ZooKeys 992: 1–58 (2020)
doi: 10.3897/zookeys.992.55977
https://zookeys.pensoft.net

RESEARCH ARTICLE

A peer-reviewed open-access journal
ZooKeys
Launched to accelerate biodiversity research

To name but a few: descriptions of five new species of *Terebellides* (Annelida, Trichobranchidae) from the North East Atlantic

Julio Parapar[1], María Capa[2], Arne Nygren[3], Juan Moreira[4]

1 *Departamento de Bioloxía, Universidade da Coruña, Spain* **2** *Departament de Biologia, Universitat de les Illes Balears, Spain* **3** *Sjöfartmuseet Akvariet, Göteborg, Sweden and Institutionen för marina vetenskaper, Göteborgs Universitet, Sweden* **4** *Departamento de Biología (Zoología) & Centro de Investigación en Biodiversidad y Cambio Global (CIBC-UAM), Facultad de Ciencias, Universidad Autónoma de Madrid, Spain*

Corresponding author: Julio Parapar (julio.parapar@udc.es)

Academic editor: C. Glasby | Received 29 June 2020 | Accepted 6 October 2020 | Published 12 November 2020

http://zoobank.org/0F038B5B-120E-4583-8E85-4092C9798566

Citation: Parapar J, Capa M, Nygren A, Moreira J (2020) To name but a few: descriptions of five new species of *Terebellides* (Annelida, Trichobranchidae) from the North East Atlantic. ZooKeys 992: 1–58. https://doi.org/10.3897/zookeys.992.55977

Abstract

The number of described species of the genus *Terebellides* Sars, 1835 (Annelida, Trichobranchidae) has greatly increased in the last years, particularly in the North East Atlantic. In this context, this paper deals with several putative species recently delineated by molecular means within a well delimited clade of *Terebellides*. Species are characterised here by a combination of morphological characters, and a complementary nucleotide diagnostic approach. Three species were identified as the nominal species *T. stroemii* Sars, 1835, *T. bigeniculatus* Parapar, Moreira & Helgason, 2011 and *T. europaea* Lavesque et al., 2019. Five species are described as new: *T. bakkeni* **sp. nov**., *T. kongsrudi* **sp. nov**., *T. norvegica* **sp. nov**., *T. ronningae* **sp. nov**. and *T. scotica* **sp. nov**. The distinctive morphological characters refer to the branchial shape, absence or presence of papillae on lamellae of anterior margin of branchial dorsal lobes, absence or presence of ciliated papillae dorsal to thoracic notopodia, geniculate chaetae in one or two chaetigers, and the morphology of thoracic and abdominal uncini teeth. Furthermore, the description of *T. bigeniculatus* is revised and complemented after examination of type specimens. An updated identification key to all species of the genus in NE Atlantic and a proposal of a classification of different types of abdominal uncini to be used in taxonomy are also included.

Keywords

DNA barcoding, DNA species delineation, identification key, integrative taxonomy, new species, North East Atlantic, polychaetes, SEM, systematics

Introduction

The species richness in the genus *Terebellides* Sars, 1835 (Annelida, Trichobranchidae) in the North East Atlantic (NEA hereafter) seemed to be well known after several taxonomic studies (Holthe 1986; Jirkov 1989, 2001; Gagaev 2009; Parapar et al. 2011, 2016c; Jirkov and Leontovich 2013; Parapar and Hutchings 2014). Nevertheless, molecular taxonomy approaches performed recently in a comprehensive sample of NEA *Terebellides* have substantially changed the understanding of the species diversity hidden within members of this genus in European waters. Studies by Nygren et al. (2018) and Lavesque et al. (2019) showed a number of genetic lineages, compatible with the species concept – independently evolving entities that are genetically (and phenotypically) distinct (Barraclough 2010). As a result, the total number of species in the NEA has increased dramatically from seven to 32 (Nygren et al. 2018; Lavesque et al. 2019), but some of these still remain unnamed or not formally described.

Terebellides is the most species-rich genus of trichobranchids, with 82 nominal species (Parapar et al. 2020; Read and Fauchald 2020) but fairly homogeneous morphologically. It is distinguished from other members in the family by their characteristic branchiae with a single mid-dorsal stalk on segment 3. However, species identification presents some difficulties as there are no clear boundaries between the intraspecific and interspecific variability of some of the morphological attributes considered of high taxonomic relevance. Species diagnostic features mainly rely on details of the branchiae, shape and size of anterior thoracic lateral lobes, and uncinal morphology (Parapar and Hutchings 2014; Parapar et al. 2016a, 2016b). Surprisingly, analyses of DNA sequences showed a large genetic diversity within the group, especially in mitochondrial markers, and while the genetic intraspecific divergence in the universal barcoding marker cytochrome c oxidase subunit I (COI) ranged from 0 to 3.4%, the interspecific distance between species varied from 8.8 to 22.9% (Nygren et al. 2018).

Phylogenetic analyses consistently showed that the NEA *Terebellides* are divided into four major clades, named Groups A–D in Nygren et al. (2018). The aim of the present paper is the systematic revision of members of Group A (according to Nygren et al. 2018), and the morphological characterization of the species assessed after phylogenetic and species delimitation analyses of DNA sequence data (Nygren et al. 2018). Given that there are some species complexes, with scarce morphological differences between the species, if any, a list of apomorphic nucleotides (present in all sequences of a certain species and unique of that species) is also provided as a complementary diagnostic feature (Rach et al. 2008; Wong et al. 2009).

Materials and methods

This paper is based on the study of 132 specimens identified as belonging to Group A as defined in Nygren et al. (2018) and corresponding to several putative species. This material is deposited in the Zoological Museum Bergen (**ZMBN**, Bergen, Norway),

Göteborg Natural History Museum (**GNM**, Goteborg, Sweden), the Norwegian University of Science and Technology, University Museum (**NTNU-VM**, Trondheim, Norway; Bakken et al. 2020) and the Senckenberg Museum Frankfurt (**SMF**, Frankfurt, Germany).

The sampling area covered in this paper is mostly the Norwegian and Swedish continental shelf but also includes some samples from the Irish and Celtic seas, North Sea, Barents Sea, Greenland Sea, South Icelandic coast and the Arctic Ocean (Suppl. material 1: Table S1; Nygren et al. 2018).

Light microscope images were obtained by means of an Olympus SZX12 stereomicroscope equipped with an Olympus C-5050 digital camera. Line drawings were made with an Olympus BX40 stereomicroscope equipped with camera lucida. Specimens for Scanning Electron Microscopy (SEM) were prepared by critical point drying, covered with gold and examined and photographed under a JEOL JSM-6400 electron microscope at the Servizos de Apoio á Investigación (SAI, Universidade da Coruña, Spain).

Methyl green (MG) staining patterns and thoracic uncini morphology were characterised based on the classification proposed by Schüller and Hutchings (2010) and Parapar et al. (2020) respectively; specimens of similar/comparable size were used.

The species dealt within the present study are quite homogenous morphologically. Therefore, common traits shared by all members of Group A are described first in order to avoid repetition of the same characters in each species description.

For each species, the list of the museum registration numbers and collection details (geographic area, locality, coordinates, depth, collecting date and habitat) is provided in Suppl. material 1: Table S1. Unless specified, each registration number holds a single specimen; associated GenBank DNA sequence accession numbers are provided in Suppl. material 2: Table S2.

The present systematic account follows the phylogenetic hypothesis presented by Nygren et al. (2018), after phylogenetic analyses of mitochondrial COI (ca. 658bp) and 16S rDNA (ca. 440 bp), and the nuclear ITS2 (290–419 bp) and 28S rDNA (ca. 760 bp) sequences from 513 specimens of *Terebellides* species from the NEA. In their topology, four strongly supported major clades were recovered, and named Groups A–D. We are herein dealing only with members of Group A. Other subgroups (A1–A4) within Group A were established after analyses of combined datasets (Fig. 1; Nygren et al. 2018). In the present study comparison of the morphological traits of species within these subgroups were performed in order to find potential characteristic diagnostic features.

The COI universal barcoding gene proved to be very informative for species delimitation purposes alone, but insufficient to resolve deeper relationships in the *Terebellides* radiation (Nygren et al. 2018). However, in the present study further analyses based on this mitochondrial marker alone have been performed in order to assess diagnostic nucleotides for each of the species and establish genetic distances between them. Phylogenetic analyses of COI *Terebellides* sequences in GenBank generated by Nygren et al. (2018) and Lavesque et al. (2019) were performed, using *Trichobranchus roseus* (Malm, 1874), *Polycirrus* sp., and *Pista cristata* (Müller, 1776) as outgroups (Nygren et

al. 2018). Four hundred and seventy-one sequences were aligned with MAFFT version 7.017 (Katoh et al. 2002), and with default parameters, trimming some starting nucleotides of the sequence of *Terebellides* sp. (MN207188) to become 659 bp alignment. Best-fit model according to Bayesian information criterion – BIC (TVM+F+I+G4), was calculated with IQTREE version 1.6.11 (Nguyen et al. 2015). Maximum likelihood phylogenetic analyses were also run in IQTREE version 1.6.11 (Nguyen et al. 2015), with ultrafast bootstrap (Hoang et al. 2018). Tree topology and support values for the nodes are found in Fig. 2. Given the morphological homogeneity in the *Terebellides* Group A species, GenBank accession numbers (COI sequences) are provided for each species, indicating those belonging to type series. Moreover, unequivocal nucleotide diagnostic characters are provided as the positions in the alignment (nucleotide), with the alignment available in Suppl. material 2: Table S2.

Abbreviations used in text, tables and figures:

abl anterior branchial lobe (lobe #5);
babv branchial afferent blood vessel;
bbv branchial blood vessel;
bdl branchial dorsal lobes;
bdlfl branchial dorsal lobes fusion line;
bdltp branchial dorsal lobe terminal papilla;
blp branchial lamellar papillae;
bst branchial stem;
bt buccal tentacles;
bvl branchial ventral lobes;
bvltp branchial ventral lobe terminal papilla;
cap capitium;
cbh contractile branchial heart;
cr ciliary row;
ct ciliary tuft;
ctrX capitium teeth row X;
dg digestive gland;
dpn dorsal projection of notopodium;
fi fore intestine;
fs fore stomach;
gc geniculate chaetae;
gr glandular region;
hs hind stomach;
loli lower lip;
MG Methyl Green;
nop notopodial protuberance;
np nephridial papilla;
oes oesophagus;
ooc oocytes;
ros rostrum;
SEM Scanning Electron Microscope;
SG segment;
STM stereomicroscope;
TC thoracic chaetiger;
tdp thoracic dorsal papilla;
tll thoracic lateral lappets;
tm tentacular membrane;
TU thoracic unciniger.

Systematics

The revision of the specimens of *Terebellides* Group A as found in Nygren et al. (2018) resulted in the identification of three nominal species: *Terebellides stroemii* Sars, 1835, *Terebellides bigeniculatus* Parapar, Moreira & Helgason, 2011 and *T. europaea* Lavesque, Hutchings, Daffe, Nygren & Londoño-Mesa, 2019, and five new species described herein as *T. bakkeni* sp. nov., *T. kongsrudi* sp. nov., *T. norvegica* sp.

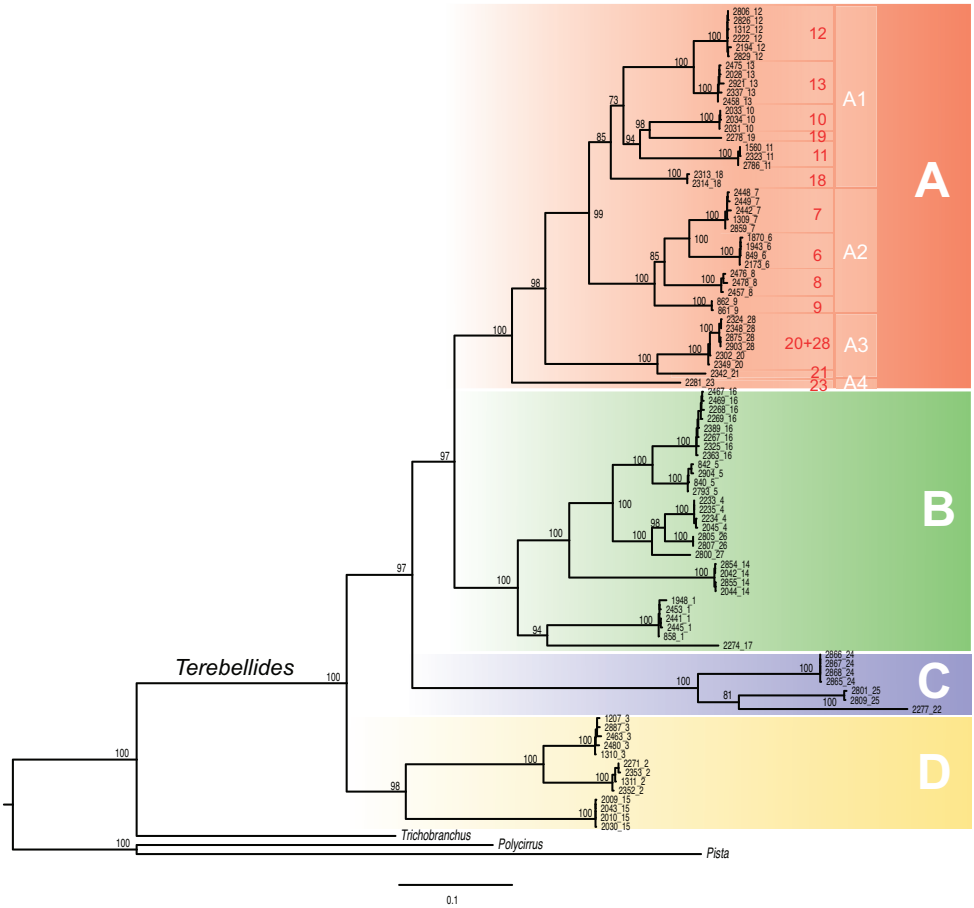

Figure 1. Phylogenetic tree after Maximum Likelihood analyses on a concatenated dataset of cox1, 16S rDNA, ITS2, and 28S rDNA (as in Nygren et al. 2018). Bootstrap support values above nodes. Coloured squares indicate the major clades referred herein as Groups A–D. Within Group A, the focus of present study, subgroups A1–A4 and species 6–13, 18–21, 23, 28 are labelled.

nov., *T. ronningae* sp. nov. and *T. scotica* sp. nov. The remaining five species will be dealt with in future studies.

Species included in Group A have been grouped as follows: A) subgroup A1 (species 10, 11, 12, 13, 18, 19; as in Nygren et al. 2018), B) subgroup A2 (species 6, 7, 8, 9; as in Nygren et al. 2018), C) subgroup A3 (clades 20 + 28, 21; as in Nygren et al. 2018) and D) subgroup A4 (species 23) (Figs 1, 2, Table 1); material will be described here following this order. Material corresponding to species 12, 18, 19 (A1), 21 (A3) and 23 (A4) is not described/named here. Species 18, 19 and 23 were represented by 1–3 specimens each (see Appendix S36 in Nygren et al. 2018) and are pending formal description until more material is available. Clades 12 and 21 will be described elsewhere by D. Gaeva and I. Jirkov (Shirshov Institute of Oceanology, Russia).

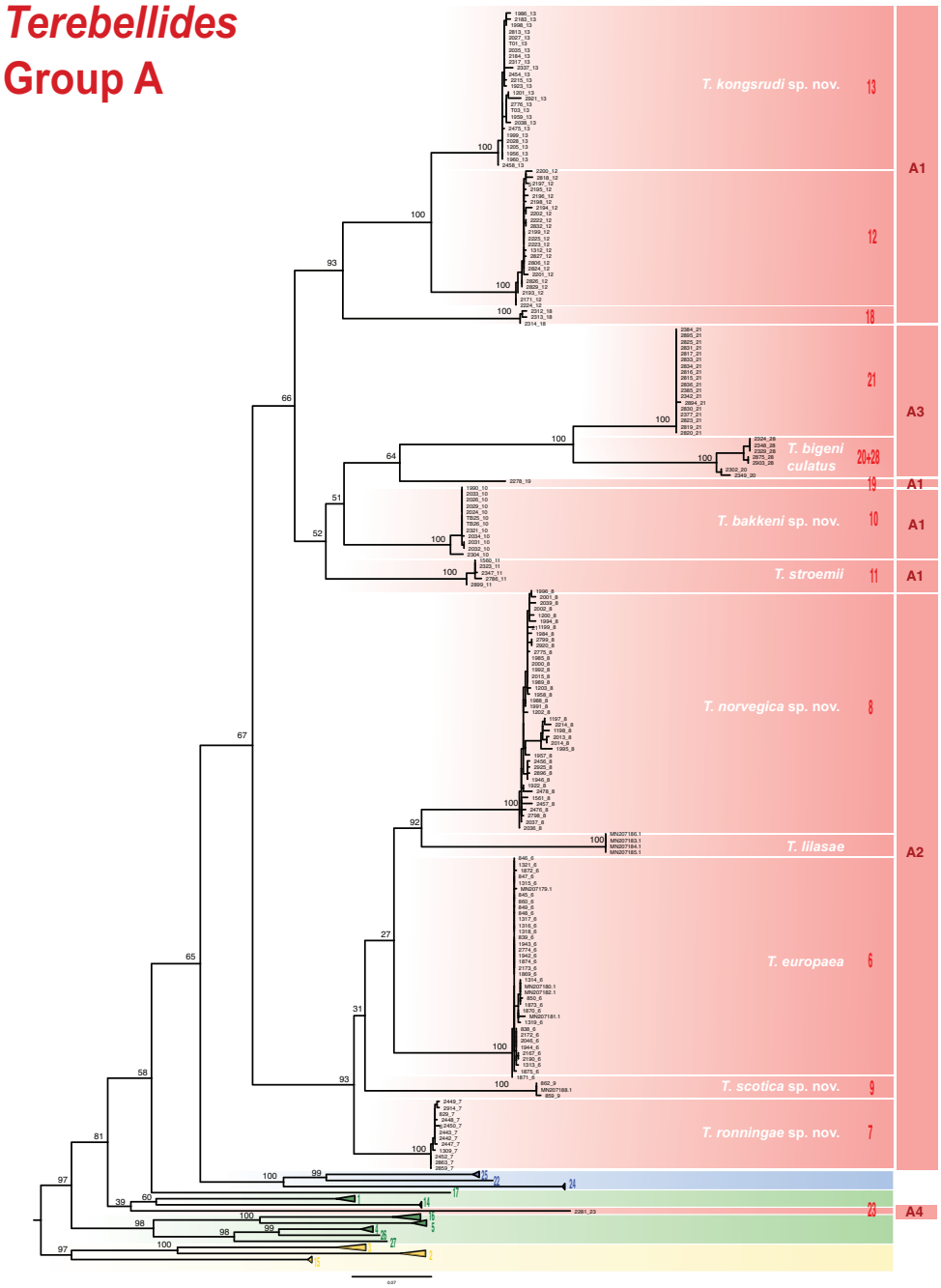

Figure 2. Phylogenetic tree after Maximum Likelihood analyses on a dataset of cox1 (including all sequences in Nygren et al. 2018 and in Lavesque et al. 2019). Bootstrap support values above nodes. Species other than members of Group A are collapsed. Species with names refer to those dealt with in present study.

Table 1. Comparison of discriminatin g taxonomic characters of the species studied in this work. Cells with text in italic show discriminatory characters of each subgroup. Species 18, 19, and 23 were not studied and 12 and 21 only examined with SEM.

Subgroups		**A1**						**A2**				**A3**		**A4**
Species sensu Nygren et al. (2018)		10	11	12	13	18	19	6	7	8	9	20 + 28	21	23
SPECIES **(as reported/described here)**		*T. bakkeni* sp. nov.	*T. stroemii* Sars, 1835	*Terebellides* sp. 1	*T. kongsrudi* sp. nov.			*T. europaea* Lavesque et al., 2019	*T. ronningae* sp. nov.	*T. norvegica* sp. nov.	*T. scotica* sp. nov.	*T. bigeniculatus* Parapar et al., 2011	*Terebellides* sp. 2	
Branchiae	type [1]	1	1	1	1	–	–	1	1	1	1	*1* [2]	*1* [2]	–
	papillae on lamellae edge	no	no	no	no	–	–	*yes*	*yes*	*yes*	*yes*	no	no	–
Thorax	ciliated papilla dorsal to notopodium	*yes*	*yes*	*yes*	*yes*	–	–	no	no (?)	no	no	*yes*	*yes*	–
	chaetiger(s) with geniculate chaetae	TC6	TC6	TC6	TC6	–	–	TC6	TC6	TC6	TC6	*TC5 + TC6*	*TC5 + TC6*	–
	uncini type [3]	3	3	3	3	–	–	3	1	3	3	3	3	–
Abdomen	uncini type [4]	1A	2	2	1A	–	–	*2*	*2*	*2*	*2*	*1B*	*1B*	–
Bathymetry – Above (A) / Below (B) 200 m depth [5]		A / **B**	A / **B**	A	A / **B**	B	B	A	A	B	A	B	A / **B**	B
Distribution – North (N) /South (S) of 60°N [5]		N	N	S	N / S	N	N	S [6]	N / S	**N** / S	S [7]	N	N	N

[1] sensu Parapar et al. (2016c); [2] sometimes irregular; [3] sensu Parapar et al. (2020); [4] this work; [5] dominant trend in bold; [6] Skagerrak and Kattegat; [7] Irish Sea

Family Trichobranchidae Malmgren, 1866

Genus *Terebellides* Sars, 1835 emended by Schüller & Hutchings, 2013

Type species. *Terebellides stroemii* Sars, 1835, redescribed by Parapar and Hutchings (2014) and neotype deposited.

Terebellides Group A (sensu Nygren et al. 2018)

Description. The morphological features shared by all studied species in Group A are itemized below. Some of these are also shared by Groups B, C and D as defined in Nygren et al. (2018) (see Remarks below).

Body appearance. Complete individuals ranging from 10.0–50.0 mm in length. Body tapering posteriorly with segments increasingly shorter and crowded towards pygidium (Fig. 14A–C). Prostomium compact; large tentacular membrane surrounding mouth (Figs 5C, 14B), with typical buccal tentacles with expanded tips (Figs 15A, 20A). SGI as an expanded structure below tentacular membrane in a lower lip (Figs 14C, 15A, 22A, 24A).

Branchiae. Branchiae arising as single structure from SGIII, with a single stalked mid-dorsal stem (Figs 5A, 11C, 15A), one pair of dorsal (upper) partially fused lobes (Figs 11B, 15B, 20A), and a pair of shorter ventral (lower) lobes (Fig. 5A, B) obscured or

not by dorsal ones (Figs 5A, C, 15A, B). Both dorsal and ventral branchial lobes ending each posteriorly in short terminal papilla (Fig. 20B). Anterior projection of dorsal lobes (fifth lobe) present but short (Fig. 5A, B) and usually obscured by tentacular membrane and buccal tentacles (Fig. 14A, C). Posterior dorsal lobes reaching TC4 (Figs 3, 4, 19). Branchial lamellae provided with several parallel rows of cilia in inner face (Fig. 15C); ciliated papillae not present, ciliary tufts present, sometimes not clearly visible (Fig. 5B, D).

Thorax. Eighteen pairs of notopodia (SGIII-SGXX) (Fig. 14B, D), those of TC1 approximately as long as following ones (Figs 20A, 22A) or slightly shorter (Fig. 15A). Lateral lappets and dorsal projections of notopodia in anterior thoracic chaetigers with different degree of development depending on size and preservation conditions, but both more conspicuous on TC2–4/5 (Figs 15A, 22A). All notochaetae as simple capillaries (Figs 11F, 15A). Neuropodia as sessile pinnules from TC5 or TC6 to body end, with uncini in single or double rows, from TC7 throughout. Neuropodia on TC5 or TC5 and TC6, provided with several sharply bent, acute-tipped, geniculate chaetae (Figs 16B, 23A) with minute teeth forming an ill-defined capitium only visible with SEM (Figs 12B, 25B). From TC7, neuropodia with one or several rows of uncini per torus (Figs 16C, 23C), with long shafted denticulate hooks, with large main fang (rostrum) longer than upper crest of teeth (capitium), which is composed by several teeth above main fang of decreasing length (Figs 23D, 25D, E).

Abdomen and pygidium. Approximately half as long as thorax and progressively thinner (Fig. 14B). Neuropodia ranging from 18–38 chaetigers and forming erect pinnules (Figs 6F, 12F) with several uncini per torus, number depending of specimen size. Uncini provided with several teeth above rostrum surmounted by a capitium composed of several teeth of decreasing length (Figs 6G, 16E, 21F). Pygidium blunt, as funnel-like depression.

Colour pattern. Colour in preserved specimens pale brown (Fig. 3). MG staining pattern 1 sensu Schüller and Hutchings (2010: 10, fig. 4) and characterised by compact green colouration in CH1–3, then turning into striped pattern in CH4–12 and fading in following segments.

Remarks. Among the aforementioned characters, branchial features might serve to distinguish most of Group A species (except for A3 species) from those in Groups B–D. Those include branchial size, lobes size (i.e., whether dorsal and ventral are of similar size or differ), presence of terminal papilla/filament on posterior lobes, and presence of ciliary structures (rows, tufts or buttons) on lamellae. Other taxa described or reported worldwide bear similar branchiae including *T. stroemii* sensu Parapar et al. (2011) from Iceland and sensu Parapar et al. (2013) from the Adriatic Sea, *T. kerguelensis* McIntosh, 1885 and *T. longicaudatus* Hessle, 1917 from Antarctic latitudes (Parapar and Moreira 2008a, 2008b), and *T. kobei* Hessle, 1917 from Japan (Imajima and Williams 1985).

The other species groups as found in Nygren et al. (2018) were not studied in depth here and will be the aim of a subsequent study. However, Group B seems to be characterised by having a shorter body and free branchial lobes; these features are shared with *T. atlantis* Williams, 1984 and *T. irinae* Gagaev, 2009 as already suggested by Nygren et al. (2018). Members of Group C are apparently not defined by any

unique shared morphological character but show the same geographic distribution as *T. irinae*. Finally, the three putative species in Group D were related to *T. gracilis* Malm, 1874 and *T. williamsae* Jirkov, 1989 by Nygren et al. (2018) even though the latter was proposed to be synonymised with the former by Parapar et al. (2011). These species seem characterised by having ventral white colouration in a number of anterior chaetigers and similar-sized branchial lobes; these characters are not shared with Group A.

Regarding Group A, six morphological characters have been considered to delineate subgroups and species (Table 1). Two characters can be determined with the aid of the STM: 1) general branchial shape, 2) number of thoracic chaetigers with geniculate chaetae; four characters require SEM examination: 3) presence of papillae on lamellae of dorsal branchial lobes, 4) presence of ciliated papillae dorsal to thoracic notopodia, 5) features of thoracic and 6) abdominal uncini shape dentition. Branchial typology (1) is defined according to Parapar et al. (2016c) and thoracic uncini (5) follows Parapar et al. (2020). Typology of abdominal uncini (6) is described here (see Discussion).

Furthermore, species will be also characterised according to geographic and bathymetric distribution according to available data.

Subgroup A1

Analyses of molecular data found low or no support for monophyly of this clade (Figs 1, 2) and there is no apparent morphological synapomorphy supporting this clade either. Cohesion of members of this group needs to be studied further, but meanwhile, it is considered herein as a morphologically homogenous gathering of species 10–13 and 18–19 (Figs 1, 2). As it was indicated above, only species 10, 11, and 13 will be described herein, of which 10 and 13 are new to science and 11 corresponds to *T. stroemii*; some comments on species 12 (*Terebellides* sp. 1 hereafter) are also provided.

Characters present only in subgroup A1

None (Table 1).

Character/s shared with subgroup A2

- Branchiae of type 1 (*stroemii*-type, comma-shaped), all four lobes fused for approximately half of their length and ventral ones usually obscured by dorsal ones (Fig. 11A–C).
- First thoracic neuropodia on TC6, with chaetiger provided with several sharply bent, acute-tipped geniculate chaetae (Figs 6A, 15A, 16B).

Character/s shared with subgroup A3

- Border of anterior region of dorsal branchial lamellae not provided with papillary projections.

- One ciliated papilla is present, dorsal to thoracic notopodia (Fig. 5F).
- Thoracic uncini type 3 (Figs 6E, 7E, F, 16D).

Character/s variable within subgroup A1

- Abdominal uncini type 1 (Fig. 6G) and 2 (Fig. 7G) (see *Conclusions* Section).

Lavesque et al. (2019) describe several species from French waters similar to those of Group A in terms of body and branchial shape. Among them, *Terebellides gralli* Lavesque, Hutchings, Daffe, Nygren & Londoño-Mesa, 2019 is described as lacking papillary projections on branchial lamellae, but no mention is made to whether or not ciliated papillae are present dorsal to thoracic notopodia. The sequences of this species do not relate with those of any putative species as defined in Nygren et al. (2018). Moreover, *T. gralli* differs morphologically from other congeners in having longer branchiae that may reach TC4–6 (Lavesque et al. 2019: 169, fig. 12A) instead of only reaching TC3–4.

***Terebellides bakkeni* sp. nov.**
http://zoobank.org/0D530A3C-65B2-4F9D-A78A-051AE5B62110
Figs 1, 2, 3A, 4A, 5, 6, 8A, 9, 17A; Table 1; Suppl. material 1: Table S1; Suppl. material 2: Table S2

Species 10 Nygren et al. 2018: 18–22, figs 6, 10.

Material examined. Type material. ***Holotype***: ZMBN116395. ***Paratypes*** (10 specimens): Barents Sea (ZMBN116388, ZMBN116389), Norwegian coast and shelf (ZMBN116390, ZMBN116391, ZMBN116392, ZMBN116393, ZMBN116394, ZMBN116396, NTNU–VM61376, NTNU–VM61377).

Holotype. Complete specimen, 32.0 mm long and 2.0 mm width (Figs 3A, 4A).

GenBank accession numbers of material examined (COI). ***Holotype***: MG025165; ***Paratypes***: MG025159, MG025160, MG025161, MG025162, MG025163, MG025164, MG025165, MG025166, MG025168, MG025169, MG025170. ***Additional material***: MG025167.

Diagnostic features of type material. Complete individuals ranging from 23.0–32.0 mm in length (Fig. 17A). Branchial dorsal lobes lamellae without papillary projections. Ventral branchial lobes generally hidden behind dorsal ones (Figs 3A, 4A, 5A–C). Lateral lappets and dorsal projection of thoracic chaetigers present on TC2(TC3)–TC5(TC4) (Fig. 5A). Geniculate chaetae in TC6 acutely bent, with low marked capitium (Fig. 6A, B). Ciliated papilla dorsal to thoracic notopodia (Fig. 5F). Thoracic uncini in one row with rostrum/capitium length ratio of approximately 2 : 1 and capitium with a first row of three or four medium-sized teeth, followed by several smaller teeth (Fig. 6C–E). Abdomen with 25–29 pairs of neuropodia (Fig. 6F) with type 1 uncini (Fig. 6G).

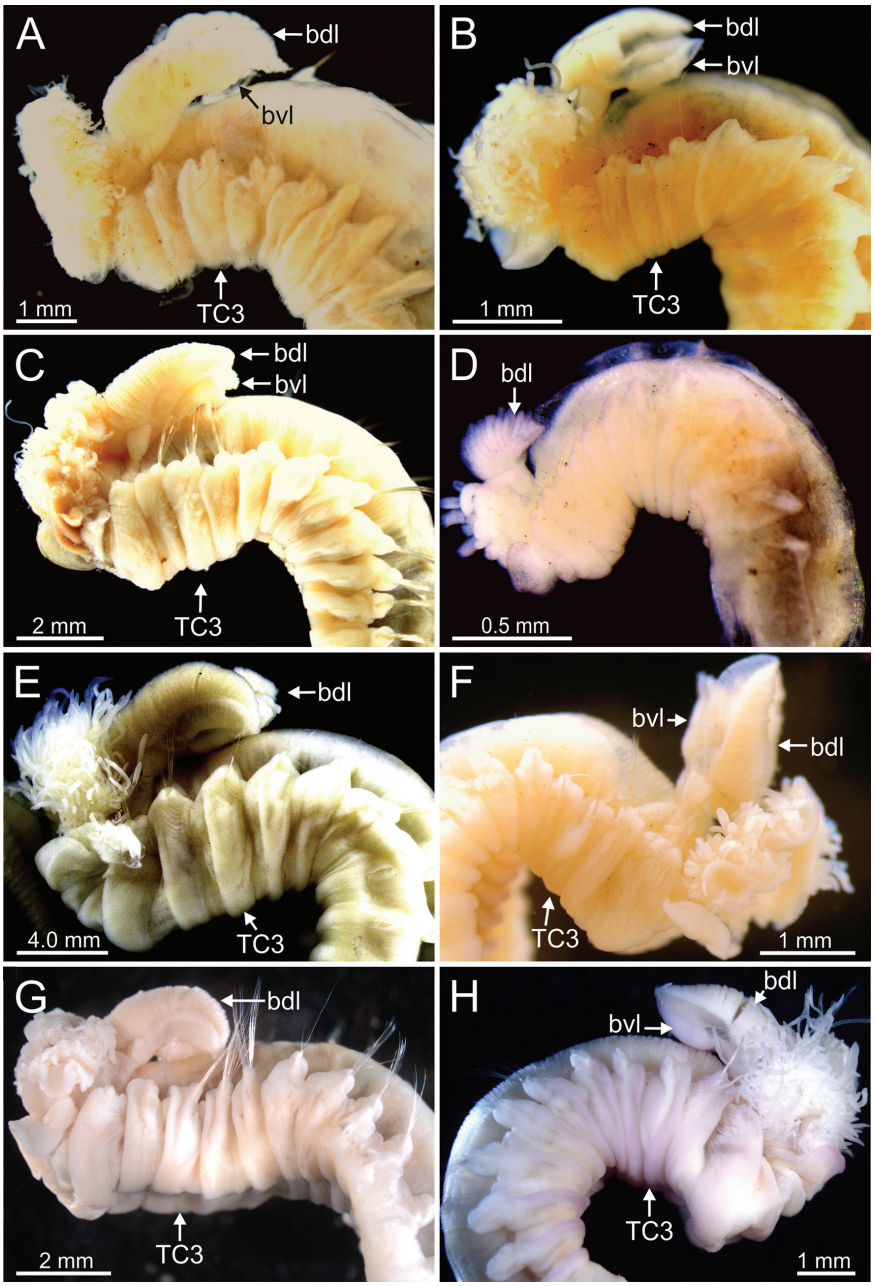

Figure 3. STM photographs of several *Terebellides* species. **A** *Terebellides bakkeni* sp. nov. (species 10; holotype, ZMBN116395) **B** *Terebellides stroemii* Sars, 1835 (species 11; non-type specimen, ZMBN116397) **C** *Terebellides kongsrudi* sp. nov. (species 13; holotype, GNM14632) **D** *Terebellides bigeniculatus* Parapar, Moreira & Helgason, 2011 (species 20 + 28; non-type specimen, ZMBN116514) **E** *Terebellides europaea* Lavesque, Hutchings, Daffe, Nygren & Londoño-Mesa, 2019 (species 6; non-type specimen, GNM14628) **F** *Terebellides ronningae* sp. nov. (species 7; holotype, ZMBN116357) **G** *Terebellides norvegica* sp. nov. (species 8; holotype, ZMBN416378) **H** *Terebellides scotica* sp. nov. (species 9; holotype, ZMBN116385). Abbreviations: bdl – branchial dorsal lobe; bvl – branchial ventral lobe; TC – thoracic chaetiger.

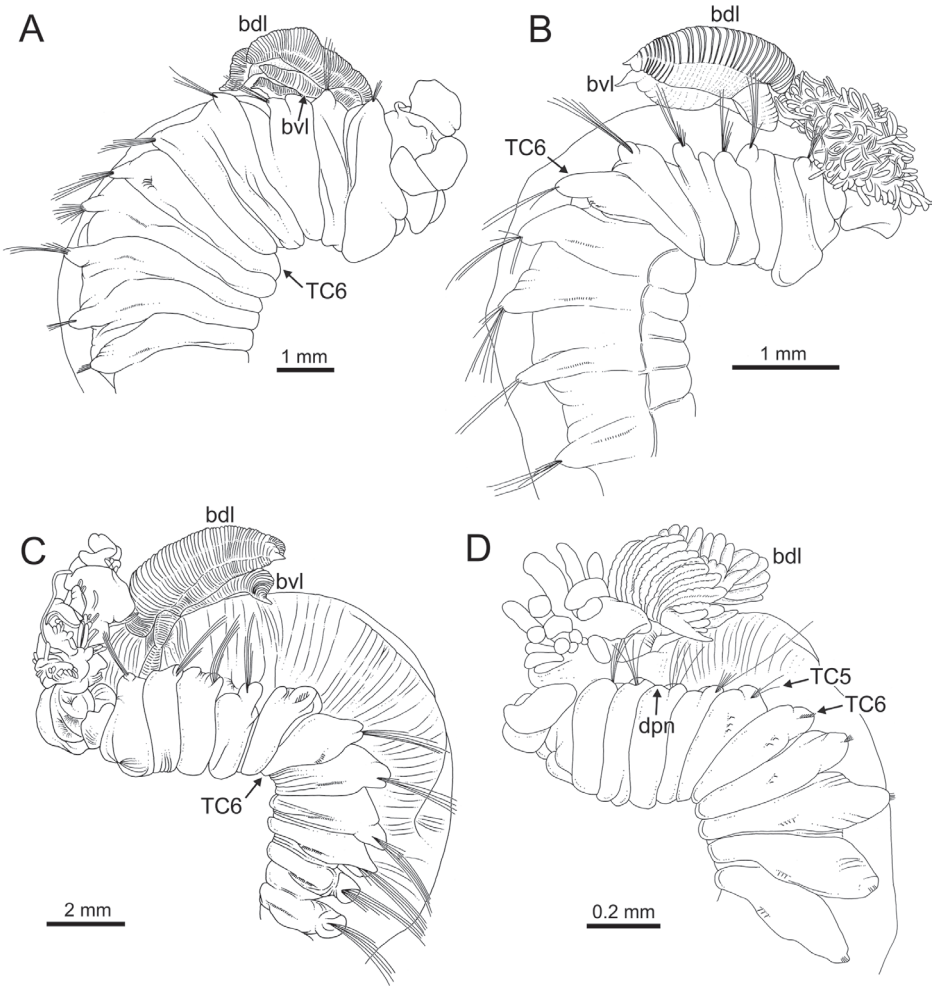

Figure 4. Line drawings of several *Terebellides* species. **A** *Terebellides bakkeni* sp. nov. (species 10; holotype, ZMBN116395), anterior end, right lateral view **B** *Terebellides stroemii* Sars, 1835 (species 11; non-type specimen, ZMBN116397), anterior end, right lateral view **C** *Terebellides kongsrudi* sp. nov. (species 13; holotype, GNM14632), anterior end, left lateral view **D** *Terebellides bigeniculatus* Parapar, Moreira & Helgason, 2011 (species 20 + 28; non-type specimen, ZMBN116514), anterior end, left lateral view. Abbreviations: bdl – branchial dorsal lobe; bvl – branchial ventral lobes; dpn – dorsal projection of notopodium ; TC – thoracic chaetiger.

Nucleotide diagnostic features. Members of *T. bakkeni* sp. nov. share the following unique nucleotides at these given positions of our alignement: 162 (G), 168 (C), 345 (G; shared only with one specimen from species 17).

Type locality. Nordland, Sortlaandssunder (Lofoten Islands); 119 m deep (Suppl. material 1: Table S1).

Distribution and bathymetry. Barents Sea, Greenland Sea, northern Norwegian coasts from the Lofoten Islands to Trondheim; at depths of102–378 m (Nygren et al.

2018) (Figs 8A, 9; Suppl. material 1: Table S1). One specimen found in North Iceland at 1,250 m deep.

Etymology. This species is named after Dr. Torkild Bakken, from the NTNU–University Museum, Trondheim (Norway), housing institution of some of the specimens used in the present study, for his dedication to the study of Norwegian polychaetes and his friendship.

Remarks. *Terebellides bakkeni* sp. nov. is a small-sized species, maximum-sized specimens reaching 20.0 mm in length (n = 3). This species is characterised by the presence of ciliated papilla dorsal to thoracic notopodia, lack of papillae on the margins of branchial lamellae and presenting abdominal uncini of type 1. Most of these features are also shared by the closest relative, *T. stroemii* (species 11 herein), but they differ in the morphology of the abdominal uncini, being of type 2 in *T. stroemii* and type 1 in *T. bakkeni* sp. nov. (Table 1). One specimen studied with SEM showed ciliary tufts in the inner side of the branchial lamellae (Fig. 5D). If this feature is not an artefact and is confirmed in all members of the species – so far only two specimens were examined under SEM – it would be an autapomorphy for the species. A similar feature was found in the non-closely related *T. gracilis*, that is also present in NEA. The ciliary tufts in *T. bakkeni* sp. nov. are, however, connected by rows of cilia (Fig. 5D), while in *T. gracilis* they are confined to isolated tufts (Parapar et al. 2011: 12, fig. 9c). On the other hand, there are no clear morphological differences between *T. bakkeni* sp. nov. and *T. kongsrudi* sp. nov. (species 13). These sympatric species differ in the southern limit of their geographic distribution: *T. bakkeni* sp. nov., as *T. kongsrudi* sp. nov. are present above 65°N (Fig. 8A, C) while the latter and *T. stroemii* reach more southern latitudes, such as the Skagerrak and Bergen respectively (Fig. 8B, C).

Of the 462 sequences, including all NEA species, and 659 positions in the COI alignment, the 12 sequences assigned to *T. bakkeni* sp. nov. hold two unique nucleotides positions, and an additional one only shared by a single specimen from another clade (see Suppl. material 2: Table S2). The species also showed 0–1.9% of intraspecific divergence in the COI marker, and a minimum of 11.5% uncorrected genetic distance with congeners (in this case *T. stroemii*) (Nygren et al. 2018).

***Terebellides stroemii* Sars, 1835**

Figs 1, 2, 3B, 4B, 7, 8B, 9, 10, 17A, 28D; Suppl. material 1: Table S1; Suppl. material 2: Table S2

Terebellides stroemii Sars, 1835: 48–50, pl. 13, fig. 31a–e. Parapar and Hutchings 2014: 10, fig. 5–10. *Non* Parapar et al. 2011: 14–17, figs 11, 12, 13G.

Species 11 – Nygren et al. 2018: 18–22, figs 6, 10. *Non* Clade 6 in Nygren et al. (2018) (see Remarks).

Type locality. Helle, Manger, Bergenfjord (Norway) (Parapar and Hutchings 2014).

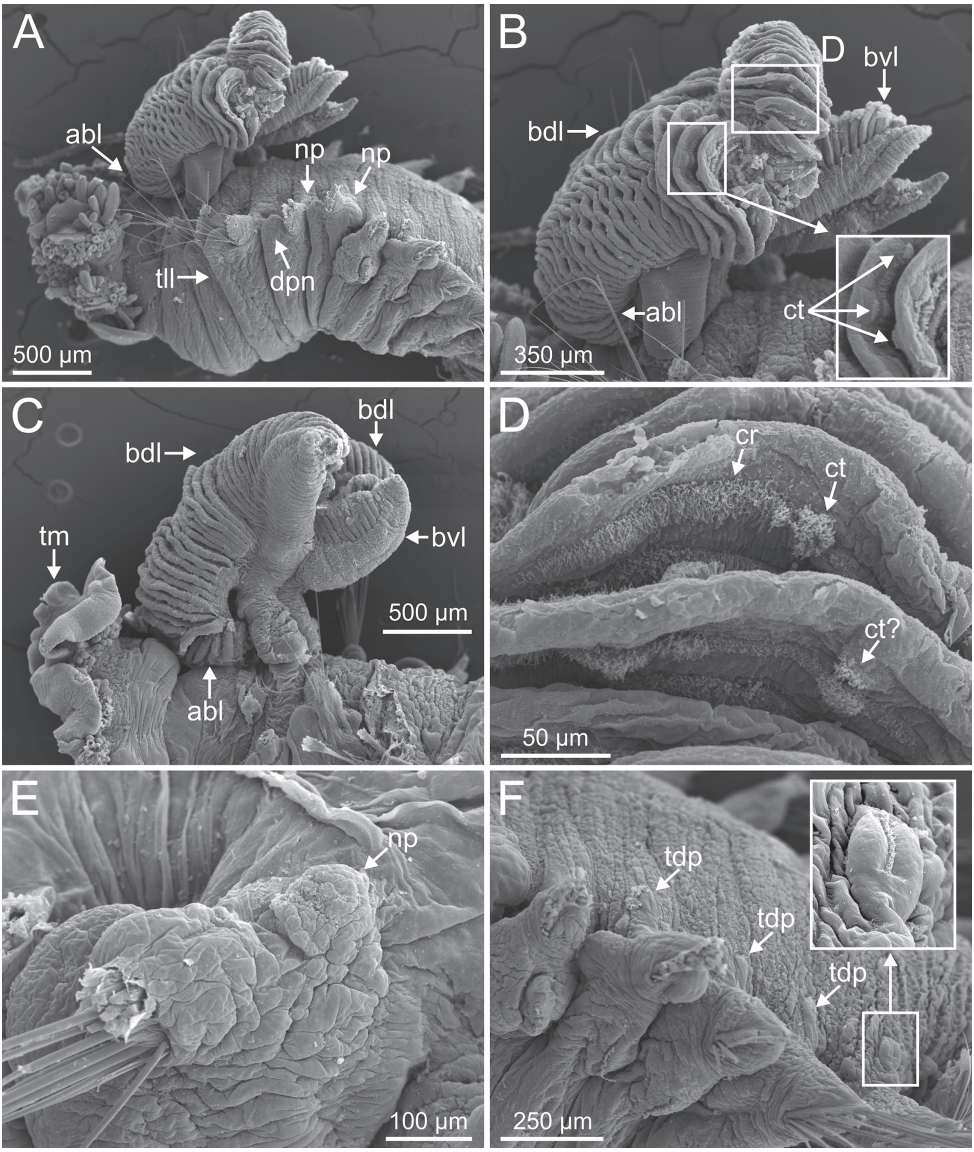

Figure 5. *Terebellides bakkeni* sp. nov. (species 10; paratypes, NTNU-VM-61376 and NTNU-VM-61377), SEM micrographs. **A** anterior end, left lateral view **B, C** branchial lamellae **D** branchial ciliary rows (framed in **B**) **E** nephridial papilla **F** thoracic notopodial papillae (framed: detail of one papilla). Abbreviations: abl – anterior branchial lobe; bdl – branchial dorsal lobe; bvl – branchial ventral lobe; cr – ciliary row; ct – ciliary tuft; dpn – dorsal projection of notopodium; np – nephridial papilla; TC – thoracic chaetiger; tdp – thoracic dorsal papilla; tll – thoracic lateral lobes; tm – tentacular membrane.

Material examined. 5 specimens (Suppl. material 1: Table S1), Norwegian coast and shelf: ZMBN 116397, ZMBN 116398, ZMBN 116399, ZMBN 116400, ZMBN 116401.

Additional material. Neotype (NHMOC5896) and seven "**neoparatypes**" (NHMOC5899, NHMOC5902, NHMOC5904, NHMOC5905, NHMOC5907, NHMOC5956, NHMOC5968) of *T. stroemii* (Suppl. material 1: Table S1).

GenBank accession numbers of material examined (COI). MG025171, MG025172, MG025173, MG025174, MG025175.

Diagnostic features of studied material. Complete individuals ranging from 6.0–20.0 mm in length (Fig. 17A). Branchial dorsal lobes lamellae without papillary projections. Ventral branchial lobes hidden behind dorsal lobes (Figs 3B, 4B). Lateral lappets present on TC1–TC4; dorsal projection well marked from TC3–TC4 (Fig. 7A). Geniculate chaetae in TC6, acutely bent (Fig. 7C) with low marked capitium. Ciliated papilla dorsal to thoracic notopodia (Fig. 7B). Thoracic uncini in one row with rostrum/capitium length ratio approximately 2 : 1 and capitium with a first row of three or four medium-sized teeth, followed by several smaller teeth (Fig. 7E, F). Abdomen with 23–32 chaetigers (Fig. 17A) with type 2 uncini (Figs 7G, 28D).

Nucleotide diagnostic features. There are no unique apomorphic nucleotides in the fragments of COI analysed for *T. stroemii*, when considering all *Terebellides* species present in the NEA (Suppl. material 2: Table S2). However, when comparing homologous nucleotide positions with members of only Group A (183 sequences in the COI alignment), the following autapomorphies arise: 174 (C), 183 (C), 453 (A), 612 (C).

Distribution and bathymetry. *Terebellides stroemii* was traditionally considered as a cosmopolitan species, but its known distribution seems in fact restricted to the Norwegian coastline (Parapar et al. 2011; Parapar and Hutchings 2014; Lavesque et al. 2019). Specimens examined by Nygren et al. (2018) and in the present paper, obtained after comprehensive sampling in the NEA, were found only in W Norway, between 115 and 388 m deep (Figs 8B, 10; Suppl. material 1: Table S1).

Remarks. In the five sequences belonging to this species, there were four haplotypes showing 0–1.1% of intraspecific divergence, and a minimum of 11.5% uncorrected genetic distance with members of the closest relative, *T. bakkeni* sp. nov. (Nygren et al. 2018).

Terebellides stroemii is a large species, reaching up to 52 mm in length (Parapar and Hutchings 2014) and is characterised by the presence of ciliated papilla dorsal to thoracic notopodia, lack of papillae on margins of branchial lamellae, thoracic uncini of type 3 and abdominal uncini of type 2. All these features are shared with *T. kongsrudi* sp. nov.; *T. bakkeni* sp. nov. is also very close morphologically to *T. stroemii* but they differ in the morphology of the abdominal uncini as explained above.

Nygren et al. (2018) misidentified species 6 as *T. stroemii*, but this was later corrected by Lavesque et al. (2019) who pointed out that the molecular sequences of these specimens fit with those of *T. europaea*.

Specimens examined here bear thoracic uncini that are most similar to other members of Group A; SEM examination showed, however, that some uncini have a rostrum distal tip that is distinctly bent downwards (deformity?) (Fig. 7E, arrow) as already described for the type specimens by Parapar and Hutchings (2014: 8, fig. 7F, G), and attributed to preservation for too long in EtOH. However, we have found similar bent rostrum

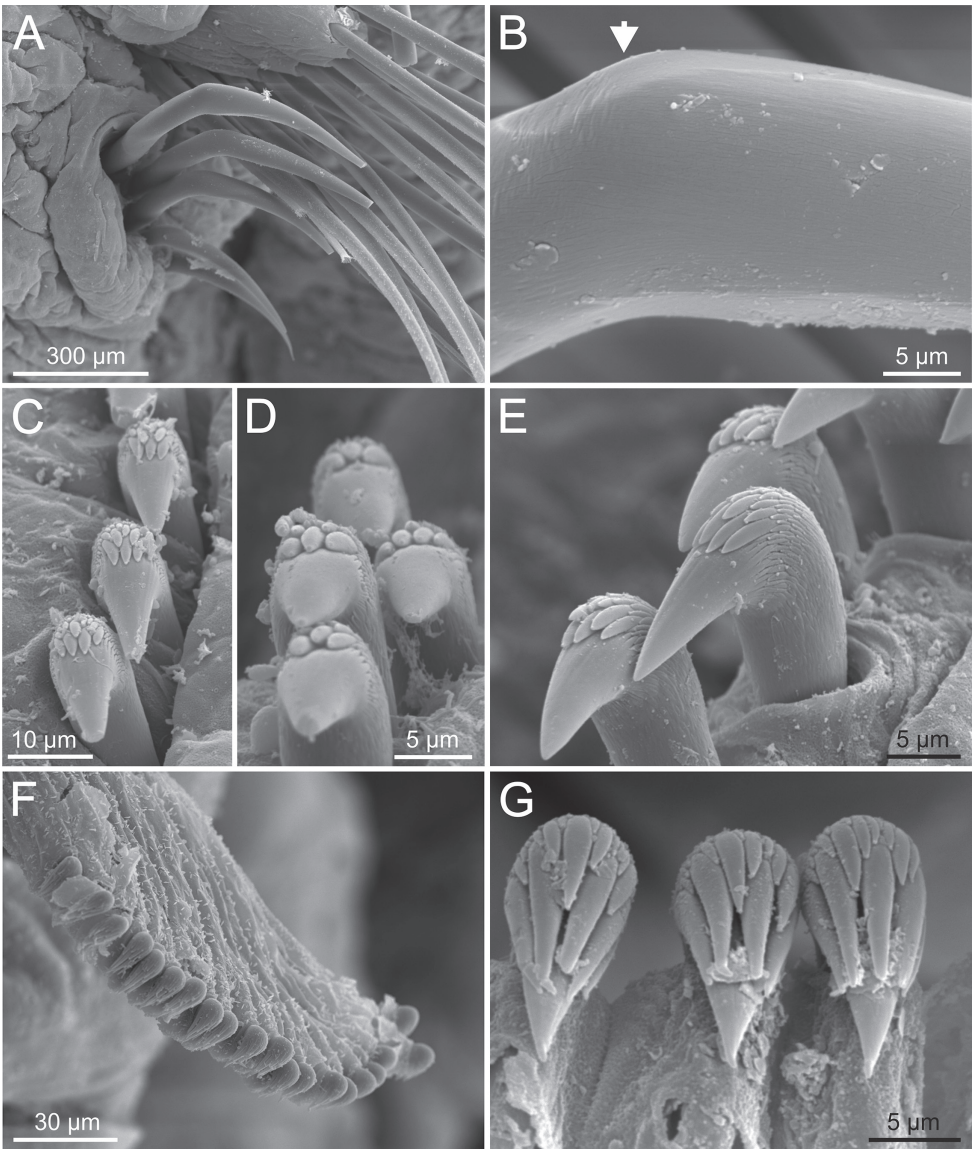

Figure 6. *Terebellides bakkeni* sp. nov. (species 10; paratypes, NTNU-VM-61376 and NTNU-VM-61377), SEM micrographs. **A** TC6 (TU1) geniculate chaetae **B** geniculate chaeta (arrow pointing to capitium) **C–E** thoracic uncini **F** abdominal unciniger **G** detail of three abdominal uncini, frontal view.

among specimens of *T. kongsrudi* sp. nov. (Fig. 12D, arrow), *T. ronningae* sp. nov. (species 7) (Fig. 21C, arrows) and *T. bigeniculatus* (species 20 + 28) (Fig. 26E, frame) suggesting this may not be related to preservation. The abdominal uncini are quite similar to those described in Parapar and Hutchings (2014: 9, fig. 8C–E) also showing a small gap among the anteriormost teeth of rostrum (Parapar and Hutchings 2014: 8–9, fig. 8F; Fig. 7G); these features are not shared by other species of subgroup A1, i.e., *T. bakkeni* sp. nov. and *T. kongsrudi* sp. nov. In all, species 11 agrees well with the redescription of *T. stroemii*.

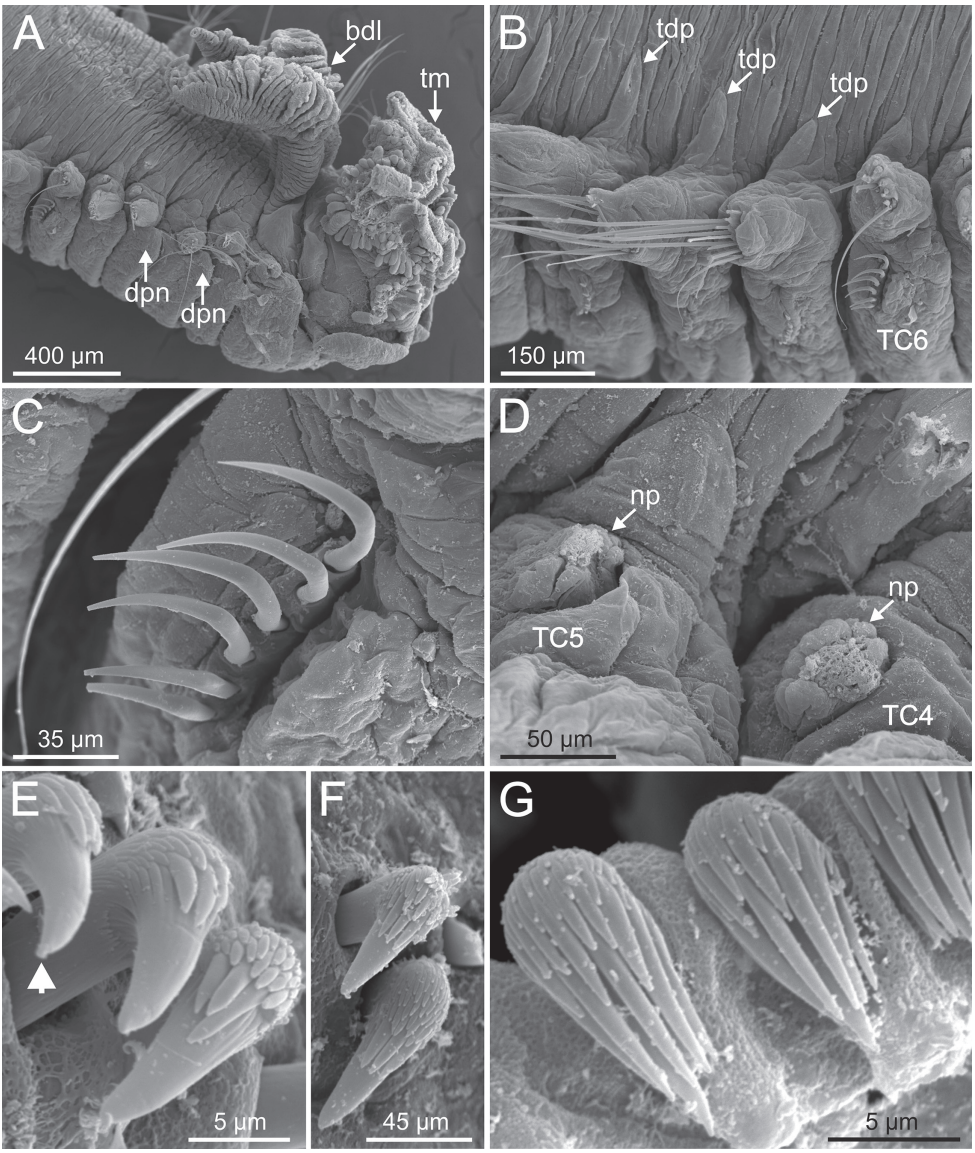

Figure 7. *Terebellides stroemii* Sars, 1835 (species 11; non-type specimen, ZMBN 116399), SEM micrographs. **A** anterior end, right lateral view **B** TC6 to TC8, lateral view **C** geniculate chaetae **D** TC4 and TC5, nephridial papillae **E, F** thoracic uncini (arrow in **E** pointing to rostrum curved at distal end) **G** abdominal uncini. Abbreviations: bdl – branchial dorsal lobes; dpn – dorsal projection of notopodium; np – nephridial papilla; TC – thoracic chaetiger; tdp – thoracic dorsal papilla; tm – tentacular membrane.

Geographic and bathymetric distribution of our specimens also agree with that of *T. stroemii* (see Parapar and Hutchings 2014), with Manger (Norway) (i.e., type locality of *T. stroemii*; Fig. 10) being its southernmost distribution limit. The other three taxa, i.e., species 5, *T. europaea* and *T. bigeniculatus*, were also found near Manger, but all can be clearly distinguished morphologically from each other (see above and below for *T. europaea*

and *T. bigeniculatus*) and species 5 belongs to Group B and seems closer morphologically to *T. atlantis*. On the other hand, type specimens of *T. stroemii* come from depths of 55–110 m (Parapar and Hutchings 2014) as well as specimens belonging to *T. europaea*, *T. ronningae* sp. nov., *T. scotica* sp. nov. (species 9) and species 12 (<200 m), and therefore they seem to constitute a shallow-water assemblage of species from an ecological point of view.

Finally, the Icelandic specimens reported as *T. stroemii* by Parapar et al. (2011) might not correspond to this species. In fact, it is likely that they represent at least two different species, namely *T. bakkeni* sp. nov. and *T. kongsrudi* sp. nov., both reported here to the North and East of Iceland. Therefore, the aforementioned specimens deserve further revision.

***Terebellides kongsrudi* sp. nov.**
http://zoobank.org/541890B5-C55E-4716-BB42-0D87E7184885
Figs 1, 2, 3C, 4C, 8C, 9, 11, 12, 17B, 28A; Table 1; Suppl. material 1: Table S1; Suppl. material 2: Table S2

Species 13 – Nygren et al. 2018: 18–22, figs 6, 10.

Material examined. Type material. ***Holotype***: GNM14632. ***Paratypes*** (20 specs): Barents Sea (ZMBN116409, ZMBN116411, ZMBN116414); Norwegian coast and shelf (ZMBN116412, ZMBN116413, ZMBN116415, ZMBN116416, ZMBN116417, ZMBN116418, NTNU-VM66568, NTNU-VM66570, NTNU-VM66571, NTNU-VM66572, NTNU-VM68195, NTNU-VM72560, NTNU-VM72561, NTNU-VM72562, NTNU-VM72563); Skagerrak (GNM15136, GNM14632, GNM14638).

Holotype. Complete specimen, 50.0 mm long and 5.0 mm width (Figs 3C, 4C).

GenBank accession numbers of material examined (COI). Paratypes: MG025201, MG025202, MG025203, MG025204, MG025210, MG025211, MG025212, MG025214, MG025216, MG025217, MG025218, MG025219, MG025223. Additional material: MG025199, MG025200, MG025205, MG025206, MG025207, MG025208, MG025209, MG025213, MG025215, MG025220, MG025221, MG025222, MG025224.

Diagnostic features of type material. Complete individuals 12.0–50.0 mm in length (Fig. 17B). Branchial dorsal lobes lamellae without papillary projections. Ventral branchial lobes hidden in between dorsal ones (Figs 3C, 4C, 11A–C). Lateral lappets and dorsal projection of thoracic notopodia on TC2(3)–TC5(4) (Fig. 11A). Geniculate chaetae in TC6, acutely bent, with low marked capitium (Fig. 12A, B). Two pairs of nephridial pores in TC4 and TC5 and ciliated papilla dorsal to thoracic notopodia (Fig. 11D, E). Thoracic uncini in one row with rostrum/capitium length ratio approximately 2 : 1 and capitium with a first row of 2–5 medium-sized teeth, followed by several smaller teeth (Fig. 12C–E). Abdomen with 25–35 uncinigers (Fig. 12F) with type 1 uncini (Figs 12G, 28A).

Nucleotide diagnostic features. All sequences of *T. kongsrudi* sp. nov. share the unique apomorphic nucleotides in positions 300 (G) and 624 (G) of our alignement.

Type locality. Skagerrak; 429–445 m deep (Fig. 8C; Suppl. material 1: Table S1).

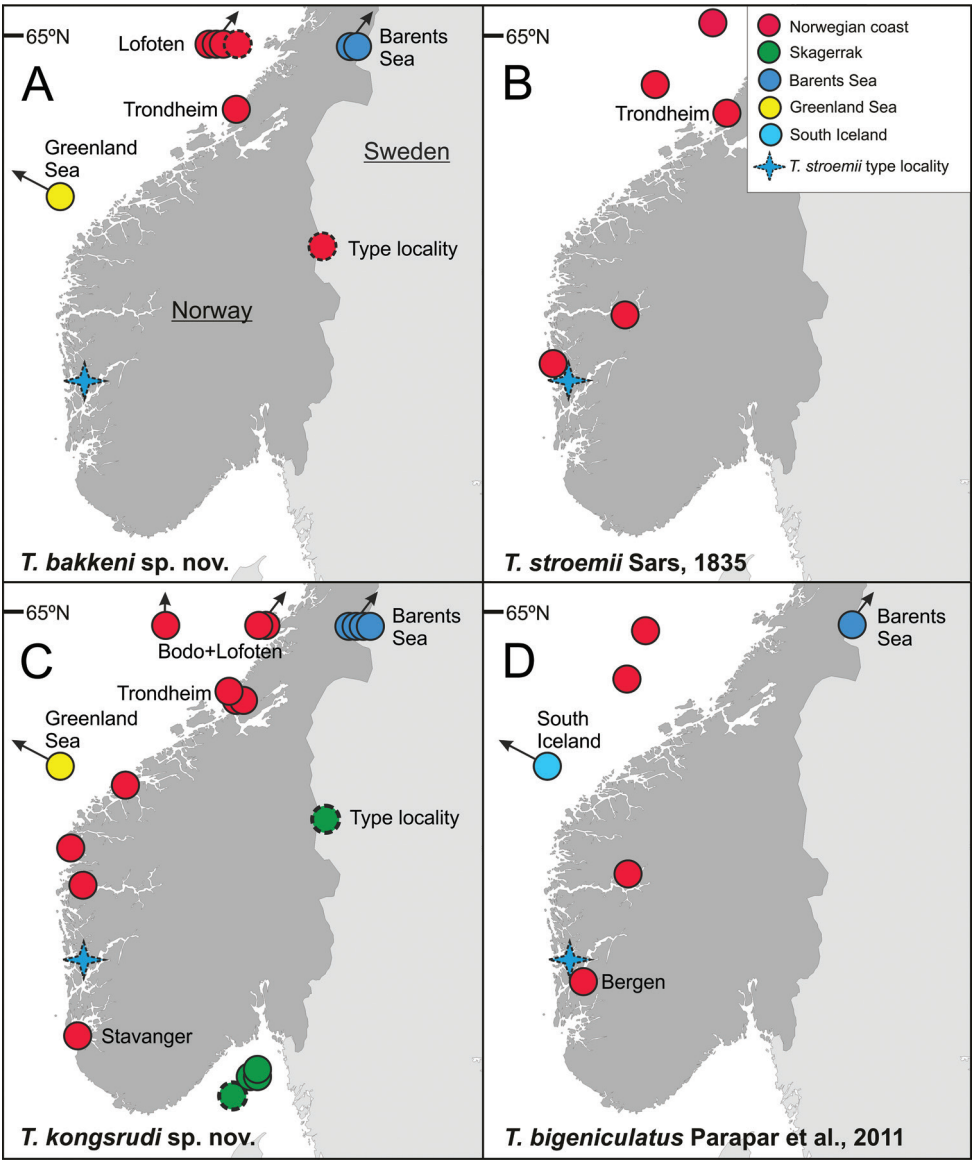

Figure 8. Geographic distribution of **A** *T. bakkeni* sp. nov. **B** *T. stroemii* Sars, 1835 **C** *T. kongsrudi* sp. nov. **D** *T. bigeniculatus* Parapar, Moreira & Helgason, 2011.

Distribution and bathymetry. Barents Sea, Greenland Sea, along the Norwegian coast and shelf, reaching the Skagerrak to the South; 108–534 m deep (Nygren et al. 2018) (Figs 8C, 9; Suppl. material 1: Table S1).

Etymology. This species is named after Dr. Jon Anders Kongsrud, Department of Natural History, Zoological Museum Bergen–ZMB (Norway), housing institution of some of the specimens used in the present study, for his dedication to the study of Norwegian polychaetes and his friendship.

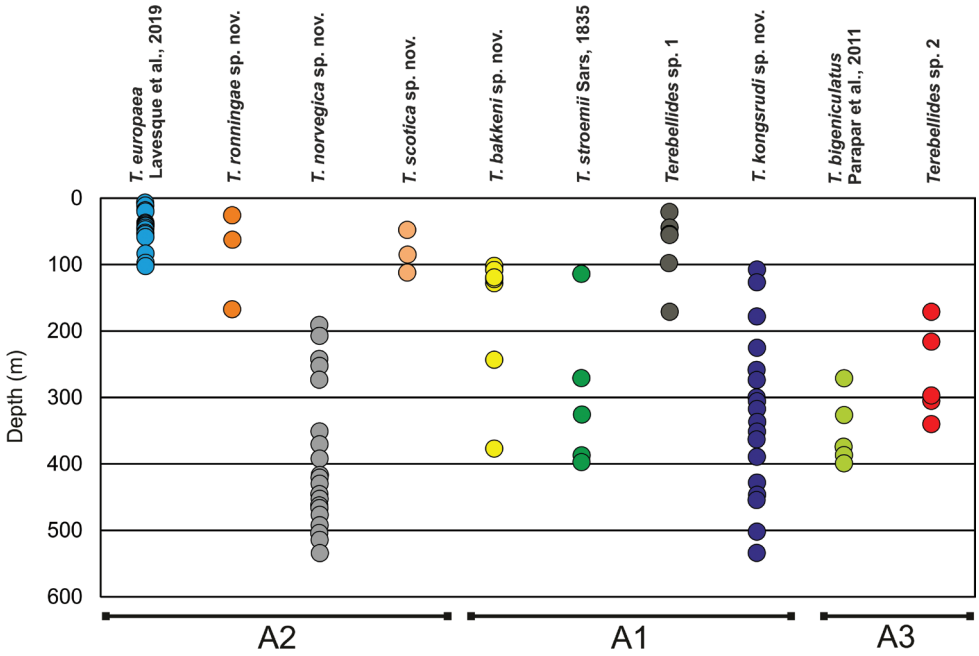

Figure 9. Bathymetric distribution of *Terebellides* species studied in this work. Subgroups (A1–3) within group A sensu Nygren et al. (2018) are indicated.

Remarks. This is a large species reaching up to 50.0 mm long, and is characterised by the presence of ciliated papilla dorsal to thoracic notopodia, lack of papillae on the margins of branchial lamellae, thoracic uncini of type 3 and abdominal uncini of type 1. These features are also shared by species 12 (sensu Nygren et al. 2018), which will be described elsewhere (Gaeva and Jirkov, pers. comm.). *Terebellides kongsrudi* sp. nov. is also morphologically similar to *T. bakkeni* sp. nov. (see above) but *T. kongsrudi* sp. nov. and species 12 show a wider geographic distribution; on the contrary, species 12 is present at shallower depths (<200 m) while *T. kongsrudi* sp. nov. extends to deeper depths (>500 m).

Finally, in the 26 sequences belonging to this species (see Suppl. material 2: Table S2), there were fourteen haplotypes showing 0–1.9% of intraspecific divergence, and a minimum of 8.2% uncorrected genetic distance with members of species 12 which is the closest relative (sensu Nygren et al. 2018).

Terebellides sp. 1

Figs 1, 2, 9, 13; Table 1; Suppl. material 1: Table S1; Suppl. material 2: Table S2

Species 12 – Nygren et al. 2018: 18–22, figs 5, 6, 10.

Material examined. 4 specimens. **Skagerrak**. GNM 14630-4; GNM 14630-8.

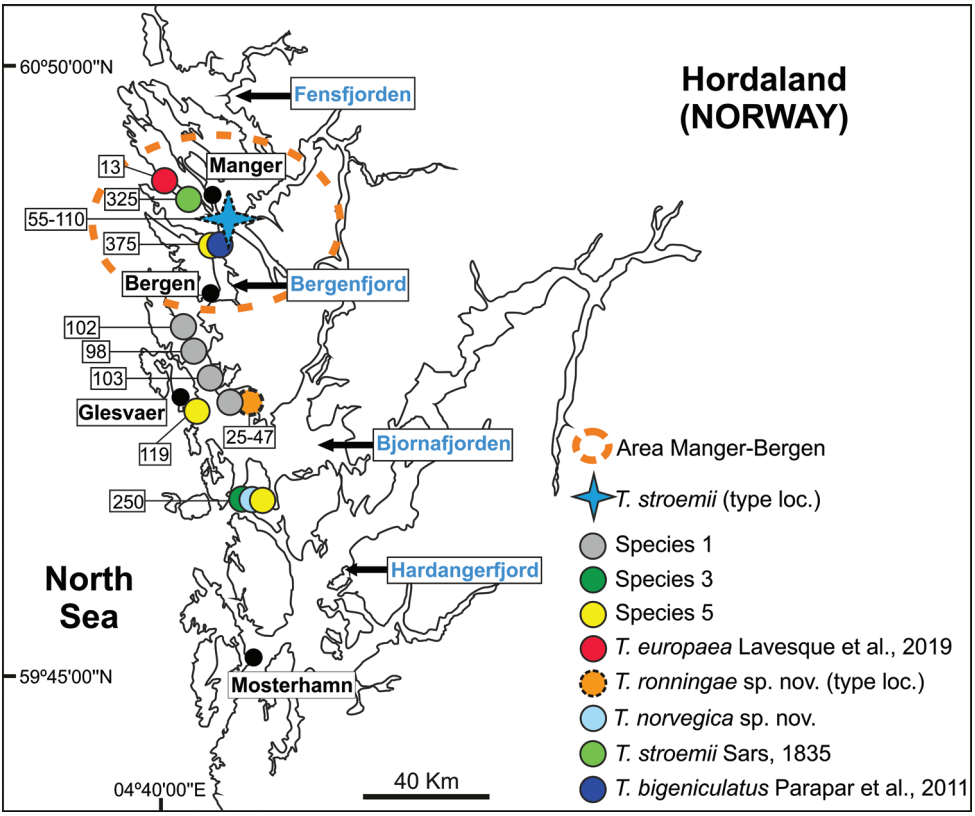

Figure 10. Map of Hordaland area (SW Norway) showing collecting sites of *Terebellides* species as found in Nygren et al. (2018) near type locality of *T. stroemii* Sars, 1835. Depth ranges shown in boxes.

Remarks. This species will be described elsewhere by D. Gaeva and I. Jirkov (pers. comm.). In order to confirm characters here used to link species within each subgroup, two specimens were examined under the SEM that share with subgroup A1 the following features: branchiae type 1 sensu Parapar et al. (2016c) (Fig. 13A), lack of papillae on border of branchial lamellae (Fig. 13B), geniculate chaetae on TC6, ciliated papilla dorsal to thoracic notopodia (Fig. 13C, D), and thoracic uncini of type 3 (Fig. 13E). Nevertheless, abdominal uncini are of type 2 (Fig. 13F), as it occurs in *T. stroemii* and differently to *T. bakkeni* sp. nov. and *T. kongsrudi* sp. nov., that are the most similar species within subgroup A1 (Table 1).

Subgroup A2

Molecular analyses of mitochondrial and nuclear markers recovered a strongly supported subgroup A2 (Fig. 1). This subgroup is composed by species 6, 7, 8, and 9 (sensu Nygren et al. 2018). Analyses of the COI dataset alone also find support for this clade, and incorporate the recently described *T. lilasae* Lavesque, Hutchings,

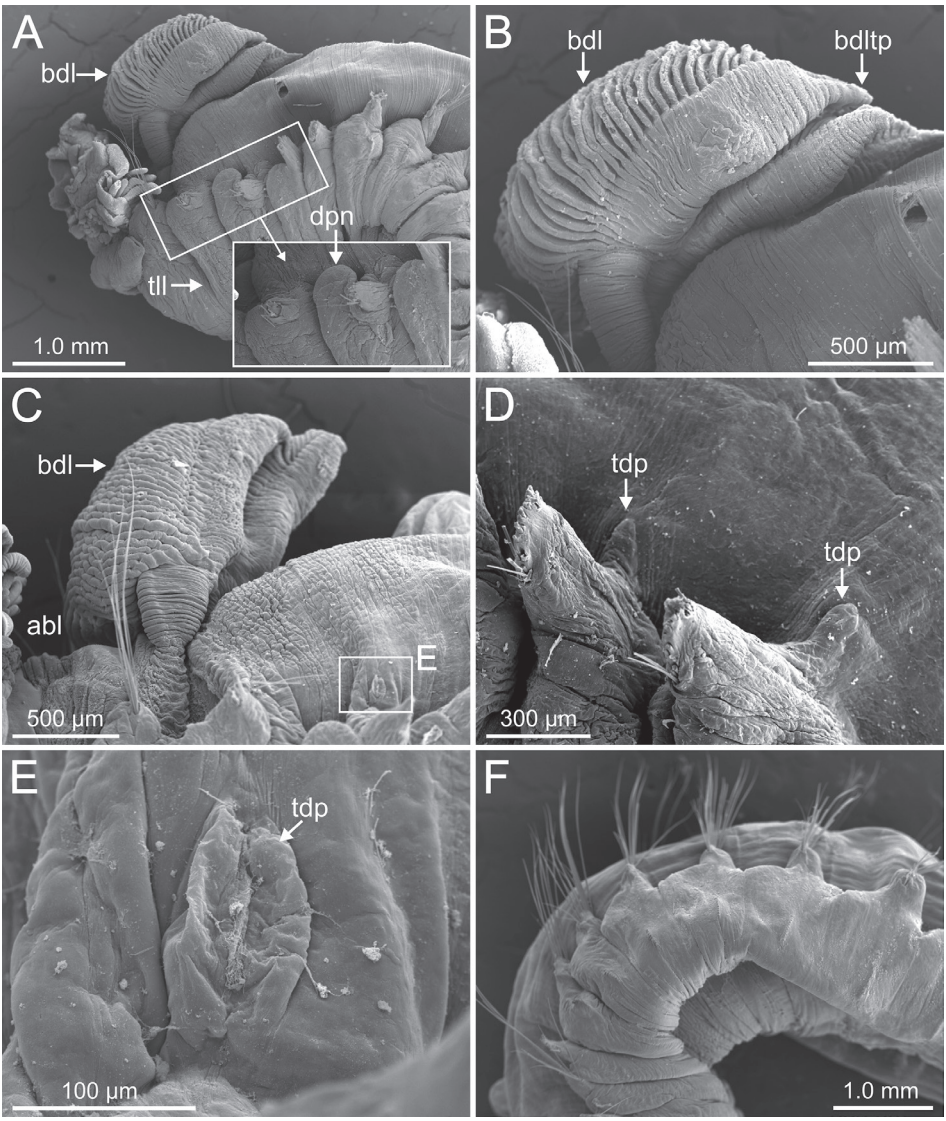

Figure 11. *Terebellides kongsrudi* sp. nov. (species 13; paratypes, ZMBN 116409 and ZMBN 116411), SEM micrographs. **A** anterior end, left lateral view **B** branchiae, left side **C** anterior end, left lateral view **D** TC1 and TC2, thoracic dorsal papillae **E** TC3, thoracic dorsal papilla (framed in **C**) **F** several thoracic chaetigers, left lateral view. Abbreviations: abl – anterior branchial lobe; bdl – branchial dorsal lobe; bdltp – branchial dorsal lobe terminal papilla; dpn – dorsal projection of notopodium; tdp – thoracic dorsal papilla; tll – thoracic lateral lobes.

Daffe, Nygren & Londoño-Mesa, 2019 (Fig. 2). There are several morphological features that are shared, and exclusive to, all members of subgroup A2, and includes other NEA species (see below). Three (7, 8, 9) of these four species are described herein as new to science and the fourth species (6) corresponds to *T. europaea*.

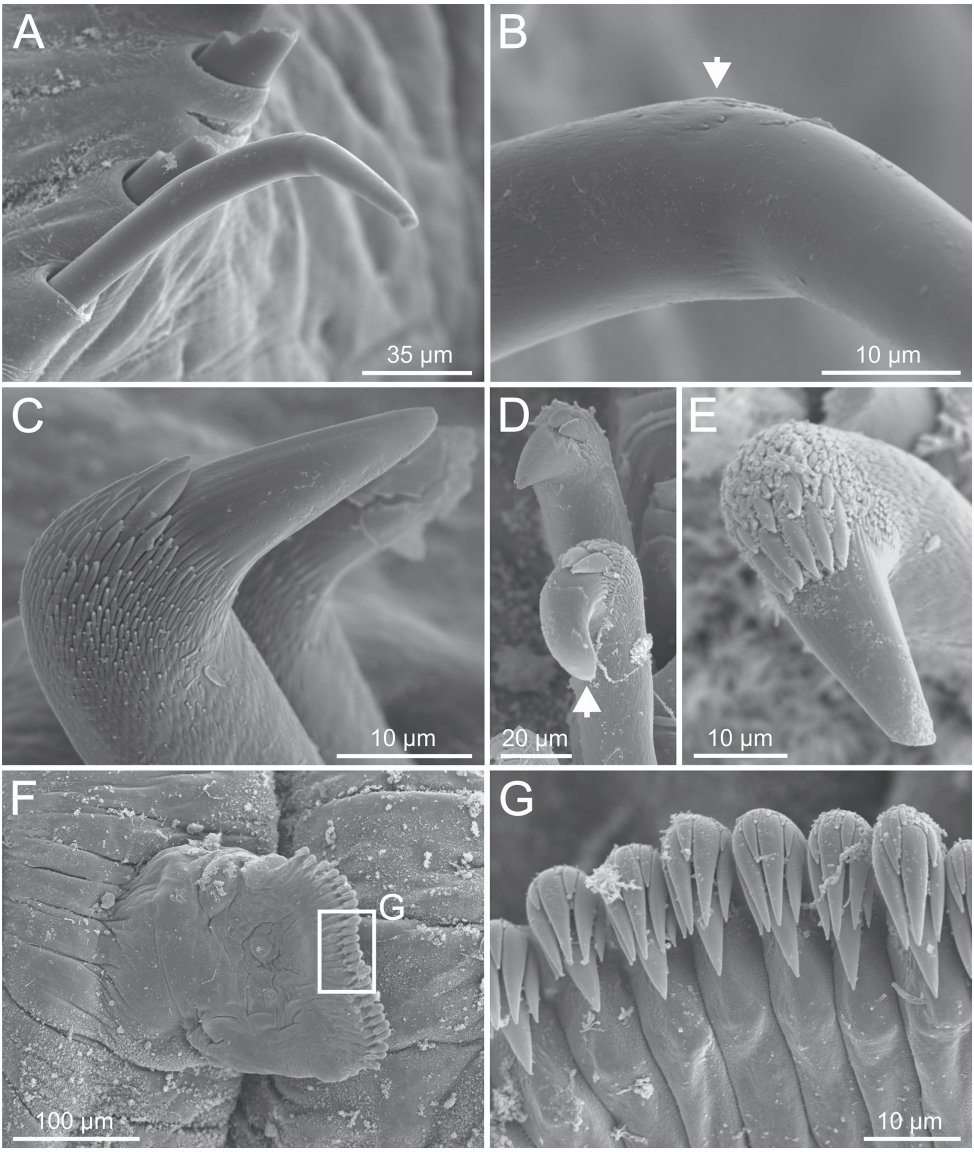

Figure 12. *Terebellides kongsrudi* sp. nov. (species 13; paratype, ZMBN 116409), SEM micrographs. **A** TC6 (TU1) geniculate chaeta **B** detail of geniculate chaeta (arrow pointing to capitium) **C–E** thoracic uncini, lateral and frontal views (arrow in **D** pointing to rostrum curved at distal end) **F** abdominal unciniger **G** abdominal uncini, frontal view (framed in **F**).

Character/s present only in Group A2

- Border of anterior region of dorsal branchial lamellae provided with papillary projections (Figs 15C, 20C, 22C).
- Ciliated papilla dorsal to thoracic notopodia not present.

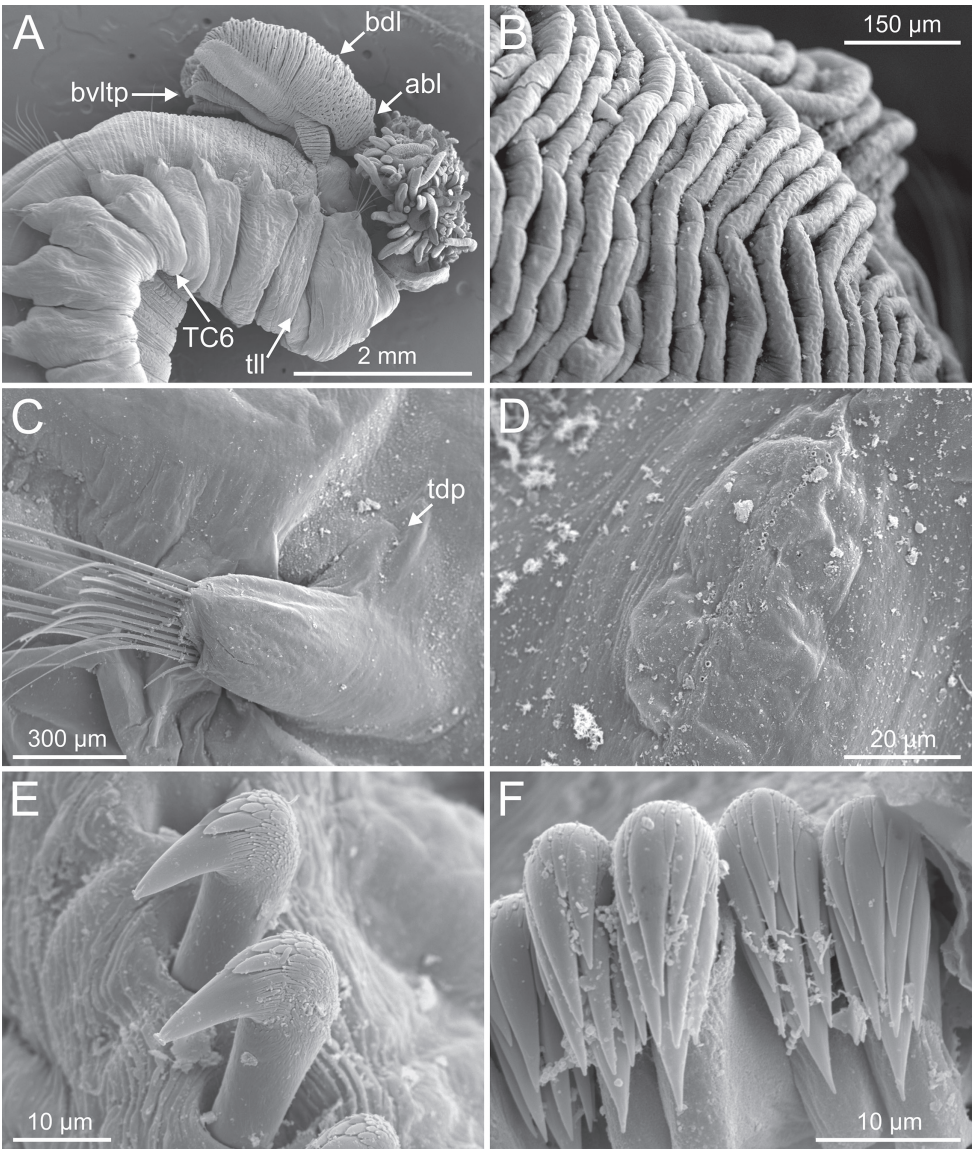

Figure 13. *Terebellides* sp. 1 (species 12; GNM 14630-4 and GNM 14640-8), SEM micrographs. **A** anterior end, right lateral view **B** detail of anterior branchial lamellae **C** TC16 **D** notopodial papilla **E** thoracic uncini **F** abdominal uncini. Abbreviations: abl – anterior branchial lobe; bdl – branchial dorsal lobe; bvltp – branchial ventral lobe terminal papilla; TC – thoracic chaetiger; tdp – thoracic dorsal papilla; tll – thoracic lateral lobes.

- Abdominal uncini type 2 (Figs 16E, 21F, 23E, 25F).

Character/s shared with subgroup A1

- Branchiae of type 1 (*stroemii*-type, comma-shaped), all four lobes fused for approximately half of their length and ventral ones usually obscured by dorsal ones (Fig. 20A).

- First thoracic neuropodia on TC6, with chaetiger provided with several sharply bent, acute-tipped geniculate chaetae (Figs 15A, 16B).

Character/s shared with subgroup A3

None (Table 1).

Character/s variable within subgroup A2

- Thoracic uncini type 1 and 3 (Figs 21E, 16D).

Several species described by Lavesque et al. (2019) have a similar body and branchiae appearance to those of subgroup A2 species; however, only four species bear papillae on the anterior border of branchial lamellae: *Terebellides bonifi* Lavesque, Hutchings, Daffe, Nygren & Londoño-Mesa, 2019, *T. europaea*, *T. gentili* Lavesque, Hutchings, Daffe, Nygren & Londoño-Mesa, 2019 and *T. lilasae*. Molecular sequences were available for all except *T. gentili*, with *T. europaea* being the only species found among the material sequenced and analysed by Nygren et al. (2018), as species 6, and initially misidentified as *T. stroemii*.

Terebellides gentili does not fit morphologically within any clade defined here because of having numerous marginal branchial lamellae that reach the posterior end of dorsal lobes, the dorsal lobes are longer and reach TC5(TC6) instead of TC3(TC4), and TC3 has a distinct whitish glandular region with a well-defined central white line. On the contrary, *T. lilasae* was found within subgroup A2 according to molecular-based analyses (Fig. 2); this species also fits well morphologically in A2 by having similar branchiae (shape), papillae on branchial lamellae, thoracic uncini of type 3 and abdominal uncini of type 2, only differing in having comparatively larger branchiae. The original description does, however, not mention whether notopodial papillae are present or not. This species was described from the French Mediterranean and Atlantic waters and is not present in northern latitudes, as suggested by Lavesque et al. (2019) and confirmed here. On the other hand, *T. bonifi* bears similar branchiae (shape, size, papillae) and thoracic uncini of type 3 (Lavesque et al. 2019: 159, fig. 4A–C) to those of A2; however, it bears abdominal uncini of type 1 instead of type 2.

***Terebellides europaea* Lavesque, Hutchings, Daffe, Nygren & Londoño-Mesa, 2019**
Figs 1, 2, 3E, 9–10, 14A, 15, 16, 17C, 18A, 19A; Table 1; Suppl. material 1: Table S1; Suppl. material 2: Table S2

Terebellides europaea Lavesque et al. 2019: 163–165, figs 1, 7, 8.
Species 6 – *T. stroemii* (*non* Sars, 1835). Nygren et al. 2018: 18–22, figs 6, 10.

Material examined. 31 specimens: Norwegian coast and shelf (GNM14625, GNM14628, GNM15107, GNM15114, GNM15115, GNM15116, GNM15120,

Figure 14. STM photographs of live specimens of several *Terebellides* species in lateral view. **A** *Terebellides europaea* Lavesque, Hutchings, Daffe, Nygren & Londoño-Mesa, 2019 (ZMBN 116343) **B** *Terebellides ronningae* sp. nov. (ZMBN 116349) **C, D** *Terebellides norvegica* sp. nov. (GNM 15131 and GNM 15130 respectively). Abbreviations: babv – branchial afferent blood vessel; bbv – branchial blood vessel; bdl – branchial dorsal lobe; bst – branchial stem; bvl – branchial ventral lobes; cbh – contractile branchial heart; dg – digestive gland; fi – fore intestine; fs – fore stomach; hs – hind stomach; loli – lower lip; oes – oesophagus; ooc – oocytes; tm – tentacular membrane.

GNM15121, GNM15122, GNM15123, GNM15124, GNM15125, GNM15126, GNM15127, GNM15128, ZMBN116334, ZMBN116335, ZMBN116343, ZMBN116344, ZMBN116346, ZMBN116347); Irish Sea (ZMBN116336,

ZMBN116337, ZMBN116338, ZMBN116339, ZMBN116340, ZMBN116341, ZMBN116342).

GenBank accession numbers of material examined (COI). MG025072, MG025073, MG025074, MG025075, MG025076, MG025077, MG025078, MG025079, MG025080, MG025081, MG025082, MG025083, MG025084, MG025085, MG025086, MG025087, MG025088, MG025089, MG025090, MG025091, MG025092, MG025093, MG025094, MG025095, MG025096, MG025097, MG025098, MG025099, MG025100, MG025101, MG025102, MG025103, MG025104. Paratypes (not examined): MN207179, MN207181. Additional sequences (material not examined): MN207180, MN207182.

Diagnostic features of type material. Complete individuals ranging from 17.0–46.0 mm in length and 2.0–5.0 mm in width (Fig. 17C). Branchial dorsal lobes lamellae provided with well-developed anterior papillary projections (Fig. 15C). Ventral branchial lobes normally hidden by dorsal ones (Figs 3E, 15B, 19A) but sometimes discernible below (Fig. 14A). Lateral lappets and dorsal projection on thorax present on TC1–TC4 (Fig. 16A) or TC2–TC3 in (Fig. 15A). Geniculate chaetae acutely bent (Fig. 16B). Ciliated papilla dorsal to thoracic notopodia not observed (Figs 15A, 16A). Thoracic uncini in one or two rows (Fig. 16C) with rostrum/capitium length ratio for approximately 2 : 1 (Fig. 16D), and capitium with a first row of four medium-sized teeth, followed by several smaller teeth. Abdomen with 29–38 uncinigers provided with type 2 uncini (Fig. 16E). Epibiont ciliates observed in some specimens (Fig. 16F).

Nucleotide diagnostic features. All sequences belonging to *T. europaea* share the unique apomorphic nucleotide in position 240 (C) of the alignement.

Type locality. Bay of Brest (Brittany, France) (Lavesque et al. 2019).

Distribution and bathymetry. Bay of Biscay (Lavesque et al. 2019); Kattegat, Skagerrak, North Sea, Irish Sea, Celtic Sea and Norwegian coast and shelf, 8–173 m deep (Nygren et al. 2018) (Figs 9, 10, 18A; Suppl. material 1: Table S1). Lavesque et al. (2019) included the Ría de Ferrol (Galicia, NW Spain) as part of the Bay of Biscay, but this locality belongs to the northern Galician Rias that are out of the western limit of this bay.

Remarks. This species is characterised by the combination of the following features: presence of papillary projections over the edge of the anterior border of dorsal branchial lamellae, lack of ciliated papilla dorsal to thoracic notopodia, thoracic uncini of type 3 and abdominal uncini of type 2. The original description states that body length is less than 17 mm, but maximal length of specimens examined here was up to 46.0 mm. Examination of live and preserved specimens has revealed that the size ratio between the ventral and dorsal branchial lobes is similar in all specimens; however, their arrangement differs among specimens, i.e., the ventral lobes are visible in some while in others are hidden behind the dorsal lobes.

Terebellides europaea was misidentified as *T. stroemii* by Nygren et al. (2018; species 6) due to their morphological similarities and coexistence near the type locality of the latter (Fig. 9). Nevertheless, Lavesque et al. (2019) found that members of species 6 have papillae on the edge of the dorsal branchial lobes, unlike the neotypes of *T. stroemii* described by Parapar and Hutchings (2014). Molecular analyses show that

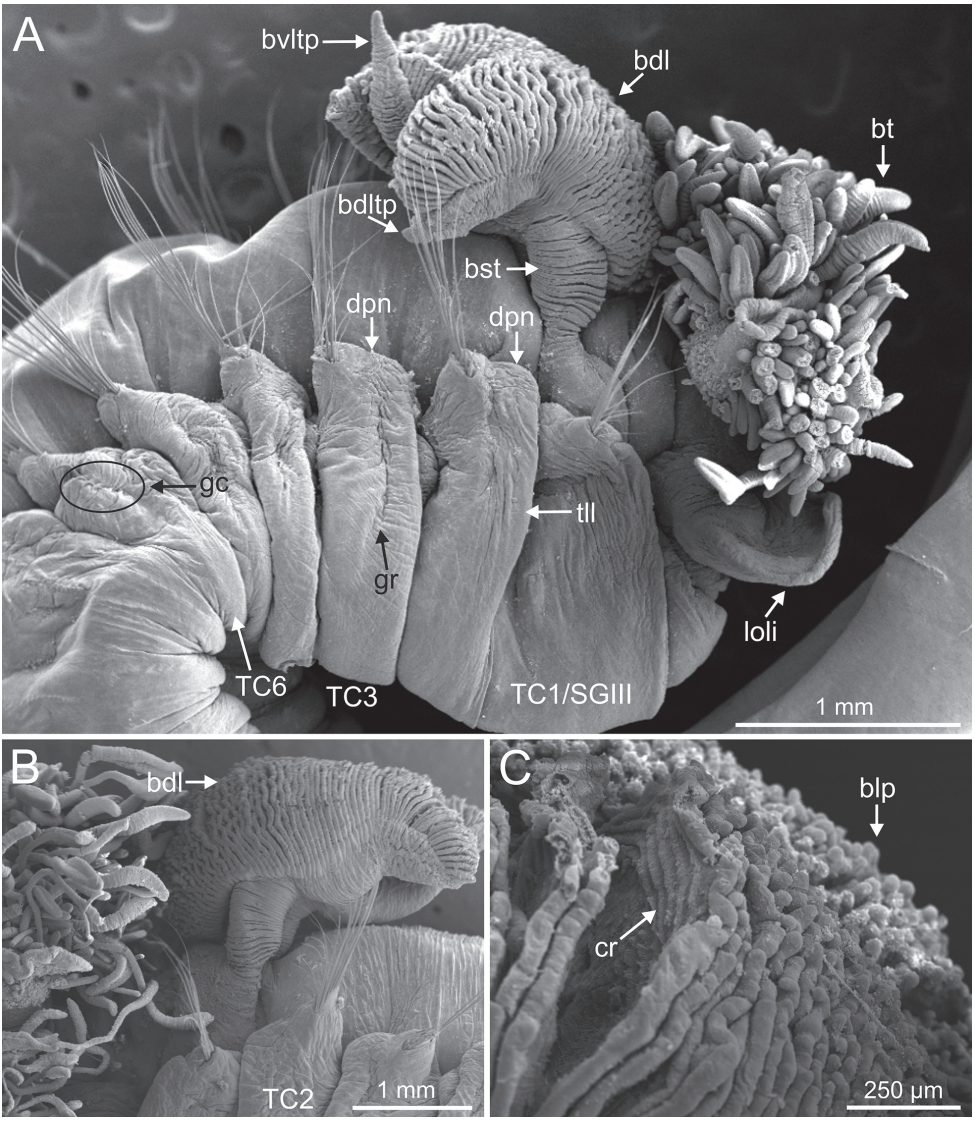

Figure 15. *Terebellides europaea* Lavesque, Hutchings, Daffe, Nygren & Londoño-Mesa, 2019 (species 6; non-type specimens, GNM15116 and GNM15118), SEM micrographs. **A** anterior end, right lateral view **B** buccal tentacles and branchiae, left lateral view **C** branchial lamellae, detail. Abbreviations: bdl – branchial dorsal lobe; bdltp – branchial dorsal lobe terminal papilla; blp – branchial lamellae papillae; bst – branchial stem; bt – buccal tentacles; bvltp – branchial terminal lobe terminal papilla; cr – ciliary row; dpn – dorsal projection of notopodium; gc – geniculate chaetae; gr – glandular region; loli – lower lip; SG – segment; TC – thoracic chaetiger; tll – thoracic lateral lobes.

the sequences of specimens found in the Bay of Biscay belong to species 6 (Lavesque et al. 2019); examination of all specimens also confirmed the presence of the aforementioned papillae. Moreover, *T. europaea* is generally found in bottoms above 100 m deep while *T. stroemii* is present in deeper environments (>100 m) (Fig. 9).

In the 37 sequences analysed attributed to this species (see Suppl. material 2: Table S2), there were ten haplotypes showing 0–0.8% of intraspecific divergence, and a minimum of 8.8% uncorrected genetic distance with members of the closest relative, *T. ronningae* sp. nov.

***Terebellides ronningae* sp. nov.**
http://zoobank.org/7A447FDE-5934-483F-95F3-D178A0857A4A
Figs 1, 2, 3F, 9, 10, 14B, 17D, 18B, 19B, 20, 21, 28C; Table 1; Suppl. material 1: Table S1; Suppl. material 2: Table S2

Species 7 – Nygren et al. 2018: 18–22, figs 5, 6, 10, Suppl. material 1: Table S1.

Material examined. Type material. ***Holotype***: ZMBN116357. ***Paratypes*** (8 specs): Norwegian coast (ZMBN 116350, ZMBN 116352, ZMBN 116353, ZMBN 116354, ZMBN 116355, ZMBN 116356, ZMBN 116358, ZMBN 116359); Skagerrak (ZMBN 116348, ZMBN 116349).

Holotype. Complete specimen, 19.0 mm long and 2.0 mm width (Figs 3F, 19B).

GenBank accession numbers of material examined (COI). ***Holotype***: MG025114; ***Paratypes***: MG025105, MG025106, MG025107, MG025109, MG025110, MG025111, MG025112, MG025113, MG025115, MG025116. ***Additional material***: MG025108,

Diagnostic features of type material. Complete individuals ranging from 12.0–35.0 mm in length and 1.5–3.0 mm in width (Fig. 17D). Branchial dorsal lobes lamellae with poorly-developed anterior papillary projections (Fig. 20C). Ventral branchial lobes hidden (Fig. 20A) or not (Figs 3F, 19B) by dorsal ones. Lateral lappets and dorsal projection ill-defined, only slightly developed on TC2 (Fig. 20A). Geniculate chaetae acutely bent (Fig. 21A, B) and with very low capitium. Ciliated papilla dorsal to thoracic notopodia not observed. Thoracic uncini in one row with rostrum/capitium length ratio of approximately 2 : 1, and capitium with a first row of four or five (sometimes six) large-sized teeth, followed by several progressively smaller teeth (Fig. 21C–E). Abdomen with 24–35 uncinigers with type 2 uncini (Figs 21F, 28C).

Nucleotide diagnostic features. All sequences of *T. ronningae* sp. nov. share the unique apomorphic nucleotides in positions 129 (G), 399 (G) and 435 (G).

Type locality. Hordaland, Lysefjord (Norway); 25–47 m deep (Figs 10, 18B).

Distribution and bathymetry. Norwegian coast and shelf, Skagerrak; 25–188 m deep (Nygren et al. 2018) (Figs 9, 18B; Suppl. material 1: Table S1).

Etymology. This species is named after Dr. Ann-Helén Rønning, Head Engineer of the Department of Technical and Scientific Conservation, Natural History Museum–NHMO (Oslo), for her help and friendship.

Remarks. *Terebellides ronningae* sp. nov. is characterised by the lack of ciliated papilla dorsal to thoracic notopodia and the presence of papillary projections pointing over the edge of the dorsal anterior border of branchial lamellae, thoracic uncini of

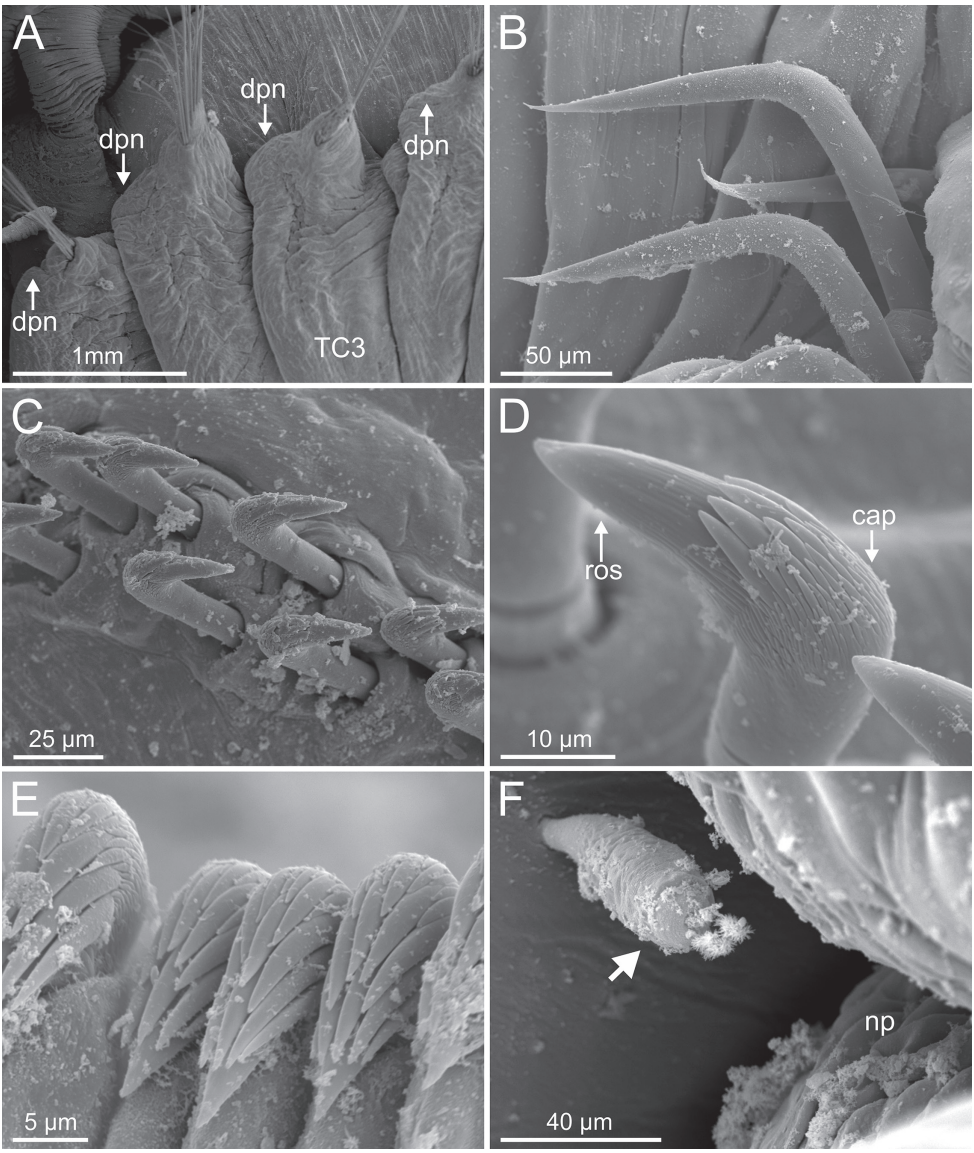

Figure 16. SEM images, *Terebellides europaea* Lavesque, Hutchings, Daffe, Nygren & Londoño-Mesa, 2019 (species 6; non-type specimen, GNM15116). **A** TC1 to TC4, lateral view **B** TC6 (TU1), geniculate chaetae **C** thoracic double row of uncini **D** thoracic uncinus, capitium, upper view **E** abdominal uncini **F** epibiont ciliate (position pointed by arrowhead) attached near TC5 nephridial papilla. Abbreviations: cap – capitium; dpn – dorsal projection of notopodium; ros – rostrum; TC – thoracic chaetiger.

type 1 and abdominal of type 2 (Table 1). It is distinguished from the closest relatives of subgroup A2 by the presence of thoracic uncini type 1 instead of type 3 (Table 1).

Specimens examined with SEM bear thoracic uncini with rostrum bendings (Fig. 21C) similar to those of other NEA species (see Discussion for *T. stroemii*). The branchial ventral lobes show variability in their arrangement that is similar to that of *T. europaea*.

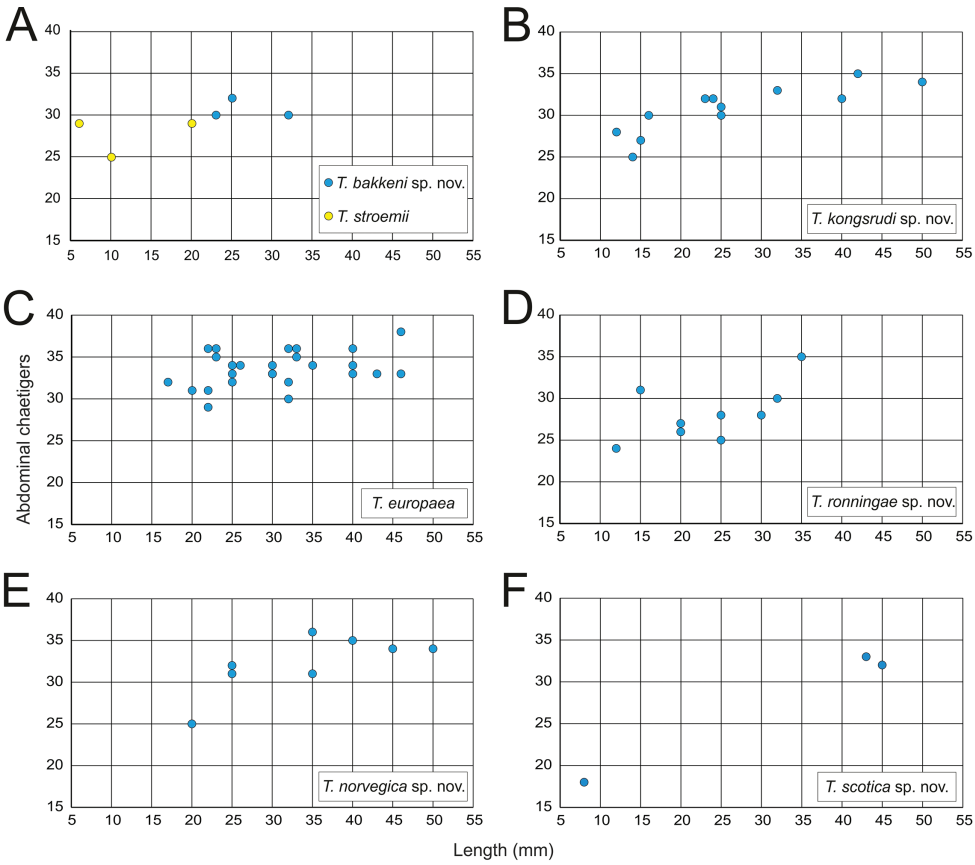

Figure 17. Relationship between number of abdominal chaetigers and body length (complete specimens) for *Terebellides* species described in this work.

Twelve sequences (see Suppl. material 2: Table S2), in ten haplotypes, have been attributed to this species (Nygren et al. 2018). They show 0–0.6% intraspecific divergence, and a minimum of 8.8% uncorrected genetic distance, its closest relative being *T. europaea* (Fig. 2).

***Terebellides norvegica* sp. nov.**
http://zoobank.org/659C513E-01DD-43A0-AC29-D1A744EDA9B0
Figs 1, 2, 3G, 9, 10, 14C–D, 17E, 18C, 19C, 22, 23; Table 1; Suppl. material 1: Table S1; Suppl. material 2: Table S2

Species 8 – Nygren et al. 2018: 18–22, figs 5, 6, 10, Suppl. material 1: Table S1.

Material examined. Type material. ***Holotype***: ZMBN116378. ***Paratypes*** (36 specs): Barents Sea (ZMBN11636, ZMBN116365, ZMBN116366, ZMBN116367); Norwegian coast (GNM146323, NTNU-VM61388, NTNU-VM61389, NTNU-

VM61390, NTNU-VM66569, NTNU-VM66573, NTNU-VM66574, NTNU-VM68197, NTNU-VM68198, ZMBN116362, ZMBN116363, ZMBN116368, ZMBN116369, ZMBN116370, ZMBN116371, ZMBN116372, ZMBN116373, ZMBN116374, ZMBN116375, ZMBN116376, ZMBN116377, ZMBN116379, ZMBN116380, ZMBN116381, ZMBN116382, ZMBN116383, ZMBN116384); Skagerrak (GNM14637, GNM15131, GNM15232, GNM15134, ZMBN116361).

Holotype. Complete specimen, 19.0 mm long and 1.5 mm wide (Figs 3G, 19C); female with oocytes in body cavity.

GenBank accession numbers of material examined (COI). Holotype: MG025148. Paratypes: MG025119, MG025120, MG025122, MG025124, MG025126, MG025127, MG025128, MG025129, MG025131, MG025132, MG025134, MG025135, MG025136, MG025137, MG025138, MG025139, MG025140, MG025141, MG025142, MG025143, MG025144, MG025145, MG025146, MG025147, MG025149, MG025151, MG025152, MG025153, MG025154, MG025155, MG025156. Additional material: MG025117, MG025118, MG025121, MG025123, MG025125, MG025130, MG025133, MG025150.

Diagnostic features of type material. Complete individuals ranging from 20.0–50.0 mm in length and 1.2–5.0 mm in width (Fig. 17E). Branchial dorsal lobes lamellae with well-developed anterior papillary projections (Fig. 22C). Ventral branchial lobes hidden (Figs 19C, 22A, B) or not (Fig. 3G) by dorsal ones. Lateral lappets and dorsal projection low marked, only partially present on TC2 (Fig. 22A, D). Geniculate chaetae acutely bent, with poorly marked capitium (Fig. 23A, B). Ciliated papilla dorsal to thoracic notopodia not observed. Thoracic uncini in one row (Fig. 23C) with rostrum/capitium length ratio of approximately 2 : 1 and capitium with a first row of two or three medium-sized teeth, followed by several progressively smaller teeth (Fig. 23D). Abdomen with 29–38 chaetigers with type 2 uncini (Fig. 23E). Epibiont ciliates observed in some specimens (Fig. 23F).

Nucleotide diagnostic features. All sequences of *T. norvegica* sp. nov. share the unique apomorphic nucleotides in positions 48 (C) and 285 (G) of the alignement.

Type locality. Rogaland (Norway); at depths of between 226 and 242 m (Fig. 18C).

Distribution and bathymetry. Barents Sea, Norwegian coast, Skagerrak; 190–1,268 m deep (Nygren et al. 2018) (Figs 9, 18C; Suppl. material 1: Table S1).

Etymology. The name of the new species refers to the country where members of this lineage were found, along the Norwegian coast from the Barents Sea to the Skagerrak Strait.

Remarks. *Terebellides norvegica* sp. nov. is characterised by the presence of marginal papillae in the anterior region of branchial dorsal lamellae, thoracic uncini of type 3 and abdominal uncini of type 2, and by lacking ciliated papilla dorsal to thoracic notopodia (Table 1). These features are shared with species of subgroup A2: *T. europaea*, *T. ronningae* sp. nov. and *T. scotica* sp. nov. (Table 1), apart from the thoracic uncini type that is different in *T. ronningae* sp. nov. Furthermore, *T. norvegica* sp. nov., *T. europaea* and *T. scotica* sp. nov. also show the same variability in whether ventral branchial lobes are hidden or not by dorsal lobes. Therefore, it seems that members of these three species can only be distinguished according to

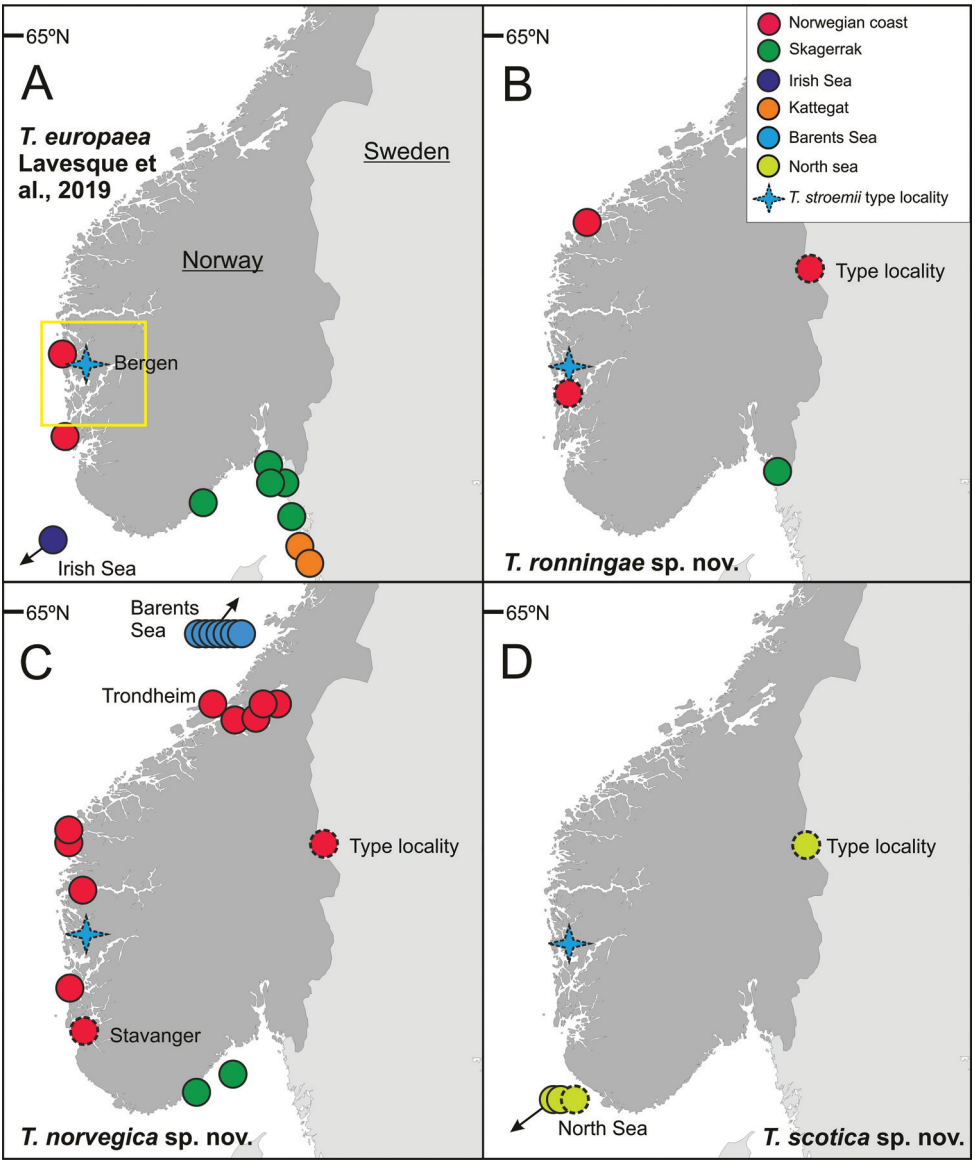

Figure 18. Geographic distribution of **A** *T. europaea* Lavesque et al., 2019, **B** *T. ronningae* sp. nov., **C** *T. norvegica* sp. nov., **D** *T. scotica* sp. nov. Yellow frame showing Hordaland (Fig. 10).

the DNA sequences. However, they show little overlapping in their geographic distribution and bathymetric ranges (Figs 9, 18A, C, D). *Terebellides norvegica* sp. nov. inhabits deep-water habitats (mostly below 200 m) along the Norwegian coast; its distribution only overlaps with that of *T. europaea* in southern waters (Skagerrak). As stated before, *T. europaea* has a broader distribution reaching to the South NW Iberian Peninsula and is generally found in shallower habitats (<100 m) similarly

to *T. scotica* sp. nov. Ciliate epibionts attached over dorsal body surface were also observed (Fig. 23F).

On the other hand, the internal anatomy of *T. norvegica* sp. nov. has been examined by transparency in one alive specimen (Fig. 14D). The digestive tract is divided in an oesophagus clearly distinguishable between TC1 and TC3, that is followed by the stomach and the associated digestive gland (TC4–TC7) and then by the intestine (from TC11). Regarding the circulatory system, a double dorsal blood vessel is present in anterior body end from which arise four afferent vessels at the level of branchial stem and into the branchiae; the coelomic cavity bears oocytes from TC11. All these internal features agree with those described by Jouin-Toulmond and Hourdez (2006) and Parapar and Hutchings (2014) for other species of the genus.

Forty sequences (see Suppl. material 2: Table S2), in 33 haplotypes, have been attributed to this species (Nygren et al. 2018). They show 0–3.1% intraspecific divergence, larger than in other *Terebellides* species, and a minimum of 10.5% uncorrected genetic distance, with its closest relative being *T. scotica* sp. nov. (Fig. 1).

***Terebellides scotica* sp. nov.**

http://zoobank.org/74511F62-C57D-4BF7-8B63-48997EB1C8E9

Figs 1, 2, 3H, 9, 17F, 18D, 19D, 24, 25; Table 1; Suppl. material 1: Table S1; Suppl. material 2: Table S2

Species 9 – Nygren et al. 2018: 18–22, figs 5, 6, 10, Suppl. material 1: Table S1.

Material examined. Type material. ***Holotype***: ZMBN116385. ***Paratypes*** (3 specs), North Sea (ZMBN 116382, ZMBN 116386, ZMBN 116387).

Holotype. Complete specimen, 45.0 mm long and 4.5 mm width (Fig. 3H, 19D).

Additional material. SMA_BR_23 (GenBank number: MN207187) and SMA_BR_33 (GenBank number: MN207188) of *Terebellides* sp. in Lavesque et al. (2019) (Suppl. material 1: Table S1).

GenBank accession numbers of material examined (COI). ***Holotype***: MG025157. ***Paratype***: MG025158.

Diagnostic features of type material. Complete individuals ranging from 6.0–45.0 mm in length and 1.0–4.0 mm in width (Figs 9, 17F). Branchial dorsal lobes lamellae provided with low anterior papillary projections (Fig. 24B). Ventral branchial lobes hidden (Fig. 24A) or not (Figs 3H, 19D) by dorsal ones. Lateral lappets and dorsal projection low marked being only discernible on TC1–3 (Fig. 24A). Geniculate chaetae acutely bent and provided with hardly distinguishable capitium (Fig. 25A, B). Ciliated papilla dorsal to thoracic notopodia not observed. Thoracic uncini in one or two rows (Fig. 25C) with rostrum/capitium length ratio of approximately 2 : 1, and capitium with a first row of 2–4 medium-sized teeth, followed by several progressively smaller teeth (Fig. 25D, E). Abdomen with 18–33 uncinigers provided with type 2 uncini (Fig. 25F).

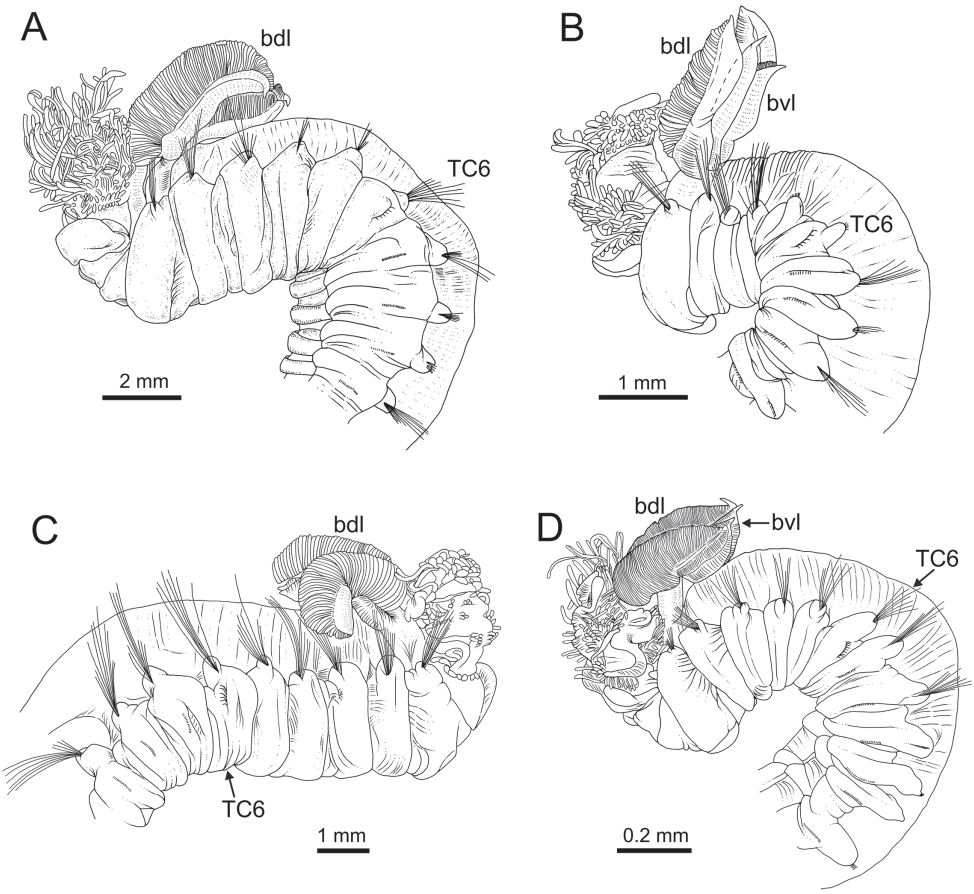

Figure 19. Line drawings of several *Terebellides* species. **A** *Terebellides europaea* Lavesque, Hutchings, Daffe, Nygren & Londoño-Mesa, 2019 (species 6; non-type specimen, GNM14628), anterior end, left lateral view **B** *Terebellides ronningae* sp. nov. (species 7; holotype, ZMBN116357), anterior end, left lateral view **C** *Terebellides norvegica* sp. nov. (species 8; holotype, ZMBN416378), anterior end, right lateral view **D** *Terebellides scotica* sp. nov. (species 9; holotype, ZMBN116385), anterior end, left lateral view. Abbreviations: bdl – branchial dorsal lobe; bvl – branchial ventral lobe; TC – thoracic chaetiger.

Nucleotide diagnostic features. There are no unique apomorphic nucleotides in the fragments of COI analysed for *T. scotica* sp. nov., when considering all *Terebellides* species present in the NEA (Suppl. material 2: Table S2). However, when comparing homologous nucleotide positions with members of only Group A (192 sequences in the COI alignment), the following autapomorphies arise: 279 (G), 444 (C), 517 (A), 630 (C).

Type locality. East Orkney Island; 85 m deep (Fig. 18D).

Distribution and bathymetry. North Sea; 48–111 m deep (Nygren et al. 2018) (Fig. 18D; Suppl. material 1: Table S1). Two specimens (*Terebellides* sp. in Lavesque et al. 2019) were identified as *T. scotica* sp. nov. according to molecular sequences; Bay of Brest (France), in rhodolith beds, 5 m deep.

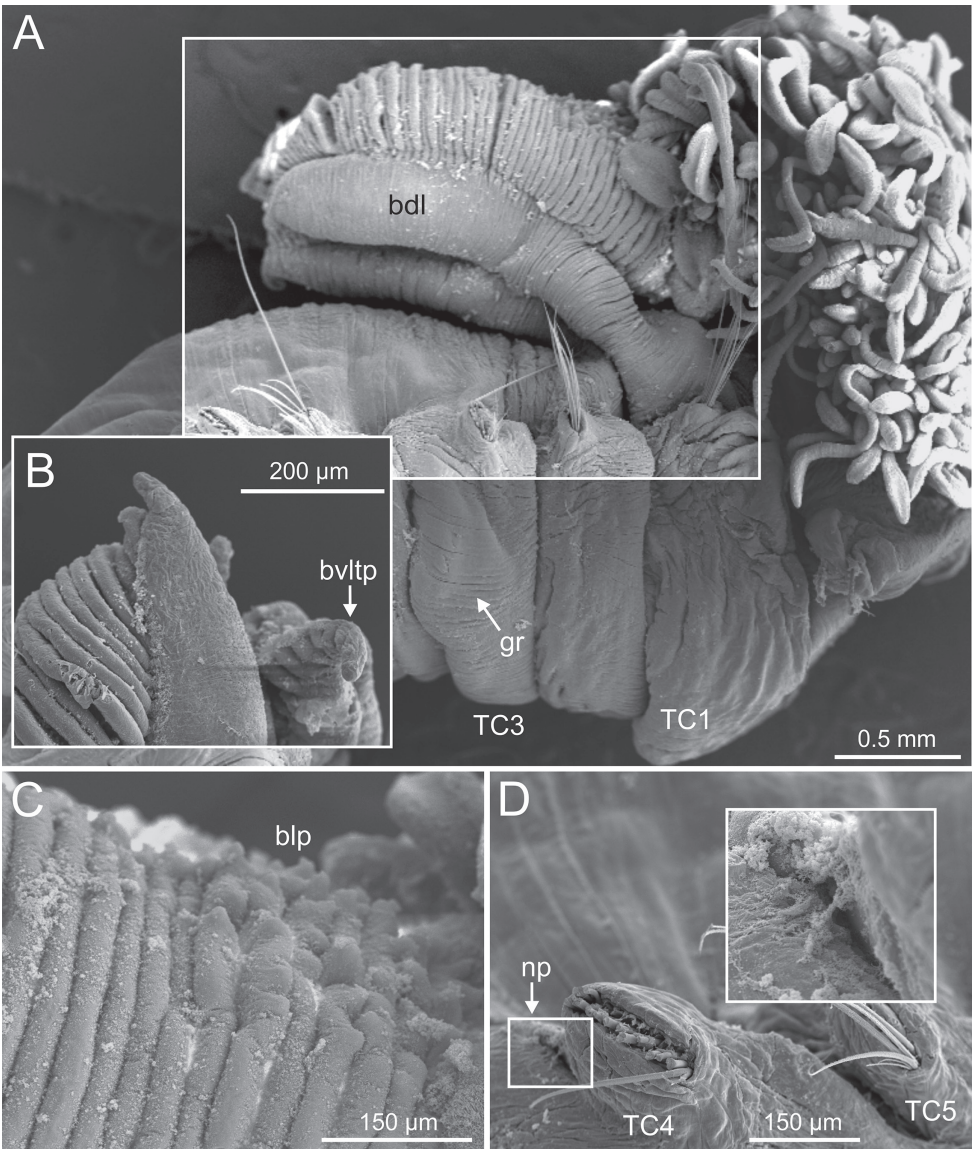

Figure 20. *Terebellides ronningae* sp. nov. (species 7; paratypes, ZMBN 116349 and ZMBN 116353), SEM micrographs. **A** anterior end, right lateral view **B** dorsal branchial lobes, terminal papilla **C** anterior branchial lamellae papillae **D** TC4, nephridial papilla (framed: detail). Abbreviations: bdl – branchial dorsal lobe; blp – branchial lamellae papillae; bvltp – branchial ventral lobe terminal papilla; gr – glandular region; np – nephridial papilla; TC – thoracic chaetiger.

Etymology. This new species is named after Scotland, since its type locality is in the Scottish Orkneys Islands.

Remarks. Among A2 species, *T. scotica* sp. nov., *T. europaea* and *T. norvegica* sp. nov. have thoracic uncini of type 3 and show ventral branchial lobes that may be

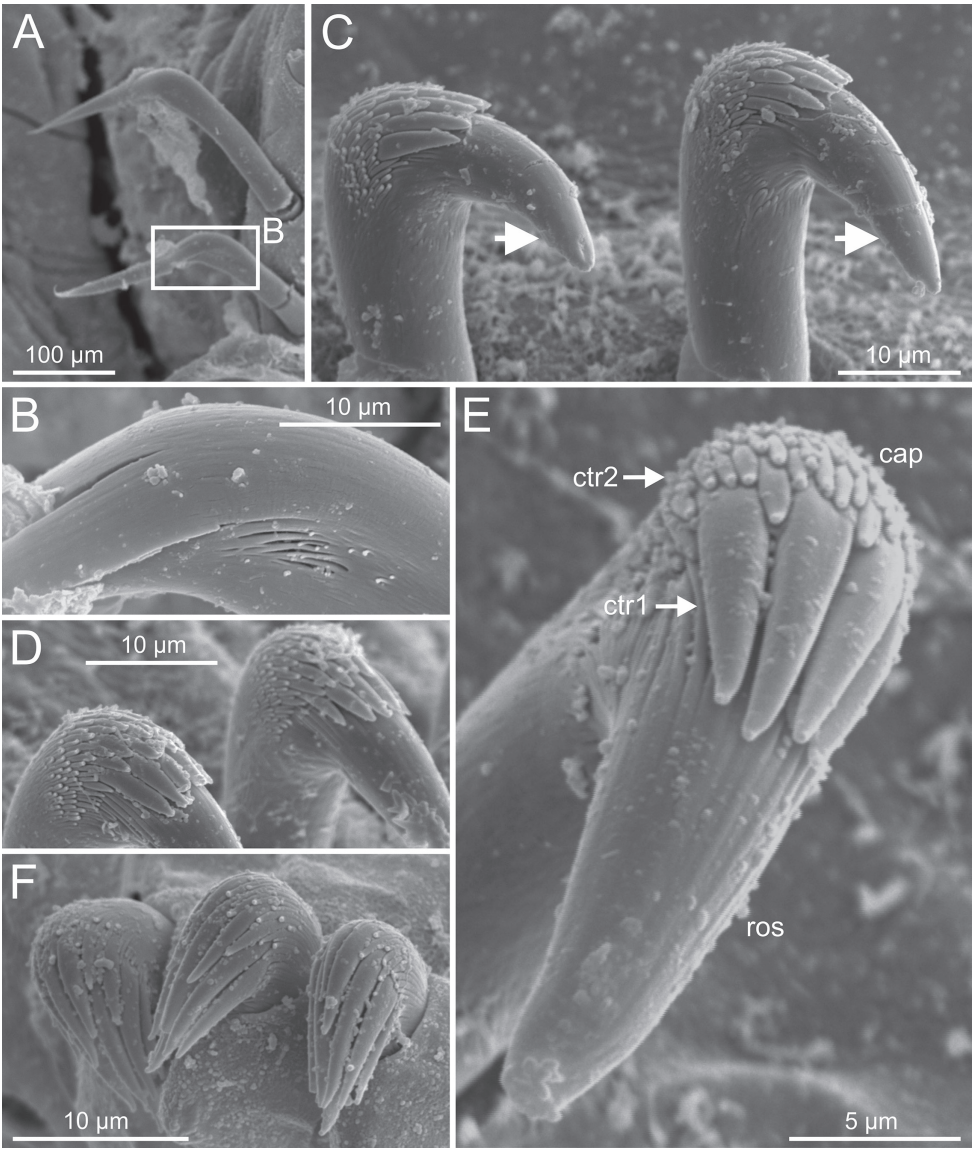

Figure 21. *Terebellides ronningae* sp. nov. (species 7; paratypes, ZMBN 116349 and ZMBN 116353), SEM micrographs. **A** TC6 (TU1), geniculate chaetae **B** geniculate chaeta, detail (framed in **A**) **C–E** thoracic uncini (arrows in **C** pointing to rostrum curved at distal end) **F** abdominal uncini. Abbreviations: cap – capitium; ctr1/2 – first and second rows of capitium teeth; ros – rostrum.

hidden in between dorsal lobes in some specimens. As stated previously, these species can only be distinguished according to DNA sequences.

The specimen studied under SEM shows a small knob near the notopodial lobe of TC1 (nop, Fig. 24C); its biological role is unknown and it may correspond to an artefact.

Two different sequences (see Suppl. material 2: Table S2; 0.2% distance) have been attributed to this species (Nygren et al. 2018). As stated above, the closest NEA congener is *T. norvegica* sp. nov., at 10.5% genetic distance.

Subgroup A3

Analyses of molecular data recovered a strongly supported subgroup A3 (Figs 1, 2; Nygren et al. 2018). This group is composed by species 20 + 28 (= *T. bigeniculatus*), and species 21; the latter will be described elsewhere (Gaeva and Jirkov, pers. comm.) but some comments are also provided here (*Terebellides* sp. 2 hereafter).

Character/s present only in subgroup A3

- Branchiae *stroemii*-type but irregular in many specimens, with all four lobes slightly fused; ventral lobes shorter and slimmer than dorsal ones and not hidden in between.
- First thoracic neuropodia on TC5; several sharply bent, acute-tipped geniculate chaetae present in two chaetigers (TC5 and TC6) (Fig. 26C).

Character/s shared with subgroup A1

- Border of anterior region of dorsal branchial lamellae not provided with papillary projections.
- Ciliated papilla present, dorsal to thoracic notopodia (Fig. 27B).
- Thoracic uncini type 3 (Fig. 26E).

Character/s shared with subgroup A2

- None (Table 1).

Character/s variable within subgroup A3

- None (Table 1).

Terebellides bigeniculatus Parapar, Moreira & Helgason, 2011

Figs 1, 2, 3D, 4D, 8D, 9, 10, 26, 28E; Table 1; Suppl. material 1: Table S1; Suppl. material 2: Table S2

Terebellides bigeniculatus Parapar, Moreira & Helgason, 2011: 6–10, figs 1b, 4–7.
Species 20 + 28 Nygren et al. 2018: 18–22, figs 6, 10.

Type locality. Off North West Iceland; 333 m deep (Parapar et al. 2011).

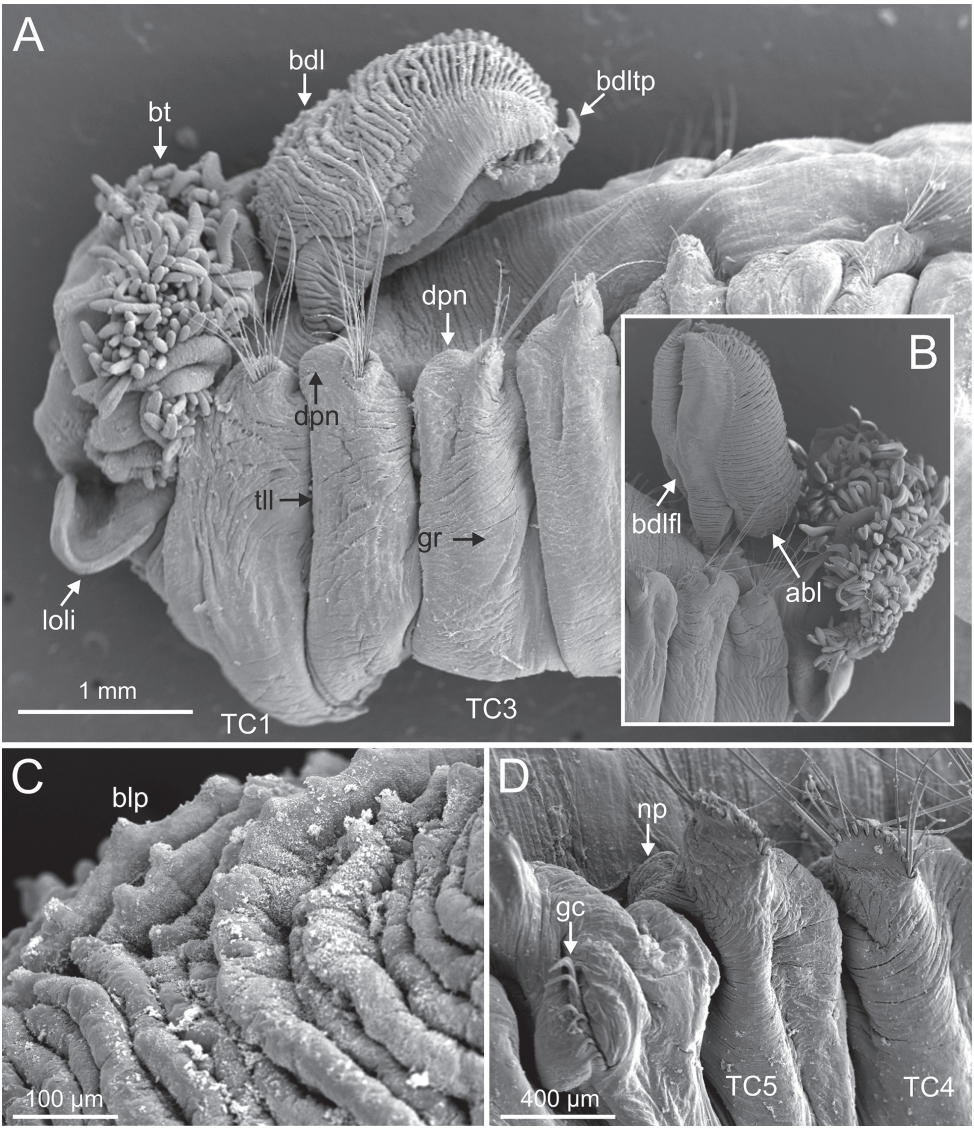

Figure 22. *Terebellides norvegica* sp. nov. (species 8; paratypes, GNM15130 and GNM15134), SEM micrographs. **A** anterior end, left lateral view **B** branchial lobes, ventral view **C** anterior dorsal branchial lamellae and papillae **D** TC4 to TC6, lateral view. Abbreviations: abl – anterior branchial lobe; bdl – branchial dorsal lobe; bdlfl – branchial dorsal lobes fusion line; bdltp – branchial dorsal lobe terminal papilla; blp – branchial lamellae papillae; bt – buccal tentacles; dpn – dorsal projection of notopodium; gc – geniculate chaetae; gr – glandular region; loli – lower lip; np – nephridial papilla; TC – thoracic chaetiger; tll – thoracic lateral lappets.

Material examined. 6 specimens: Barents Sea (ZMBN 116511); Norwegian coast and shelf (ZMBN 116417, ZMBN 116510, ZMBN 116512, ZMBN 116513, ZMBN 116514).

Additional material. *T. bigeniculatus*: ***Holotype*** (IIH 24923) and 5 ***paratypes*** (IINH 24925) (Suppl. material 1: Table S1).

GenBank accession numbers of material examined (COI). MG025318, MG025319, MG025351, MG025352, MG025353, MG025354, MG025355.

Diagnostic features of studied material. Complete individuals ranging from 10.0–24.0 mm in length. Branchiae clearly fitting with type 1 only in some specimens, irregular in others; dorsal lobes lamellae not provided with papillary projections. Lateral lappets from TC1-TC5 and well-marked dorsal projection of notopodia in TC3 (Figs 3D, 4D). Geniculate chaetae present in TC5 and TC6 (Fig. 26C), acutely bent and provided with hardly distinguishable capitium (Fig. 26D). Ciliated papilla dorsal to thoracic notopodia. Thoracic uncini of type 3, with rostrum/capitium length ratio of approximately 2 : 1 (Fig. 26E), and capitium with a first row of four medium-sized teeth, followed by several progressively smaller teeth. Abdomen with 20–25 chaetigers provided with type 1 uncini (Figs 26F, 28B).

Material examined herein corresponds to a few small and incomplete specimens. Therefore, the list of diagnostic characters given was developed with the aid of the type specimens re-examined and the original description.

Nucleotide diagnostic features. All sequences of *T. bigeniculatus* share the unique apomorphic nucleotides in positions 67 (G) and 138 (G) of the alignement.

Distribution and bathymetry. Around Iceland at both sides of the GIF Ridge; 179–968 m deep (Parapar et al. 2011). Material examined here also confirms its presence in shallow and deep bottoms of Norway and Barents Sea (Fig. 8D).

Remarks. In some of the species delimitation analyses performed, Nygren et al. (2018) were able to distinguish between two closely related lineages, clades 20 and 28, but some analyses of nuclear and mitochondrial datasets lump them together in a single entity. Given that all specimens examined share characteristic features that are distinct from other *Terebellides* species studied herein, clades 20 and 28 have been considered in the present study as a single species and identified as *T. bigeniculatus*.

As stated above, the sequenced specimens are small and not well preserved, hindering the examination of relevant morphological features with taxonomic value (i.e., branchial type). However, this species is characterised by having geniculate chaetae on TC5 and TC6 instead of only on one chaetiger (Parapar et al. 2011: 7) as in congeners listed in the Key of the present study. Furthermore, *T. bigeniculatus* is characterised by the low fusion of the usually irregularly-shaped branchial lobes (Parapar et al. 2011: 7–8, figs 4, 5a, b), ventral lobes are not obscured by dorsal ones, the lack of marginal papillae in the anterior region of the branchial dorsal lamellae, the presence of ciliated papilla dorsal to thoracic notopodia, and by having thoracic uncini of type 3 and abdominal uncini of type 1. However, it is likely that the irregular shape of the branchiae may correspond to an artefact related to fixation/preservation; other specimens show instead well-defined branchiae that agree with those of A1 and A2 species but less developed (Fig. 26A, B; Parapar et al. 2011: 8, fig. 5a). Regarding the four branchial types as defined by Parapar et al. (2016c), branchiae of *T. bigeniculatus* might correspond therefore to type 3 but with lobes showing a more variable shape.

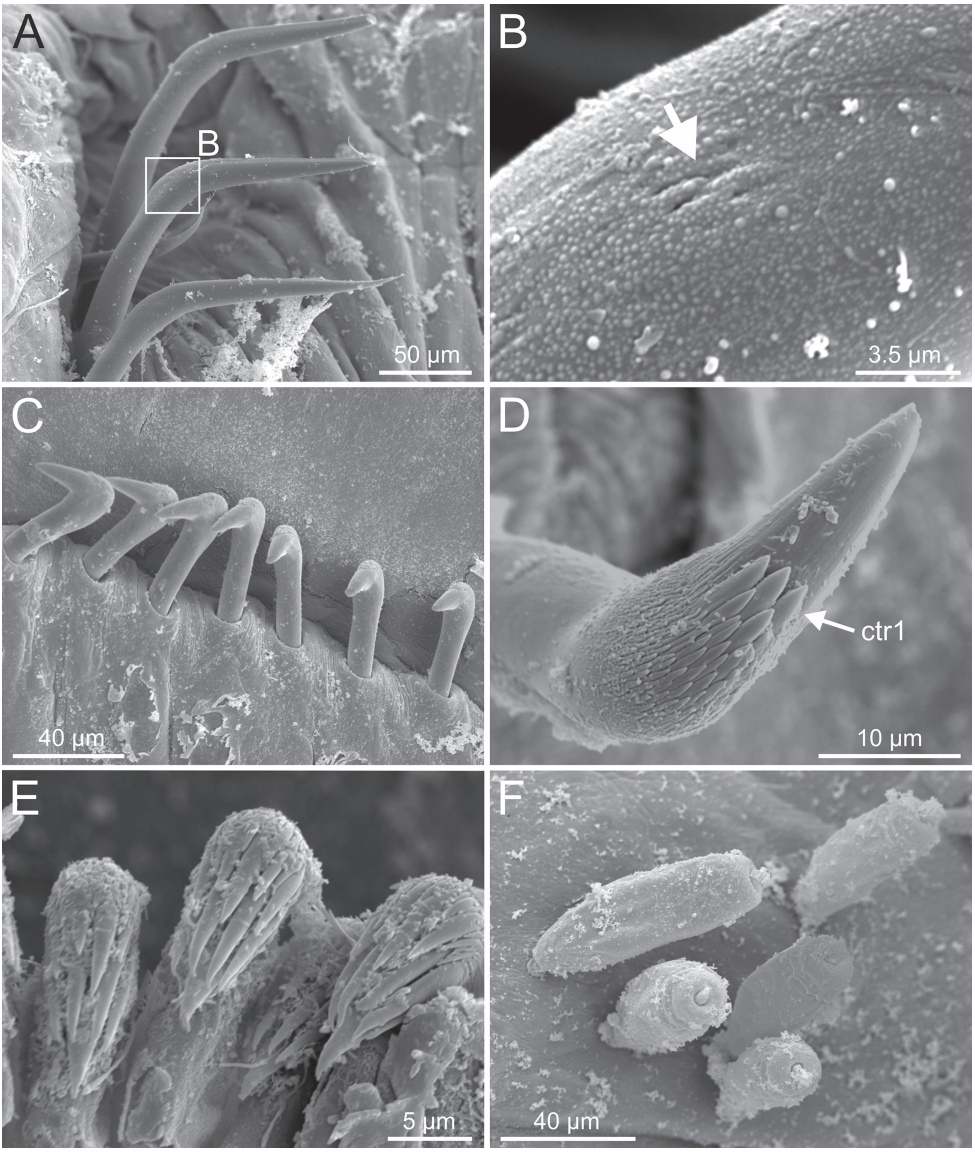

Figure 23. *Terebellides norvegica* sp. nov. (species 8; paratypes, GNM15130 and GNM15134), SEM micrographs. **A** TC6 (TU1), geniculate chaetae **B** detail of geniculate chaeta, arrow pointing to capitium (framed in **A**) **C** simple row of uncini **D** thoracic uncinus, capitium **E** abdominal uncini **F** ciliate epibionts. Abbreviations: ctr1 – first row of capitium teeth.

The original description states that nephridial papillae are located on TC3–TC4 or TC4–TC5 (Suppl. material 1: Table S1; Parapar et al. 2011: 7–9, figs 5c, 6d). Examination of the holotype and several paratypes confirmed that pores are on TC4 and TC5, as in other Group A species. Nephridial pores, as found in most *Terebellides* species, are usually flat and can be easily overlooked when examined with STM and even

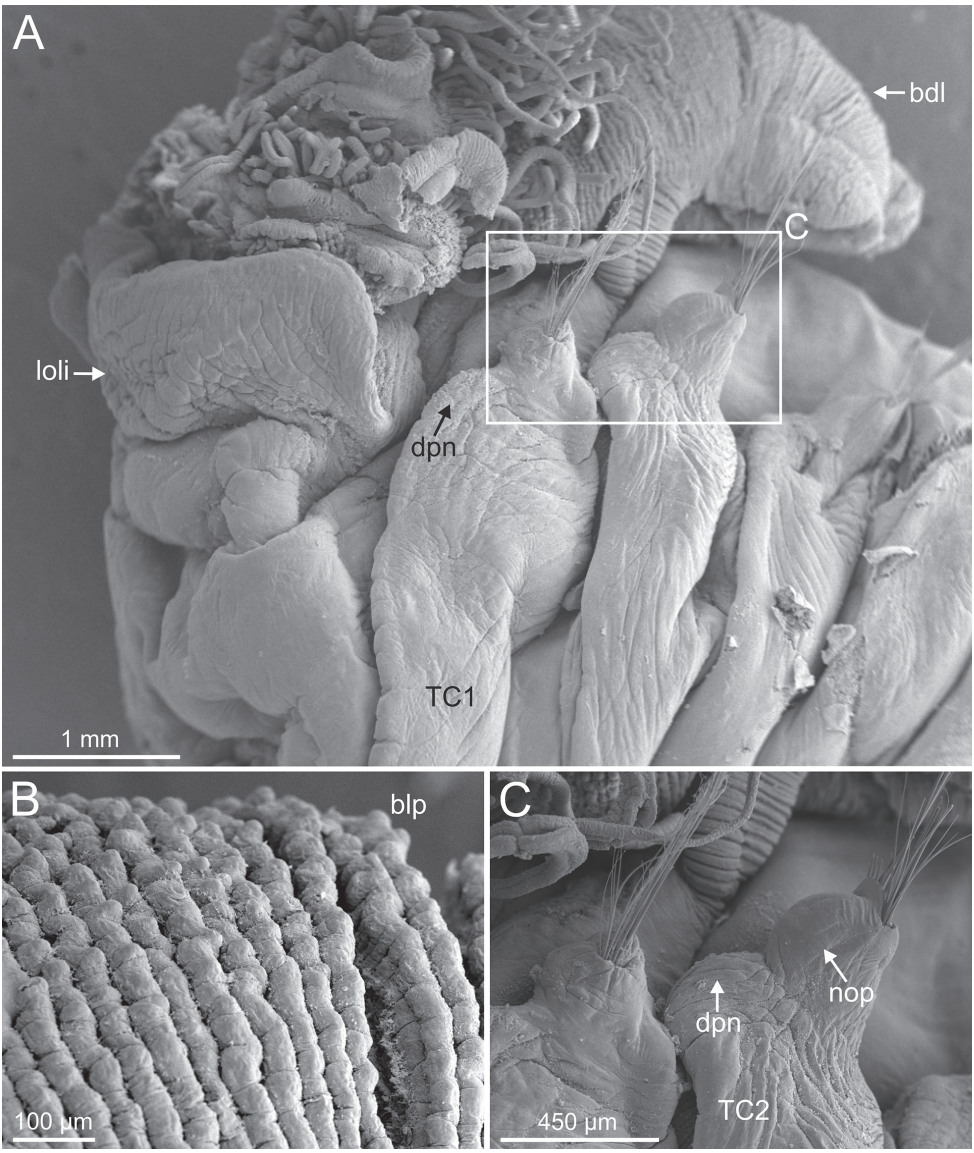

Figure 24. *Terebellides scotica* sp. nov. (species 9; paratype, ZMBN 1163887), SEM micrographs. **A** anterior end, left lateral view **B** anterior dorsal branchial lamellae and papillae **C** TC1 and TC2, lateral view (framed in **A**). Abbreviations: bdl – branchial dorsal lobe; blp – branchial lamellae papillae; dpn – dorsal projection of notopodium; loli – lower lip; nop – notopodial protuberance; TC – thoracic chaetiger.

SEM; those of *T. bigeniculatus* are larger and easier to distinguish comparatively with STM (Parapar et al. 2011: 9, fig. 6d).

Members of species 21 (see below, as *Terebellides* sp. 2) also bear geniculate chaetae in two chaetigers; this feature had been considered as unique to *T. bigeniculatus* regarding other NEA species. However, species 21 is present in Arctic waters (cf. Nygren et al.

2018: fig. 6) while the distribution of members of species 20 + 28 and identified here as *T. bigeniculatus* agrees with that of the type specimens (see Fig. 8D).

***Terebellides* sp. 2**

Figs 1, 2, 9, 27; Table 1; Suppl. material 1: Table S1; Suppl. material 2: Table S2

Species 21 Nygren et al. 2018: 18–22, figs 5, 6, 10.

Material examined. 4 specimens: **Barents Sea**. ZMBN 116481; ZMBN 116486.

Remarks. As explained for *Terebellides* sp. 1, two specimens were examined under SEM; these share with *T. bigeniculatus* the irregular shape of branchial lobes (Fig. 27A), the presence of geniculate chaetae on TC5 and TC6 (Fig. 27C–E) and abdominal uncini of type 1B (Fig. 27G). They share with subgroup A1 the presence of one ciliated papilla dorsal to thoracic notopodium (Fig. 27B) and thoracic uncini of type 3 (Fig. 27F).

On the other hand, species 18 and 19 of A1 (not described here because of the few specimens being available) and 23 (A4) have a geographic distribution similar to that of *T. bigeniculatus* but their position in the cladogram by Nygren et al. (2018: fig. 5) suggests that they may not bear geniculate chaetae in two chaetigers.

There are no unique diagnostic nucleotide positions that are shared by the two haplotypes (in 18 sequences) in COI. Eighteen sequences, in one single haplotype, have been attributed to this species (Nygren et al. 2018). Members of this species show a minimum of 3.0% uncorrected genetic distance, with its closest relative being *T. bigeniculatus* (Fig. 1).

Key to European species of *Terebellides*

The following key of European *Terebellides* species is based on Lavesque et al. (2019) and updated by including all species of Group A (in bold) apart from those that will be described elsewhere. The known geographic or bathymetric distribution has been used when there is a lack of discriminatory morphological characters between some species (e.g., subgroup A2).

1 Geniculate chaetae on TC5 and TC6[1] ..... **(subgroup A3)** ***T. bigeniculatus* Parapar, Moreira & Helgason, 2011**
– Geniculate chaetae on TC6 only **2**
2 Branchial lamellae margins lacking papillae[2] **3**
– Branchial lamellae margins with papillae **11**
3 Lower branchial lobes with long posterior projections as filaments **4**
– Lower branchial lobes with short posterior projections **5**

1 This character is also present in clade 21, which will be described elsewhere.
2 This character is also present in clade 12, which will be described elsewhere.

4 Glandular region on TC3 present; branchial lamellae pointed; notochaetae from TC1 longer than following ones; dorsal papillae absent ....***T. parapari*** **Lavesque, Hutchings, Daffe, Nygren & Londoño-Mesa, 2019**

– Glandular region on TC3 absent; branchial lamellae rounded; all notochaetae equal-sized; dorsal papillae present .... ***T. shetlandica*** **Parapar, Moreira & O'Reilly, 2016**

5 Ventral white band present on TC4 after MG staining **6**

– No distinct pattern on TC4 after MG staining **7**

6 Large species (>30 mm in length); 5th branchial lobe present; notochaetae of TC1 similar to following ones; main fang of thoracic uncini straight .... ***T. gracilis*** **Malm, 1874**

– Small species (<20 mm in length); 5th branchial lobe absent; notochaetae of TC1 absent or shorter than following ones; main fang of thoracic uncini 'eagle head'-shaped .... ***T. ceneresi*** **Lavesque, Hutchings, Daffe, Nygren & Londoño-Mesa, 2019**

7 First notopodia and notochaetae longer than following ones..... ..... ***T. mediterranea*** **Parapar, Mikac & Fiege, 2013**

– First notopodia and notochaetae similar or shorter than following ones..... **8**

8 Large-sized species (>50 mm); dorsal rounded projections on TC1–TC5 conspicuous..... **(subgroup A1) 9**

– Small-sized species (<20 mm); dorsal rounded projections on TC1–TC5 absent; main fang of thoracic uncini straight **10**

9 Abdominal uncini type 1[3] ..... ***T. kongsrudi*** **sp. nov.** and ***T. bakkeni*** **sp. nov.**

– Abdominal uncini type 2[3] ..... ***T. stroemii*** **Sars, 1835**

10 5th branchial lobe absent ..... ***T. atlantis*** **Williams, 1984**

– 5th lobe present ....***T. gralli*** **Lavesque, Hutchings, Daffe, Nygren & Londoño-Mesa, 2019**

11 Glandular region on TC3 round or oval **12**

– Glandular region on TC3 otherwise..... **13**

12 Glandular region on TC3 stained white; branchial lamellae with rounded papillae; TC1–3 without conspicuous dorsal projection ....***T. lilasae*** **Lavesque, Hutchings, Daffe, Nygren & Londoño-Mesa, 2019**

– Glandular region on TC3 stained blue; branchial lamellae with conical papillae; TC1–3 with conspicuous dorsal projection..... ...***T. bonifi*** **Lavesque, Hutchings, Daffe, Nygren & Londoño-Mesa, 2019**

13 Most branchial lamellae with marginal papillae; upper lip elongated..... ...***T. resomari*** **Lavesque, Hutchings, Daffe, Nygren & Londoño-Mesa, 2019**

– Only anterior branchial lamellae with marginal papillae; upper lip not elongated..... **(subgroup A2) 14**

14 Thoracic uncini type 1[4] ..... ***T. ronningae*** **sp. nov.**

– Thoracic uncini type 3[4] **15**

---

3 Types of abdominal uncini as described in this work.

4 Types of thoracic uncini sensu Parapar et al. (2020).

15 Deep-water species; mostly below 200 m deep..... ***T. norvegica* sp. nov.**
– Shallow-water species; mostly above 100 m deep **16**
16 Present from Southern Norway to NW Iberian Peninsula.....
... ***T. europaea* Lavesque, Hutchings, Daffe, Nygren & Londoño-Mesa, 2019**
– Present in the Shetland and Orkneys Islands and in Brittany .....
.....***T. scotica* sp. nov.**

Discussion

Group A species: taxonomy and distribution

The comprehensive study by Nygren et al. (2018) revealed that the genus *Terebellides* holds a large species diversity in NEA waters regardless its morphological homogeneity. Over 25 molecular entities that meet the requirements to be recognized as species were recovered forming four main and robust clades (A–D); Group A is composed, in turn, by thirteen species. Among the latter, members of only three species were identified herein as current nominal species: *T. stroemii*, *T. bigeniculatus*, and *T. europaea*; the remaining ten represent undescribed taxa.

Within Group A, three subgroups (A1–A3) can be defined based on molecular data, being only A2 and A3 well supported and congruent among all molecular analyses and datasets (Figs 1, 2; Nygren et al. 2018) but also by morphological features. A1 and A2 gather species morphologically similar to *T. stroemii*, while species included in subgroup A3 share morphological features with *T. bigeniculatus*. The original description of *T. stroemii* by Sars (1835) lacks detailed specific diagnostic features as are recognised nowadays in many closely related species, most of them described in the last years. On the contrary, *T. bigeniculatus* belongs to a small group of species bearing geniculate chaetae in two thoracic chaetigers (TC5 and TC6) instead of one (TC6), a distinct morphological trait for the group; *T. bigeniculatus* was described from deep Icelandic waters by Parapar et al. (2011), and only later reported NEA by Nygren et al. (2018). *Terebellides europaea* was recently described after molecular analyses by Lavesque et al. (2019) and fits within species of A1+A2. Other species from NEA, namely *T. gracilis*, *T. atlantis*, *T. williamsae*, *T. irinae* and *T. shetlandica* Parapar, Moreira & O'Reilly, 2016, differ from members of Group A in shape and body length, ventral colouration in a number of thoracic chaetigers, branchiae shape and degree of fusion and relative size of dorsal/ventral lobes (see Holthe 1986; Jirkov 2001; Parapar et al. 2011, 2016c). The aforementioned species fit either within groups B, C, or D sensu Nygren et al. (2018) and will be dealt with in a forthcoming paper.

The characters considered to delineate morphologically the aforementioned subgroups (A1–A3) should be taken with care because there are limitations due to number of specimens available to be studied and their condition of preservation. However, considering the variety and origin of the material examined we were able to elucidate some general patterns on taxonomy and distribution of the studied species. Thus, all studied species seem quite homogeneous in terms of general body features and share

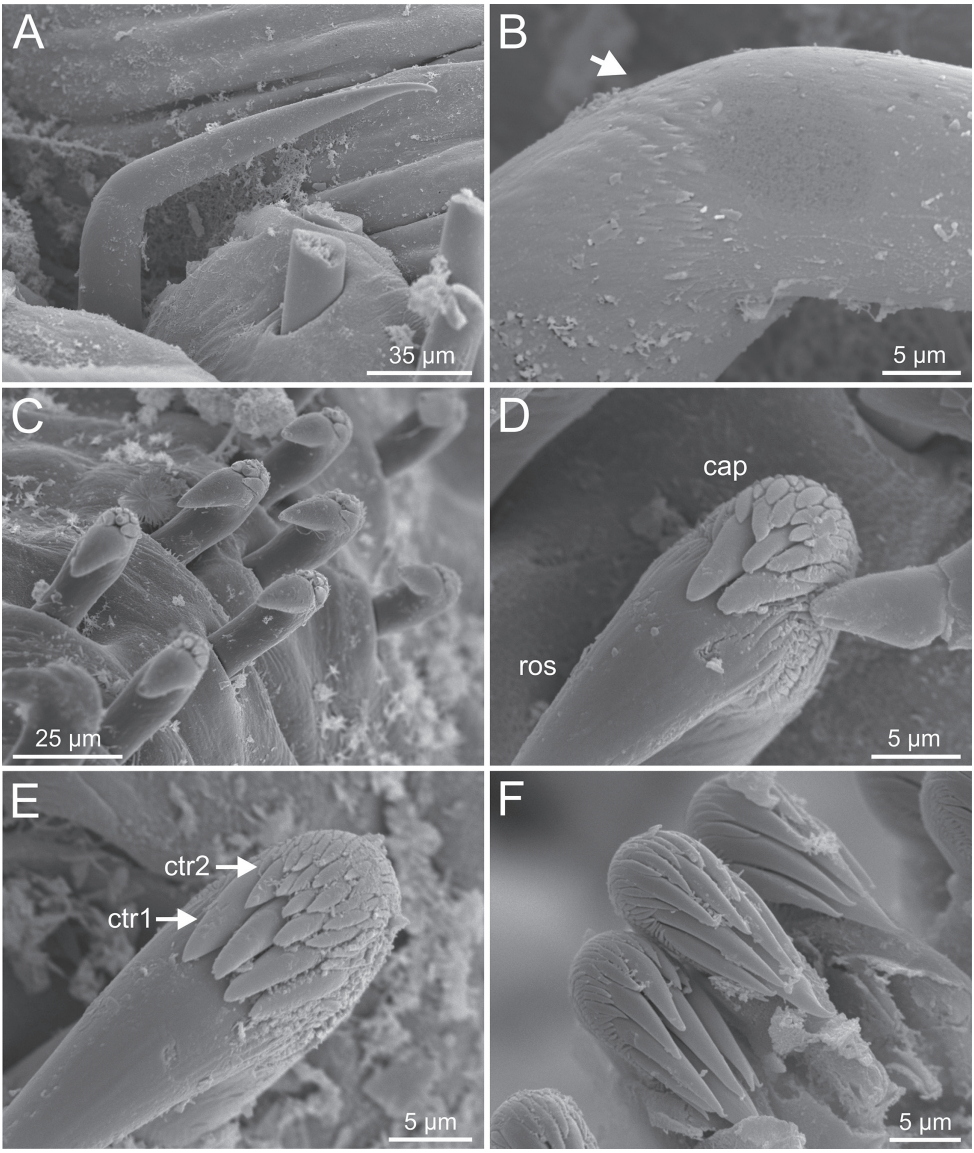

Figure 25. *Terebellides scotica* sp. nov. (species 9; paratype, ZMBN 1163887), SEM micrographs. **A** TC6 (TU1), geniculate chaetae **B** detail of geniculate chaeta (arrow pointing to capitium) **C** double row of thoracic uncini **D, E** thoracic uncini, capitium **F** abdominal uncini. Abbreviations: cap – capitium; ctr1 – first row of capitium teeth; ros – rostrum.

many characters; however, presence/absence of some macroscopic/microscopic characters has allowed their organization in the subgroups proposed above. Nevertheless, some species could not be differentiated according to morphological characters but genetic data. On the other hand, geographic distributions of species do not show apparent gaps; some species have a wider distribution and were more frequent in samples such as *T. norvegica* sp. nov. and *T. kongsrudi* sp. nov.; this suggests that many previous

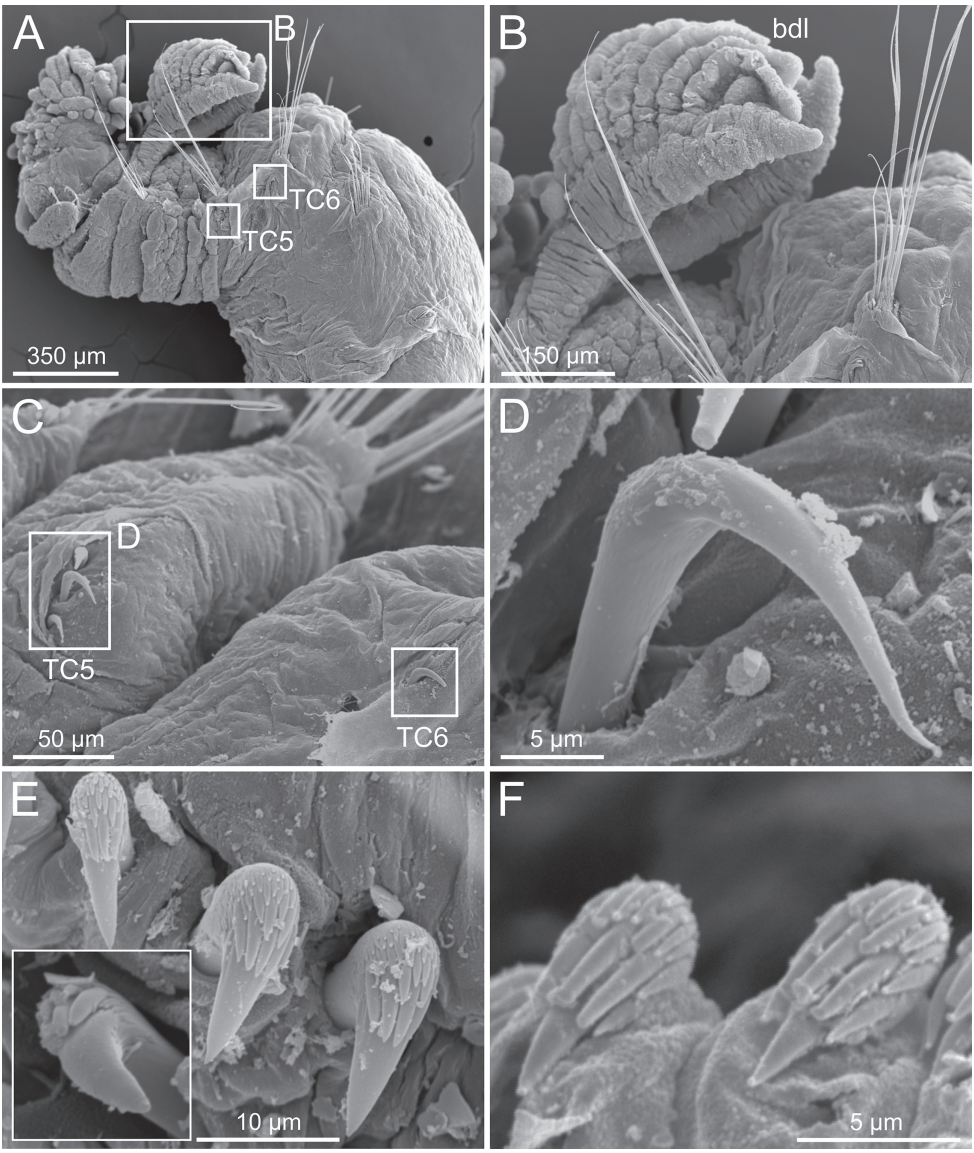

Figure 26. *Terebellides bigeniculatus* Parapar, Moreira & Helgason, 2011 (species 20 + 28; non-type specimens, ZMBN 116512 and ZMBM 116513), SEM micrographs. **A** anterior end, left lateral view **B** branchiae, ventral view **C** TC5 and TC6 (framed: geniculate chaetae location) **D** geniculate chaeta (framed in **C**) **E** thoracic uncini (framed: uncinus rostrum with curved distal end) **F** abdominal uncini. Abbreviations: bdl – branchial dorsal lobe; TC – thoracic chaetiger.

reports of *T. stroemii* in NEA might correspond to the aforementioned species. Other species apparently show a more restricted distribution, i.e., *T. bakkeni* sp. nov. in northern Norway or have their limit of distribution in southern Norway, as *T. europaea*. Similarly, there are no gaps in the bathymetric distribution of species, but some seem to appear typically at shallow depths, reaching the continental shelf (0–200 m) such as

T. europaea, *T. ronningae* sp. nov. and *T. scotica* sp. nov. On the contrary, *T. bigeniculatus* and *T. norvegica* sp. nov. are found at depths of below 200 m while *T. stroemii*, *T. bakkeni* sp. nov. and *T. kongsrudi* sp. nov. show a wider bathymetric distribution.

Given the morphological homogeneity, DNA sequences have been shown to provide advantageous data and support when it comes to species delineation in *Terebellides*. The most informative markers in previous studies are COI and ITS (Nygren et al. 2018; Lavesque et al. 2019). In the present study, analyses have been mainly based on mitochondrial COI, the universal barcoding gene, because it offers no ambiguities in the alignment process, and is the most commonly used in molecular taxonomy in annelids (e.g., Borda et al. 2013; Tomioka et al. 2016; Álvarez-Campos et al. 2017; Aguado et al. 2019; Grosse et al. 2020) and other taxa (e.g., Kekkonen and Hebert 2014). After species delimitation, identification to the correct nominal species level is ideal, as species names allow the communication, study, quantification, classification, use and management of life on the planet. This has been the motivation of recognising unequivocal diagnostic nucleotides in specific positions for the species described in the present study. As with morphological traits, molecular diagnostic characters are tested continuously when additional intraspecific and interspecific variation within the groups has been found. Nevertheless, and as pointed out by previous studies, diagnostic nucleotides may be an effective and relatively simple way for species identification (Rach et al. 2008; Wong et al. 2009).

Comparisons with other NE Atlantic *Terebellides*

Lavesque et al. (2019) described eight new species of *Terebellides* from continental France considering an integrative taxonomy approach. Those species could be informally grouped in two assemblages:

1. Species similar to Group A sensu Nygren et al. (2018) regarding body colour and shape, and branchiae features: *T. bonifi*, *T. europaea*, *T. gentili*, *T. gralli* and *T. lilasae*.
2. Species closer to groups B, C or D sensu Nygren et al. (2018): *T. ceneresi*, *T. parapari* and *T. resomari.*

The first five species were already discussed above. Regarding the remaining three species, only *T. ceneresi* was sequenced by Lavesque et al. (2019) and according to their phylogenetic analyses, it is not related to any species of Group A; in fact, it differs from Group A species: a) in having a very distinct MG staining pattern corresponding to a solid stain manifested in the first ten thoracic chaetigers, being lighter in TC4; b) the anterior branchial lobe (5th lobe) is not present; c) the outer edge of branchial lamellae bears tufts of cilia. These characters would relate *T. ceneresi* to Group D sensu Nygren et al. (2018). This species was described with 'eagle head'-shaped thoracic uncini, which are similar to those of *T. stroemii*, *T. ronningae* sp. nov. and *T. kongsrudi* sp. nov. as described here and *T. stroemii* sensu Parapar and Hutchings (2014). However, as explained above (see Remarks for *T. stroemii*), the taxonomic value of this character

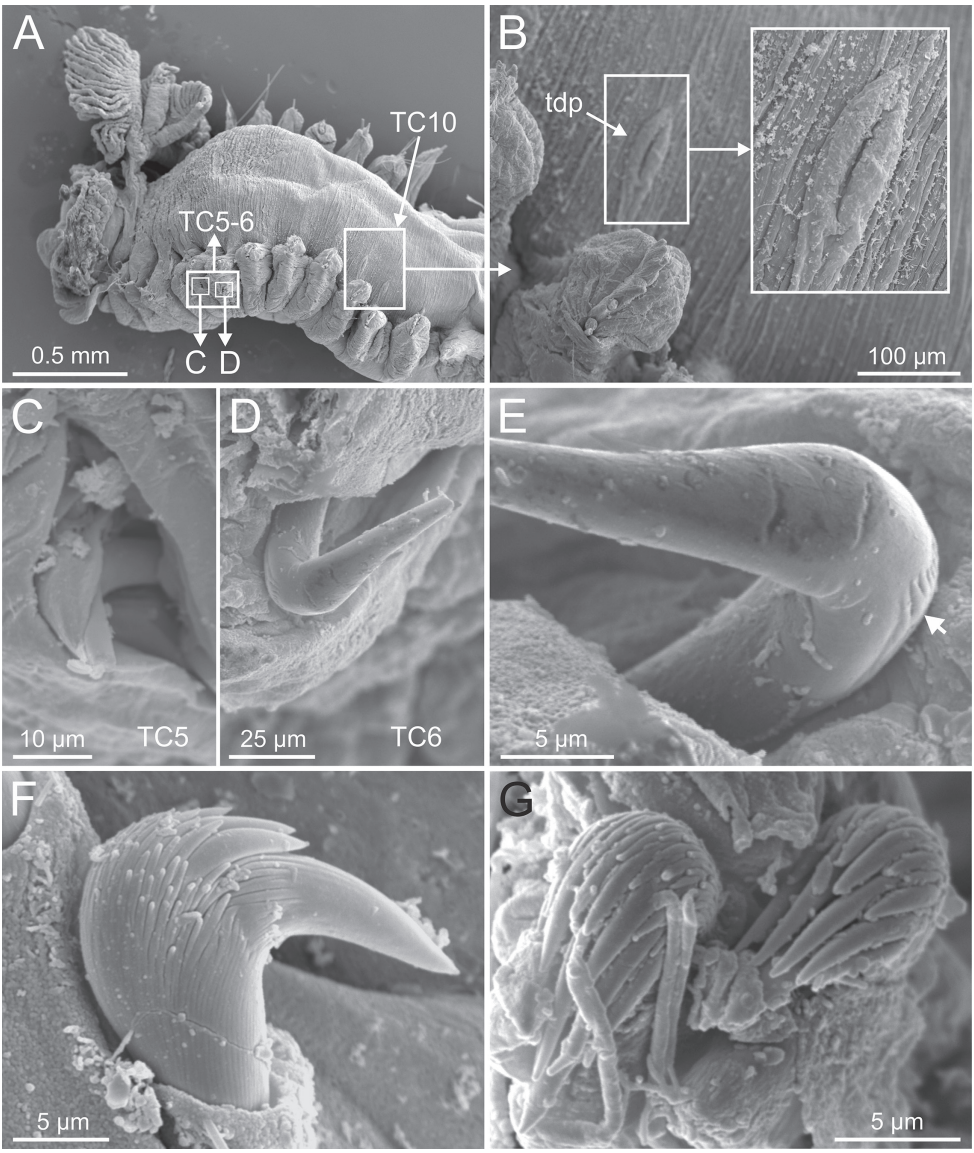

Figure 27. *Terebellides* sp. 2 (species 21; ZMBN 116481 and ZMBN 116486), SEM micrographs. **A** anterior end, left lateral view **B** TC10, thoracic dorsal papilla (framed in **A**) **C, D** geniculate chaetae of TC5 and TC6 respectively (framed in **A**) **E** TC6, geniculate chaeta (arrow pointing to capitium teeth) **F** thoracic uncinus **G** abdominal uncini. Abbreviations: TC – thoracic chaetiger; tdp – thoracic dorsal papilla.

should be viewed cautiously and its consistent presence across the three aforementioned species needs to be assessed.

Terebellides parapari differs from Group A species in the shape and arrangement of branchial lobes that are free from each other, and by the presence of terminal filament in ventral lobes. These features and its short body length relate *T. parapari* to

T. shetlandica and Group B sensu Nygren et al. (2018). Finally, *T. resomari* is unique among NEA *Terebellides* because of having "not well packed (separated) disposition of the branchial lamellae" (Lavesque et al. 2019: 177, fig. 18B) and therefore branchiae seem lacking a defined shape. In addition, this species also shows the "upper lip very elongated with convoluted margins" (Lavesque et al. 2019: 177, fig. 18C), that was also reported by Parapar et al. (2020) for *Terebellides* sp. from the Atlantic African coast. Therefore, these unusual features do not allow for the allocation of *T. resomari* to any group as defined by Nygren et al. (2018).

Discriminant vs. non-discriminant body characters in species delineation

This study has revealed that some of the traditionally morphological-based taxonomic characters are not appropriate for *Terebellides* species identification. The number of species in the genus is now large and their morphological homogeneity high. Regarding Group A, two macroscopic characters have, however, been useful: 1) presence of geniculate chaetae in one or two chaetigers (A1+A2 vs A3), 2) presence of papillary projections in the border of branchial lamellae (A2 vs A1+A3). On the contrary, we found that the development of lateral lappets and the presence of a dorsal projection on the anterior thoracic notopodia seem dependent on size/age and preservation, and therefore these characters should be taken with care for species identification. Similarly, the species in Group A seem quite homogeneous when considering branchial morphology, particularly within A1 and A2. Some of the morphological differences observed between *Terebellides* species rely in the exposure of the ventral lobes (hidden or not behind the dorsal lobes). However, we have also observed some degree of variability between specimens belonging to the same species and could be due to size or the contraction of specimens after fixation.

Morphology of thoracic and abdominal uncini seems useful for species identification; such features need to be examined under SEM and are being considered in descriptions of *Terebellides* in the last years. Recently, Parapar et al. (2020) describe tentatively several types of thoracic uncini. The uncini of the NEA species treated here are quite similar because of their phylogenetic proximity, being *T. ronningae* sp. nov. the only species that differ in uncini type from other congeners of subgroup A2. There were, however, differences in abdominal uncini that correspond to two morphologies that agree well, in turn, with groups of species as defined by molecular-based phylogenetic analyses. Following Parapar et al. (2020), we propose here the use of similar criteria for the characterization of abdominal uncini, that are based on the rostrum vs. capitium length ratio (RvC), and the number of the capitium teeth and their relative size. Therefore, considering our results after SEM examination and other previous work, two main types of abdominal uncini can be defined:

Type 1

Capitium of ca. 0.7 of total length of rostrum (RvC = 1/0.7); capitium simple, composed of a few wide denticles, being 3(5) in first row and 1(2) in a second row

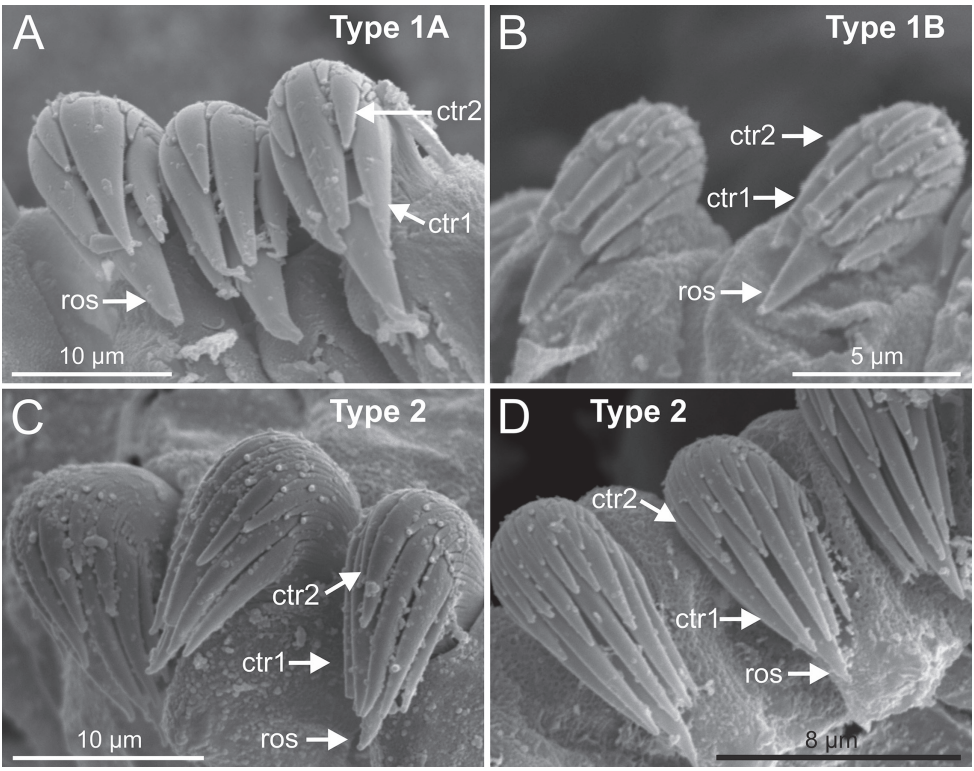

Figure 28. SEM micrographs of abdominal uncini types of *Terebellides* species. **A** *T. kongsrudi* sp. nov. (species 13; ZMBN-116409) **B** *T. bigeniculatus* Parapar, Moreira & Helgason, 2011 (species 20 + 28; ZMBN-116513) **C** *T. ronningae* sp. nov. (species 7; ZMBN-116353) **D** *Terebellides stroemii* Sars, 1835 (species 11; ZMBN-116399). Abbreviations: ctr – capitium teeth row; ros – rostrum.

(Fig. 28A, B). In turn, Type 1A and 1B would differ in number of capitium teeth, being higher in B (Fig. 28A, B, Table 1). This typology is present in *T. bakkeni* sp. nov. (1A), *T. kongsrudi* sp. nov. (1A) and *T. bigeniculatus* (1B; see also Parapar et al. 2011: fig. 7f). Type 1 uncini are apparently also present in *T. gracilis* (sensu Parapar et al. 2011, 2013), *T. narribri* Schüller & Hutchings, 2010, *T. mediterranea* Parapar, Mikac & Fiege, 2013, *T. toliman* Schüller & Hutchings, 2013, *T. ectopium* Zhang & Hutchings, 2018, *T. kirkegaardi* Parapar, Martin & Moreira, 2020 and *T. longiseta* Parapar, Martin & Moreira, 2020 (Parapar et al. 2013, 2020; Schüller and Hutchings 2010, 2013; Zhang and Hutchings 2018).

Type 2

Capitium of almost same length as rostrum (RvC = 1/0.9); capitium much complex than in Type 1, composed of a first row of 4(5) denticles and a variable number of teeth in two more rows with decreasing number and size posterior to them (Fig. 28C, D). Present in *T. europaea*, *T. ronningae* sp. nov., *T. norvegica* sp. nov., *T. scotica* sp.

nov., and *T. stroemii* (Table 1). Type 2 is apparently also present in *T. kergelensis* McIntosh, 1885 (sensu Parapar and Moreira 2008a), *T. jitu* Schüller & Hutchings, 2010, *T. canopus* Schüller & Hutchings, 2013, *T. persiae* Parapar, Moreira, Gil & Martin, 2016, *T. baliensis* Hsueh & Li, 2017, *T. guangdongensis* Zhang & Hutchings, 2018, *T. augeneri* Parapar, Martin & Moreira, 2020, *T. fauveli* Parapar, Martin & Moreira, 2020, *T. nkossa* Parapar, Martin & Moreira, 2020, and *T. ramili* Parapar, Martin & Moreira, 2020 (Parapar et al. 2016a, 2020; Hsueh and Li 2017; Zhang and Hutchings 2018). This "more complex" type 2 condition of abdominal uncini does not seem related to body size; for instance, small species such as *T. atlantis* sensu Parapar et al. (2011: 5, fig. 3f) and *T. shetlandica* (Parapar et al. 2016c: 218, fig. 6f) are provided with such uncini. The validity of this proposed uncini classification should be assessed across species considering specimens of different sizes and across abdominal chaetigers.

On the other hand, we observed differences in whether the capitium is defined or not in geniculate chaetae of TC5/TC6, as previously highlighted by Parapar et al. (2011, 2013, 2016a, 2016b, 2016c). For instance, *T. ginkgo* Schüller & Hutchings, 2012 shows a well-defined capitium conformed by many large-sized teeth whereas other species bear an almost inconspicuous capitium (e.g., *T. bakkeni* sp. nov., *T. kongsrudi* sp. nov.) (Schüller and Hutchings 2012: 10, fig. 5a–c; Figs 6G, 12G); Parapar et al. (2011) also reported from Iceland several species with conspicuous capitium, i.e., *T. atlantis*, *T. gracilis* and *T. stroemii*. In this sense, the specimens of *T. stroemii* examined here bear a low capitium in comparison to those aforementioned from Iceland (Parapar et al. 2011); this suggests that the latter might not correspond to *T. stroemii* but to other taxa as explained above. Again, the taxonomic value of this character should be tested in other species considering potential intraspecific variation.

Methyl Green staining pattern

The MG staining pattern was mostly similar across the studied species and according to type 1 sensu Schüller and Hutchings (2010), being solid in three to five anterior chaetigers, TC1–TC3(5), striped in subsequent seven or eight chaetigers, i.e., TC4(6)–TC10(11), and fading towards the end of the thorax at TC18; minor observed differences can be attributed to body size, degree of contraction and preservation of specimens. Parapar et al. (2011) reported a similar pattern for specimens identified as *T. stroemii* from Iceland: solid in the first six chaetigers after turning into a striped pattern and fading in the posterior thoracic segments, while for *T. bigeniculatus* staining is solid from TC1 to TC11, striped between TC12 and TC14, and then fading in the following segments. The first pattern only partially agrees with that of *T. stroemii* (species 11) and the second one would match better with that of *T. bigeniculatus* (species 20 + 28) as examined here. Parapar and Hutchings (2014) reported a MG staining pattern for neotypes of *T. stroemii* being solid from TC1 to TC3, striped from TC4 to TC12 and fading in the last thoracic segments; this is exactly the same pattern as observed in *T. stroemii* from Norway (Suppl. material 1: Table S1).

Nephridial papillae

Schüller and Hutchings (2010) and Parapar et al. (2011), among others, suggest that position of thoracic papillae (nephridial/genital) should be considered as of taxonomic value. We agree with this and have found that papillae are present always in TC4 and TC5 in the species/clades studied here. This position has also been reported in *T. gracilis* sensu Parapar et al. (2011, 2013), *T. mediterranea*, *T. kerguelensis*, and *T. hutchingsae* Parapar, Moreira & Martin, 2016. On the contrary, other species reported elsewhere have such papillae in TC1 instead, including *T. persiae* Parapar, Moreira, Gil & Martin, 2016, *T. mediterranea*, and *T. hutchingsae*.

Conclusions

To sum up all results and according to the discussion of the aforementioned characters, the general characteristics for each subgroup of Group A sensu Nygren et al. (2018) are listed below. A1 and A2 are particularly close to each other and were informally designed by Nygren et al. (2018) as "*stroemii*-group"; subgroup A3 is the most dissimilar, with *T. bigeniculatus* as the typical species.

Subgroup A1

Species are similar morphologically and differ from A2 in lacking papillae on branchial lamellae and in having ciliated papillae on thoracic notopodia. Regarding morphology and distribution, *T. bakkeni* sp. nov. and *T. kongsrudi* sp. nov. are closest to each other than to *T. stroemii*. *Terebellides stroemii* (as species 11 here) shows also a similar geographic and bathymetric distribution (Table 1), but seems less frequent across Norway and differs in abdominal uncini type (cf. Fig. 7G vs. Figs 6G, 12G).

Subgroup A2

The subgroup is morphologically homogeneous. It differs from A1 in having lamellae papillae and by the lack of thoracic ciliated papillae (at least not observed with SEM). The most recognisable species is *T. ronningae* sp. nov. because of having thoracic uncini of type 1, a long rostrum and a capitium provided with long first row teeth; the other three species bear thoracic uncini of type 3 and differ of each other in the geographic (*T. europaea*, *T. scotica* sp. nov.) and bathymetric distribution (*T. norvegica* sp. nov.).

Subgroup A3

This subgroup is composed by *T. bigeniculatus* (species 20 + 28) and species 21 (not formally described here). Branchial shape is irregular and geniculate chaetae are present in two thoracic chaetigers (TC5 and TC6). Other features are shared with A1 such as

lack of lamellae papillae; thoracic uncini type 3 or presence of thoracic ciliated papillae. The bathymetric distribution of species is similar to A1.

Acknowledgements

We would like to thank all people involved in Nygren et al. (2018) paper, specially Torkild Bakken (NTNU–University Museum, Trondheim, Norway) and Jon Anders Kongsrud (Zoological Museum, Bergen, Norway), for providing part of the specimens of the different species studied here. Many thanks also to Ann Helén Rønning and Åse Ingvild Wilhelmsen (Natural History Museum–University of Oslo, Norway) and Gudmundur Gudmundsson (Icelandic Institute of Natural History, Reykjavik) for providing the type specimens of *T. stroemii* and *T. bigeniculatus* respectively. Thanks also to Ada Castro and Catalina Sueiro (Servizos de Apoio á Investigación, Universidade da Coruña) for SEM assistance, to María Candás (Estación de Bioloxía Mariña da Graña–Ferrol, Universidade de Santiago de Compostela, Spain) for assistance with the stereomicroscope photographs, and to Antonio Fernández y García de Vinuesa (Ministerio de Transición Ecológica y Reto Demográfico, Spain) and Juana Agudo González (DHL España) for their unvaluable help with Customs paperwork related to the shipment of type specimens of *T. stroemii* and *T. bigeniculatus*.

This study was partly supported by the FAUNA IBÉRICA research project Polychaeta VII, Palpata, Canalipalpata II (PGC2018–095851–B–C64) funded by the Agencia Estatal de Investigación, Ministerio de Ciencia e Innovación, and coordinated by JP. Funding was also provided from the Ramón y Cajal program (RYC-2016- 20799) funded by Spanish MINECO, Agencia Estatal de Investigación, Comunidad Autónoma de las Islas Baleares and the European Social Fund to MC. Financial support was also provided by the Norwegian Taxonomy Initiative (Cryptic polychaete species in Norwegian waters, knr 49-13, project no. 70184228 to AN; Polychaetes in the Norwegian Sea, project no. 70184227; Polychaetes in Skagerrak, project no.70184216; and the MAREANO program.

Authors deeply thank Pat Hutchings and one anonymous reviewer as well as Chris Glasby, Zookeys Subject Editor, for their constructive comments on the manuscript.

References

Aguado MT, Capa M, Lago-Barcia D, Gil J, Pleijel F, Nygren A (2019) Species delimitation in *Amblyosyllis* (Annelida, Syllidae). PLOS One 14(4): e0214211. https://doi.org/10.1371/journal.pone.0214211

Álvarez-Campos P, Giribet G, Riesgo A (2017) The *Syllis gracilis* species complex: a molecular approach to a difficult taxonomic problem (Annelida, Syllidae). Molecular Phylogenetics and Evolution 109: 138–150. https://doi.org/10.1016/j.ympev.2016.12.036

Bakken T, Hårsaker K, Daverdin M (2020) Marine invertebrate collection NTNU University Museum. Version 1.535. NTNU University Museum. [Occurrence dataset:] https://doi.org/10.15468/ddbs14 [accessed via GBIF.org on 26 June 2020]

Barraclough TG (2010) Evolving entities: towards a unified framework for understanding diversity at the species and higher levels. Philosophical Transactions of the Royal Society B – Biological Sciences 365(1547): 1801–1813. https://doi.org/10.1098/rstb.2009.0276

Borda E, Kudenov JD, Chevaldonné P, Blake JA, Desbruyères D, Fabri M-C, Hourdez S, Pleijel F, Shank TM, Wilson NG, Schulze A, Rouse GW (2013) Cryptic species of *Archinome* (Annelida: Amphinomida) from vents and seeps. Proceedings of the Royal Society B – Biological Sciences 28(1770): e20131876. https://doi.org/10.1098/rspb.2013.1876

Gagaev SY (2009) *Terebellides irinae* sp. n., a new species of *Terebellides* (Polychaeta: Terebellidae) from the Arctic basin. Russian Journal of Marine Biology 35: 474–478. https://doi.org/10.1134/S1063074009060042

Grosse M, Bakken T, Nygren A, Kongsrud JA, Capa M (2020) Species delimitation analyses of NE Atlantic *Chaetozone* (Annelida, Cirratulidae) reveals hidden diversity among a common and abundant marine annelid. Molecular Phylogenetics and Evolution 149: e106852. https://doi.org/10.1016/j.ympev.2020.106852

Hoang DT, Chernomor O, Von Haeseler A, Minh BQ, Vinh LS (2018) UFBoot2: improving the ultrafast bootstrap approximation. Molecular Biology and Evolution 35(2): 518–522. https://doi.org/10.1093/molbev/msx281

Holthe T (1986) Polychaeta Terebellomorpha. Marine Invertebrates of Scandinavia 7: 1–194.

Hsueh P-W, Li K-R (2017) Additions of new species to *Thelepus* (Thelepodidae), with description of a new *Terebellides* (Trichobranchidae) from Taiwan. Zootaxa 4244(3): 429–439. https://doi.org/10.11646/zootaxa.4244.3.10

Imajima M, Williams SJ (1985) Trichobranchidae (Polychaeta) chiefly from the Sagami and Saruga Bays, collected by R/V Tansei-Maru (Cruises KT-65/76). Bulletin of the National Science Museum of Tokyo 11(1): 7–18.

Jirkov IA (1989) Bottom fauna of the USSR. Polychaeta. Moscow State University Press, Moscow, 141 pp. [English translation from Russian]

Jirkov IA (2001) Polychaeta of the Arctic Ocean. Yanus-K, Moskva, 632 pp. [in Russian]

Jirkov IA, Leontovich MK (2013) Identification keys for Terebellomorpha (Polychaeta) of the eastern Atlantic and the North Polar Basin. Invertebrate Zoology 10: 217–243. https://doi.org/10.15298/invertzool.10.2.02

Jouin-Toulmond C, Hourdez S (2006) Morphology, ultrastructure and functional anatomy of the branchial organ of *Terebellides stroemii* (Polychaeta: Trichobranchidae) and remarks on the systematic position of the genus *Terebellides*. Cahiers de Biologie Marine 47: 287–299.

Katoh K, Misawa K, Kuma KI, Miyata T (2002) MAFFT: a novel method for rapid multple sequence alignment based on fast Fourier transform. Nucleic Acids Research 30 (14): 3059–3066. https://doi.org/10.1093/nar/gkf436

Kekkonen M, Hebert PD (2014) DNA barcode-based delineation of putative species: efficient start for taxonomic workflows. Molecular Ecology Resources 14(4): 706–715. https://doi.org/10.1111/1755-0998.12233

Lavesque N, Hutchings P, Daffe G, Nygren A, Londoño-Mesa MH (2019) A revision of the French Trichobranchidae (Polychaeta), with descriptions of nine new species. Zootaxa 4664(2): 151–190. https://doi.org/10.11646/zootaxa.4664.2.1

Malmgren AJ (1866) Nordiska Hafs–Annulater. Öfversigt af Königlich Vetenskapsakademiens förhandligar, Stockholm 22: 51–410.

McIntosh WC (1885) Report on the Annelida Polychaeta collected by H.M.S. Challenger during the years 1873–1876. Challenger Reports 12: 1–554.

Nguyen LT, Schmidt HA, Von Haeseler A, Minh BQ (2015) IQ-TREE: a fast and effective stochastic algorithm for estimating maximum-likelihood phylogenies. Molecular Biology and Evolution 32(1): 268–274. https://doi.org/10.1093/molbev/msu300

Nygren A, Parapar J, Pons J, Meißner K, Bakken T, Kongsrud JA, Oug E, Gaeva D, Sikorski A, Johansen RA, Hutchings PA, Lavesque N, Capa M (2018) A mega-cryptic species complex hidden among one of the most common annelids in the North East Atlantic. PLOS ONE 13(6): e0198356. https://doi.org/10.1371/journal.pone.0198356

Parapar J, Hutchings P (2014) Redescription of *Terebellides stroemii* (Polychaeta, Trichobranchidae) and designation of a neotype. Journal of the Marine Biological Association of the United Kingdom 95: 323–337. https://doi.org/10.1017/S0025315414000903

Parapar J, Martin D, Moreira J (2020) On the diversity of *Terebellides* (Annelida, Trichobranchidae) in West Africa, seven new species and the redescription of *T. africana* Augener, 1918 stat. prom. Zootaxa 4771(1): 1–61. https://doi.org/10.11646/zootaxa.4771.1.1

Parapar J, Mikac B, Fiege D (2013) Diversity of the genus *Terebellides* (Polychaeta: Trichobranchidae) in the Adriatic Sea with the description of a new species. Zootaxa 3691 (3): 333–350. https://doi.org/10.11646/zootaxa.3691.3.3

Parapar J, Moreira J (2008a) Redescription of *Terebellides kerguelensis* stat. nov. McIntosh, 1885 (Polychaeta: Trichobranchidae) from Antarctic and subantarctic waters. Helgoland Marine Research 62: 143–152. https://doi.org/10.1007/s10152-007-0085-4

Parapar J, Moreira J (2008b) Revision of three species of *Terebellides* (Polychaeta: Trichobranchidae) described by C. Hessle in 1917 from the Southern Ocean. Journal of Natural History 42: 1261–1275. https://doi.org/10.1080/00222930801989997

Parapar J, Moreira J, Gil J, Martin D (2016a) A new species of the genus *Terebellides* (Polychaeta, Trichobranchidae) from the Iranian coast. Zootaxa 4117(3): 321–340. https://doi.org/10.11646/zootaxa.4117.3.2

Parapar J, Moreira J, Helgason GV (2011) Taxonomy and distribution of *Terebellides* (Polychaeta, Trichobranchidae) in Icelandic waters, with the description of a new species. Zootaxa 2983: 1–20. https://doi.org/10.11646/zootaxa.2983.1.1

Parapar J, Moreira J, Martin D (2016b) On the diversity of the SE Indo-Pacific species of *Terebellides* (Annelida; Trichobranchidae), with the description of a new species. PeerJ 4: e2313. https://doi.org/10.7717/peerj.2313

Parapar J, Moreira J, O'Reilly M (2016c) A new species of *Terebellides* (Polychaeta: Trichobranchidae) from Scottish waters with an insight into branchial morphology. Marine Biodiversity 46: 211–225. https://doi.org/10.1007/s12526-015-0353-5

Rach J, DeSalle R, Sarkar IN, Schierwater B, Hadrys H (2008) Character-based DNA barcoding allows discrimination of genera, species and populations in Odonata. Proceedings of the Royal Society B – Biological Sciences 275 (1632): 237–247. https://doi.org/10.1098/rspb.2007.1290

Read G, Fauchald K (2020) World Polychaeta database. *Terebellides* Sars, 1835. [Accessed through: World Register of Marine Species at] http://www.marinespecies.org/aphia.php?p=taxdetails&id=129717 [accessed on 23 Sept 2020]

Sars M (1835) Beskrivelser og iagttagelser over nogle maerkelige eller nye i Havet ved den Bergenske Kyst levende Dyr af Polypernes, Acephalernes, Radiaternes, Annelidernes og Molluskernes Classer, med en kort Oversigt over de hidtil af Forfatteren sammesteds fundne Arter og deres Forekommen. Thorstein Hallagers Forlag hos Chr. Dahl, Bergen, 81 pp. https://doi.org/10.5962/bhl.title.13017

Schüller M, Hutchings PA (2010) New insights in the taxonomy of Trichobranchidae (Polychaeta) with the description of a new *Terebellides* from Australia. Zootaxa 2395: 1–16. https://doi.org/10.11646/zootaxa.2395.1.1

Schüller M, Hutchings PA (2012) New species of *Terebellides* (Polychaeta: Trichobranchidae) indicate long-distance dispersal between western South Atlantic deep-sea basins. Zootaxa 3254: 1–31. https://doi.org/10.11646/zootaxa.3254.1.1

Schüller M, Hutchings PA (2013) New species of *Terebellides* (Polychaeta: Trichobranchidae) from deep Southern Ocean. Zootaxa 3619: 1–45. https://doi.org/10.11646/zootaxa.3619.1.1

Tomioka S, Kondoh T, Sato-Okoshi W, Ito K, Kakui K, Kajihara H (2016) Cosmopolitan or cryptic species? A case study of *Capitella teleta* (Annelida: Capitellidae). Zoological Science 33(5): 545–554. https://doi.org/10.2108/zs160059

Wong EHK, Shivji MS, Hanner RH (2009) Identifying sharks with DNA barcodes: assessing the utility of a nucleotide diagnostic approach. Molecular Ecology Resources 9: 243–256. https://doi.org/10.1111/j.1755-0998.2009.02653.x

Zhang J, Hutchings P (2018) Taxonomy and distribution of *Terebellides* (Polychaeta: Trichobranchidae) in the northern South China Sea, with description of three new species. Zootaxa 4377(3): 387–411. https://doi.org/10.11646/zootaxa.4377.3.4

Supplementary material 1

Table S1. Locality and collecting data, museum registration numbers and references to figures of *Terebellides* specimens

Authors: Julio Parapar, María Capa, Arne Nygren, Juan Moreira

Data type: occurences

Explanation note: Locality and collecting data, museum registration numbers and references to figures of *Terebellides* specimens described in this work. Country names are transcribed from original museum vials.

Link: https://doi.org/10.3897/zookeys.992.55977.suppl1

Supplementary material 2

Table S2. List of COI sequences considered in present study (Group A), museum vouchers and GenBank accession numbers

Authors: Julio Parapar, María Capa, Arne Nygren, Juan Moreira

Data type: COI sequences, museum vouchers and GenBank accession numbers

Explanation note: List of COI sequences considered in present study (Group A), museum vouchers and GenBank accession numbers. Abbreviations of housing institutions: ZMBN = Department of Natural History, University Museum of Bergen; GNM = The Gothenburg Museum of Natural History; NTNU-VM = Norwegian University of Science and Technology, University Museum, Trondheim; SMF = Senckenberg Museum Frankfurt.

Link: https://doi.org/10.3897/zookeys.992.55977.suppl2

ZooKeys 992: 59–104 (2020)
doi: 10.3897/zookeys.992.54856
https://zookeys.pensoft.net

RESEARCH ARTICLE

A peer-reviewed open-access journal
ZooKeys
Launched to accelerate biodiversity research

Four new *Cyclopina* (Copepoda, Cyclopinidae) from South Korea

Tomislav Karanovic[1]

1 *Hanyang University, College of Natural Sciences, Department of Life Science, Seoul 04763, Republic of Korea*

Corresponding author: Tomislav Karanovic (tomislav.karanovic@gmail.com)

Academic editor: D. Defaye | Received 29 May 2020 | Accepted 23 October 2020 | Published 12 November 2020

http://zoobank.org/E604D905-F161-482D-9944-75496EEFF427

Citation: Karanovic T (2020) Four new *Cyclopina* (Copepoda, Cyclopinidae) from South Korea. ZooKeys 992: 59–104. https://doi.org/10.3897/zookeys.992.54856

Abstract

Copepods are well studied in South Korea, with the exception of marine non-parasitic cyclopoids, and especially cyclopinids; only three species were found so far here, and only one of them is endemic. A survey of intertidal interstitial faunas from sandy beaches revealed four endemic members of the genus *Cyclopina* Claus, 1863, which represents the first record of the largest cyclopinid genus in South Korea. A detailed study of their morphology revealed numerous differences, including in rarely studied cuticular organs. Some of these micro-characters could easily be homologised and showed little intraspecific variability, which might prove invaluable for matching sexes and reconstructing phylogenetic relationships. *Cyclopina busanensis* **sp. nov.** is described from both sexes collected near Busan (South Coast of South Korea), and is most similar to the only congener from Japan: *C. kiraensis* Horomi, 1984. *Cyclopina koreana* **sp. nov.** is described from both sexes collected near Gangneung (East Coast), and has no close relatives among currently known species. *Cyclopina curtijeju* **sp. nov.** is described from two females from Jeju (off South Coast); it is possibly closely related to *C. smirnovi* Herbst, 1982, but the latter is known from a single male from the Russian Far East. *Cyclopina wido* **sp. nov.** is described from both sexes from Wido (West Coast), and shows numerous reductions in segmentation and armature of appendages, most of them probably a consequence of its diminutive size. A table of 26 discrete and continuous characters commonly used in the taxonomy of this group is provided for 48 valid species and subspecies of *Cyclopina*.

Keywords

Cyclopoida, intertidal zone, meiofauna, new species, stygofauna, taxonomy

Introduction

Marine cyclopoids, and especially cyclopinids, are poorly studied globally because their diversity is highest in marginal habitats, such as intertidal interstitial and anchialine caves, or in highly inaccessible abyssal and hadal depths. Only three cyclopinids have been reported so far from Korea: *Cyclopinoides orientalis* Chang, 2011; *Cyclopinopsis deformata* Lee & Chang, 2019; and *Paracyclopina nana* Smirnov, 1935. The first species was described by Chang (2011) from one beach on the East Coast of mainland Korea, one beach on Jeju Island (Korea), and one beach on Tsushima Island (Japan). The second species was described by Lee and Chang (2019) from a shallow littoral (25 m) on the East Coast and intertidal sands on the West Coast of South Korea. The third species was described by Smirnov (1935) from Vladivostok (Russia) and was subsequently reported also from China (Shen 1979), Japan (Ueda et al. 2001), and South Korea (Chang 2009, 2010); interestingly, this cyclopinid has become a model organism for various genomic and physiological studies in recent years (Jeong et al. 2015; Lee et al. 2015, 2017). Chang (2011) also mentioned unidentified specimens belonging to the genus *Cyclopina* Claus, 1863 accompanying *Cyclopinoides orientalis*, but it is unclear if these were collected in South Korea or Japan. It is possible that these specimens are conspecific with one (or more) of the four South Korean species described in this paper, but it is also possible that they belong to *Cyclopina kiraensis* Hiromi, 1984, which is the only species from this genus described so far from Japan and seems to be relatively widely distributed there (Hiromi 1984; Ueda et al. 2001).

Copepods are generally relatively well studied in South Korea, both as free-living forms in marine (Soh et al. 2010; Lee et al. 2012) and freshwater environments (Chang 2009, 2010), as well as parasites of other organisms (Kim 2008). However, utilisation of novel taxonomic methods, such as the study of microstructures (Karanovic and Cho 2012, 2016, 2017; Karanovic and Lee 2012; Karanovic et al. 2013) and DNA (Karanovic and Kim 2014a, b; Karanovic et al. 2014, 2015; Kim et al. 2014), and survey of marginal and previously understudied habitats, such as marine interstitial (Karanovic 2014, 2017; Karanovic et al. 2012a, b; Karanovic and Lee 2016), resulted in numerous recent additions. While most interstitial copepods are harpacticoids (Giere 1993), a recent survey of selected intertidal beaches in South Korea brought to light four new species of *Cyclopina* presented here. There are no published data on how much of the South Korean coastline is sandy, but it is a significant ecosystem without any doubt. South Korea has 12,478 kilometres of coastline along three seas (Pruett and Cimino 2000) and some three-quarters of the world's ice-free coastlines consist of sandy shores (Brown and McLachlan 2006). Like in most developed economies, this ecosystem is under constant anthropogenic pressure and, being a marginal habitat, is rarely included in protected natural reserves. However, marine interstitial harbours a disproportionate level of biodiversity (Gray 1997; Thrush et al. 2006; Karanovic 2008), which is yet to be fully appreciated and understood (Armonies and Reise 2000; Gray 2002; Zeppelli et al. 2015).

Cyclopina is the oldest and type cyclopinid genus, as well as the largest by number of species (Boxshall and Halsey 2004). It was established by Claus (1963), with *C. gracilis* Claus, 1863 as the type species. Approximately 70 other species and subspecies have been described since then, but many of them were subsequently transferred to newly established genera or synonymised. However, this genus still contains more than 30% of cyclopinid species (Boxshall and Halsey 2004; Walter and Boxshall 2020). The most recent key to species and subspecies was provided by Vervoort (1964) and it was based on an earlier one provided by Lindberg (1953). This makes identification of species difficult. A lack of morphological detail in early species descriptions (including nearly half of them described only after one sex) and wide intraspecific variability between highly disjunct populations in some presumably widely distributed species make it impossible to construct a reliable key to species (Karanovic 2008). Also, there are no published lists of characters for all species in the genus; most authors usually comparing new or redescribed species with only a few congeners. Apparent differences in the armature of mouthparts between disjunct populations were often ignored, usually based on suspicion of earlier inadequate descriptions (Jaume and Boxshall 1996), although they proved valuable in distinguishing some Australian congeners (Karanovic 2008). Most *Cyclopina* species, however, have never been recorded and redescribed after their original description, which is arguably the largest problem for the taxonomy of this genus.

Cyclopinid systematics at large is also still in a state of flux (Boxshall and Jaume 2012 and references therein), which is perhaps best illustrated by the fact that Walter and Boxshall (2020) list *Heterocyclopina* Pleşa, 1969 in the family Cyclopinidae and the supposedly closely related genus *Procyclopina* Herbst, 1955 in the family Hemicyclopinidae. Both genera were considered members of the allegedly monophyletic Hemicyclopinidae by Martínez Arbizu (2001a), in addition to *Pseudocyclopina* Lang, 1946 and five other genera. However, the genus *Pseudocyclopina* was considered a member of Cyclopinidae by Elwers et al. (2001), with one of the co-authors being Martínez Arbizu. As noted by Boxhall and Halsey (2004), the phylogenetic analysis presented by Martínez Arbizu (2001a) as a justification for the establishment of the Hemicyclopinidae was not parsimony based and hinged on a single character, which is also present in at least four unrelated genera. Some of the characters used by Martínez Arbizu (2000a, b, 2001a, b, 2006) to define supposedly monophyletic families of cyclopinids were shown to be part of intraspecific variability, and sometimes even asymmetries (Karanovic 2008). A polyphyletic nature of cyclopinids was already suspected by Ho (1986), Ho and Thatcher (1989), and Huys and Boxshall (1991), based on the analysis of morphological characters. It was confirmed by Khodami et al. (2017), based on the analysis of four genes and 205 copepod species. However, the molecular phylogeny presented by Khodami et al. (2017) did not recover monophyly of previously proposed monophyletic families (where they had representatives of more than one genus). The same authors proposed another two new families, each containing a single cyclopinid genus, and one of them a single species. This certainly contributes very little to our understanding of the phylogenetic relationships between cyclopinid

genera, but unfortunately, no comprehensive, parsimony-based test of the validity of the new families has yet been carried out (Boxshall and Jaume 2012). It should be noted that subsequent re-analyses of the molecular dataset published by Khodami et al. (2017) failed to reproduce both their topology and branch supports, despite the use of the same methods and software (Mikhailov and Ivanenko 2019a). It is reasonable to conclude that we are still in the early stages of understanding cyclopoid systematics, with wider taxon and character sampling continuing to raise as many questions as they answer (Khodami et al. 2019; but see Mikhailov and Ivanenko 2019b). Validity of many genera is widely disputed among different researches (see, for example, Karanovic 2008; Ivanenko et al. 2019). The fact that nearly 60% of all cyclopinid genera are monotypic (Boxshall and Halsey 2004; Karanovic 2008; Suárez-Morales and Almeyda-Artigas 2015; Walter and Boxshall 2020) clearly indicates that we are not even close to discovering the major extent of their diversity. There is no doubt that we will have to look for alternative characters when trying to reconstruct phylogenetic relationships between cyclopinids. Cuticular organs on somites were recently suggested as suitable micro-characters for reconstructing phylogenetic relationships between some harpacticoid copepods (Karanovic and Kim 2014b) and also for distinguishing closely related species using geometric morphometrics (Karanovic et al. 2016, 2018). However, in cyclopoids they seem to be more numerous, variable, and difficult to homologise (Karanovic and Blaha 2019).

Aims of this study were to describe four new species from South Korea in fine detail, asses their affinities using morphological characters, provide a global list of valid *Cyclopina* species and subspecies, and assemble a table of discrete and morphometric morphological characters most commonly used to identify species in this genus.

Materials and methods

All specimens were collected from the intertidal zone in four localities in South Korea, using the Karaman-Chappuis method. This sampling technique involves digging a hole on the beach down to the water level and then decanting the inflowing interstitial water and filtering it through a plankton net (mesh size 30 µm). All samples were fixed in 99% ethanol, sorted in the laboratory also in 99% ethanol, using an Olympus SZX12 dissecting microscope with PLAPO objectives and magnification of up to 200 ×. Locality data and number of specimens are listed for each species separately and all material is deposited in the National Institute of Biological Resources (**NIBR**), Incheon, South Korea.

Some specimens were dissected and mounted on microscope slides in Faure's medium (see Stock and von Vaupel Klein 1996), and dissected appendages were then covered by a coverslip. For the urosome, two human hairs of appropriate thickness were mounted between the slide and coverslip during examination, to prevent squashing. All line drawings were prepared using a drawing tube attached to a Leica MB2500 phase-interference compound microscope, equipped with N-PLAN (5 ×, 10 ×, 20 ×, 40 ×, and 63 × dry) or PL FLUOTAR (100 × oil) objectives. Specimens that were not

drawn were examined in glycerol and, after examination, were stored in 99.9% ethanol. Specimens for scanning electron microscopy (SEM) were transferred into pure isoamyl-acetate for two hours, critical-point dried, mounted on stubs, coated in gold, and observed under a Hitachi S-4700 scanning microscope on the in-lens detector, with an accelerating voltage of 10 kV and working distances between 12 mm and 13.5 mm; micrographs were taken with a digital camera.

The terminology for morphological characters mostly follows Huys and Boxshall (1991), except for the numbering of setae on the caudal rami (not used) and small differences in the spelling of some appendages (antennula, mandibula, maxillula instead of antennule, mandible, maxillule); the latter as an attempt to standardise the terminology for homologous appendages in different crustacean groups. However, the terminology of maxilla and maxilliped follows revisions proposed by Ferrari and Ivanenko (2008). In order to save space and avoid unnecessary repetitions, species descriptions are comparative.

Results

***Cyclopina busanensis* sp. nov.**
http://zoobank.org/F8FFA47A-D9C4-4826-A6F1-5F286041EE1A
Figures 1–6, 17A

Type locality. South Korea, South Coast, Busan, Sonjong Beach, intertidal sand, 35°10.741'N, 129°12.317'E.

Specimens examined. ***Holotype*** ovigerous female dissected on one slide, collected from the type locality, 6 May 2016, leg. T. Karanovic. ***Paratypes*:** one male (allotype) and two females dissected on one slide each, seven females (one ovigerous) and five copepodids in alcohol, and five females on one SEM stub (together with specimens of other three species described here; row no. 2), all collected from the type locality, 6 May 2016, leg. T. Karanovic.

Etymology. The species name refers to the type locality. It is an adjective for place, made with the Latin suffix *-ensis*.

Description. Female (based on holotype and seven paratypes). ***Body length***, excluding caudal setae, from 515 to 535 µm. ***Colour*** of preserved specimens light brown, nauplius eye not visible (Fig. 17A). Integument on all somites smooth (Figs 1–3), with light bacterial cover, spinules only on genital and anal somites and caudal rami, cuticular pores on all somites, and sensilla on all but penultimate somite; hyaline fringes of prosomites smooth, of urosomites serrated. ***Habitus*** (Figs 1A, 3A) ca. 2.8 × as long as wide in dorsal view, with pronounced distinction between prosome and urosome; prosome ovoid, ca. 1.6 × as long as wide in dorsal view, nearly 1.3 × as long and 2.6 × as wide as urosome, its greatest width at posterior end of first pedigerous somite; urosome gently tapering towards posterior end, 3.3 × as long as wide, its greatest width at posterior end of fifth pedigerous somite (first urosomite). First pedigerous somite (Fig. 1A, F) not

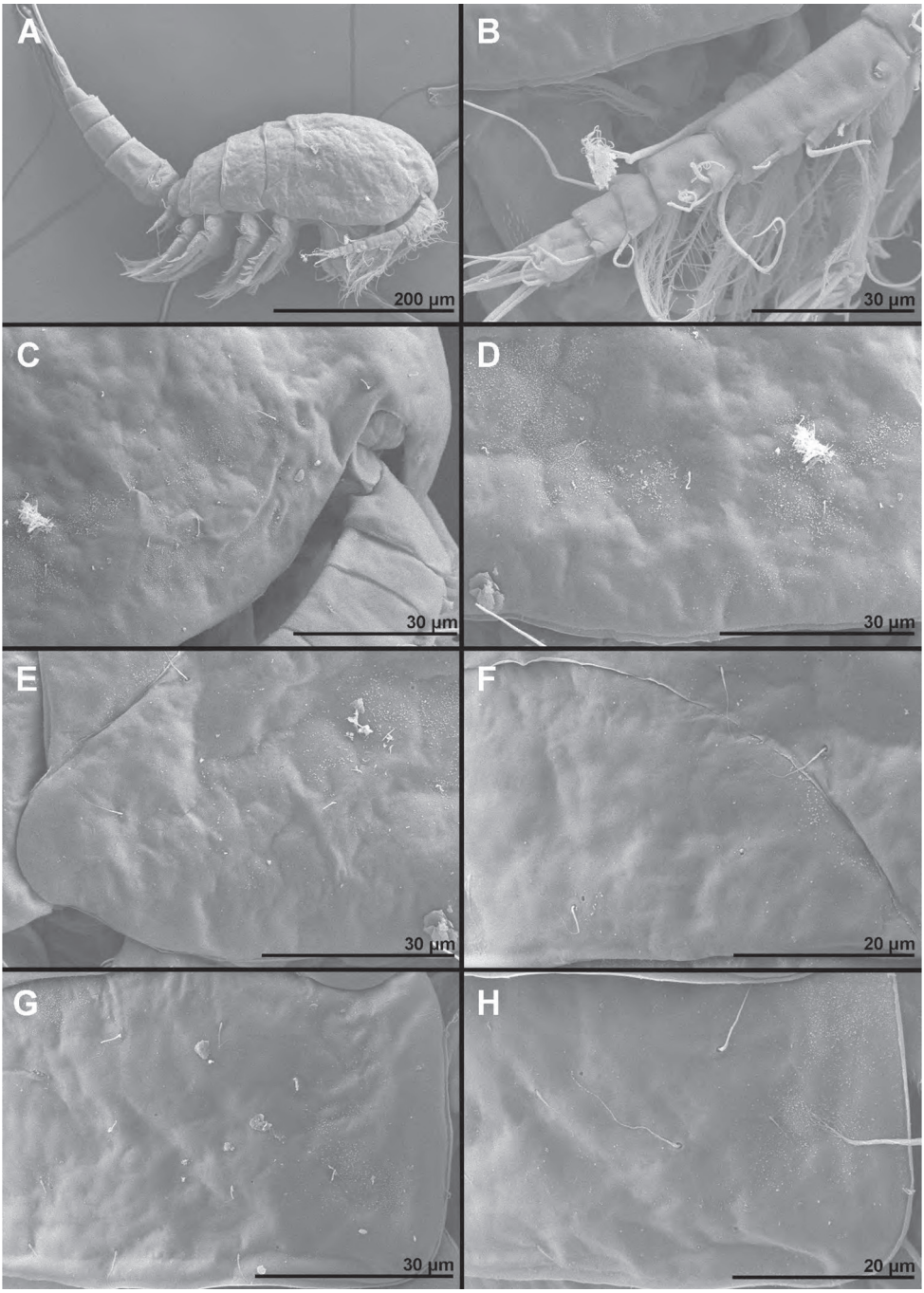

Figure 1. *Cyclopina busanensis* sp. nov., paratype female 1, SEM photographs, all in lateral view **A** habitus **B** distal part of antennula **C** anterior part of cephalothorax with rostrum **D** central part of cephalothoracic shield **E** postero-lateral corner of cephalothoracic shield **F** tergite of first pedigerous somite (= first free prosomite), mostly covered by postero-lateral corner of cephalothoracic shield **G** tergite of second pedigerous somite **H** tergite of third pedigerous somite.

fused to cephalothorax, but its tergites partly covered with posterior extensions of cephalothoracic shield (Fig. 1A, E). Pedigerous somites without lateral expansions. ***Rostrum*** (Fig. 1C, B) well-developed, membranous, very broad. ***Cephalothorax*** (Figs 1A, C–E, 3B, C) nearly conical,approximately as long as wide, and 1.3 × as long as free prosomites combined. Second to fourth free prosomites (Figs 1A, G, H, 2A, 3D) progressively shorter and narrower towards posterior end, and with fewer cuticular organs.

First urosomite (Figs 1A, 2C, 3A) shortest, laterally expanded in posterior part.

Genital double-somite (Figs 2C–E, 3E, F, 4A) ca. 1.2 × as long as wide in dorsal view, laterally expanded anterior part nearly 1.4 × as wide as posterior margin; anterior part (second urosomite) with one pair of narrowly spaced posterior dorsal sensilla (Fig. 3E), large dorsal medial pore in between them (Fig. 3E), one pair of widely spaced anterior dorsal sensilla, one pair of small widely spaced anterior dorsal pores, one pair of narrowly spaced ventral pores next to copulatory pore (Fig. 4A), and two pairs of large pores, two pairs of small pores, and longitudinal row of spinules next to genital apertures (Fig. 2D); posterior part (third urosomite) with also with one pair of narrowly spaced posterior sensilla and large dorsal medial pore in between them (Fig. 3F), one pair of lateral posterior sensilla (Fig. 2E), one pair of large lateral pores (Fig. 2E), one pair of widely spaced ventral pores (Fig. 4A), and two pairs of posterior ventral sensilla (Fig. 4A). Medial copulatory pore (Fig. 4A) hardly bigger than cuticular pores next to it, situated in first third. Copulatory duct (Fig. 4A) narrow, rigidly sclerotised, T-shaped. Seminal receptacles (Fig. 4A) weakly sclerotised, simple, ovoid, with space between them slightly wider than one receptacle, reaching posteriorly slightly beyond level of copulatory pore. Oviducts weakly sclerotised, short. Genital apertures situated laterally, covered by reduced sixth legs. Paired egg sacs ovoid, each containing 8–10 eggs, twice as long and ca. 1.2 × as wide as genital double-somite. Fourth urosomite (Figs 2F, 3G, 4A) ca. 0.6 × as long as genital double-somite, with sensilla and pores as in third urosomite, except ventral pores situated slightly more posteriorly and more narrowly spaced. Fifth urosomite (Figs 2F, 3G, 4A) 0.8 × as long as fourth urosomite, with medial dorsal pore and one pair of widely spaced ventral pores. Sixth (anal) urosomite (Figs 2G, H, 3H, 4A) nearly 0.8 × as long as fifth urosomite, with one pair of large dorsal sensilla, one pair of dorsal pores, two pairs of ventral pores, and three rows of slender spinules fringing anal sinus; anal operculum smooth, short, broad, slightly concave, situated in first third, represents 66% of somite's width.

Caudal rami (Figs 2G, 4A) cylindrical, ca. 3.7 × as long as wide and twice as long as anal somite, narrowly spaced on anal somite, diverging posteriorly; armed with one proximal lateral seta, one dorsal seta, and four terminal setae; ornamented with row of small spinules at base of proximal lateral seta, and posterior ventral row of spinules. All setae slender and pinnate, and all except dorsal seta uni-articulated at base; two central terminal setae much longer and stronger than others and both with breaking planes; dorsal seta inserted close to posterior margin, biarticulated at base; proximal lateral seta inserted atapproximately two fifths of ramus' length; medial terminal seta 1.2 × as long as caudal ramus, 1.6 × as long as lateral terminal seta, 1.5 × as long as dorsal seta, and 2.5 × as long as proximal lateral seta.

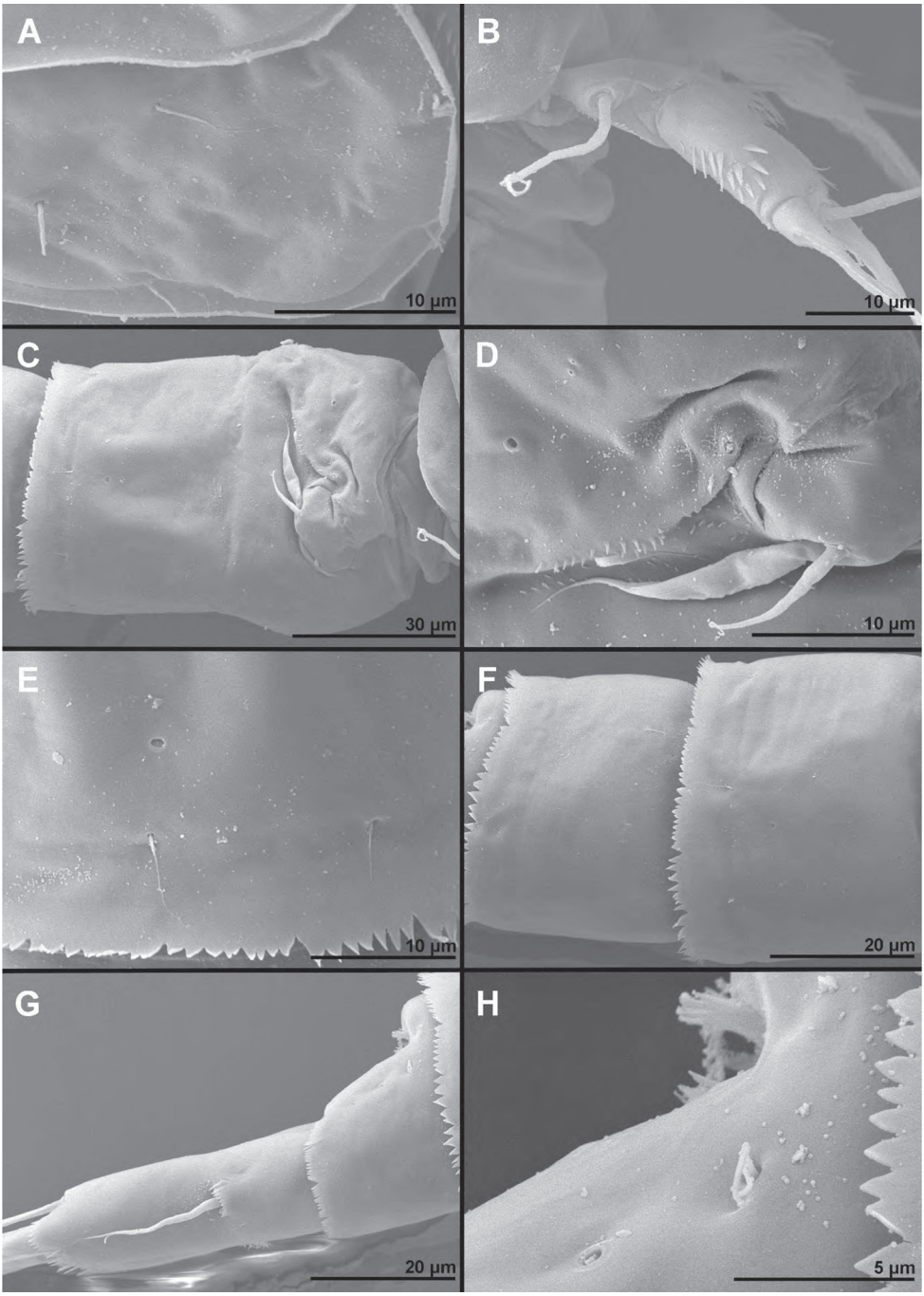

Figure 2. *Cyclopina busanensis* sp. nov., paratype female 1, SEM photographs, all in dorsal view **A** tergite of fourth pedigerous somite **B** fifth leg **C** genital double-somite (=fused second and third urosomites) **D** sixth leg **E** detail of posterior part of genital double-somite **F** fourth and fifth urosomites **G** sixth urosomite (= anal somite) and caudal ramus **H** detail of sixth urosomite.

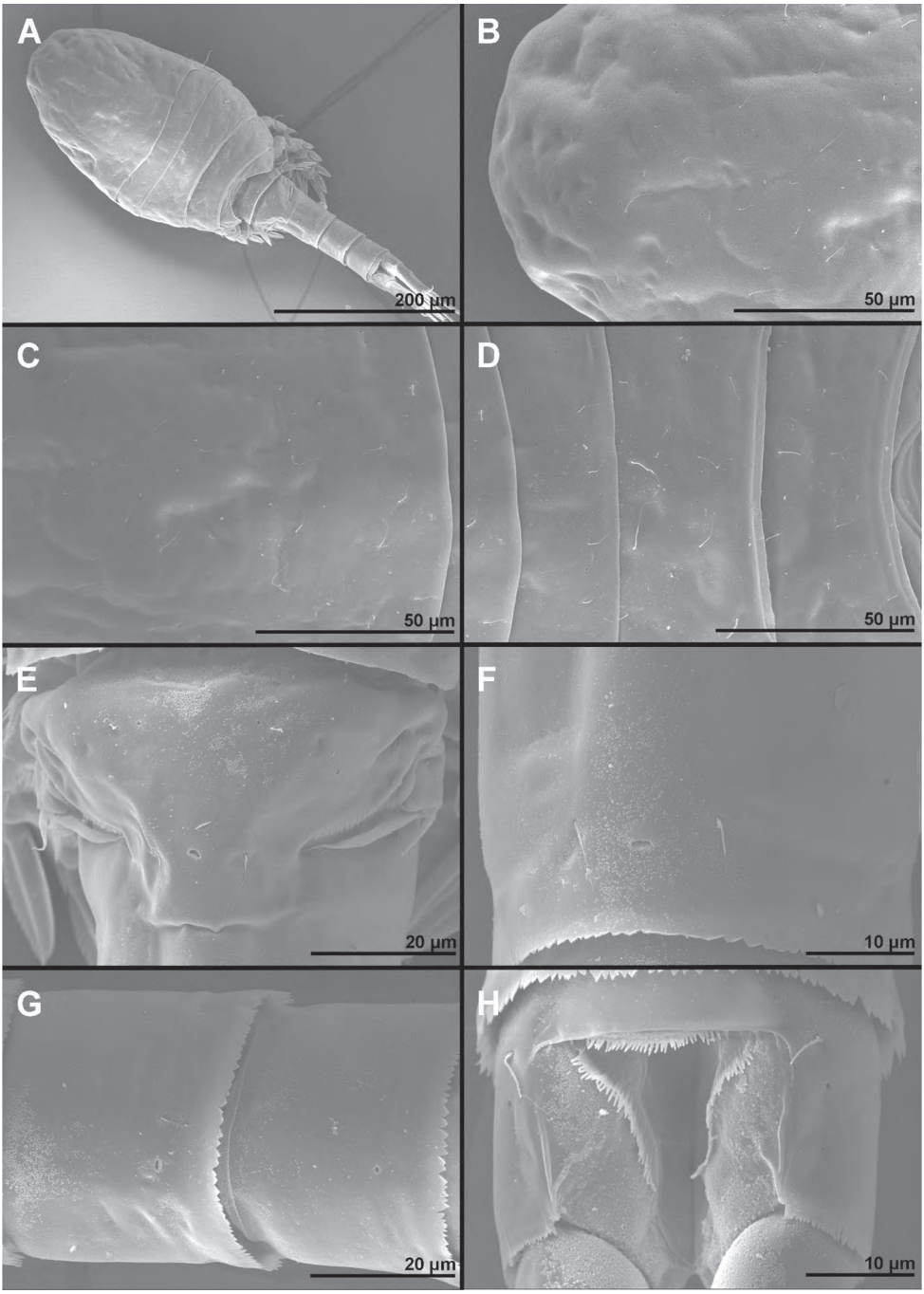

Figure 3. *Cyclopina busanensis* sp. nov., paratype female 2, SEM photographs, all in dorsal view **A** habitus **B** anterior part of cephalothorax **C** posterior part of cephalothorax **D** free prosomites **E** anterior part of genital double-somite **F** posterior part of genital double-somite **G** fourth and fifth urosomite **H** sixth urosomite.

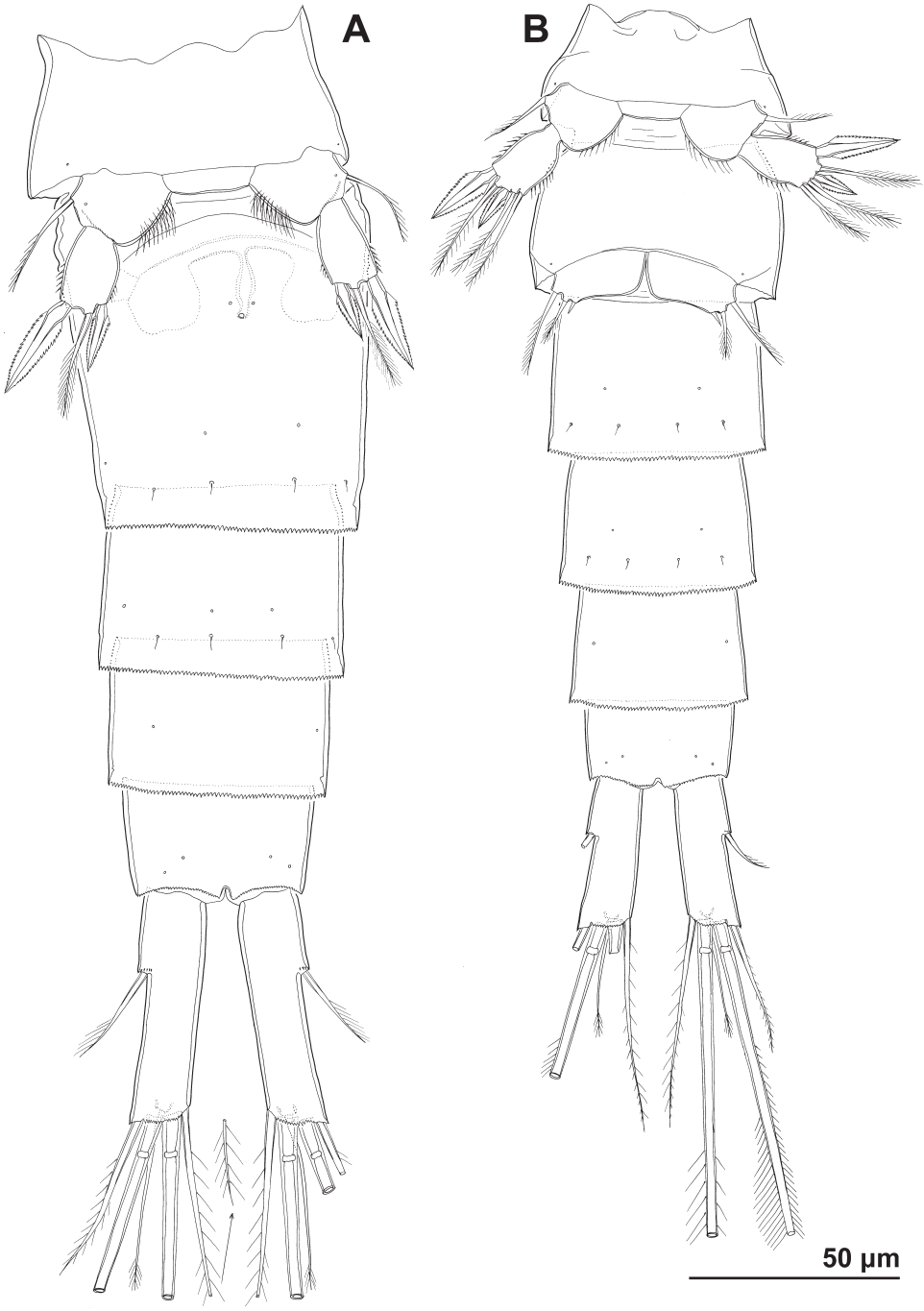

Figure 4. *Cyclopina busanensis* sp. nov., line drawings **A** holotype female, urosome, ventral view **B** allotype male, urosome, ventral view.

Antennula (Figs 1A, B, 5A) reaching two thirds of cephalothoracic shield with its distal tip, stout, smooth, cylindrical but tapering towards distal end, 10-segmented; no setae with breaking planes or biarticulated, one seta on fifth segment short and spiniform, largest seta on ultimate segment and seven setae on second and third segments bipinnate, all other setae smooth and slender; single slender aesthetasc on ultimate segment fused basally to slender seta; armature formula (ae = aesthetasc) 3.5.8.4.5.7.4.3.2.7+ae; sixth segment longest, ca. 2.8 × as long as wide, and more than 0.8 × as long as subsequent four segments combined; tenth segment 1.5 × as long as wide.

Antenna (Fig. 5B) slender, cylindrical, four-segmented, with highly mobile joint between second and third segment; first segment (probably allobasis) longest and widest, twice as long as wide, slightly curved, unornamented, armed with single strong medial-distal seta and twice as long exopodal seta; second segment (probably first endopodal) 0.8 × as long as basis, twice as long as wide, with spinules along medial convex margin, and with single medial seta inserted mid-length; second endopodal segment slightly narrower and only half as long as first endopodal, with spinules along lateral margin, and with four medial setae (shortest one inserted in proximal half, three near distal-medial corner; one distal seta spiniform, others slender); third endopodal segment 1.4 × as long as second endopodal and twice as long as wide, with spinules along lateral margin and seven apical setae (four strong and prehensile, three slender).

Mandibula (Fig. 5C, D) with large coxa, and smaller palp consisting of basis, two-segmented endopod, and four-segmented exopod; coxal gnathobase with relatively wide cutting edge consisting of four polycuspidate large teeth (ventralmost largest), three smaller unicuspid teeth (dorsalmost with serrated edges, others smooth), row of spinules at base of two central polycuspidate teeth, and two short setae; dorsalmost seta on cutting edge smooth, ca. 1.5 × as long as other, bipinnate seta; basis ovoid, 1.7 × as long as wide, with single medial seta; endopod 0.6 × as long as basis, with three setae on first and five setae on second segment; exopod slightly shorter than basis but much more slender, with armature formula 1.1.1.2; all setae on basis, endopod, and exopod slender and pinnate.

Maxillula (Fig. 5E, F) unornamented, composed of well-developed praecoxa and three-segmented palp; arthrite of praecoxa with six strong and pinnate apical spines, one isolated smooth spine on posterior surface, two spiniform plumose setae, and two smooth minute setae (or perhaps large spinules?) in between plumose setae and spines; proximalmost seta longest and strongest element, three × as long as other seta and ca. 1.1 × as long as longest and strongest (ventralmost) spine; coxa reduced to small endite partly fused to arthrite of praecoxa, bearing single slender seta, and another slender seta probably belonging to former epipodite; palp slightly smaller than praecoxa, composed of large rectangular basis, small ovoid endopod, and also ovoid but shorter and wider exopod; basis twice as long as wide, with short proximal and distal endites bearing three and two setae respectively; endopod slightly longer than greatest width of basis, ca. 1.5 × as long as wide, with two medial and four distal slender setae (one smooth,

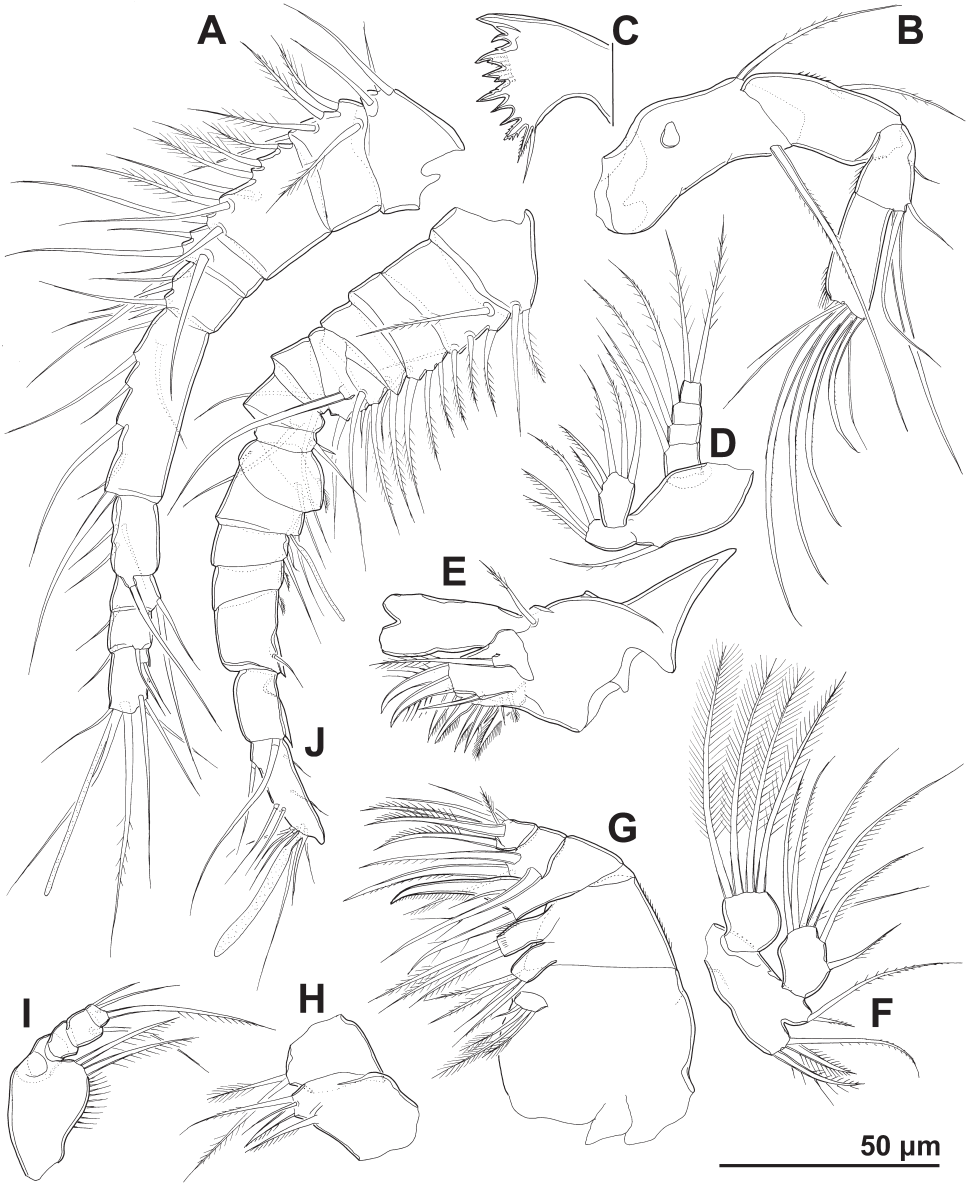

Figure 5. *Cyclopina busanensis* sp. nov., line drawings **A–I** holotype female **J** allotype male: **A** antennula **B** antenna **C** cutting edge of mandibula **D** mandibular palp **E** praecoxa of maxillula **F** maxillular palp **G** maxilla **H** syncoxa and basis of maxilliped **I** endopod of maxilliped **J** antennula.

others unipinnate); exopod 0.8 × as long as endopod, as long as wide, with four distal slender and plumose setae.

Maxilla (Fig. 5G) stout, 1.6 × as long as wide, tapering towards distal end, ornamented with row of spinules along lateral margin and several spinules on endites,

composed of syncoxa (fused praecoxa and coxa), basis, and three-segmented endopod; syncoxa largest, quadrate, with four setae on proximal endite and one seta on distal endite; basis ca. 0.6 × as long as syncoxa, also quadrate, with three setae on proximal endite and three setae on distal endite; first endopodal segment half as long as coxa, with basally fused, smooth and robust claw and two articulated setae, proximal seta strong and bipinnate, slightly longer than claw, distal seta smooth and minute; second and third endopodal segments combined slightly longer than first, second segment somewhat longer than third and armed with four strong setae, third segment armed with three strong and three slender setae.

Maxilliped (Fig. 5H, I) prehensile, slender, almost 3.5 × as long as wide, seven-segmented, composed of syncoxa, basis, and five-segmented endopod; syncoxa rhomboidal, approximately as long as wide, unornamented, with one element on proximal endite and three on distal endite; basis slightly smaller than syncoxa, quadrate, unornamented, with two setae on only endite; first endopodal segment nearly as long as syncoxa and basis combined, 1.6 × as long as wide, with row of long spinules along swollen medial margin, and with two spiniform setae near distal medial corner; distal part of endopod cylindrical, 0.7 × as long as basis, 2.4 × as long as wide, with armature formula 0.0.1.3, second endopodal segment partly fused to first endopodal and last segment half as long as any other; medial apical seta spiniform, 1.7 × as long as last four endopodal segments, twice as long as central apical seta, and 1.4 × as long as setae on first endopodal segment; other three endopodal setae slender.

Swimming legs (Figs 1A, 6A–E) large, composed of short praecoxa, rectangular large coxa, triangular basis, three-segmented exopod, three-segmented endopod, and coxae of opposite appendages connected with squarish intercoxal sclerite; coxae of all legs with pore on anterior surface, row of spinules along lateral margin, and slender seta on medial-distal corner; intercoxal sclerites unornamented, with nearly straight distal margin; basis with slender lateral seta, anterior pore, row of long spinules along convex medial margin, row of minute spinules at base of lateral seta, and strong medial spine on first leg and short spiniform process instead on other legs; all exopodal segments with short spinules along lateral margin, and all endopodal segments with long and slender spinules along lateral margin; second endopodal segment of first to third leg with single anterior pore, third endopodal segment of first leg with two anterior pores, and third endopodal segments of second to fourth leg with single anterior pore; first and second exopodal segments with single lateral spine and single medial seta; first endopodal segments of all legs and second endopodal segment of first leg with single medial seta; second endopodal segments of second to fourth legs with two medial setae; third endopodal segments seta formula 6.6.6.5; third exopodal segment seta formula 4.5.5.5 and spine formula 4.4.4.3; third endopodal segment of fourth leg 1.7 × as long as wide and third exopodal segment of fourth leg ca. 1.5 × as long as wide; all setae slender and all spines lanceolate.

Fifth leg (Figs 2B, 4A) small, two-segmented, with short intercoxal sclerite; first segment (presumably basis)approximately as long as wide, with single lateral seta, single anterior pore, several parallel rows of long spinules along convex medial margin,

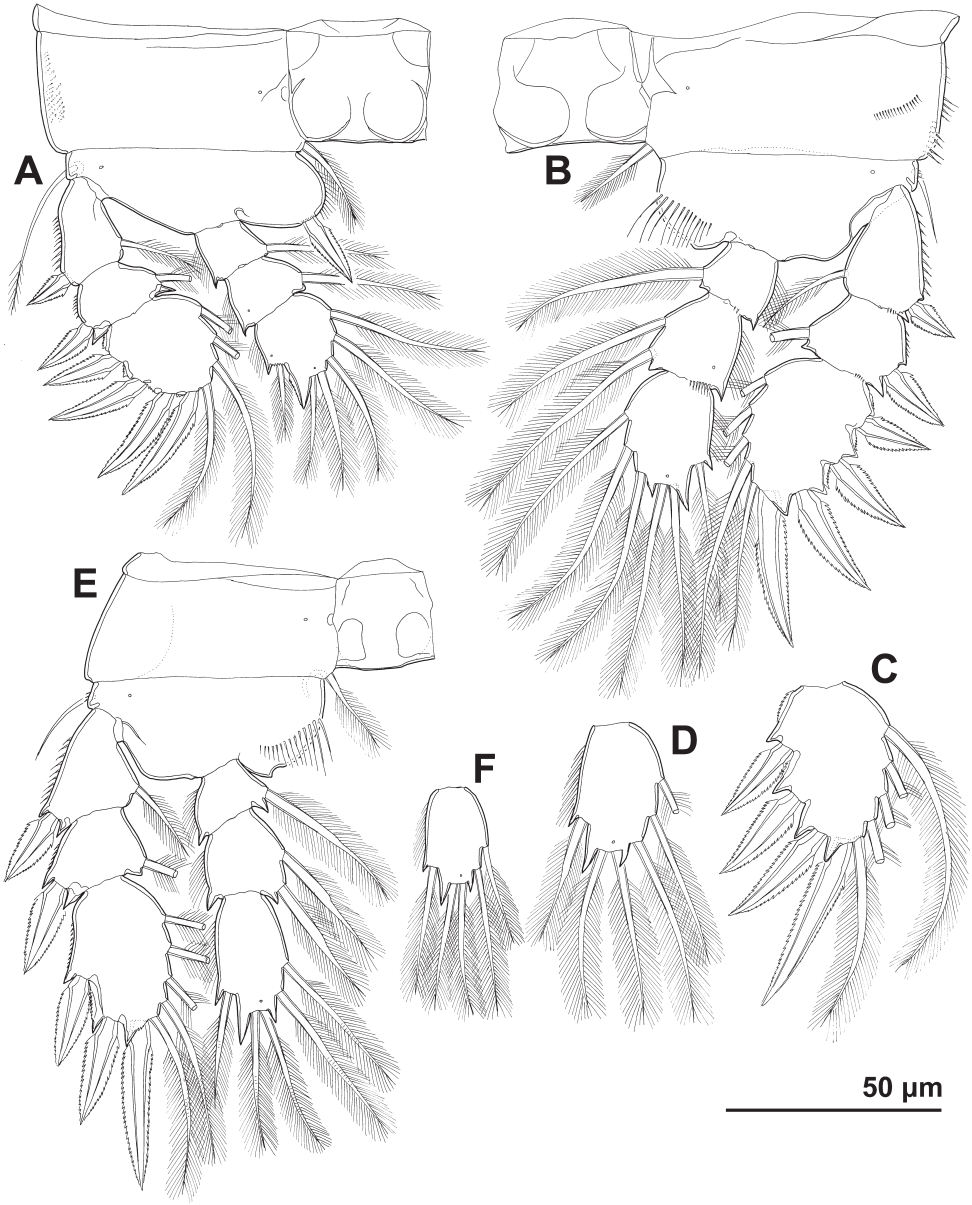

Figure 6. *Cyclopina busanensis* sp. nov., line drawings **A–E** holotype female **F** allotype male: **A** first swimming leg **B** second swimming leg **C** third exopodal segment of third swimming leg **D** third endopodal segment of third swimming leg **E** fourth swimming leg **F** third endopodal segment of fourth swimming leg.

and distal row of minute spinules; second segment (presumably exopod) ca. 1.3 × as long as first but much narrower, 1.6 × as long as wide, with spinules along both medial and lateral slightly convex margins, apical central seta and two subapical spines; lateral spine 1.2 × as long as exopod and 1.6 × as long as medial spine.

Sixth leg (Fig. 2D) simple semi-circular flap, mostly fused to genital somite, approximately twice as wide as long, unornamented, with two dorsally directed setae; lateral seta much stronger and nearly twice as long as medial seta.

Male (based on allotype). ***Body*** length 503 µm. ***Urosome*** (Fig. 4B) slenderer than in female, and second and third urosomites fully articulated; ornamentation as in female, except ventral pores on third and fourth urosomites more widely spaced.

Caudal rami (Fig. 4B) slightly shorter than in female, but armature and ornamentation without significant differences.

Antennula (Fig. 5J) digeniculate, 15-segmented, with proximal geniculation between eighth and ninth and segments, and distal geniculation between thirteenth and fourteenth segments; armature formula: 2.5.4.2.6.1.1.2.2.1+ae.2.1.2.1.11+ae; thirteenth and fourteenth segments with strong cuticular ridges along anterior (geniculating) surface; ninth, eleventh, twelfth, and thirteenth segments with short spiniform seta each, all other setae slender and most also smooth.

Antenna, mandibula, maxillula, maxilla, maxilliped, and all four swimming legs as in female. Third endopodal segment of fourth leg (Fig. 6F) ca. 1.5 × as long as wide.

Fifth leg (Fig. 4B) segmentation, ornamentation, and armature of proximal segment as in female; armature of distal segment with two slender medial setae in addition to two spines and central apical seta as in female; lateral spine as long as distal segment and ca. 1.8 × as long as medial spine.

Sixth leg (Fig. 4B) also simple semi-circular flap, but better articulated than in female, with medial minute spine and two slender setae; lateral seta 1.7 × as long as central seta and more than 5 × as long as spine.

Variability. Cuticular organs on the cephalothorax (Figs 1C–E, 3B, C) often exhibited asymmetries in position and/or absence on one side and in different specimens, to the point that a complete survey was probably impossible. Cuticular organs on free prosomites showed fewer asymmetries in position (Fig. 3D) and rarely any absence, while those on urosomites showed no variability in position or number (Figs 2D, 3E). There was no variability in the segmentation or armature formulae of appendages, and any variability in the proportion of segments or armature elements could not be confidently discounted as resulting from slight difference in position due to mounting of specimens and appendages.

Cyclopina koreana **sp. nov.**
http://zoobank.org/9ACBBC99-22DF-4150-8938-666F7099CC05
Figures 7–11, 17B

Type locality. South Korea, East Coast, Gangneung, small beach, intertidal sand, 37°47.824'N, 128°55.085'E.

Specimens examined. ***Holotype*** female dissected on one slide, collected from the type locality, 29 March 2013, leg. T. Karanovic.

Paratypes**:** two males and one female dissected on one slide each; three males, two females, and four copepodids in alcohol; one male and two females on one SEM stub

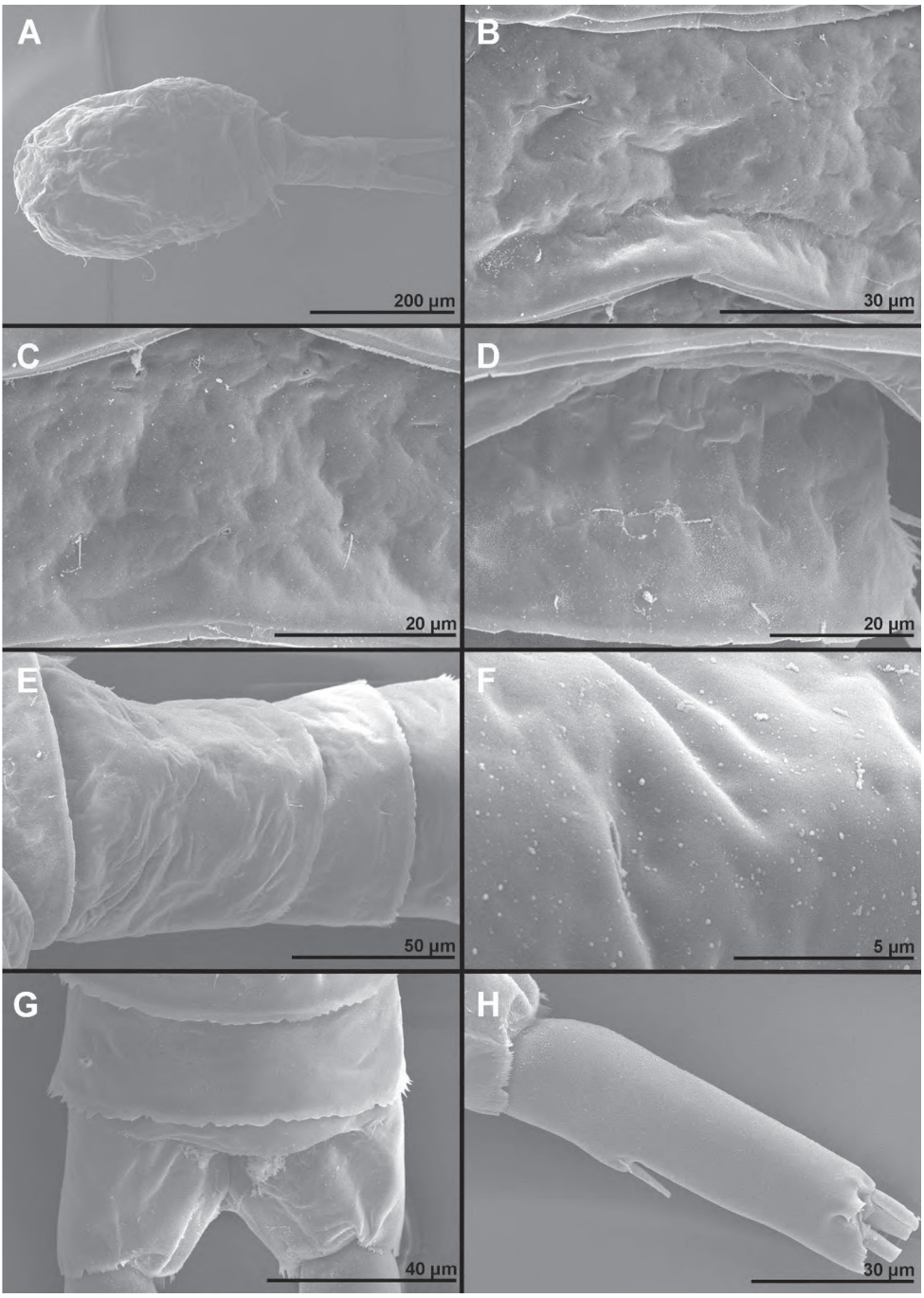

Figure 7. *Cyclopina koreana* sp. nov., paratype female 1, SEM photographs, all in dorsal view **A** habitus **B** second pedigerous somite **C** third pedigerous somite **D** first urosomite **E** genital double-somite and fourth urosomite **F** anterior medial pore on genital double-somite **G** fifth and sixth urosomites **H** caudal ramus.

(together with specimens of other three species described here; row no. 4); all collected from the type locality, 29 March 2013, leg. T. Karanovic.

Etymology. The species name refers to South Korea. It is an adjective, agreeing in gender with the feminine genus name.

Description. Female (based on holotype and three paratypes). ***Body length*** from 620 to 635 µm. ***Colour*** of preserved specimens yellowish, nauplius eye not visible (Fig. 17B). Integument on all somites (Figs 7, 8) smooth, with light bacterial cover, cuticular pores on all somites, spinules only on genital somite and caudal rami, and sensilla on all but penultimate somite; hyaline fringes of prosomites smooth, of urosomites serrated. ***Habitus*** (Fig. 7A) ca. 2.6 × as long as wide in dorsal view, with pronounced distinction between prosome and urosome; prosome ovoid, ca. 1.5 × as long as wide in dorsal view, nearly 1.4 × as long and 2.6 × as wide as urosome, its greatest width at posterior end of first pedigerous somite; urosome nearly cylindrical, ca. 3 × as long as wide, its greatest width at posterior end of fifth pedigerous somite (first urosomite). ***First pedigerous somite*** (Fig. 7A) not fused to cephalothorax, but its tergites partly covered with posterior extensions of cephalothoracic shield as in *C. busanensis*. ***Cephalothorax*** (Fig. 7A) broader in anterior part than in *C. busanensis*, ca. 1.2 × as long as wide, and twice as long as free prosomites combined. Second to fourth free prosomites (Figs 7A–C, 8F) progressively shorter and narrower towards posterior end, and with fewer cuticular organs; not many prosomal cuticular organs clearly homologous to those in previous species (compare Figs 2A, 8F), except dorsal medial pores and several posterior sensilla (Fig. 7B, C).

First urosomite (Figs 7D, 8G, 9A) short, slightly laterally expanded in posterior part, with four dorsal sensilla and single dorsal medial pore.

Genital double-somite (Figs 7E, F, 8G, 9A) ca. 0.9 × as long as wide in dorsal view, laterally expanded anterior part only ca. 1.1 × as wide as posterior margin; sensilla and pores as in *C. busanensis*. Copulatory pore, copulatory duct, seminal receptacles, oviducts, and genital apertures as in *C. busanensis*, except first part of copulatory duct slightly wider. Fourth urosomite (Figs 7E, 9A) ca. 0.6 × as long as genital double-somite, with sensilla and pores as in *C. busanensis*. Fifth urosomite (Figs 7G, 8H, 9A) 0.7 × as long as fourth urosomite, with medial dorsal pore and one pair of widely spaced ventral pores as in *C. busanensis*. Sixth urosomite (Figs 7G, 8H, 9A) 1.2 × as long as fifth urosomite, with one pair of dorsal sensilla, two pairs of dorsal pores, and single pair of ventral pores; no spinules on fringes of anal sinus; anal operculum smooth, short, broad, slightly convex, situated in first third, represents 62% of somite's width.

Caudal rami (Figs 7H, 8H, 9A) cylindrical, ca. 3.5 × as long as wide and 1.5 × as long as anal somite, very widely spaced on anal somite, diverging posteriorly; armed as in *C. busanensis*; ornamented with single sensilla near proximal lateral seta, row of small spinules at base of proximal lateral seta, and posterior ventral row of spinules. Proximal lateral seta inserted at ca. two fifths of ramus' length; medial terminal seta nearly 0.9 × as long as caudal ramus, 1.6 × as long as lateral terminal seta, 0.8 × as long as dorsal seta, and 2.3 × as long as proximal lateral seta.

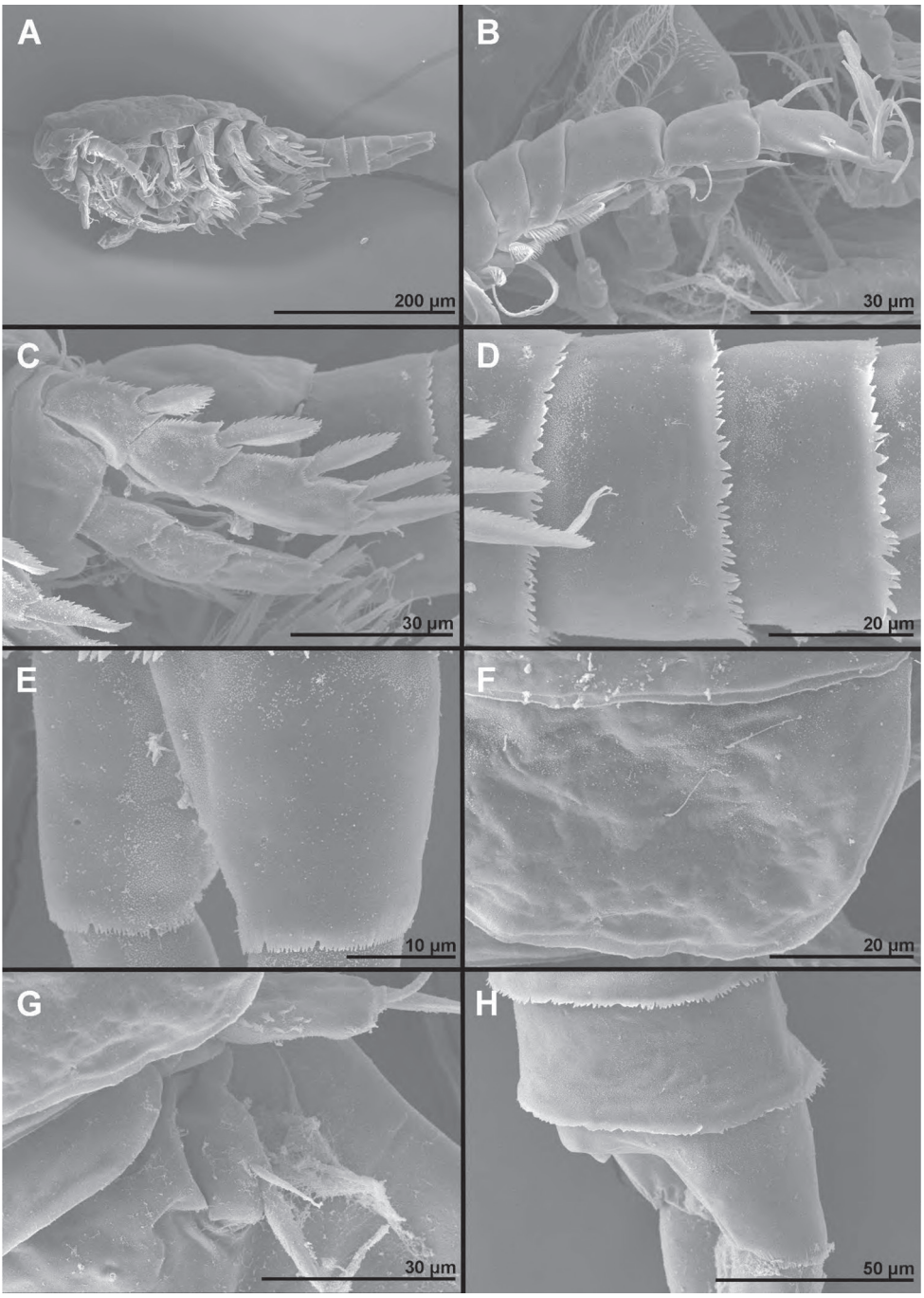

Figure 8. *Cyclopina koreana* sp. nov., SEM photographs **A–E** paratype male 1, ventral view **F–H** paratype female 2, lateral view: **A** habitus **B** distal part of antennula **C** fourth swimming leg **D** fourth and fifth urosomites **E** sixth urosomite **F** tergite of fourth pedigerous somite **G** anterior part of urosomite, with fifth and sixth legs **H** fifth and sixth urosomites.

Figure 9. *Cyclopina koreana* sp. nov., line drawings **A** holotype female, urosome, ventral view **B** holotype female, antennula **C** allotype male, urosome, ventral view.

Antennula (Fig. 9B) segmentation and most armature as in *C. busanensis*, but proximal half stouter and distal half slenderer; armature formula 3.6.8.4.5.6.4.2.2.7+ae; apical aesthetasc significantly shorter than in *C. busanensis* and fifth segment with two short setae; sixth segment longest, ca. 3 × as long as wide, and nearly 0.9 × as long as subsequent four segments combined; tenth segment nearly twice as long as wide.

Antenna (Fig. 10A) as in *C. busanensis*, but another small exopodal seta present and second endopodal segment slightly longer.

Mandibula (Fig. 10B) as in *C. busanensis*, except second endopodal segment with six setae, apical setae on fourth exopodal segment of markedly different lengths (outer one twice as long as inner one), and additional row of minute spinules at base of unicuspid teeth.

Maxillula (Fig. 10C) segmentation and armature formula as in *C. busanensis*, but only one minute seta on praecoxal arthrite smooth, one seta on endopod markedly shorter than other endopodal setae, and both endopod and exopod slightly slenderer.

Maxilla (Fig. 10D) as in *C. busanensis*, but with only three setae on proximal syncoxal endite, proximal basal endite less mobile and with one seta minute, endopodal claw smooth, and endopod four-segment.

Maxilliped (Fig. 10E) segmentation and armature formula as in *C. busanensis*, but with longer syncoxa, shorter first endopodal segment, and two long setae on ultimate endopodal segment.

Swimming legs (Fig. 10A–E) shape, segmentation, and ornamentation as in *C. busanensis*; armature formula as in *C. busanensis*, except third exopodal segment of fourth leg with only four setae; all spines lanceolate; three setae on endopod of fourth leg also lanceolate, other setae slender; third endopodal segments seta formula 6.6.6.5; third exopodal segment seta formula 4.5.5.4 and spine formula 4.4.4.3; third endopodal segment of fourth leg 1.7 × as long as wide and third exopodal segment of fourth leg ca. 1.6 × as long as wide.

Fifth leg (Fig. 8A, G) shape, segmentation, armature formula, and ornamentation as in *C. busanensis*, but first segment slightly shorter (ca. 0.6 × as long as wide) and lateral spine on second segment also proportionately shorter (approximately as long as second segment and 1.3 × as long as medial spine).

Sixth leg (Fig. 8G) as in *C. busanensis*.

Male (based on allotype and two other paratypes). ***Body*** length from 440 to 500 µm. Habitus (Fig. 8A) similar to female, but slenderer. ***Urosome*** (Figs 8D, E, 9C) also slenderer than in female, and second and third urosomites fully articulated as in *C. busanensis*; ornamentation as in female.

Caudal rami (Fig. 9C) slightly less widely spaced than in female, but armature and ornamentation without significant differences (perhaps dorsal seta somewhat shorter).

Antennula (Figs 8B, 11F) shape, geniculation, segmentation, ornamentation, and almost all armature as in *C. busanensis*, but fifth segment with traces of additional segmentation, both aesthetascs longer, and tenth segment with additional short seta (armature formula therefore: 2.5.4.2.6.1.1.2.2.2+ae.2.1.2.1.11+ae).

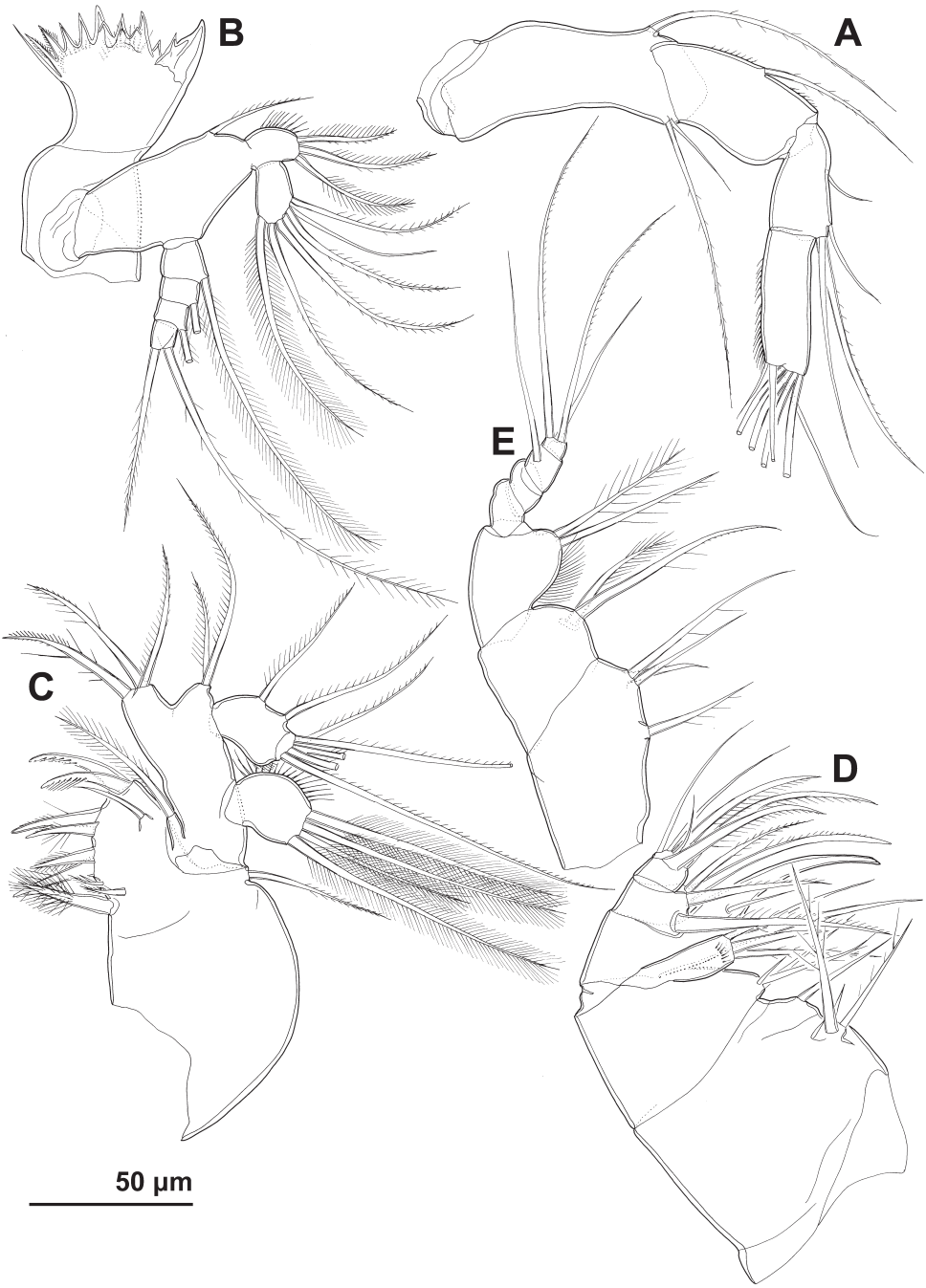

Figure 10. *Cyclopina koreana* sp. nov., line drawings, holotype female **A** antenna **B** mandibula **C** maxillula **D** maxilla **E** maxilliped.

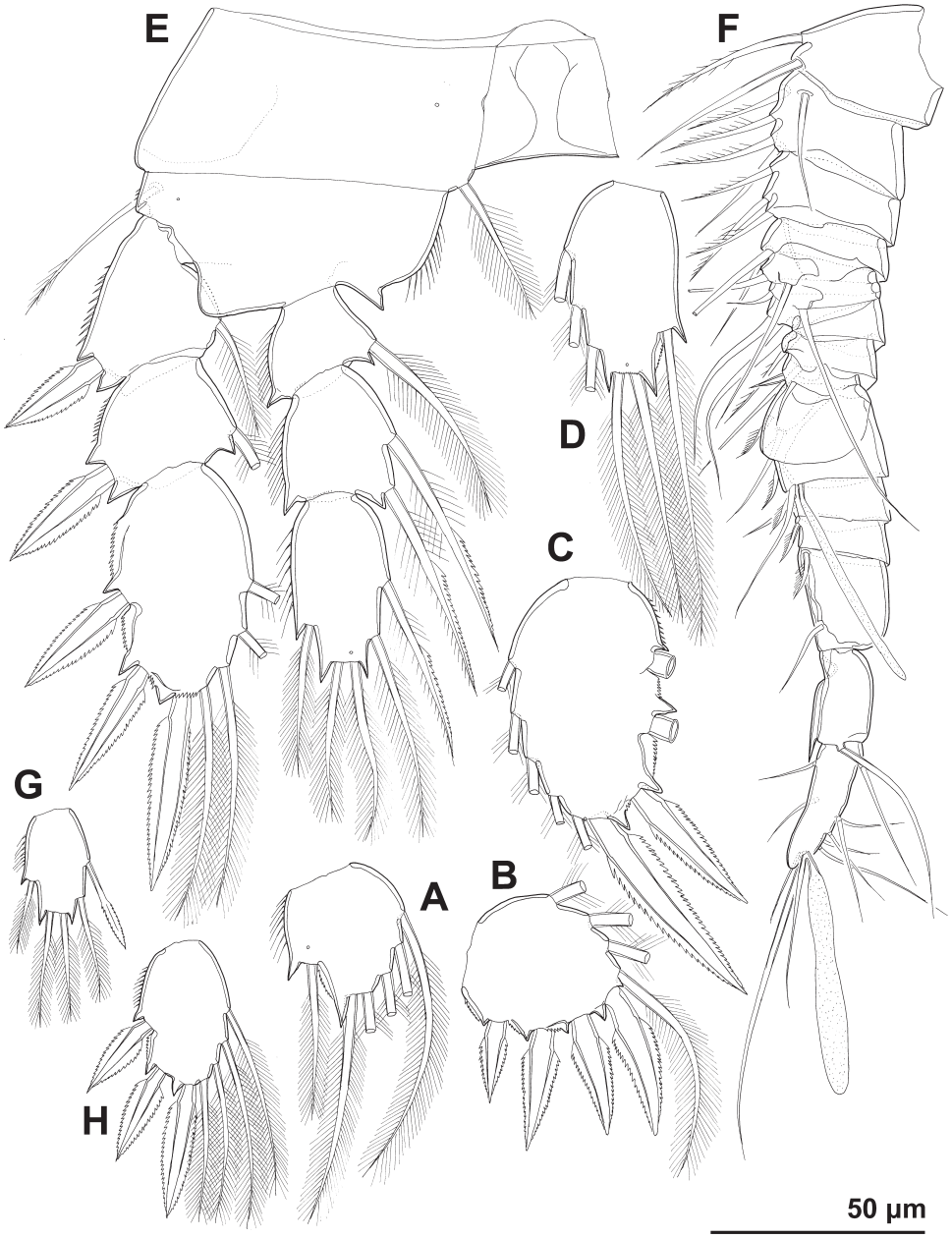

Figure 11. *Cyclopina koreana* sp. nov., line drawings **A–E** holotype female **F–H** allotype male: **A** third endopodal segment of first swimming leg **B** third exopodal segment of first swimming leg **C** third exopodal segment of second swimming leg **D** third endopodal segment of second swimming leg **E** fourth swimming leg **F** antennula **G** third endopodal segment of fourth swimming leg **H** third exopodal segment of fourth swimming leg.

Antenna, mandibula, maxillula, maxilla, maxilliped, and all four swimming legs (Fig. 8A, C) as in female. Third endopodal segment of fourth leg (Fig. 11G) ca. 1.6 × as long as wide, with proximal medial seta lanceolate along both sides; third exopodal segment (Fig. 11H) with only four setae as in female, ca. 1.6 × as long as wide.

Fifth leg (Fig. 9C) segmentation, ornamentation, and armature formula as in *C. busanensis*, i.e., with two medial setae on second segment; proximal segment as in female; lateral spine ca. 0.7 × as long as second segment and 1.1 × as long as medial spine.

Sixth leg (Fig. 9C) as in *C. busanensis*, but broader and without minute medial spine; lateral seta 1.5 × as long as medial seta.

Variability. Except for small differences in body size no other forms of variability were observed, but some specimens were damaged (e.g., with some setae broken off; see Fig. 7H) so comparisons were somewhat limited.

***Cyclopina curtijeju* sp. nov.**
http://zoobank.org/D1D520C8-2BC3-4A0B-B00C-A9BBC730D4A8
Figures 11, 12, 17C

Type locality. South Korea, South Coast, Jeju Island, Gwangchigi Beach near Seongsan Sunrise Peak, 33°27.122'N, 126°55.481'E.

Specimens examined. ***Holotype*** female dissected on one slide, collected from the type locality, 14 April 2014, leg. T. Karanovic. ***Paratype*** female on an SEM stub (together with specimens of other three species described here; row no. 3), collected from the type locality, 14 April 2014, leg. T. Karanovic.

Etymology. The species name is composed of the Latin adjective *curtus* (= short), referring to its short caudal rami, and the name of the type locality (Jeju). It should be treated as a noun (gender feminine) in apposition to the generic name.

Description. Female (based on holotype and one paratype). ***Body length*** 400 µm. ***Colour*** (Fig. 17C), nauplius eye, body segmentation, integument on somites (Fig. 12), and general habitus as in *C. busanensis*, except for different sensilla and pores pattern on prosomites (Fig. 12A–D) and hyaline fringes of urosomites (except anal somite) rather wavy than serrated (Fig. 12F–H). Prosome ca. 1.4 × as long as urosome.

Genital double-somite (Fig. 12E, F) as in *C. busanensis*, except with two additional dorsolateral pair of pores, one additional ventrolateral pair of pores, posterior lateral pore almost at same level as posterior lateral sensillum (instead of being anterior to posterior lateral sensillum), and sensillum instead of large pore at dorsal end of lateral row of spinules. Genital field not clearly observed because of mounting, but in lateral view seems very similar to that in *C. busanensis*. Fourth urosomite (Fig. 12G) as in *C. busanensis*, except with one additional pair of dorsal pores in anterior half. Fifth urosomite (Fig. 12G) and sixth urosomite (Fig. 12H) as in *C. busanensis*.

Caudal rami (Fig. 12A, H) cylindrical, ca. 1.3 × as long as wide, 1.2 × as long as anal somite, narrowly spaced on anal somite, parallel; ornamented as in *C. busanensis*;

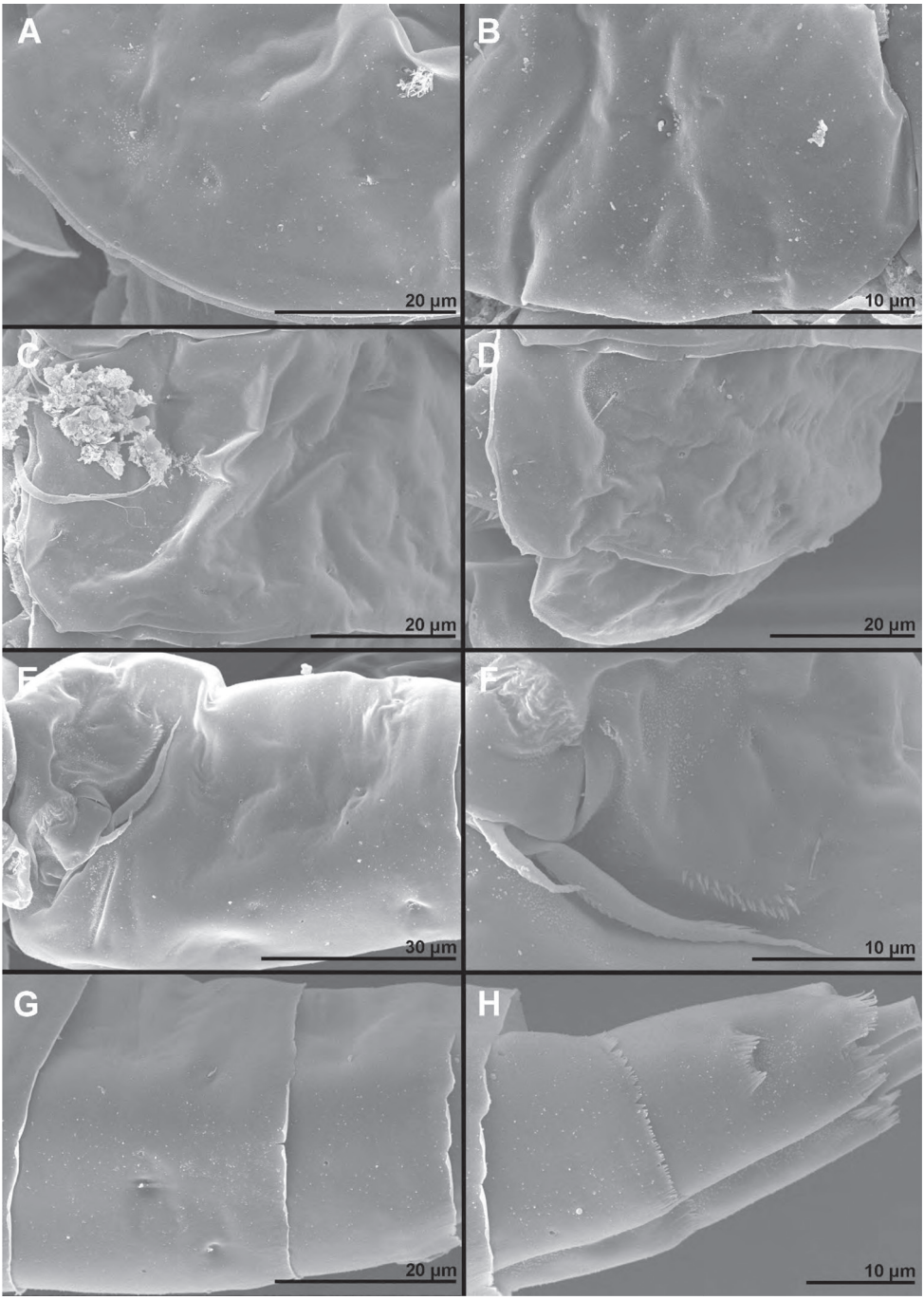

Figure 12. *Cyclopina curtijeju* sp. nov., paratype female, SEM photographs, all in lateral view **A** anterior part of cephalothoracic shield **B** posterio-lateral corner of cephalothoracic shield **C** tergite of second pedigerous somite **D** tergites of third and fourth pedigerous somites **E** genital double-somite **F** sixth leg **G** fourth and fifth urosomites **H** sixth urosomite and caudal rami.

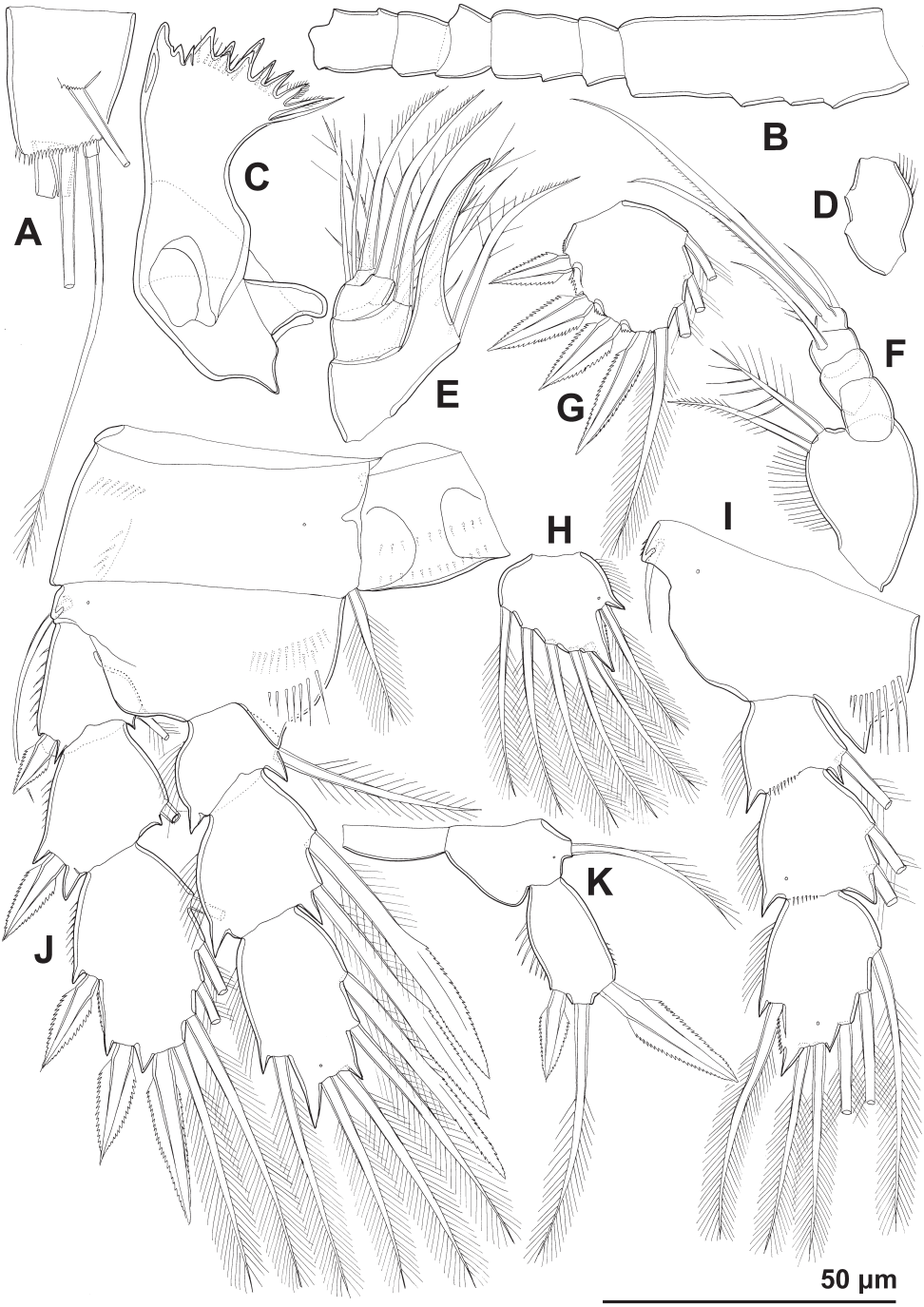

Figure 13. *Cyclopina curtijeju* sp. nov., holotype female, line drawings **A** caudal ramus, lateral view **B** distal part of antennula, without armature **C** coxa of mandibula **D** endopod of maxillula **E** endopod of maxilla **F** endopod of maxilliped **G** third exopodal segment of first swimming leg **H** third endopodal segment of first swimming leg **I** basis and endopod of second swimming leg **J** fourth swimming leg **K** fifth leg.

most armature broken off; dorsal seta nearly 3 × as long as ramus; proximal lateral seta inserted at approximately midlength of ramus.

Antennula (Fig. 13B) 11-segmented, but all armature as in *C. koreana*; armature formula 3.6.8.4.5.6.2.2.2.2.7+ae; sixth segment ca. 2.7 × as long as wide, nearly 0.9 × as long as subsequent five segments combined; tenth segment 1.5 × as long as wide.

Antenna and mandibula (Fig. 13C) shape, segmentation, armature, and ornamentation as in *C. koreana*.

Maxillula (Fig. 13D) also as in *C. koreana*, except endopod slightly slenderer.

Maxilla (Fig. 13E) with only two setae on second endopodal segment; everything else as in *C. koreana*.

Maxilliped (Fig. 13F) generally as in *C. koreana*, except first endopodal segment slightly slenderer, seta on fourth endopodal segment shorter, large setae on fifth endopodal segment stronger, and slender seta on fifth endopodal segment shorter.

Swimming legs (Fig. 13G–J) shape, segmentation, armature formula, and most ornamentation as in *C. busanensis*; fourth leg (Fig. 13J) with three setae on endopod lanceolate as in *C. koreana*, five setae on third exopodal segment as in *C. busanensis*, but unlike these species with two parallel posterior rows of spinules on intercoxal sclerite and with posterior row of spinules on basis; third endopodal segment of fourth leg 1.6 × as long as wide and third exopodal segment of fourth leg ca. 1.5 × as long as wide.

Fifth leg (Fig. 13K) shape, segmentation, and armature formula as in *C. busanensis*, but first segment without inner spinules and second segment slightly longer (1.5 × as long as first segment and 1.9 × as long as wide); lateral spine ca. 1.3 × as long as second segment and nearly 1.8 × as long as medial spine.

Sixth leg (Fig. 12F) as in *C. busanensis*.

Male unknown.

Variability. Only two females were examined, both partly damaged, one in detail with a light microscope (holotype), and the other with a scanning electron microscope (paratype), so variability could not be properly assessed. However, the paratype female was also beforehand examined with a light microscope (although without dissection) and no variability was observed in the most important diagnostic characters (caudal rami length, antennula segmentation, swimming legs armature, or fifth leg proportions); mouth appendages could not be examined without dissection.

Cyclopina wido **sp. nov.**

http://zoobank.org/06FD35E8-BD0D-4592-BAE3-717CEB70AF9C
Figures 14–16, 17D

Type locality. South Korea, West Coast, Wido Island, small beach, intertidal sand, 35°35.089'N, 126°15.196'E.

Specimens examined. ***Holotype*** ovigerous female dissected on one slide, collected from the type locality, 12 April 2013, leg. T. Karanovic.

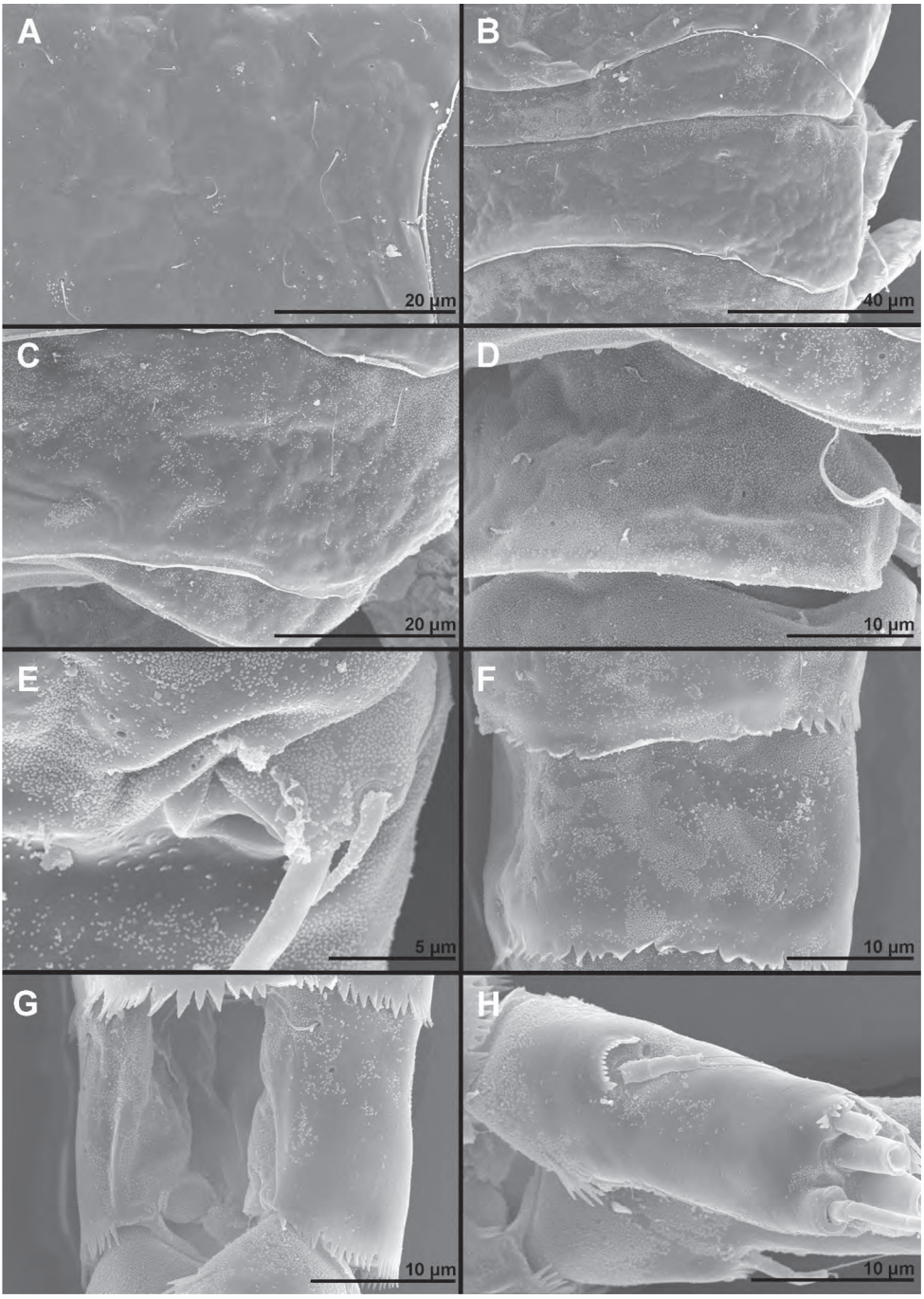

Figure 14. *Cyclopina wido* sp. nov., paratype female 1, SEM photographs, all in dorsal view **A** posterior part of cephalothorax **B** first and second pedigerous somites **C** third and fourth pedigerous somites **D** first urosomite **E** sixth leg **F** posterior part of genital double-somite and fourth urosomite **G** hyaline fringe of fifth urosomite and sixth urosomite **H** caudal rami.

***Paratypes*:** one male (allotype) dissected on one slide; one female on one SEM stub (together with specimens of other three species described here; row no. 1); both collected from the type locality, 12 April 2013, leg. T. Karanovic.

Etymology. The species name refers to its type locality (Wido). It should be treated as a noun (gender feminine) in apposition to the generic name.

Description. Female (based on holotype and one paratype). ***Body length*** of holotype 327 µm, that of paratype 323 µm. ***Colour*** of preserved specimens yellowish, nauplius eye not visible (Fig. 17D). Integument on all somites (Fig. 14) smooth, with moderate bacterial cover, cuticular pores on all somites, spinules only on genital somite and caudal rami, and sensilla on all but penultimate somite; hyaline fringes of prosomites smooth, of urosomites serrated. ***Habitus*** ca. 2.6 × as long as wide in dorsal view, with pronounced distinction between prosome and urosome; prosome ovoid but with more flared posterior end than in *C. busanensis*, ca. 1.6 × as long as wide in dorsal view, nearly 1.6 × as long and 2.7 × as wide as urosome, its greatest width at posterior end of first pedigerous somite; urosome nearly cylindrical, ca. 3 × as long as wide, its greatest width at posterior end of fifth pedigerous somite (first urosomite). ***First pedigerous somite*** (Fig. 14B) not fused to cephalothorax, but its tergites largely covered with posterior extensions of cephalothoracic shield. ***Cephalothorax*** (Fig. 14A) shape as in *C. busanensis*, nearly conical, approximately as long as wide, and 1.2 × as long as free prosomites combined; however, cuticular sensilla and pores pattern unique. Second to fourth free prosomites (Fig. 14B, C) progressively shorter and narrower towards posterior end, and with fewer cuticular organs; not many prosomal cuticular organs obviously homologous to those in previous species, except perhaps dorsal medial pores and several posterior sensilla.

First urosomite (Fig. 14D) as in *C. busanensis* and *C. koreana*, short, slightly laterally expanded in posterior part, with two pairs of dorsal sensilla, single dorsal medial pore, one pair of dorsolateral pores, and one pair of ventrolateral pores (at base of fifth legs).

Genital double-somite (Figs 14E, 15A) as in *C. busanensis*, except ventral posterior pores slightly closer to ventral posterior sensilla, pair of small lateral anterior pores closer to sixth leg, somite ca. 1.1 × as long as wide, and laterally expanded anterior part nearly 1.4 × as wide as posterior margin. Copulatory pore, copulatory duct, seminal receptacles, oviducts, and genital apertures as in *C. busanensis*. Fourth urosomite (Figs 14F, 15A) ca. half as long as genital double-somite, with sensilla and pores as in *C. busanensis*. Fifth urosomite (Figs 14G, 15A) almost as long as fourth urosomite, with medial dorsal pore and one pair of widely spaced ventral pores as in *C. busanensis*, but dorsal hyaline fringe coarsely serrated and expanded posteriorly almost as pseudo-operculum (completely covering anal operculum). Sixth urosomite (Figs 14G, 15A) 0.85 × as long as fifth urosomite, with one pair of dorsal sensilla, two pairs of dorsal pores, and single pair of ventral pores; no spinules on fringes of narrow anal sinus; anal operculum smooth, very short, narrow, slightly concave, situated in first fourth, represents approximately 40% of somite's width.

Caudal rami (Figs 14H, 7H, 8H, 9A) robust, cylindrical, ca. 2.3 × as long as wide and 1.4 × as long as anal somite, very narrowly spaced on anal somite, nearly parallel;

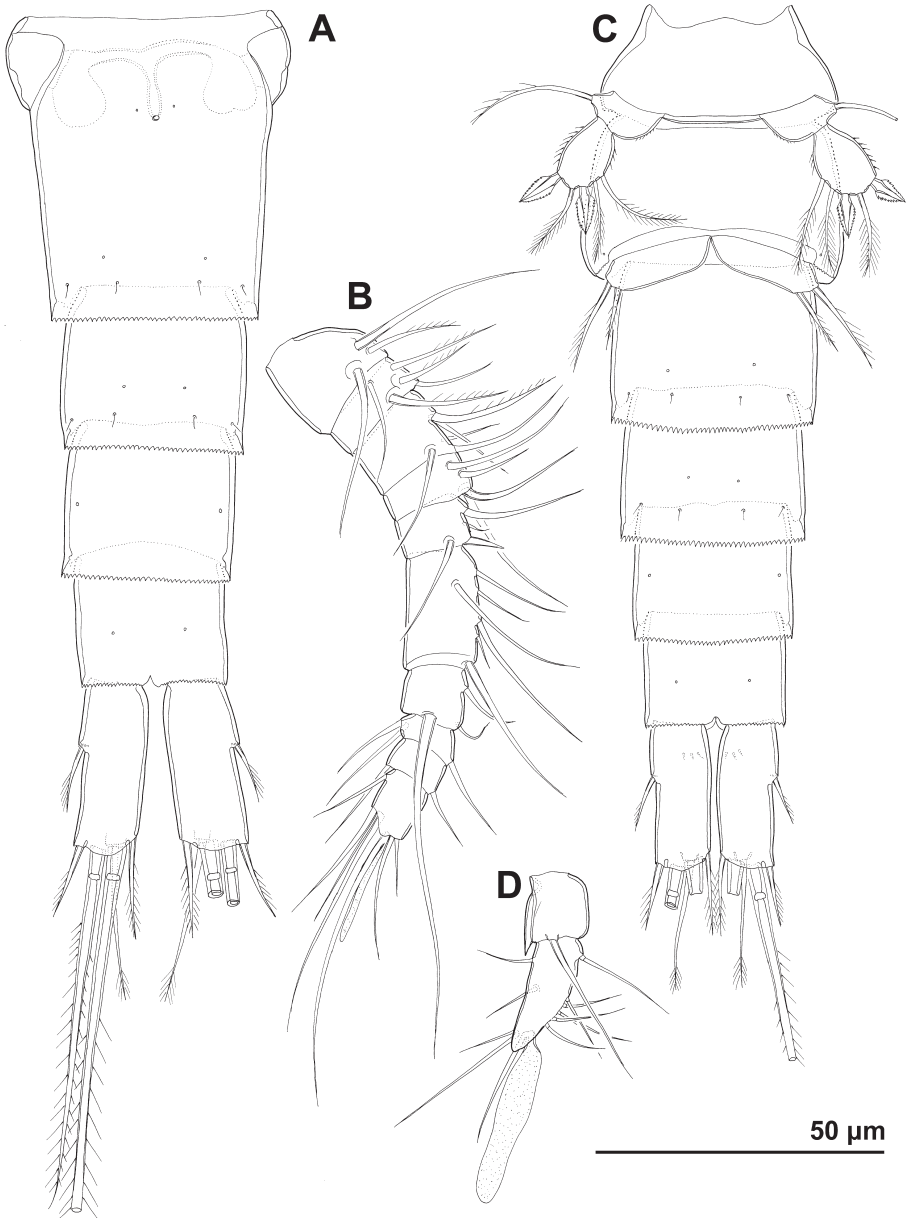

Figure 15. *Cyclopina wido* sp. nov., line drawings **A, B** holotype female **C, D** allotype male: **A** urosome without first urosomal somite, ventral view **B** antennula **C** urosome, ventral view **D** penultimate and ultimate segments of antennula.

armed with six setae as in *C. busanensis*; ornamented with single pore near proximal lateral seta, row of small spinules at base of proximal lateral seta, posterior ventral row of spinules, and short diagonal dorsomedial row of large spinules in anterior half.

Proximal lateral seta inserted at ca. two fifths of ramus' length; medial terminal seta only ca. 0.6 × as long as caudal ramus, 1.2 × as long as lateral terminal seta, 0.6 × as long as dorsal seta, and 1.6 × as long as proximal lateral seta.

Antennula (Fig. 15B) 10-segmented, very stout, nearly cylindrical (proximal part only slightly wider than distal part); armature formula 3.5.5.4.4.6.3.3.2.7+ae; apical aesthetasc significantly shorter than in *C. busanensis* and fifth segment with two short setae, as in *C. koreana*; sixth segment longest, ca. 1.5 × as long as wide, and 0.6 × as long as subsequent four segments combined; tenth segment ca. 1.3 × as long as wide.

Antenna (Fig. 16A) shape, segmentation, most ornamentation, and most armature as in *C. koreana*, but no exopodal setae and inner-distal seta on basis significantly shorter.

Mandibula (Fig. 16B) as in *C. koreana*, except cutting edge somewhat narrower, basis slenderer, exopod stouter, setae on fourth exopodal segment of equal length, and no spinules at base of unicuspid teeth.

Maxillula (Fig. 16C) as in *C. koreana*, except endopod shorter and with only six setae, as well as setae on distal basal endite of equal length.

Maxilla (Fig. 16D) as in *C. curtijeju*, i.e., with only two setae on second endopodal segment.

Maxilliped (Fig. 16E) as in *C. koreana*, except apical setae slightly shorter.

Swimming legs (Fig. 16F–I) shape, most segmentation, most ornamentation, and most armature as in *C. busanensis*, except endopod of first leg two-segmented and with one less seta, as well as second endopodal segments of second to fourth legs with single medial seta; all spines lanceolate and all setae slender; third exopodal segment seta formula 4.5.5.5 and spine formula 4.4.4.3; third endopodal segment of fourth leg 1.3 × as long as wide and third exopodal segment of fourth leg only ca. 1.1 × as long as wide.

Fifth leg (Fig. 16J) shape, segmentation, armature formula, and ornamentation as in *C. koreana*, but second segment longer and lateral spine shorter than medial; second segment ca. 1.9 × as long as first segment and ca. 1.7 × as long as wide; lateral spine ca. 0.5 × as long as second segment and 0.7 × as long as medial spine.

Sixth leg (Fig. 14E) as in *C. busanensis*.

Male (based on allotype). ***Body length*** 305 µm. ***Habitus*** similar to female, but slightly slenderer. ***Urosome*** (Fig. 15C) also slenderer than in female, and second and third urosomites fully articulated as in *C. busanensis*; ornamentation as in female.

Caudal rami (Fig. 15C) slightly shorter and slenderer than in female, but armature and ornamentation without significant differences.

Antennula (Fig. 15D) geniculation, segmentation, ornamentation, and all armature as in *C. koreana*, but all segments shorter.

Antenna, mandibula, maxillula, maxilla, maxilliped, and all four swimming legs (Fig. 16K–M) as in female. Endopod of first leg (Fig. 16K) also two-segmented, with only seven setae; third endopodal segment of fourth leg (Fig. 16L) nearly 1.4 × as long as wide; third exopodal segment of fourth leg (Fig. 16M) ca. 1.2 × as long as wide.

Fifth leg (Fig. 15C) segmentation, ornamentation, and armature formula as in *C. busanensis*, except second segment more rounded and lateral spine shorter; second segment twice as long as first segment and 1.5 × as long as wide; lateral spine ca. 0.6 × as long as distal segment and 0.9 × as long as medial spine.

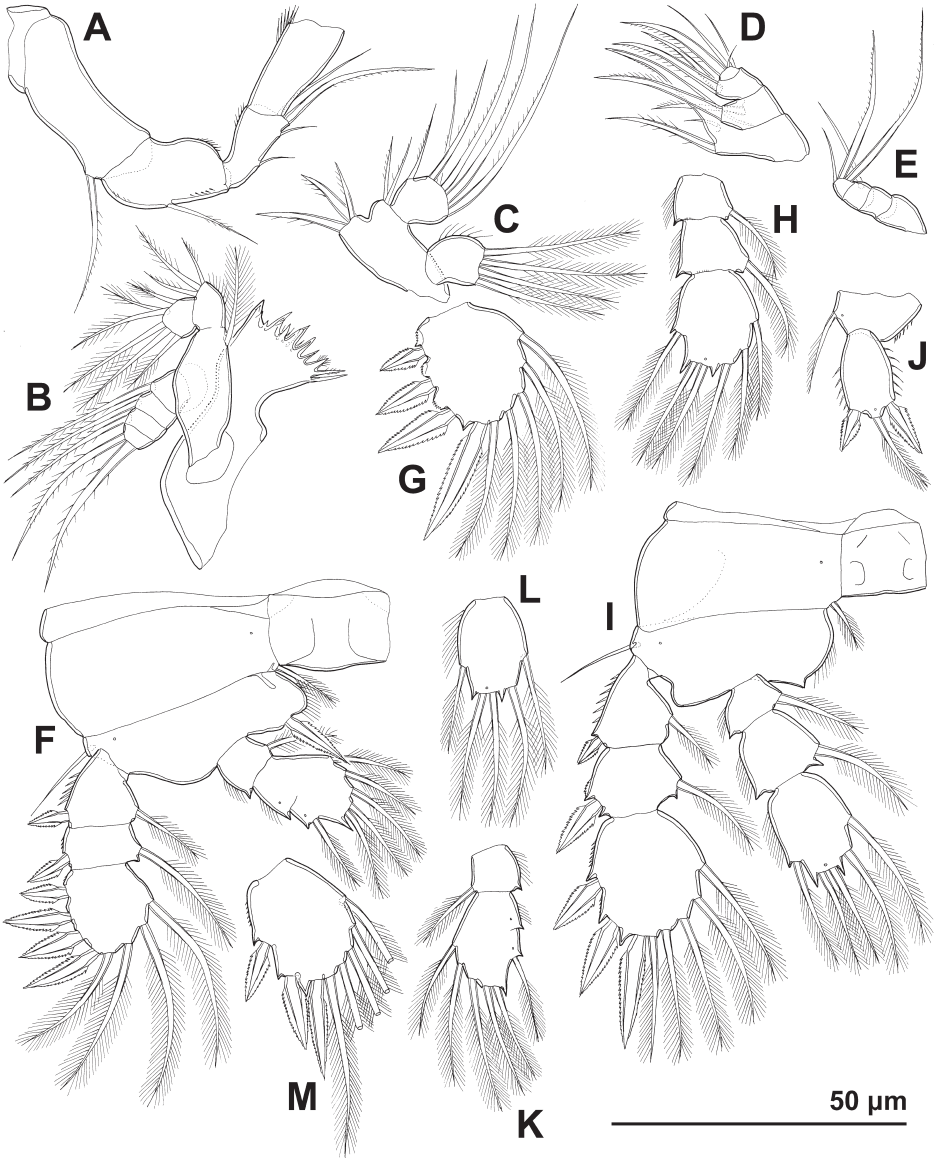

Figure 16. *Cyclopina wido* sp. nov., line drawings **A–J** holotype female **K–M** allotype male: **A** antenna, without apical armature **B** mandibula **C** maxillular palp **D** endopod of maxilla **E** last four endopodal segments of maxilliped **F** first swimming leg **G** third exopodal segment of second swimming leg **H** endopod of second swimming leg **I** fourth swimming leg **J** fifth leg **K** endopod of first swimming leg **L** third endopodal segment of fourth swimming leg **M** third exopodal segment of fourth swimming leg.

Sixth leg (Fig. 15C) without medial spine as in *C. koreana*; lateral seta 1.4 × as long as medial seta.

Variability. Only one male and two females were examined, so variability could not be properly assessed. One female was examined in detail with a light microscope

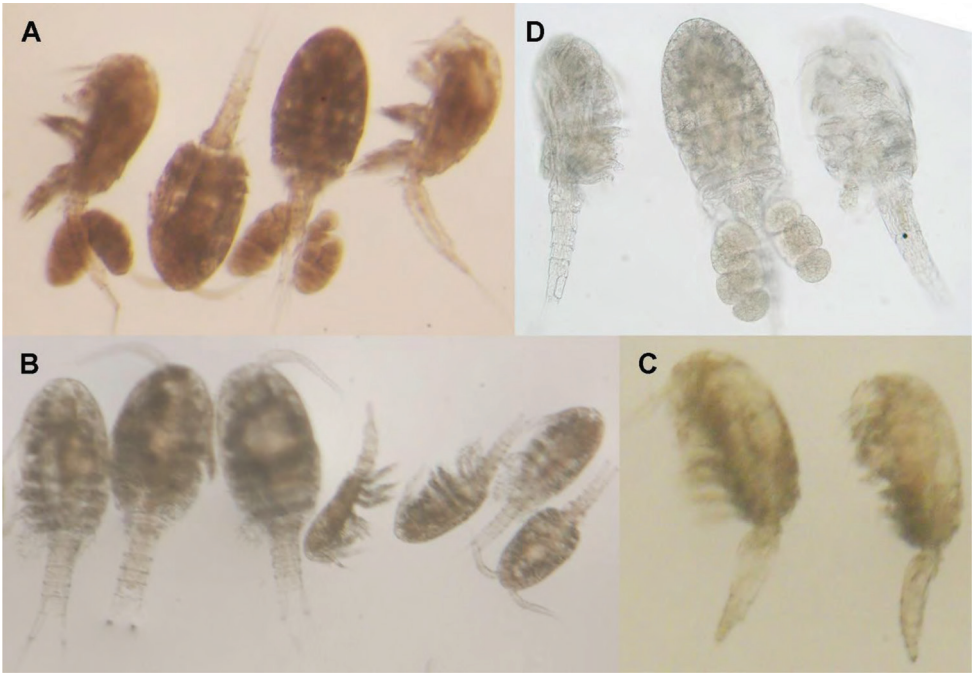

Figure 17. Light photographs of four new species (not to scale) **A** *Cyclopina busanensis* sp. nov., four females (two ovigerous) **B** *Cyclopina koreana* sp. nov., three females and four males **C** *Cyclopina curtijeju* sp. nov., two females **D** *Cyclopina wido* sp. nov., two females (one ovigerous) and one male.

(holotype), and the other with a scanning electron microscope (paratype). However, the paratype female was also beforehand examined with a light microscope (although without dissection) and no variability was observed in the most important diagnostic characters (caudal rami length, antennula segmentation, swimming legs segmentation and armature, or fifth leg proportions); mouth appendages could not be examined without dissection. Male characters that are not sexually dimorphic show only minute differences from female characters in proportions of somites, segments, or armature.

Discussion

Four new species from South Korea share a number of characters that are considered important in cyclopoid taxonomy and systematics, such as free first pedigerous prosomite, extended postero-lateral corners of the cephalothoracic shield, T-shaped copulatory duct and ovoid seminal receptacles on the completely fused genital double-somite, very short anal operculum, relatively short caudal rami armed with only six setae, short female antennula (10- or 11-segmented) with longest sixth segment, four-segmented antenna with armature formula of the last three segments 1/4/7, four-segmented mandibular exopod with armature formula 1/1/1/2, one-segmented maxillular exopod

armed with four setae, maxillipedal armature formula 4/2/2/0/0/1/3, three-segmented exopods of all swimming legs with spine formula of the third segments 4/4/4/3, three-segmented endopods of second to fourth legs with seta formula of the third segments 6/6/5, two-segmented female fifth leg with two spines and central seta on the second segment, and male fifth legs (in three species with known males) with two additional medial setae on the second segment. All of these characters are within the currently recognised boundaries of the genus *Cyclopina* (see Lotufo 1994; Gómez and Martínez Arbizu 2004; Karanovic 2008). However, the four South Korean congeners can easily be distinguished from each other by a multitude of features, including size, caudal rami shape, proportions of caudal setae, proportions of ultimate endopodal and exopodal segments on the fourth leg, proportions of segments and armature on the fifth leg, and cuticular sensilla and pores pattern on prosomites and some urosomites. Other distinguishing characters include: space between caudal rami (less than the width of one ramus in *C. busanensis*, *C. curtijeju*, and *C. wido*; more than the width of one ramus in *C. koreana*), antennula segmentation (10-segmented in *C. busanensis*, *C. koreana*, and *C. wido*; 11-segmented in *C. curtijeju*), number of exopodal setae on the antenna (one in *C. busanensis*, two in *C. koreana* and *C. curtijeju*, and none in *C. wido*), number of setae on the mandibular endopod (five in *C. busanensis*, six in other species), number of setae on the second endopodal segment of maxilla (four in *C. busanensis* and *C. koreana*, two in *C. curtijeju* and *C. wido*), number of long setae on the ultimate segment of maxilliped (one in *C. busanensis*, two in other species), first leg endopod segmentation (two-segmented in *C. wido*, three-segmented in other species), number of setae on the first leg endopod (seven in *C. wido*, eight in other species), number of setae on the second endopodal segment of second to fourth legs (one in *C. wido*, two in other species), number of setae on the third exopodal segment of fourth leg (four in *C. koreana*, five in other species), and nature of setae on the second endopodal segment of fourth leg (plumose in *C. busanensis* and *C. wido*, lanceolate in *C. koreana* and *C. curtijeju*). Other smaller differences are highlighted in their comparative descriptions above. It should be clear from the presented distribution of character states among the four species that there are no clear sister-species pairs here. The only thing about their phylogenetic relationships that can be concluded from morphological characters is that *C. wido* stands apart from the other three species by a number of reductions in segmentation and armature, which are perhaps related to its diminutive size.

Cuticular organs (sensilla and pores) on somites certainly show some differences between the four new South Korean species described here, but some of these rarely studied micro-characters could easily be homologised (especially on urosomites) and showed little intraspecific variability. This could be invaluable in future studies trying to match opposite sexes, especially because numerous *Cyclopina* species are known after only one sex (Karanovic 2008). It might also be useful in reconstructing difficult phylogenetic relationships among cyclopinids at large, as was shown for some harpacticoid copepods (Karanovic and Kim 2014b).

Cyclopina busanensis is probably most similar to the Japanese *C. kiraensis* Horomi, 1984, described from the Pacific Coast of Honshu (Hiromi 1984) and later reported

from the same island, but from the Sea of Japan (Ueda et al. 2001). However, the Japanese species can easily be distinguished from its South Korean congener by slightly shorter caudal rami and ultimate endopodal and exopodal segments of the fourth leg, as well as by the presence of lanceolate setae on the fourth leg endopod and modified apical seta on the mandibular exopod. Both share many morphological details with a large group of species around the widely distributed *C. gracilis* Claus, 1863 (which is the type species of the genus) and the Mediterranean *C. esilis* Brian, 1928 (see Claus 1863; Sars 1913; Brian 1928; Steuer 1940; Lang 1946; Herbst 1964; Pallares 1968; Monchenko 1979; Wells and McKenzie 1973; Jaume and Boxshall 1996), but can be distinguished by at least some details in the proportion of certain segments and armature (Table 1). It should be noted that this whole complex is in need of revision, with intraspecific variability between some highly disjunct populations sometimes exceeding interspecific variability. For example, specimens redescribed as *C. esilis* from the Black Sea by Monchenko (1979) almost certainly represent a different species from those redescribed from Mallorca by Jaume and Boxshall (1996). Discrepancies in body size and caudal rami shape in some Mallorcan specimens reported by Jaume and Boxshall (1996) could indicate further sympatric cryptic species, as recently demonstrated using molecular tools for several groups of copepods (Karanovic and Cooper 2012; Karanovic et al. 2016). However, Jaume and Boxshall (1996) were probably well justified in synonymising with *C. esilis* specimens from France that were tentatively reported by Herbst (1953) as *C. kieferi* Schëfer, 1936. Problems surrounding distribution and variability of *C. gracilis* are of similar nature: while Sars (1913) stated that the male fifth leg is exactly the same as in the female in a population from Norway, Herbst (1964) illustrated a male fifth leg with one additional medial seta in a population from the Red Sea, and Pallares (1968) redescribed a population from Argentina that cannot possibly be conspecific with these two.

Cyclopina koreana is easily distinguishable from most congeners by its slender and widely spaced caudal rami, as well as by only four setae on the third exopodal segment of fourth leg. Only *C. adelphae* Karanovic, 2008 has somewhat similar caudal rami, but this Australian species has a completely different armature formula of the antennula, antenna, and swimming legs, as well as a more bulbous copulatory duct and slenderer fifth leg. Four setae on the third exopodal segment of fourth leg is a character so far reported only for three other congeners (see Table 1): *C. caroli* Lotufo, 1994 from Brazil; *C. parapsammophila* Monchenko, 1981 from the Black Sea; and *C. psammophila* Steuer, 1940 from the Mediterranean and Red Sea (see Steuer 1940; Herbst, 1964; Monchenko 1981; Lotufo 1994). All three, however, have very short caudal rami, and the latter two also have four setae on the third exopodal segment of third leg. Note that Lotufo (1994) stated in his description that *C. caroli* has five setae on the third exopodal segment of the fourth leg, but his fig. 13 clearly shows four and he did not mention this character as variable.

Including *C. curtijeju*, there are currently only seven species of *Cyclopina* with caudal rami that are less than 1.5 × as long as wide (Table 1). Among them the new South Korean species is the only one with an 11-segmented antennula. In fact, they all differ

Table 1. List of selected character states for valid species and subspecies of the genus *Cyclopina* Claus, 1963. Abbreviations used: ?, unknown; +, present; –, absent; A, anterior; A1, antennula; A2, antenna; AnSo, anal somite; Bp, basis; Cr, caudal ramus; Enp, endopod; Exp, exopod; L, length; Md, mandibula; Mxl, maxillula; Mxp, maxilliped; P, posterior; P1, first leg; P4, fourth leg; P5, fifth leg; P6, sixth leg; W, width. See text for more details.

	Cr, L/W	Cr /AnSo	medial seta/Cr	Cr, medial/dist. lateral seta	Cr, medial/dorsal seta	Cr, prox. lat. seta position	Cr, space between rami	Female A1, segmentation	A2, no. of exopodal setae	A2Bp, no. of medial setae	A2Enp2, no. of setae	MdEnp, armature formula	MxlEnp, no. of setae	MxpEnp, armature formula	P1Enp, no. of segments	P1Enp, no. of setae	P4Exp3, L/W	P4Exp3, no of setae	P4Enp3, L/W	P4Enp, lanceolate setae	P5, Exp/Bp	P5Exp, L/W	P5, lateral spine/Exp	P5Exp, lateral/medial spine	Male P5, no. of medial setae	Male P6, medial spine
C. adelphe Karanovic, 2008	3	1.2	?	?	?	A	2.2	11	1	2	5	3/4	6	0/0/1/3	3	7	?	5	1.4	–	1.9	2.5	0.4	0.7	?	?
C. adriatica Petkovski, 1955	1.6	1	3	1.5	1.1	P	0.3	10	1	1	5	3/6	7	0/0/1/3	?	8	?	5	?	?	2.1	2.2	0.9	1	?	?
C. americana Herbst, 1982	1.5	1	2.7	2	1.5	P	0.5	10	0	1	4	3/6	?	0/0/1/2	3	?	1.5	5	1.5	–	1.5	2	1.3	2.5	1	–
C. amita Karanovic, 2008	1.8	0.9	2.3	2.2	1.2	P	0.4	11	1(0)	1(2)	4(5)	3/4	6	0/0/0/3	3	8	1.7	5	1.5	–	1.4	2.1	1.3	2.2	2	–
C. arenosa Lotufo, 1994	3.4	1.4	0.8	1.4	1.2	A	0.6	10	2	1	5	3/5	7	?	2	8	1.4	5	?	?	1.2	1.5	1	1.2	?	?
C. balearica (Jaume & Boxshall, 1996)	2.9	1.2	1.7	2.9	1.7	A	0.7	10	2	1	5	3/6	7	0/0/4	3	7	1.6	5	1.5	–	1.4	2.4	0.9	1.2	2	+
C. brachystylis Sars, 1921	1.5	0.9	2.7	1.5	1.4	P	0.2	10	?	?	?	?	?	?	?	?	?	?	?	?	1.2	2.2	1.3	2	?	?
C. brevifurca Sars, 1913	0.8	0.5	4.6	1.1	1	P	0.3	12	1	1	4	3/6	7	1/1/2	3	8	1.9	5	1.7	–	1.4	2.5	1.5	1.7	?	?
C. busanensis sp. nov.	3.7	2	1.2	1.6	1.5	A	0.5	10	1	1	4	3/5	7	0/0/1/3	3	8	1.5	5	1.6	–	1.3	1.6	1.2	1.6	2	+
C. caiala Lotufo & Rocha, 1991	1.7	0.8	2.6	1.7	2	P	0.2	10	1	1	5	3/6	7	1/0/1/3	3	8	1.3	5	1.3	+	1.5	1.6	0.5	1	0	+
C. caissara Lotufo, 1994	1.5	0.9	3.1	1.2	1.3	P	0.2	12	1	1	5	3/6	7	0/0/1/4	3	8	1.8	5	1.8	–	0.9	2	1.7	6.5	2	+
C. campechana (Suarez & Almeyda, 2015)	1.2	1	3	1.5	1.3	P	0.5	10	1	1	5	3/5	7	0/0/1/4	3	8	1.4	5	1.4	–	1.5	2	0.9	2.4	2	+
C. caroli Lotufo, 1994	1.5	1.1	3.5	2.2	2.3	P	0.3	10	2	1	5	3/5	7	0/0/1/4	3	8	1.5	4	1.4	+	1.7	1.7	1	1.3	1	+
C. confusa (Ivanenko & Defaye, 2004)	3.7	1.3	1.5	1.7	1.7	A	0.6	10	2	1	5	3/6	7	0/0/1/4	3	8	1.4	5	1.5	–	1.3	2.1	0.8	1.4	2	+

	Cr, L/W	Cr /AnSo	medial seta/Cr	Cr, medial/dist. lateral seta	Cr, medial/dorsal seta	Cr, prox. lat. seta position	Cr, space between rami	Female A1, segmentation	A2, no. of exopodal setae	A2Bp, no. of medial setae	A2Enp2, no. of setae	MdEnp, armature formula	MxlEnp, no. of setae	MxpEnp, armature formula	P1Enp, no. of segments	P1Enp, no. of setae	P4Exp3, L/W	P4Exp3, no of setae	P4Enp3, L/W	P4Enp, lanceolate setae	P5, Exp/Bp	P5Exp, L/W	P5, lateral spine/Exp	P5Exp, lateral/medial spine	Male P5, no. of medial setae	Male P6, medial spine
C. crassisetosa Herbst, 1953	3.7	1.4	1.1	1.9	0.7	P	0.3	10	0	1	4	3/?	7	0/0/1/3	3	?	?	?	1.4	–	1.6	1.5	1	1	?	?
C. curtijeju sp. nov.	1.3	1.2	?	?	?	P	0.3	11	2	1	4	3/6	7	0/0/1/3	3	8	1.5	5	1.6	+	1.5	1.9	1.3	1.8	?	?
C. dorae Lotufo, 1994	1.9	1.1	1.1	1.3	0.8	P	0.6	10	2	1	5	3/5	7	0/0/1/4	3	8	1.5	5	?	?	1.3	2	0.7	0.9	?	?
C. ensifera Grandori, 1925	3	1.4	1.7	1.6	1.4	P	0.3	10	1	1(0)	5	3/6	7	0/0/1/3	3	8	1.3	5	1.7	+	2	2	1.1	1.1	0	–
C. esilis Brian, 1938	3	1.5	1.6	2.5	1.5	A(P)	0.6	10	1(0)	1(0)	5	3/6	7	0/0/1/3(4)	3	8	1.8	5	2	+(–)	1.4	1.7	1.1	2.8	2	+(–)
C. gracilis Claus, 1863	4	2	0.8	1.2	0.8	A	0.8	10	1	1	4	2/6	6	0/1/2	3	8	1.8	5	1.4	–	1.2	1.3	1.5	1.2	1(0)	+
C. hadzii Petkovski, 1955	2.8	1.7	0.7	1.7	1	A	0.5	10	1	1	3	?	?	?	?	7	?	5	?	?	1.4	1.9	1	1	1	?
C. kasignete Karanovic, 2008	2.3	0.9	1.5	1.9	0.9	P	0.4	10	1	1	5	3/6	6	0/0/0/3	3	8	?	5	1.4	–	1.7	2.1	1.1	1.2	0	+
C. kasis Karanovic, 2008	2.4	1.2	2.2	1.6	1.6	P	0.2	9	1	1	5	2/4	6	0/0/3	3	8	?	5	1.5	–	1.5	1.6	1.1	2.1	?	?
C. kieferi elongata Herbst, 1953	3.3	1.5	1.7	1.9	1.4	A	0.4	10	0	1	4	3/6	7	0/0/1/4	3	8	?	5	1.6	+	1.8	1.7	1.4	1.5	?	?
C. kieferi Schäfer, 1936	1.5	1	2.9	1.8	1.9	P	0.3	?	1	1	5	3/6	7	0/0/1/3	3	8(7)	?	5	1.5	+	1.9	2.1	1.2	2.5	1(0)	?
C. kiraensis Hiromi, 1984	3.3	1.2	1	1.4	0.8	A	0.6	10	1	1	5	3/6	7	0/0/1/3	3	8	1.5	5	1.4	+	1.1	1.8	1.5	1.7	2	+
C. koreana sp. nov.	3.5	1.6	0.9	1.7	0.9	A	1.4	10	2	1	4	3/6	7	0/0/1/3	3	8	1.6	4	1.7	+	1.3	1.6	1	1.3	2	–
C. laurentica Nicholls, 1939	0.5	0.5	8.2	1.4	?	P	0.3	12	0	1	3	3/5	7	0/0/0/4	3	8	1.5	5	1.6	–	1.2	1.9	1	1.5	?	?
C. mediterranea Steuer, 1940	1.5	1	2.9	2	1.2	P	0.3	10	1	1	5	3/6	7	0/0/1/3	?	8	1.3	5	1.3	+	1.5	1.8	0.6	1	1	–
C. norvegica Boeck, 1865	2.5	1.2	1.1	2.2	2.7	A	0.6	10	?	?	?	?	?	?	?	?	?	?	?	?	1.3	2	1.4	1.8	?	?
C. oblivia Monchenko, 1981	2.3	1	1.9	1.6	1.3	P	0.3	10	1	1	5	3/6	6	0/0/1/3	3	8	1.4	5	1.4	–	1.3	1.5	0.7	1	?	?
C. pacifica Smirnov, 1935	2.4	1.1	3	1.4	1.5	P	0.3	13	1	1	5	3/6	?	?	3	?	?	?	?	?	1	2	1.2	1.8	?	?

	C_5, L/W	Cr /AnSo	medial seta/Cr	C_5, medial/dist. lateral seta	C_5, medial/dorsal seta	C_6, prox. lat. seta position	C_5, space between rami	Female A1, segmentation	A2, no. of exopodal setae	A2Bp, no. of medial setae	A2Enp2, no. of setae	MdEnp, armature formula	MxlEnp, no. of setae	MxpEnp, armature formula	P1Enp, no. of segments	P1Enp, no. of setae	P4Exp3, L/W	P4Exp3, no of setae	P4Enp3, L/W	P4Enp, lanceolate setae	P5, Exp/Bp	P5Exp, L/W	P5, lateral spine/Exp	P5Exp, lateral/medial spine	Male P5, no. of medial setae	Male P6, medial spine
C. parapsammophila Monchenko, 1981	1.3	0.8	2.4	3	2.1	P	0.6	10	2	1	4	3/6	7	0/0/1/3	3	8	1.8	4	1.3	–	1	1.7	0.8	1.4	0	+
C. phoenicia Lindberg, 1953	3	1	1.5	1.6	1.6	P	0.3	10	1	1	4	3/5	?	?	?	?	?	5	1.4	?	2	2	1.2	1.2	?	?
C. pontica Monchenko, 1977	3.7	1.3	0.9	1.6	1.5	A	0.7	10	1	0	4	3/5	7	0/0/1/3	2	8	1.6	5	1.6	–	1.8	1.8	1	1.2	?	?
C. psammophila Steuer, 1940	1	0.7	4.7	1.8	1.8	P	0.3	10	0	1	5	?	6	0/0/1/3	3	8	?	4	1.5	–	1	1.7	0.8	1.8	0	?
C. pygmaea Sars, 1918	5.5	2	0.8	1.8	2	A	0.8	10	1	1	4	?	?	?	3	7	?	?	?	?	1.1	1.5	1.2	0.9	?	?
C. rotundipes Herbst, 1952	2.5	1.2	1	1.4	1.4	A	0.6	10	0	1	4	3/5	6	0/1/2	3	7	1.1	5	1.1	–	1.4	1.3	0.9	1	1	+
C. schneideri Scott T., 1903	1.6	0.9	?	?	?	P	0.5	12	1	1	3	3/6	?	?	3	8	?	?	?	?	1	1.5	0.9	1.5	?	?
C. sinaitica (Por, 1979)	2.9	1.4	1.3	1.8	1.7	A	0.5	10	1	1	5	3/5	6	1/1/3	2	7	1.3	5	1.6	–	1.3	1.7	1.2	1.4	2	–
C. smirnovi Herbst, 1982	1.3	0.9	?	?	?	P	?	?	?	?	?	?	?	?	?	?	?	?	?	?	1.1	1.4	1.5	4.1	1	–
C. soror Karanovic, 2008	1.5	0.7	3.4	1.8	1.4	P	0.2	11	1	1	5	3/4	6	0/0/1/3	3	8	?	5	1.7	–	1.9	2.9	0.3	0.6	?	?
C. steueri Früchtl, 1923	2.2	1.2	2	1.6	1.9	A	0.5	10	0(1)	0	5	3/6	6(7)	0/0/1/3	3	7	1.5	5	1.5	–	1.5	1.6	1.1	1.1	1	+
C. tuberculata Herbst, 1962	3.2	1.8	0.8	1.8	2.1	A	0.2	10	1	1	5	3/6	6	0.1.3	3	?	1.5	5	?	–	1.4	2.5	1.6	1.3	?	?
C. unisetosa Karanovic, 2008	2	1	2.2	1.9	1.9	P	0.3	10	1(2)	1	4	3/4	6	0/0/0/3	3	8	1.5	5	1.5	–	1.4	2	1	1.7	?	?
C. vachoni Nicholls, 1939	2	1.1	0.7	1.1	?	P	0.2	10	0	1	3	2/6	7	0/0/0/4	3	8	1.5	5	1.6	–	1.1	1.7	0.6	1.2	?	?
C. wido sp. nov.	2.3	1.4	0.6	1.2	0.6	A	0.3	10	0	1	4	3/6	6	0/0/1/3	2	7	1.1	5	1.3	–	1.9	1.7	0.5	0.7	2	–
C. yutimaete Lotufo, 1994	2.7	1.5	1.5	1.9	1.7	A	0.3	10	2	1	5	3/5	7	0/0/1/4	2	8	1.4	5	1.5	+	1.3	1.8	1.1	1.5	?	?

markedly in so many morphological details that it is probably safe to assume that short caudal rami originated convergently in this genus a number of ×. A further 12 species have caudal rami that are between 1.5 and 1.9 × as long as wide (Table 1). Among them, only two have an 11-segmented antennula, both of them Australian endemics: *C. amita* Karanovic, 2008 and *C. soror* Karanovic, 2008. However, they both have no lanceolate setae on the fourth leg endopod, and have only six setae on the maxillular endopod (vs. seven in *C. curtijeju*) and four setae on the second segment of mandibular endopod (vs. six in *C. curtijeju*); additionally, *C. amita* has a different maxillipedal armature formula, while the fifth leg in *C. soror* has the medial spine longer than lateral spine (Karanovic 2008). Most of the other 12 species with relatively short caudal rami have a 10-segmented antennula, except the Brazilian *C. caissara* Lotufo, 1994 and the Scandinavian *C. schneideri* Scott T., 1903, which both have a 12-segmented antennula (see Scott T. 1903; Sars 1913; Lotufo 1994). Note that both Sars (1921) and Gurney (1927) considered *C. brevifurca* Sars, 1913 a subjective junior synonym of *C. schneideri*, presumably because both species were described from Norway and Sars (1913) was not aware of Scott's (1903) paper, but morphological differences between them are significant enough to consider them as separate species (Table 1). For two *Cyclopina* species with short caudal rami we don't know the segmentation of female antennula: *C. kieferi* Schäfer, 1936 and *C. smirnovi* Herbst, 1982. The former is presumably widely distributed in Europe (see Schäfer 1936; Steuer 1940; Petkovski 1955) and differs from *C. curtijeju* by antennal armature and proportions of the fifth leg. The latter was proposed as a new name by Herbst (1982) for a single male from Vladivostok, originally identified by Smirnov (1935) as *C. brachystylis* Sars, 1921 and illustrated by two simple drawings. This species could be closely related to *C. curtijeju*, but the lack of information on *C. smirnovi* and the fact that only females were found for the South Korean new species preclude further discussion.

Cyclopina wido has a completely unique swimming legs armature formula in the genus. It shares its two-segmented endopod of the first leg with only four congeners: *C. arenosa* Lotufo, 1994 from Brazil; *C. pontica* Monchenko, 1977 from the Black Sea; *C. sinaitica* (Por, 1979) from the Red Sea; and *C. yutimaete* Lotufo, 1994 from Brazil. All these species, however, have two setae on the second endopodal segment of second to fourth legs and differ from *C. wido* in many additional morphological characters (see Monchenko 1977; Por 1979; Lotufo 1994; Table 1). There could be very little doubt that the two-segmented condition evolved in this group convergently. This is further supported by the fact that a two-segmented endopod of the first leg could be found in several unrelated cyclopinid genera (see Herbst 1952, 1964; Krishnaswamy 1957; Plesa 1961; Rao and Ganapati 1969; Herbst 1974; Lotufo and Rocha 1991), and was also once reported as intraspecific variability (Ivanenko and Defaye 2004).

Several problems illustrated above should make it obvious that the genus *Cyclopina* is in need of revision. Unfortunately, as already mentioned by several researchers (Jaume and Boxshall 1996; Ivanenko and Defaye 2004; Karanovic 2008), incomplete descriptions of many species and a lack of one sex in some make this task impossible. To help facilitate further studies in this genus a list of characters is provided below for

48 species and subspecies currently considered as valid (Table 1). It does not include the Chinese *C. heterospina* Shen & Bai, 1956, which appears to have an 18-segmented antennula without elongated sixth segment and a fifth leg exopod with only two elements (see Shen and Bai 1956). This is obviously a completely different genus, but so many morphological details are missing from the species description that it is impossible to postulate phylogenetic relationships with the existing cyclopinid genera. On the other hand, very detailed descriptions and illustrations (including SEM photographs) of the Mexican *Mexiclopina campechana* Suárez-Morales & Almeyda-Artigas, 2015 leave very little double that this is a member of *Cyclopina* in its current (broad) definition, which could be already guessed from a very comprehensive comparison Suárez-Morales and Almeyda-Artigas (2015) provided with *C. esilis* Brian, 1938 and *C. kieferi* Schäfer, 1936. Therefore, it is included in Table 1 as *Cyclopina campechana* (Suárez-Morales & Almeyda-Artigas, 2015) comb. nov. Characters and measurements in this table were scored from original descriptions but also from subsequent redescriptions. Reported variability and/or asymmetries for discrete characters (such as armature formulae) are included in brackets, while those for continuous characters (such as various proportions) were averaged and rounded to the first decimal. The latter are, of course, approximate, which is one of the reasons they should be taken with caution and not used to construct keys to species. In addition to original species descriptions, which are automatically included in the reference list below, and papers already mentioned above, the following publications were consulted for species listed in Table 1: *C. brevifurca* Sars, 1913 (see also Lang 1946); *C. caissara* Lotufo, 1994 (see also Gómez & Martínez Arbizu 2004); *C. ensifera* Grandori, 1926 (see also Brian 1928; Petkovski 1955); *C. mediterranea* Steuer, 1940 (see also Petkovski 1955; Lotufo 1994); *C. norvegica* Boeck, 1865 (see also Sars 1921; Lang 1946); and *C. steueri* Früchtl, 1923 (see also Herbst 1955; Plesa 1963; Monchenko 1976). Armature formula for the maxillipedal endopod is given for the last four segments only. Unfortunately, state of the terminal seta on tip of the exopod of mandibular palp is unknown in most *Cyclopina* species, and therefore is not included in the table. However, there is no doubt that the state of this character would be very important in any phylogenetic analysis; this seta is modified (umbrella-like) in *C. esilis* (see Jaume and Boxshall 1996), as well as in *C. gracilis* and probably several other congeners (D. Jaume, pers. comm. July 2020). All South Korean new species, as well as all Australian species (Karanovic 2008), have this seta unmodified, so any revision of this genus will have to test the significance of this morphological character using molecular tools.

Acknowledgments

This work was supported by a grant from the National Institute of Biological Resources (NIBR), funded by the ministry of Environment (MOE) of the Republic of Korea (NIBR202004101). I am very grateful to Prof Gi-Sik Min (Inha University, Incheon) for a continuous support through the research project 'Discovery of Korean Indigenous

Species'. I would also like to thank Prof Ivana Karanovic and Ms Pham Thi Minh Huyen (both from Hanyang University, Seoul) for their generosity in sharing research facilities and providing administrative help respectively. The scanning electron microscope was made available through the courtesy of Prof. Jin Hyun Jun, and I also want to thank Mr. Junho Kim for the technical help provided (both from Eulji University, Seoul).

References

Armonies W, Reise K (2000) Faunal diversity across a sandy shore. Marine Ecology Progress Series 196: 49–57. https://doi.org/10.3354/meps196049

Boeck A (1865) Oversigt over de ved Norges Kyster jagttagne Copepoder henhorende til Calanidernes, Cyclopidernes og Harpactidernes Familier. Forhandlinger i Videnskabs-Selskabet i Christiania 1864: 226–282.

Boxshall GA, Halsey SH (2004) An Introduction to Copepod Diversity 1 & 2. The Ray Society, London, 966 pp.

Boxshall GA, Jaume D (2012) Three new species of copepods (Copepoda: Calanoida and Cyclopoida) from anchialine habitats in Indonesia. Zootaxa 3150: 36–58. https://doi.org/10.11646/zootaxa.3150.1.2

Brian A (1928) I Copepodi bentonici marini. Archivio Zoologico Italiano 12: 293–343.

Brian A (1938) Description d'une nouvelle espèce de Copépode Cyclopoïde du genre Cyclopina. Bulletin de la Société Zoologique de France 63: 13–18.

Brown AC, McLachlan A (2006) The Ecology of Sandy Shores. Elsevier, Amsterdam, 328 pp. https://doi.org/10.1016/B978-012372569-1/50001-X

Chang CY (2009) Inland-water Copepoda. Illustrated Encyclopedia of Fauna and Flora of Korea 42: 1–687.

Chang CY (2010) Continental Cyclopoids I. Invertebrate Fauna of Korea 21(19): 1–92.

Chang CY (2011) First record of the genus *Cyclopinoides* (Copepoda, Cyclopoida, Cyclopinidae) from the Pacific. Animal Cells and Systems 15: 63–72. https://doi.org/10.1080/19768354.2011.555132

Claus C (1863) Untersuchungen über die Organisation und Verwandtschaft der Copepoden. (Im Auszuge zusammengestellt). Verhandlungen der physikalisch-medizinischen Gesellschaft zu Würzburg 3: 51–103.

Elwers K, Martínez Arbizu P, Fiers F (2001) The genus *Pseudocyclopina* Lang in Antarctic waters: Redescription of the type-species, *P. belgicae* (Giesbrecht, 1902) and the description of four new species (Copepoda: Cyclopinidae). Ophelia 54: 143–165. https://doi.org/10.1080/00785236.2001.10409462

Ferrari FD, Ivanenko VN (2008) The identity of protopodal segments and the ramus of maxilla 2 of copepods (Copepoda). Crustaceana 81: 823–835. https://doi.org/10.1163/156854008784771702

Früchtl F (1923) Cladocera und Copepoda der Aru-Inseln. (Vorläufige Mitteilung: Artenliste und kurze Diagnosen der neuen Formen). Abhandlungen Senckenbergische Naturforschende Gesellschaft 375: 449–457.

Giere O (1993) Meiobenthology, the Microscopic Fauna in Aquatic Sediments. Springer-Verlag, Berlin, 328 pp. https://doi.org/10.1007/978-3-540-68661-3

Gómez S, Martínez Arbizu P (2004) First record of the genus *Cyclopina* (Copepoda: Cyclopoida), and fully illustrated redescription of *Cyclopina caissara* from northwestern Mexico. Anales del Instituto de Biología, Universidad Nacional Autónoma de México, Serie Zoología 75: 121–134.

Grandori R (1926) Nuove specie di Copepodi della Laguna Veneta. Bollettino di Istituto di Zoologia, Reale Università di Roma 3: 38–70.

Gray JS (1997) Marine biodiversity: patterns, threats and conservation needs. Biodiversity and Conservation 6: 153–175. https://doi.org/10.1023/A:1018335901847

Gray JS (2002) Species richness of marine soft sediments. Marine Ecology Progress Series 244: 285–297. https://doi.org/10.3354/meps244285

Gurney R (1927) Report on the Crustacea. Copepoda of brine-pools at Kabret. Zoological results of the Cambridge Expedition to the Suez Canal, 1924. Transactions of the Zoological Society of London 22: 173–177. https://doi.org/10.1111/j.1096-3642.1927.tb00329.x

Herbst HV (1952) Neue Cyclopoida Gnathostoma (Crustacea Copepoda) des Küstengrundwassers. Kieler Meeresforschungen 9: 94–111.

Herbst HV (1953) Weitere Cyclopoidea Gnathostoma (Crustacea Copepoda) des Küstengrundwassers. Kieler Meeresforschungen 9: 257–270.

Herbst HV (1955) Cyclopoida Gnathostoma (Crustacea Copepoda) von der brasilianischen Atlantikküste. Kieler Meeresforschungen 11: 214–229.

Herbst HV (1962) Marine Cyclopoida Gnathostoma (Copepoda) von der Bretagne-Küste als Kommensalen von Polychaeten. Crustaceana 4: 191–206. https://doi.org/10.1163/156854062X00346

Herbst HV (1964) Cyclopoida Gnathostoma (Crustacea Copepoda) aus dem Litoral und Küstengrundwasser des Roten Meeres. Kieler Meeresforschungen 20: 155–169.

Herbst HV (1974) Drei interstitielle Cyclopinae (Copepoda) von der Nordseeinsel Sylt. Mikrofauna Meeresbodens 35: 1–17.

Herbst HV (1982) Drei neue marine Cyclopoida Gnathostoma (Crustacea: Copepoda) aus dem nordamerikanischen Küstenbereich. Gewässer und Abwässer 68/69: 107–124.

Hiromi J (1984) Studies on littoral copepods in Mikawa Bay and adjacent waters. 1. Description of a new species of the genus *Cyclopina*. Proceedings of the Japan Society of Systematic Zoology 29: 16–23.

Ho J-S (1986) Phylogeny of Cyclopoida. In: Schriever G, Schminke HK, Shih C-T (Eds) Proceedings of the Second International Conference on Copepoda, Ottawa, Canada, 13–17 August 1984. Syllogeus 58: 177–183.

Ho J-S, Thatcher VE (1989) A new family of cyclopoid copepods (Ozmanidae) parasitic in the hemocoel of a snail from the Brazilian Amazon. Journal of Natural History 23: 903–911. https://doi.org/10.1080/00222938900770471

Huys R, Boxshall GA (1991) Copepod Evolution. Ray Society, London, 468 pp.

Ivanenko VN, Defaye D (2004) A new genus and species of deep-sea cyclopoids (Crustacea, Copepoda, Cyclopinidae) from the Mid-Atlantic Ridge (Azores Triple Junction, Lucky Strike). Zoosystema 26: 49–64.

Ivanenko VN, Lee J, Chang CY, Kim I-H (2019) Description of *Barathricola thermophilus*, a new species from a deep-sea hydrothermal vent field in the Indian Ocean with redescription of the *Barathricola* type species (Crustacea, Copepoda, Cyclopoida). ZooKeys 865: 103–121. https://doi.org/10.3897/zookeys.865.35827

Jaume D, Boxshall GA (1996) Two new genera of cyclopinid copepods (Crustacea) from anchihaline caves on western Mediterranean and eastern Atlantic islands. Zoological Journal of the Linnean Society 117: 283–304. https://doi.org/10.1111/j.1096-3642.1996.tb02191.x

Jaume D, Boxshall GA (1997) Rare cyclopoid copepods (Crustacea) from Mediterranean littoral caves. Bulletin of The Natural History Museum, Zoology 62: 83–99.

Jeong C-B, Lee MC, Lee K-W, Seo JS, Park HG, Rhee J-S, Lee J-S (2015) Identification and molecular characterization of dorsal and dorsal-like genes in the cyclopoid copepod *Paracyclopina nana*. Marine Genetics 24: 319–327. https://doi.org/10.1016/j.margen.2015.08.002

Karanovic T (2008) Marine interstitial Poecilostomatoida and Cyclopoida (Copepoda) of Australia. Crustaceana Monographs 9: 1–331. https://doi.org/10.1163/ej.9789004164598.i-332

Karanovic T (2014) On the phylogeny of Euryteinae (Crustacea, Copepoda, Cyclopoida), with description of one new species from Korea. Zoologischer Anzeiger 253: 512–525. https://doi.org/10.1016/j.jcz.2014.07.002

Karanovic T (2017) Two new *Phyllopodopsyllus* (Copepoda, Harpacticoida) from Korean marine interstitial. Journal of Species Research 6: 185–214. https://doi.org/10.12651/JSR.2017.6(S).185

Karanovic T, Blaha M (2019) Taming extreme morphological variability through coupling of molecular phylogeny and quantitative phenotype analysis as a new avenue for taxonomy. Scientific Reports 9: 1–14. https://doi.org/10.1038/s41598-019-38875-2

Karanovic T, Cho J-L (2012) Three new ameirid harpacticoids from Korea and first record of *Proameira simplex* (Crustacea: Copepoda: Ameiridae). Zootaxa 3368: 91–127. https://doi.org/10.11646/zootaxa.3368.1.5

Karanovic T, Cho J-L (2016) Four new *Schizopera* (Copepoda, Harpacticoida) from marine interstitial habitats in Korea. Zootaxa 4114: 1–32. https://doi.org/10.11646/zootaxa.4114.1.1

Karanovic T, Cho J-L (2017) Second member of the harpacticoid genera *Pontopolites* and *Pseudoleptomesochra* (Crustacea, Copepoda) are new species from Korean marine interstitial. Marine Biodiversity 48: 367–393. https://doi.org/10.1007/s12526-017-0731-2

Karanovic T, Cho J-L, Lee W (2012a) Redefinition of the parastenocaridid genus *Proserpinicaris* (Copepoda: Harpacticoida), with description of three new species from Korea. Journal of Natural History 46: 1573–1613. https://doi.org/10.1080/00222933.2012.681316

Karanovic T, Djurakic M, Eberhard SM (2016) Cryptic species or inadequate taxonomy? Implementation of 2D geometric morphometrics based on integumental organs as landmarks for delimitation and description of copepod taxa. Systematic Biology 65: 304–327. https://doi.org/10.1093/sysbio/syv088

Karanovic T, Grygier M, Lee W (2013) Endemism of subterranean *Diacyclops* in Korea and Japan, with descriptions of seven new species of the *languidoides*-group and redescriptions of *D. brevifurcus* Ishida, 2006 and *D. suoensis* Ito, 1954 (Crustacea, Copepoda, Cyclopoida). ZooKeys 267: 1–76. https://doi.org/10.3897/zookeys.267.3935

Karanovic T, Kim K (2014a) New insights into polyphyly of the harpacticoid genus *Delavalia* (Crustacea, Copepoda) through morphological and molecular study of an unprecedented diversity of sympatric species in a small South Korean bay. Zootaxa 3783: 1–96. https://doi.org/10.11646/zootaxa.3783.1.1

Karanovic T, Kim K (2014b) Suitability of cuticular pores and sensilla for harpacticoid copepod species delineation and phylogenetic reconstruction. Arthropod Structure and Development 43: 615–658. https://doi.org/10.1016/j.asd.2014.09.003

Karanovic T, Kim K, Lee W (2014) Morphological and molecular affinities of two East Asian species of *Stenhelia* (Crustacea, Copepoda, Harpacticoida). ZooKeys 411: 105–143. https://doi.org/10.3897/zookeys.411.7346

Karanovic T, Kim K, Lee W (2015) Concordance between molecular and morphology-based phylogenies of Korean *Enhydrosoma* (Copepoda: Harpacticoida: Cletodidae) highlights important synapomorphies and homoplasies in this genus globally. Zootaxa 3990: 451–496. https://doi.org/10.11646/zootaxa.3990.4.1

Karanovic T, Lee S, Lee W (2018) Instant taxonomy: choosing adequate characters for species delimination and description through congruence between molecular data and quantitative shape analysis. Invertebrate Systematics 32: 551–580. https://doi.org/10.1071/IS17002

Karanovic T, Lee W (2012) A new species of *Parastenocaris* from Korea, with a redescription of the closely related *P. biwae* from Japan (Copepoda: Harpacticoida: Parastenocarididae). Journal of Species Research 1: 4–34. https://doi.org/10.12651/JSR.2012.1.1.004

Karanovic T, Lee W (2016) First records of *Hemicyclops tanakai* Itoh and Nishida, 2002 and *Tisbe ensifer* Fisher, 1860 (Crustacea, Copepoda) in Korea. Journal of Species Research 5: 289–299. https://doi.org/10.12651/JSR.2016.5.3.289

Karanovic T, Yoo H, Lee W (2012b) A new cyclopoid copepod from Korean subterranean waters reveals an interesting connection with the Central Asian fauna (Crustacea: Copepoda: Cyclopoida). Journal of Species Research 1: 155–173. https://doi.org/10.12651/JSR.2012.1.2.156

Khodami S, McArthur JV, Blanco-Bercial L, Martínez Arbizu P (2017) Molecular phylogeny and revision of copepod orders (Crustacea: Copepoda). Scientific Reports 7: 1–11. https://doi.org/10.1038/s41598-017-06656-4

Khodami S, Mercado-Salas NF, Tang D, Martinez Arbizu P (2019) Molecular evidence for the retention of the Thaumatopsyllidae in the order Cyclopoida (Copepoda) and establishment of four suborders and two families within the Cyclopoida. Molecular Phylogenetics and Evolution 138: 43–52. https://doi.org/10.1016/j.ympev.2019.05.019

Kim I-H (2008) Sea Lice. Invertebrate Fauna of Korea 21(1): 1–66. https://doi.org/10.1038/s41598-017-06656-4

Kim K, Trebukhova Y, Lee W, Karanovic T (2014) A new species of *Enhydrosoma* (Copepoda: Harpacticoida: Cletodidae) from Korea, with redescription of *E. intermedia* and establishment of a new genus. Proceedings of the Biological Society of Washington 127: 248–283. https://doi.org/10.2988/0006-324X-127.1.248

Krishnaswamy S (1957) Studies on the Copepoda of Madras. Ph. D thesis, University of Madras, India, 168 pp.

Lang K (1946) Einige für die schwedische Fauna neue marine Cyclopoida Gnathostoma, nebst Bemerkungen uber die Systematik der Unterfamilie Cyclopodinae. Arkiv för Zoologi (A) 38: 1–16.

Lee B-Y, Kim H-S, Choi B-S, Hwang D-S, Choi AY, Han J, Won E-J, Choi I-Y, Lee S-H, Om A-S, Park HG, Lee J-S (2015) RNAseq based whole transcriptome analysis of the cyclopoid copepod *Paracyclopina nana* focusing on xenobiotics metabolism. Comparative Biochemistry and Physiology D 15: 12–19. https://doi.org/10.1016/j.cbd.2015.04.002

Lee J, Chang CY (2019) A new cyclopinid species of the rarely known genus *Cyclopinopsis* (Copepoda, Cyclopinidae) from Korea. Animal Systematics Evolution and Diversity 35: 114–122. https://doi.org/10.5635/ASED.2019.35.3.016

Lee S-H, Lee M-C, Puthumana J, Park JC, Kang S, Han J, Shin K-H, Park HG, Om A-S, Lee J-S (2017) Effects of temperature on growth and fatty acid synthesis in the cyclopoid copepod *Paracyclopina nana*. Fish Science 83: 725–734. https://doi.org/10.1007/s12562-017-1104-2

Lee W, Park E, Song SJ (2012) Marine Harpacticoida. Invertebrate Fauna of Korea 21(11): 1–276.

Lindberg K (1953) La sous-famille des Cyclopininae Kiefer (Crustacés Copépodes). Arkiv för Zoologi n. ser. 4(16): 311–325.

Lotufo GR (1994) *Cyclopina* (Copepoda, Cyclopoida) from Brazilian sandy beaches. Zoologica Scripta 23: 147–159. https://doi.org/10.1111/j.1463-6409.1994.tb00381.x

Lotufo GR, Rocha CEF (1991) Copepods from intertidal interstitial water of Salvador, Brazil, 1. *Cuipora janaina* gen. n., sp. n. and *Cyclopina caiala* sp. n. (Cyclopoida: Cyclopinidae). Bijdragen tot de Dierkunde 61: 107–118. https://doi.org/10.1163/26660644-06102003

Martínez Arbizu P (2000a) A new species of *Cyclopetta* from the Laptev Sea (Arctic Ocean), with the recognition of Cyclopettidae fam. nov., a new monophylum of free-living Cyclopoida (Copepoda). Bulletin de l'Institut Royal des Sciences Naturelles de Belgique, Biologie 70: 91–101.

Martínez Arbizu P (2000b) Giselinidae fam. nov., a new monophyletic group of cyclopoid copepods (Copepoda, Crustacea) from the Atlantic deep sea. Helgoland Marine Research 54: 190–212. https://doi.org/10.1007/s101520000051

Martínez Arbizu P (2001a) Hemicyclopinidae n. fam., a new monophyletic group of marine cyclopinid Cyclopoida, with description of one new genus and two new species (Crustacea, Copepoda, Cyclopoida). Senckenbergiana Biologica 81: 37–54.

Martínez Arbizu P (2001b) Psammocyclopinidae fam. n., a new monophyletic group of marine Cyclopoida (Copepoda, Crustacea), with the description of *Psammocyclopina georgei* sp. n. from the Magellan Region. Senckenbergiana Biologica 81: 37–54.

Martínez Arbizu P (2006) Phylogenetic relationships within Schminkepinellidae fam. n., a new monophyletic group of marine cyclopinids (Cyclopoida: Copepoda), description of two new genera and four new species. Zoologiya Bespozvonochnykh 3: 185–207. https://doi.org/10.15298/invertzool.03.2.04

Mikhailov KV, Ivanenko VN (2019a) Low support values and lack of reproducibility of molecular phylogenetic analysis of Copepoda orders. BioRxiv: e650507. https://doi.org/10.1101/650507

Mikhailov KV, Ivanenko VN (2019b) Lack of reproducibility of molecular phylogenetic analysis of Cyclopoida. Molecular Phylogenetics and Evolution 139 (106574). https://doi.org/10.1016/j.ympev.2019.106574

Monchenko VI (1976) A new for the Soviet Union fauna species *Cyclopina* cf. *steueri* Früchtl (Crustacea, Copepoda). Dopovidi Akademiyi Nauk Ukrayins'koiy RSR, Kiev (B) 1976(9): 844–848. [in Ukrainian with Russian and English summaries]

Monchenko VI (1977) On two Cyclopinidae (Crustacea, Copepoda) from interstitial biotope of the Black Sea. Russian Journal of Marine Biology 1977(5): 16–23. [in Russian with English summary]

Monchenko VI (1979) The second finding of *Cyclopina esilis* Brian (Crustacea, Copepoda) and redescription of the species. Doklady Akademii Nauk SSSR (B) 1979(5): 387–39l. [in Ukrainian with Russian and English summaries]

Monchenko VI (1981a) *Cyclopina oblivia* sp.n. (Crustacea, Copepoda) from the interstitial of the Black Sea. Vestnik Zoologii 5: 10–16. [in Russian with English summary]

Monchenko VI (1981b) *Cyclopina parapsammophila* sp. n. (Crustacea, Copepoda), a new species from the Black Sea. Biologiya Morya 6: 35–40. [in Russian with English summary]

Nicholls AG (1940) Marine Harpacticoids and Cyclopoids from the Shores of the St. Lawrence, Station Biologique du Saint-Laurent. Fauna et Flora Laurentianae 2: 241–292.

Pallares RE (1968) Copépodos marinos de la Ría Deseado (Santa Cruz, Argentina), Contribución sistemática-ecológica I. Contribuciones Científicas del Centro de Investigaciones de Biología Marina (CIBIMA), Buenos Aires (Servício de Hidrografía Naval H. 1024) 27: 1–125.

Petkovski TK (1955) IV Beitrag zur Kenntnis der Copepoden. Acta Musei Macedonici Scientiarum Naturalium Skopje 3: 71–104.

Plesa C (1961) New cyclopoids (Crustacea, Copepoda) of the interstitial fauna from the beaches of Ghana. Journal of the West African Science Association 7: 1–13.

Plesa C (1963) Étude sur la faune interstitielle litorale de la mer Noire, III. Résultats préliminaires des recherches sur la côte Roumaine, avec aperçu spécial sur les Cyclopoides Gnathostomes (Crustacea, Copepoda). Vie et Milieu 14: 775–813.

Por FD (1979) The Copepoda of Di Zahav pool (Gulf of Elat, Red Sea). Crustaceana 37: 13–30. https://doi.org/10.1163/156854079X00825

Pruett L, Cimino J (2000) Coastal length based on the World Vector Shoreline, United States Defense Mapping Agency, 1989. Global Maritime Boundaries Database (GMBD), Veridian – MRJ Technology Solutions, Fairfax, VA.

Rao GC, Ganapati PN (1969) On some interstitial copepods from the beach sands of Waltair coast. Proceedings of the Indian Academy of Sciences (B) 70: 262–286. https://doi.org/10.1007/BF03052153

Sars GO (1913) Copepoda Cyclopoida. Parts I & II. Oithonidae, Cyclopinidae, Cyclopidae (part). An Account of the Crustacea of Norway, with short descriptions and figures of all the species, Bergen Museum 6: 1–32.

Sars GO (1918) Copepoda Cyclopoida. Parts XIII & XIV. Lichomolgidae (concluded), Oncaeidae, Corycaeidae, Ergasilidae, Clausiidae, Eunicicolidae, Supplement. An Account of the Crustacea of Norway, with short descriptions and figures of all the species, Bergen Museum 6: 173–225.

Sars GO (1921) Copepoda Supplement. Parts IX & X. Harpacticoida (concluded), Cyclopoida. An Account of the Crustacea of Norway, with short descriptions and figures of all the species, Bergen Museum 7: 93–121.

Schäfer HW (1936) Cyclopiniden (Crustacea Copepoda) aus der deutschen Nordsee. Zoologischer Anzeiger 114: 225–234.

Scott T (1903) Notes on some Copepoda from the Arctic Seas collected in 1890 by the Rev. Canon A.M. Norman, F.R.S. In: Norman AM (Ed.) Notes on the Natural History of East

Finmark, I. Annals and Magazine of Natural History 11: 4–32. https://doi.org/10.5962/bhl.title.38697

Shen C-J [Ed.] (1979) Fauna Sinica, Crustacea Freshwater Copepoda. Fauna Editorial Commission, Academia Sinica, 450 pp.

Smirnov SS (1935) Zur Systematik der Copepoden-Familie Cyclopinidae G.O. Sars. Zoologischer Anzeiger 109: 203–210.

Soh HY, Moon SY, Wi JH (2010) Marine Planktonic Copepods II. Invertebrate Fauna of Korea 21(28): 1–157.

Steuer A (1940) Über einige Copepoda Cyclopoida der mediterranen Amphioxussande. Note dell'Istituto Italo-Germanico di Biologia Marina di Rovigno d'Istria 2: 1–27.

Stock JK, Von Vaupel Klein JC (1996) Mounting media revisited: the suitability of Reyne's fluid for small crustaceans. Crustaceana 69: 749–798. https://doi.org/10.1163/156854096X00826

Suárez-Morales E, Almeyda-Artigas RJ (2015) A new genus and species of cyclopoid (Crustacea, Copepoda, Cyclopinidae) from a coastal system in the Gulf of Mexico. ZooKeys 534: 17–34. https://doi.org/10.3897/zookeys.534.6019

Thrush SF, Grey JS, Hewitt JE, Ugland KI (2006) Predicting the effect of habitat homogenization on marine biodiversity. Ecological Applications 16: 1636–1642. https://doi.org/10.1890/1051-0761(2006)016[1636:PTEOHH]2.0.CO;2

Ueda H, Ohtsuka S, Seike Y, Ohtani S (2001) Second record of *Cyclopina kiraensis*, a small, brackish-water cyclopoid copepod, in Japan. Limnology 2: 49–50. https://doi.org/10.1007/s102010170016

Vervoort W (1964) Free-living Copepoda from Ifaluk Atoll in the Caroline Islands with notes on related species. Bulletin of the United States National Museum 236: 1–431. https://doi.org/10.5479/si.03629236.236.1

Walter TC, Boxshall G (2020) World Copepoda database [Database]. http://www.marinespecies.org/copepoda [accessed on 21 June 2020]

Wells JBJ, McKenzie KG (1973) Report on a small collection of benthic copepods from marine and brackish waters of Aldabra, Indian Ocean. Crustaceana 25: 133–146. https://doi.org/10.1163/156854073X00786

Zeppilli D, Sarrazin J, Leduc D, Marinez Arbizu P, Fontaneto D, Fonanier C, Gooday AJ, Kristensen RM, Ivanenko VN, Sorensen MV, Vanreusel A, Thebault J, Mea M, Allio N, Andro T, Arvigo A, Castrec J, Danielo M, Foulon V, Fumeron R, Hermabessiere L, Hulot V, James T, Lanfonne-Augen R, Le Bot T, Long M, Mahabror D, Morel Q, Panralos M, Pouplard E, Raimondeau L, Rio-Cabello A, Seite S, Traisnel G, Urvoy K, Van Der Stegen T, Weyand M, Fernandes D (2015) Is the meiofauna a good indicator for climate change and anthropogenic impacts? Marine Biodiversity 45: 505–535. https://doi.org/10.1007/s12526-015-0359-z

ZooKeys 992: 105–138 (2020)
doi: 10.3897/zookeys.992.56921
https://zookeys.pensoft.net

RESEARCH ARTICLE

A peer-reviewed open-access journal
ZooKeys
Launched to accelerate biodiversity research

Contribution to the knowledge of Neanurinae of north-western Iran with description of seven new species (Collembola, Neanuridae)

Adrian Smolis[1], Dariusz Skarżyński[1]

1 *Institute of Environmental Biology, Department of Invertebrate Biology, Evolution and Conservation, University of Wrocław, Przybyszewskiego 65, 51-148 Wrocław, Poland*

Corresponding author: Dariusz Skarżyński (dariusz.skarzynski@uwr.edu.pl)

Academic editor: W. M. Weiner | Received 25 July 2020 | Accepted 29 September 2020 | Published 12 November 2020

http://zoobank.org/F143D360-4A50-4567-AEBC-4F7425D6FEC0

Citation: Smolis A, Skarżyński D (2020) Contribution to the knowledge of Neanurinae of north-western Iran with description of seven new species (Collembola, Neanuridae). ZooKeys 992: 105–138. https://doi.org/10.3897/zookeys.992.56921

Abstract

Seven new species of the subfamily Neanurinae from north-western Iran are described and illustrated in detail. *Endonura agnieskae* **sp. nov.** differs from the most similar congener, *E. reticulata* (Axelson, 1905), in chaetotaxic details and the arrangement of tubercles on the dorsal side of the body. *Endonura annae* **sp. nov.** can be easily recognised by its wide labrum, the absence of chaetae C on the head and the presence of a toothed claw. *Endonura schwendingeri* **sp. nov.** is especially distinctive due to the absence of chaetae A and Ocp on the head and the presence of the male ventral organ. *Deutonura breviseta* **sp. nov.** is related and most similar to *D. persica* Smolis, Shayanmehr & Yoosefi-Lafooraki, 2018, described recently and known from Mazandran Province in Iran. The new species can be easily distinguished by the following set of features: dark pigmented body, presence of chaetae C and Dl3 on the head, absence of microchaetae on the furca rudimentary, presence of thickened macrochaetae on dorsal side of body and absence of cryptopygy. The main characteristics of *Deutonura sengleti* **sp. nov.** include a white body with dark pigmented eyes, the fusion of tubercles Di and De on the first thoracic segment and the presence of the male ventral organ. *Deutonura iranica* **sp. nov.** is superficially similar to *D. gibbosa* Porco, Bedos & Deharveng, 2010, a species known from the Alps and Jura in Europe, but it differs in the body colour and the number of labial chaetae and chaetae (L+So) on the head. *Paravietnura rostrata* **sp. nov.**, the first member of this enigmatic and intriguing genus known from Iran, is characterised by an unusually

elongate ogival labrum and extreme reduction of dorsal chaetotaxy. Furthermore, new records of several other species of the subfamily: *Cryptonura maxima* Smolis, Falahati & Skarżyński, 2012; *C. persica* Smolis, Falahati & Skarżyński, 2012; *Deutonura persica*; *Endonura longirostris* Smolis, Shayanmehr, Kuznetsova & Yoosefi-Lafooraki, 2017; *E. paracentaurea* Smolis, Shayanmehr, Kuznetsova & Yoosefi-Lafooraki, 2017; *Neanura deharvengi* Smolis, Shayanmehr & Yoosefi-Lafooraki, 2018; *N. muscorum* (Templeton, 1835) and *Protanura papillata* Cassagnau & Delamare Deboutteville, 1955 are given. The present study is based on the rich material collected by Antoine Senglet and loaned by Peter J. Schwendinger.

Keywords
Asia, new records, springtails, taxonomy, western Palearctic

Introduction

Springtails, classified within the subfamily Neanurinae, differ significantly in terms of morphology and behaviour from other Collembola. First of all, they have completely lost the furcula and their movement may be defined as exceptionally slow compared to the majority of springtails. Another noticeable difference between them and the majority of other Collembola is the covering of the dorsal and lateral sides of the body by spherical structures naming tubercles, which make them resemble a mulberry. In addition, chaetae covering Neanurinae body are usually strongly developed, elongated and considerably widened, as well as covered with numerous teeth (Deharveng 1983; Smolis 2008). Paradoxically, although they do not have a furcula, i.e. structures enabling express escape from predators, Neanurinae are an example of an evolution success, demonstrated by its over 800 currently described taxa which constitutes nearly one tenth of all the known Collembola (Bellinger et al. 2020; Smolis and Greenslade 2020). Regarding the actual distribution of the subfamily, the largest species diversity is observed both in tropical and temperate forests on all continents, excluding Antarctica (i.e. Yosii 1976; Cassagnau and Deharveng 1984; Deharveng and Weiner 1984; Cassagnau 1988; Deharveng 1989; Deharveng and Bedos 1992; Cassagnau 1996; Deharveng and Suhardjono 2000; Palacios-Vargas and Simón Benito 2007; Zhi-Chun and Jian-Xiu 2008; Palacios-Vargas and Deharveng 2014; Smolis and Deharveng 2015; Luo and Palacios-Vargas 2016; Ji-Gang et al. 2018). Nevertheless, knowledge on global diversity of the subfamily is still insufficient and far from complete as many areas, i.e. the Middle East, North Africa, New Guinea or Central Asia, are poorly surveyed in this respect.

An examination of an exceptionally-rich material of Neanurinae from north-western Iran (Provinces: Gilan, Golestan, Kermanshah, Mazandaran, North Khorasan, Semnan and West Azerbaijan), collected in the early 1970s by Antoine Senglet and loaned for the presented studies by Peter J. Schwendinger (curator of the Muséum d'histoire naturelle in Geneva, Switzerland), has revealed seven unknown species of this subfamily. Their detailed and illustrated descriptions are provided with new records of several other known species classified to Neanurinae.

Materials and methods

The specimens were cleared in Nesbitt's fluid, subsequently mounted on slides in Swan's medium and studied using a Nikon Eclipse E600 phase contrast microscope. Figures were drawn with a camera lucida and prepared for publication using Adobe Photoshop CS3.

The whole material, types as well as the other material, is deposited in the Muséum d'histoire naturelle in Geneva, Switzerland.

Terminology

Terminology and layout of the tables used in the paper follow Deharveng (1983), Deharveng and Weiner (1984), Smolis and Deharveng (2006) and Smolis (2008).

Abbreviations

General morphology:

Abd. abdomen;
Ant. antenna;
AOIII sensory organ of antennal segment III;
Cx coxa;
Fe femur;
Scx2 subcoxa 2;
T tibiotarsus;
Th. thorax;
Tr trochanter;
VT ventral tube.

Groups of chaetae:

Ag antegenital;
An chaetae of anal lobes;
Ap apical;
Ca centroapical;
Cm centromedial;
Cp centroposterior;
D dorsal;
Fu furcal;
Vc ventrocentral;
Ve or **ve** ventroexternal;
Vea ventroexternoanterior;
Vem ventroexternomedial;
Vep ventroexternoposterior;
Vel ventroexternolateral;
Vec ventroexternocentral;
Vei ventroexternointernal;
Vi or **vi** ventrointernal;
Vl ventrolateral.

Tubercles:

Af antenno-frontal;
Cl clypeal;
De dorsoexternal;
Di dorsointernal;
Dl dorsolateral;
L lateral;
Oc ocular;
So subocular.

Types of chaetae:

Ml	long macrochaeta;	**iv**	ordinary chaetae on ventral Ant. IV;
Mc	short macrochaeta;	**or**	organite of Ant. IV;
Mcc	very short macrochaeta;	**brs**	border s-chaeta on Ant. IV;
Me	mesochaeta;	**i**	ordinary chaeta on Ant. IV;
mi	microchaeta;	**mou**	cylindrical s-chaetae on Ant. IV ("soies mousses");
ms	s-microchaeta;	**x**	labial papilla x;
S or **s**	chaeta s;	**L'**	ordinary lateral chaeta on Abd. V;
Bs	s-chaeta on Ant. IV;	**B4**, **B5**	ordinary chaetae on tibiotarsi.
miA	microchaetae on Ant. IV;		

Taxonomy

***Endonura agnieskae* sp. nov.**
http://zoobank.org/B8FE7E36-B1F9-4D2E-BA23-1588CCA1126D
Figs 1–13, Tables 1–3

Type material. ***Holotype*:** adult female on slide, Iran, Mazandaran Province, Nashtarud, forest reserve, sifting, 10.VII.1973, leg. A. Senglet, sample 7318. ***Paratypes*:** 4 females, 2 males and 2 juveniles on slide, same data as holotype.

Other material. Female on slide, Iran, Mazandaran Province, Kiasar (36°16'N, 53°25'E), 10.VII.1975, leg. A. Senglet, 7546; 9 females, 2 males and juvenile on slide, Gilan Province, Limir, large trees in marsh, sifting, 28.VI.1973, leg. A. Senglet, 7306; female on slide, Iran, Gilan Province, Paresar, tree holes, leaves, sifting, 2.VII.1973, leg. A. Senglet, 7310; female on slide, Gilan Province, road to Jirandeh, 1000 m a.s.l., forest, 9.VIII.1974, leg. A. Senglet, 7486; female on slide, Semnan Province, near Loveh (37°19'N, 55°46'E / 1300 m a.s.l.), 22.VIII.1975, leg. A. Senglet, 7574.

Etymology. The new species is dedicated to Agnieszka, wife of the first author.

Diagnosis. Habitus typical of the genus *Endonura*. Dorsal tubercles present and well developed. 2+2 large pigmented eyes. Buccal relatively short, labrum nonogival. Central area of head with complete chaetotaxy. Tubercles Cl and Af separate. Tubercles Dl and (L+So) on head with 6 and 10 chaetae, respectively. Tubercles Di on Th. I present and fused with tubercle De. Tubercles De on Th. II and III with 3 and 4 chaetae, respectively. Tubercles L on Abd. III and IV with 3–4 and 7 chaetae, respectively. Abd. IV and V with 8 and 3 tubercles, respectively. Furcal rest without mi. Claw without inner tooth. Tibiotarsi with chaetae B4 and B5 rather short.

Description. General. Body length (without antennae): 0.8 (juvenile) to 1.7 mm (holotype: 1.5 mm). Colour of the body bluish-grey. 2+2 large black eyes, in a typical arrangement for the genus (one anterior and one posterior eye, Fig. 3).

Chaetal morphology. Dorsal ordinary chaetae of five types: long macrochaetae (Ml), short macrochaetae (Mc), very short macrochaetae (Mcc), mesochaetae and

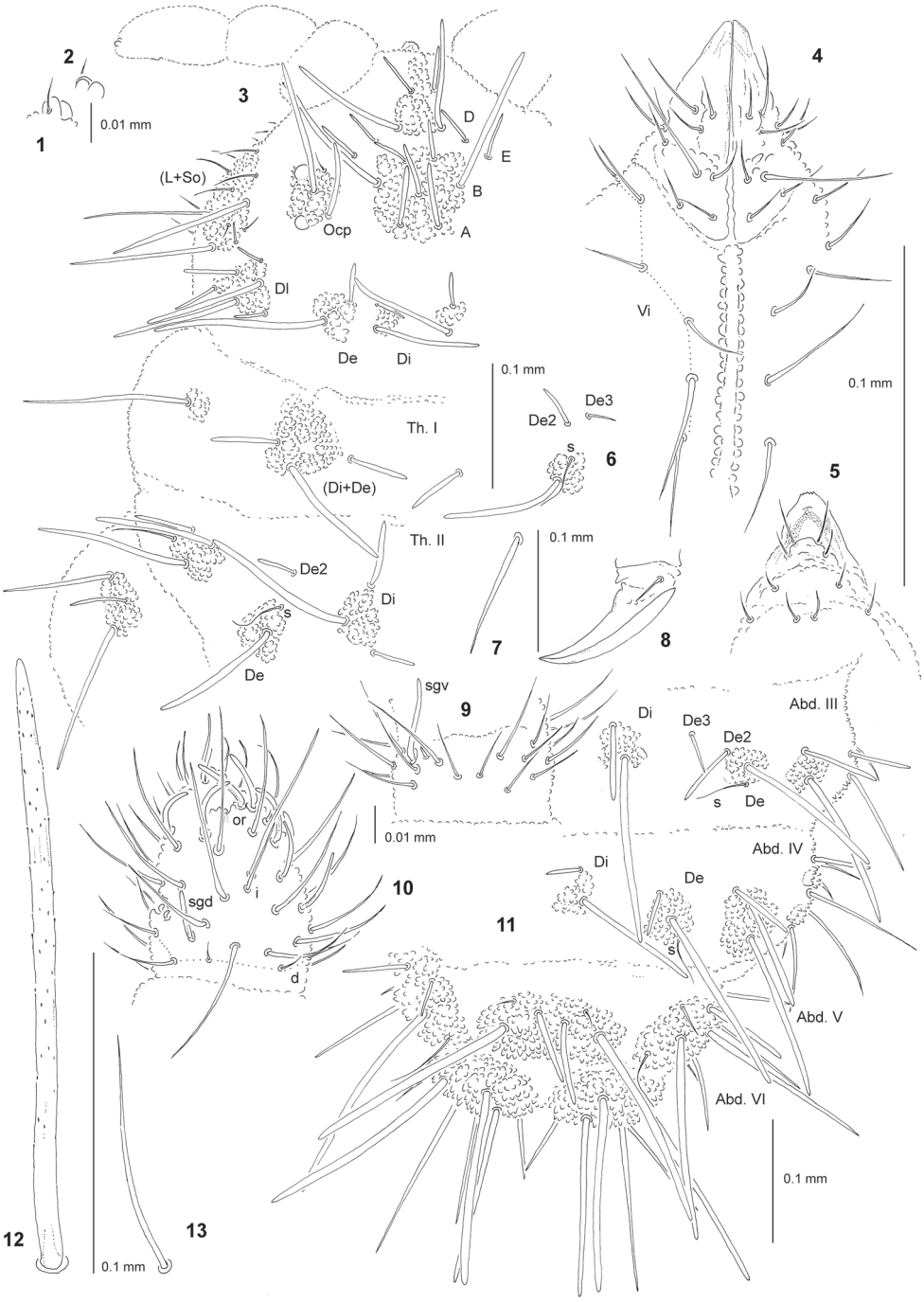

Figures 1–13. *Endonura agnieskae* sp. nov.: **1** apical bulb, dorsal view **2** apical bulb, ventral view **3** chaetotaxy of head and Th., dorsolateral view **4** chaetotaxy of labium and group Vi (holotype) **5** chaetotaxy and ventral sclerifications of labrum (holotype) **6** tubercle De of Th. III **7** chaeta B4 of leg III **8** claw of leg III, lateral view **9** ventral chaetotaxy of Ant. III **10** dorsal chaetotaxy of Ant. III–IV (holotype) **11** dorsal chaetotaxy of Abd. III–VI **12** chaeta Di1 of Abd. V **13** sensillum of Abd. V.

Table 1. Chaetotaxy of *Endonura agnieskae* sp. nov.: Cephalic chaetotaxy–dorsal side.

Tubercle	Number of chaetae	Types of chaetae	Names of chaetae
Cl	4	Ml	F
		me	G
Af	11	Ml	B
		Mc	A, O, C, D, E
Oc	3	Ml	Ocm
		Mc	Ocp
		mi	Oca
Di	2	Ml	Di1
		Mcc	Di2
De	2	Ml	De1
		Mcc	De2
Dl	6	Ml	Dl5, Dl1
		Mc	Dl3
		Mcc	Dl2, Dl4, Dl6
(L+So)	10	Ml	L1, L4, So1
		Mcc	L2
		mi	L3, So2
		me	So3–6

Table 2. Chaetotaxy of *Endonura agnieskae* sp. nov.: Chaetotaxy of antennae.

Segment, Group	Number of chaetae	Segment, Group	Number of chaetae adult
I	7	IV	or, 8 S, i, 12 mou, 6 brs, 2 iv
II	12		
III	5 sensilla AO III		
ve	5	ap	8 bs, 5 miA
vc	4	ca	2 bs, 3 miA
vi	4	cm	3 bs, 1 miA
d	5	cp	8 miA, 1 brs

microchaetae. Long macrochaetae thick, slightly arc-like or straight, narrowly sheathed, feebly serrated, apically rounded (Figs 3, 6, 11, 12). Macrochaetae Mc and Mcc morphologically similar to long macrochaetae, but much shorter. Mesochaetae similar to ventral chaetae, thin, smooth and pointed. Microchaetae similar to mesochaetae, but clearly shorter. S-chaetae of terga thin, smooth and short, distinctly shorter than nearby macrochaetae (Figs 3, 6, 11, 13).

Antennae. Typical of the genus. Dorsal chaetotaxy of Ant. III–IV as Fig. 10 and Table 2. S-chaetae of Ant. IV of medium length and moderately thickened (Fig. 10). Apical vesicle distinct, trilobate (Figs 1 and 2). Ventral chaetotaxy of Ant. III–IV as Fig. 9 and Table 2, sensillum sgv long and slightly s-shaped.

Mouthparts. Buccal cone rather short with labral sclerifications nonogival. Labrum chaetotaxy: 4/2, 4 (Fig. 5). Labium with four basal, three distal and three lateral chaetae, papillae x absent (Fig. 4). Maxilla styliform, mandible thin and tridentate.

Dorsal chaetotaxy and tubercles. Chaetotaxy of head complete (Fig. 3). Tubercles Di on head present, on Th. I differentiated and fused with De. Th. III and Abd. I–III with chaetae De3 free (Figs 6 and 11). On Abd. I–III, the line of chaetae De1–chaeta s parallel to the dorsomedian line (Fig. 11). On Abd. IV chaetae Di1 short. Cryptopygy absent, Abd. VI well visible from above. Chaeta Di2 on Abd. V as Mc, Mcc or mi.

Table 3. Chaetotaxy of *Endonura agnieskae* sp. nov.: Postcephalic chaetotaxy.

	Terga				Legs				
	Di	De	Dl	L	Scx2	Cx	Tr	Fe	T
Th. I	3		1	–	0	3	6	13	19
Th. II	3	2+s	3+s+ms	3	2	7	6	12	19
Th. III	3	3+s	3+s	3	2	8	6	11	18
							Sterna		
Abd. I	2	3+s	2	3			VT: 4		
Abd. II	2	3+s	2	3			Ve: 5; chaeta Ve1 present		
Abd. III	2	3+s	2	3			Vel:5–6; Fu: 5 me, 0 mi		
Abd. IV	2	2+s	3	5–6			Vel: 4; Vec: 2; Vei: 2; Vl: 4		
Abd. V	(3+3)		7–8+s				Ag: 3; Vl: 1		
Abd. VI		7					Ve: 14; An: 2 mi		

Ventral chaetotaxy. On head, groups Vea, Vem and Vep with 3, 3–4, 4 chaetae, respectively. Group Vi on head with 6 chaetae (Fig. 4). On Abd. IV, furca rudimentary without microchaetae. On Abd. IV, tubercle L without free chaeta.

Legs. Chaetotaxy of legs as in Table 3. Claw without internal tooth (Fig. 8). On tibiotarsi, chaeta M present and chaetae B4 and B5 rather short and pointed (Fig. 7).

Remarks. Due to the general appearance, dorsal and ventral chaetotaxy, *E. agnieskae* sp. nov. strongly resembles *E. reticulata* (Axelson, 1905), Holarctic and circumboreal species occurring in tundra, boreal and temperate biotopes of northern Europe (Scandinavian Peninsula), north-eastern Asia and North America (Smolis et al. 2011). Nevertheless, these species can be easily distinguished from each other by the set of characters: size of the eyes (expressed by the ratio of anterior eye diameter and diameter of base of chaeta Ocm, in *agnieskae* 2:1, in *reticulata* 1:1 or 5:4), the number of lateral labial chaetae (in *agnieskae* three, in *reticulata* four), the length of chaetae Ocp and A on the head (in *agnieskae*, equal in length, in reticulata chaeta Ocp, longer than chaeta A), the presence of tubercle Di on Th. I (in *agnieskae*, present and fused with De, in *reticulata*, absent), the location of chaeta De2 on Abd. I–III (in *agnieskae*, connected with tubercle De, in *reticulata*, free), the location of chaeta s on Abd. I–III (in *agnieskae*, the line of chaetae De1–chaeta s parallel to the dorsomedian line, in *reticulata*, not parallel) and the length of chaeta Di1 on Abd. IV (in *agnieskae*, distinctly shorter than chaeta Di1 on Abd. III, in *reticulata*, longer or equal to chaeta Di1 on Abd. III).

Endonura annae sp. nov.

http://zoobank.org/A26E5348-95D7-4E84-BB9A-C50383757D11
Figs 14–27, Tables 4–6

Type material. ***Holotype*:** adult female on slide, Iran, Gilan Province, road to Dyavaherdeh, 1100–1300 m a.s.l., 7.VIII. 1974, leg. A. Senglet, sample 7484. ***Paratypes*:** 2 females, male and juvenile on slide, same data as holotype.

Other material. Iran, 7 females and male on slide, Gilan Province, near Asalem, 300–600 m a.s.l., large beeches, sifting, 30.VI.1973, leg. A. Senglet, 7308; 3 females on

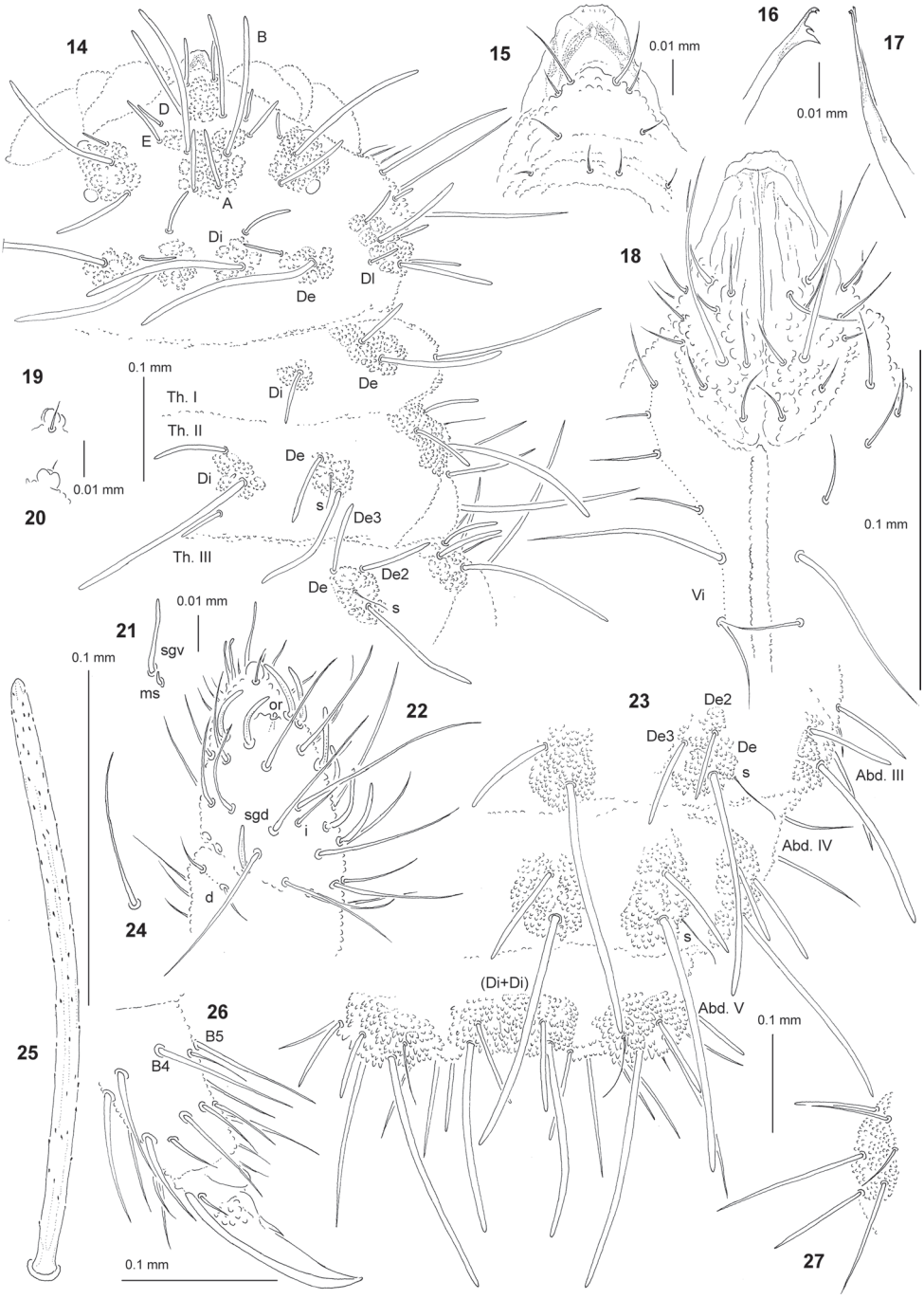

Figures 14–27. *Endonura annae* sp. nov.: **14** chaetotaxy of head and Th. (holotype), dorsolateral view **15** chaetotaxy and ventral sclerifications of labrum **16** Mandible **17** Maxilla **18** chaetotaxy of labium and group Vi **19** apical bulb, dorsal view **20** apical bulb, ventral view **21** sensillum sgv and microsensillum of Ant. III **22** dorsal chaetotaxy of Ant. III–IV **23** dorsal chaetotaxy of Abd. III–VI (holotype) **24** sensillum of Abd. V **25** chaeta Di1 of Abd. V **26** tibiotarsus and claw of leg III, lateral view **27** tubercle L of Abd. IV.

Table 4. Chaetotaxy of *Endonura annae* sp. nov.: Cephalic chaetotaxy–dorsal side.

Tubercle	Number of chaetae	Types of chaetae	Names of chaetae
Cl	4	Ml	F
		me	G
Af	8	Ml	B
		Mc	A, E
		Mcc	D
Oc	3	Ml	Ocm
		Mc	Ocp
		Mcc	Oca
Di	2	Ml	Di1
		Mc	Di2
De	2	Ml	De1
		Mcc	De2
Dl	6	Ml	Dl5, Dl1
		Mc	Dl4
		Mcc	Dl2, Dl3, Dl6
(L+So)	8	Ml	L1, L4, So1
		Mcc	L2
		me	So3–6

slide, Gilan Province, Shahrbijar, tree hole, humus, sifting, 6.IX.1973, leg. A. Senglet, 7366; 4 females and juvenile on slide, Gilan Province, Asalem (37°45'N, 48°57'E), leaves and tree holes, sifting, 11.VI.1975, leg. A. Senglet, 7519; juvenile on slide, Mazandaran Province, Pol-e Zanguleh, 2300 m a.s.l., 12.VII.1973, leg. A. Senglet, 7320.

Etymology. The new species is dedicated to Anna, wife of the second author.

Diagnosis. Habitus typical of the genus *Endonura*. Dorsal tubercles present and well developed. 2+2 large pigmented eyes. Buccal cone short, labrum nonogival. Head with chaetae A, B, D and E. Chaetae O and C absent. Tubercles Cl and Af separate. Tubercles Dl and (L+So) on head with 6 and 8 chaetae, respectively. Tubercles Di on Th. I present. Tubercles De on Th. II and III with 3 and 4 chaetae, respectively. Tubercles L on Abd. III and IV with 3 and 6 chaetae, respectively. Abd. IV and V with 8 and 3 tubercles, respectively. Furcal rest without mi. Claw with inner tooth. Tibiotarsi with chaetae B4 and B5 rather short.

Description. General. Body length (without antennae): 0.8 to 1.45 mm (holotype: 1.25 mm). Colour of the body white. 2+2 large black eyes, in a typical arrangement for the genus (Fig. 14).

Chaetal morphology. Dorsal ordinary chaetae of four types: long macrochaetae (Ml), short macrochaetae (Mc), very short macrochaetae (Mcc) and mesochaetae. Long macrochaetae thick, slightly arc-like, narrowly sheathed, feebly serrated, apically rounded (Figs 14, 23, 25). Macrochaetae Mc and Mcc morphologically similar to long macrochaetae, but shorter. Mesochaetae similar to ventral chaetae, thin, smooth and pointed. S–chaetae of terga thin, smooth and short, notably shorter than nearby macrochaetae (Figs 14, 23, 24).

Antennae. Typical of the genus. Dorsal chaetotaxy of Ant. III–IV as Fig. 22 and Table 5. S-chaetae of Ant. IV of medium length and moderately thickened, sensillum sgd notably short (Fig. 22). Ant. III with two chaetae d. Apical vesicle distinct, trilobate (Figs 19, 20). Ventral chaetotaxy of Ant. III as in Table 5, sensillum sgv long and slightly s-shaped (Fig. 21).

Table 5. Chaetotaxy of *Endonura annae* sp. nov.: Chaetotaxy of antennae.

Segment, Group	Number of chaetae	Segment, Group	Number of chaetae adult
I	7	IV	or, 8 S, i, 12 mou, 6 brs, 2 iv
II	12		
III	5 sensilla AO III		
ve	5	ap	8 bs, 5 miA
vc	4	ca	2 bs, 3 miA
vi	4	cm	3 bs, 1 miA
d	2	cp	8 miA, 1 brs

Table 6. Chaetotaxy of *Endonura annae* sp. nov.: Postcephalic chaetotaxy.

	Terga				Legs				
	Di	De	Dl	L	Scx2	Cx	Tr	Fe	T
Th. I	1	2	1	–	0	3	6	13	19
Th. II	3	2+s	3+s+ms	3	2	7	6	12	19
Th. III	3	3+s	3+s	3	2	8	6	11	18
							Sterna		
Abd. I	2	3+s	2	3			VT: 4		
Abd. II	2	3+s	2	3			Ve: 5; chaeta Ve1 present		
Abd. III	2	3+s	2	3			Vel: 5; Fu: 4–5 me, 0 mi		
Abd. IV	2	2+s	3	6			Vel: 4; Vec: 2; Vei: 2; Vl: 4		
Abd. V	(2+2)		5+s				Ag: 3; Vl: 1, L‘: 1		
Abd. VI		7					Ve: 13–14; An: 2 mi		

Mouthparts. Buccal short and wide with labral sclerifications nonogival (Fig. 15). Labrum chaetotaxy: 4/2, 4 (Fig. 15). Labium with four basal, three distal and four lateral chaetae, papillae x absent (Fig. 18). Maxilla styliform (Fig. 17), mandible with four teeth and relatively thin (Fig. 16).

Dorsal chaetotaxy and tubercles. Head without chaetae O, C, So2 and L3 (Fig. 14). Chaetae D free and not connected with tubercle. Tubercles Di on Th. I differentiated, not fused with tubercles De (Fig. 14). Th. III and Abd. I–III without free chaetae De2 and De3 (Figs 14, 23). On Abd. I–III, the line of chaetae De1–chaeta s perpendicular to the dorsomedian line. On Abd. III–IV, chaetae Di1 notably longer than chaetae Di1 of Abd. V (Fig. 23). On Abd. V, tubercle (Di+Di) with 2+2 chaetae. Cryptopygy strongly developed, Abd. VI practically not visible from above (Fig. 23).

Ventral chaetotaxy. On head, groups Vea, Vem and Vep with 3, 4, 4 chaetae, respectively. Group Vi on head with 6 chaetae (Fig. 18). On Abd. IV, furca rudimentary without macrochaetae, tubercle L with 6 chaetae (Fig. 27). On Abd. V, chaetae Vl and L’ present.

Legs. Chaetotaxy of legs as in Table 6. Claw with internal tooth. On tibiotarsi, chaeta M present and chaetae B4 and B5 relatively short and pointed (Fig. 26).

Remarks. Morphologically, *E. annae* sp. nov. is strongly reminiscent of *E. persica* Smolis, Kahrarian, Piwnik & Skarżyński, 2016, taxon described from Kermanshah Province in northern Iran (Smolis et al. 2016a). Nevertheless, the new species can be easily recognised by several characters, including: the absence of chaeta C on the head (in *persica* present), the presence of 6 chaetae Dl on the head (in *persica* 5), wide and short buccal cone (in *persica* narrow and long), chaetae E on the head connected with tubercle Af (in *persica* free), chaetae De2 and De3 on Th. II–III, connected with

tubercle De (in *persica* free), 2+2 chaetae Di on Abd. V (in *persica* 3+3) and strong cryptopygy (in *persica*, slightly developed).

E. annae sp. nov. is also similar to two species with toothed claw: *E. dentifera* Smolis, Skarżyński, Pomorski & Kaprus', 2007 and *E. dobrolyubovae* Smolis & Kuznetsova, 2018, described from the Crimea and the Caucasus, respectively (Smolis et al. 2007; Smolis and Kuznetsova 2018). These species differ, however, in a number of details: the shape of the buccal cone (in *annae*, wide and short, in *dentifera* and *dobrolyubovae*, narrow and relatively long), the presence of chaeta C on the head (in *annae*, absent, in *dentifera* and *dobrolyubovae*, present), the presence and location of chaeta E on the head (in *annae*, present and connected with tubercle Af, in *dentifera*, present and free, in *dobrolyubovae*, absent), the number of chaetae (L+So) on the head (in *dentifera*, 10 chaetae, in *annae* and *dobrolyubovae*, 8 chaetae), the presence of tubercle Di on Th. I (in *annae*, present, in *dentifera* and *dobrolyubovae*, absent), the location of chaetae De3 on Th. III and Abd. I–III (in *annae*, connected with tubercle De, in *dentifera* and *dobrolyubovae*, free), the presence of male ventral organ (in *annae* and *dentifera*, absent, in *dobrolyubovae*, present) and the presence of cryptopygy (in *annae*, present, in *dentifera* and *dobrolyubovae*, absent).

***Endonura schwendingeri* sp. nov.**
http://zoobank.org/19378FF6-D560-4C9E-A729-B7681C695986
Figs 28–41, Tables 7–9

Type material. ***Holotype*:** female on slide, Iran, Gilan Province, Paresar, tree holes, leaves, sifting, 2.VII.1973, leg. A. Senglet, sample 7310. ***Paratypes*:** 3 females and male on slide, same data as holotype.

Other material. Iran, 3 females and male on slide, Gilan Province, Lunak, 600 m a.s.l., forest, leaves, trunk, sifting, 6.VII.1973, leg. A. Senglet, 7313.

Etymology. The new species is dedicated to Peter J. Schwendinger, curator of the Muséum d'histoire naturelle in Geneva and prominent Austrian Arachnologist.

Diagnosis. Habitus typical of the genus *Endonura*. Dorsal tubercles present. 2+2 large pigmented eyes. Buccal cone relatively long, labrum nonogival. Head with chaetae B, C and D. Chaeta O absent. Tubercles Cl and Af separate. Tubercles Dl and (L+So) on head with 5 and 7 chaetae, respectively. Tubercles Di on Th. I absent. Tubercles De on Th. II and III with 3 and 4 chaetae, respectively. Tubercles L on Abd. III and IV with 2 and 4 chaetae, respectively. Abd. IV and V with 8 and 3 tubercles, respectively. Furcal rest without mi. Claw with inner tooth. Tibiotarsi with chaetae B4 and B5 long.

Description. General. Body length (without antennae): 0.5 (juvenile) to 1.15 mm (holotype: 1.1 mm). Colour of the body bluish-grey. 2+2 large black eyes, in a typical arrangement for the genus (Fig. 29).

Chaetal morphology. Dorsal ordinary chaetae of five types: long macrochaetae (Ml), short macrochaetae (Mc), very short macrochaetae (Mcc), mesochaetae and mi-

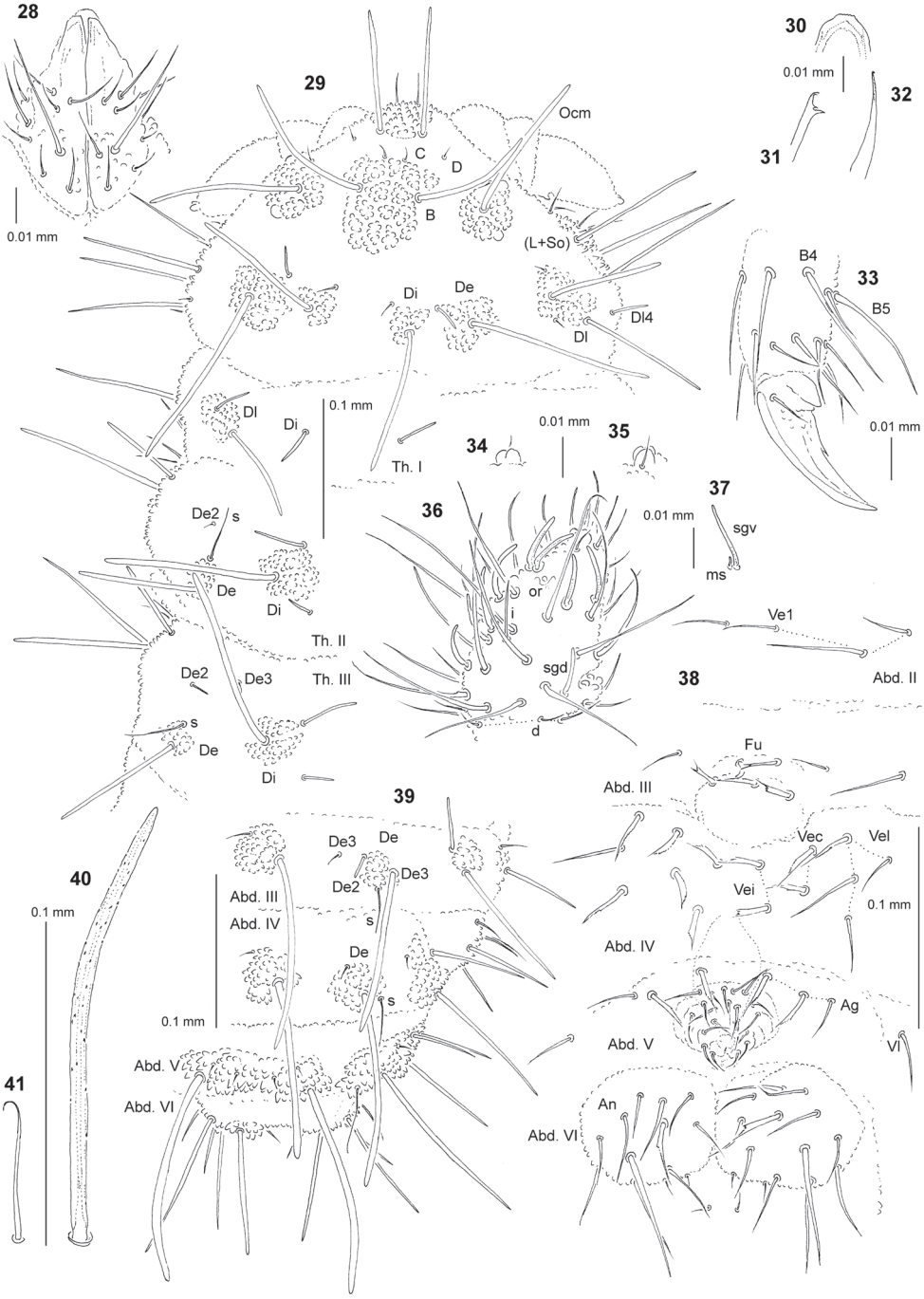

Figures 28–41. *Endonura schwendingeri* sp. nov.: **28** chaetotaxy of labium **29** chaetotaxy of head and Th. (holotype), dorsolateral view **30** apical part of labrum **31** Mandible **32** Maxilla **33** tibiotarsus and claw of leg III, lateral view **34** apical bulb, ventral view **35** apical bulb, dorsal view **36** dorsal chaetotaxy of Ant. III–IV **37** sensillum sgv and microsensillum of Ant. III **38** ventral chaetotaxy of Abd. II–VI (adult male) **39** dorsal chaetotaxy of Abd. III–VI **40** chaeta Di1 of Abd. V **41** sensillum of Abd. V.

Table 7. Chaetotaxy of *Endonura schwendingeri* sp. nov.: Cephalic chaetotaxy–dorsal side.

Tubercle	Number of chaetae	Types of chaetae	Names of chaetae
Cl	4	Ml	F
		me	G
Af	6	Ml	B
		mi	C, D
Oc	2	Ml	Ocm
		mi	Oca
Di	2	Mc	Di1
		mi	Di2
De	2	Ml	De1
		Mcc	De2
Dl	5	Ml	Dl5, Dl1
		Mcc	Dl4
		mi	Dl2, Dl6
(L+So)	7	Ml	L1, L4, So1
		me	So3–6

crochaetae. Long macrochaetae relatively thin, straight or slightly arc-like, narrowly sheathed, feebly serrated, apically rounded (Figs 29, 39, 40). Macrochaetae Mc and Mcc morphologically similar to long macrochaetae, but much shorter (Figs 29, 39). Mesochaetae similar to ventral chaetae, thin, smooth and pointed. Microchaetae similar to mesochaetae, but clearly shorter (Figs 29, 39). S–chaetae of terga thin, smooth and short, notably shorter than nearby macrochaetae (Figs 29, 39, 41).

Antennae. Typical of the genus. Dorsal chaetotaxy of Ant. III–IV as Fig. 36 and Table 8. S–chaetae of Ant. IV of medium length and thickened, sensillum sgd short and straight (Fig. 36). Apical vesicle distinct, trilobate (Figs 34, 35). Ventral chaetotaxy of Ant. III–IV Table 8, sensillum sgv as Fig. 37.

Mouthparts. Buccal cone relatively short with labral sclerifications nonogival (Fig. 30). Labrum chaetotaxy: 4/2, 4. Labium with four basal, three distal and three lateral chaetae, papillae x absent (Fig. 28). Maxilla styliform (Fig. 32), mandible relatively thin with two basal and two apical teeth (Fig. 31).

Dorsal chaetotaxy and tubercles. Head without chaetae A, E, Ocp, Dl3, So2, L2 and L3 absent (Fig. 29), chaeta D free. Tubercles Di on Th. I not differentiated (Fig. 29). On Th. III chaetae De2 and De3 free, on Abd. I–III chaetae De3 free (Figs 29, 39). On Abd. I–III, the line of chaetae De1–chaeta s non perpendicular to the dorsomedian line. Cryptopygy present, but weakly developed, Abd. VI partially visible from above (Fig. 39).

Ventral chaetotaxy. On head, groups Vea, Vem and Vep with 3, 4 and 4 chaetae, respectively. Group Vi on head with 6 chaetae. On Abd. IV, furca rudimentary without microchaetae (Fig. 38). On Abd. IV, group L without free chaeta. On Abd. V, chaetae Vl present, chaetae L' absent (Fig. 38). Male with thick and forked chaetae (male ventral organ) on anal plates (Abd. VI) and in groups: Ag (Abd. V); Vei, Vec and Vel (Abd. IV) and Fu (Abd. III) (Fig.38).

Legs. Chaetotaxy of legs as in Table 9. Claw with internal tooth. On tibiotarsi, chaeta M present and chaetae B4 and B5 relatively long and pointed (Fig. 33).

Remarks. Since *E. schwendingeri* sp. nov. is characterised by chaetotaxic features unknown in other members of the genus, for example, the absence of chaetae A and

Table 8. Chaetotaxy of *Endonura schwendingeri* sp. nov.: Chaetotaxy of antennae.

Segment, Group	Number of chaetae	Segment, Group	Number of chaetae adult
I	7	IV	or, 8 S, i, 12 mou, 6 brs, 2 iv
II	12		
III	5 sensilla AO III		
ve	5	ap	8 bs, 5 miA
vc	4	ca	2 bs, 3 miA
vi	4	cm	3 bs, 1 miA
d	5	cp	8 miA, 1 brs

Table 9. Chaetotaxy of *Endonura schwendingeri* sp. nov.: Postcephalic chaetotaxy.

	Terga				Legs				
	Di	**De**	**Dl**	**L**	**Scx2**	**Cx**	**Tr**	**Fe**	**T**
Th. I	1	2	1	–	0	3	6	13	19
Th. II	3	2+s	3+s+ms	3	2	7	6	12	19
Th. III	3	3+s	3+s	3	2	8	6	11	18
							Sterna		
Abd. I	2	3+s	2	2			VT: 4		
Abd. II	2	3+s	2	2			Ve: 4–5; chaeta Ve1 present		
Abd. III	2	3+s	2	2			Vel: 3–4; Fu: 5 me, 0 mi		
Abd. IV	2	2+s	3	4			Vel: 4; Vec: 2; Vei: 2; Vl: 4		
Abd. V	(3+3)		5+s				Ag: 3; Vl: 1		
Abd. VI		7					Ve: 11–12; An: 2 mi		

Ocp on the head, its closer affinities with other *Endonura* species are currently uncertain and hard to assess. However, taking into account the weak development of tuberculation, delicate buccal cone and the presence of well-developed male ventral organ, the new species seems to be most similar to *E. quadriseta* Cassagnau & Péja, 1979, a form shortly described from Greece (Cassagnau and Péja 1979), but recently re-described, based on types and a new material from the Crimea (Smolis et al. 2007). Nevertheless, besides characters mentioned above, these taxa differ in numerous features: the number of lateral labial chaetae (in *schwendingeri*, three, in *quadriseta*, four), the presence of chaetae C and O on the head (in *schwendingeri*, absent, in *quadriseta*, present), the number of chaetae (L+So) on the head (in *schwendingeri*, 7, in *quadriseta*, 9), the number of chaetae Dl on the head (in *schwendingeri*, 5, in *quadriseta*, 6), the number of chaetae L on Abd. III and IV (in *schwendingeri*, 2 and 4, in *quadriseta*, 4 and 7) and the presence of an internal tooth on claws (in *schwendingeri*, present, in *quadriseta*, absent).

Deutonura breviseta **sp. nov.**

http://zoobank.org/98297969-EFC7-42C8-9597-14ED4612CD03
Figs 42–52, Tables 10–12

Type material. ***Holotype*:** male on slide, Iran, Gilan Province, near Asalem, 300–600 m a.s.l., large beeches, sifting, 30.VI.1973, leg. A. Senglet, sample 7308. ***Paratypes*:** 3 females and 2 males on slide, same data as holotype.

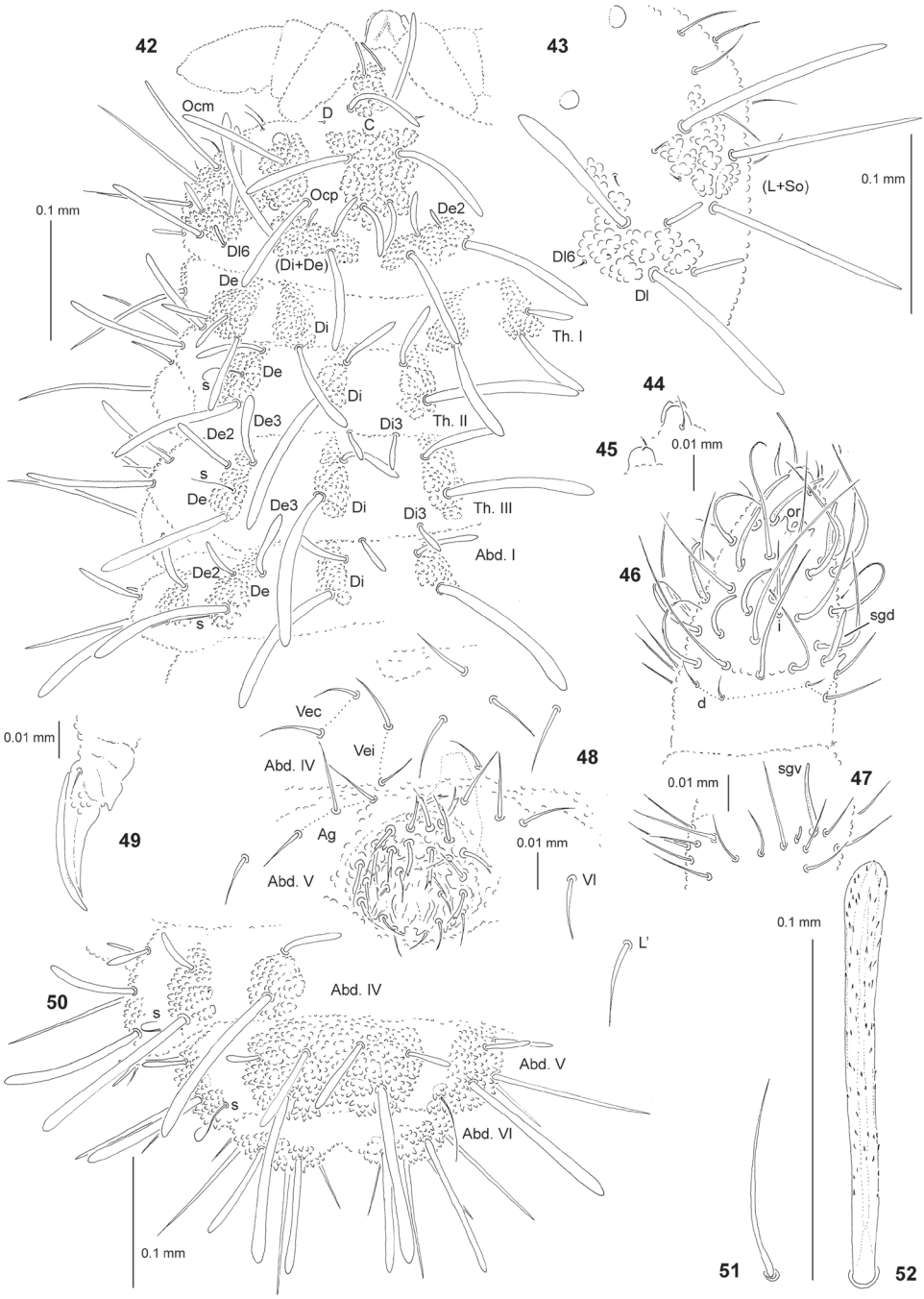

Figures 42–52. *Deutonura breviseta* sp. nov.: **42** chaetotaxy of head, Th. and Abd. I (holotype), dorsolateral view **43** chaetotaxy of tubercles Dl and (L+So), lateral view **44** apical bulb, dorsal view **45** apical bulb, ventral view **46** dorsal chaetotaxy of Ant. III–IV **47** ventral chaetotaxy of Ant. III **48** ventral chaetotaxy of Abd. IV–V (adult male) **49** claw of leg III, lateral view **50** dorsal chaetotaxy of Abd. IV–VI (holotype) **51** sensillum of Abd. V **52** chaeta Di1 of Abd. V.

Table 10. Chaetotaxy of *Deutonura breviseta* sp. nov.: Cephalic chaetotaxy–dorsal side.

Tubercle	Number of chaetae	Types of chaetae	Names of chaetae
Cl	4	Ml	F
		Mc	G
Af	8	Ml	B
		Mc	A
		mi	C
		mi or me	D
Oc	3	Ml	Ocm, Ocp
		mi	Oca
(Di+De)	4	Ml	Di1, De1
		Mc	Di2
		Mcc or mi	De2
Dl	6	Ml	Dl5, Dl1
		Mc	Dl3, Dl4
		Mcc or mi	Dl6
		mi	Dl2
(L+So)	9	Ml	L1, L4, So1
		me	So3–6
		mi	L2, So2

Other material. Iran, female on slide, Gilan Province, Asalem (37°45'N, 48°57'E), leaves and tree holes, sifting, 11.VI.1975, leg. A. Senglet, 7519; female, male and 2 juveniles on slide, Gilan Province, Paresar, tree holes, leaves, sifting, 2.VII.1973, leg. A. Senglet, 7310; male on slide, Mazandaran Province, Nashtarud, forest, reserve, sifting, 10.VII.1973, leg. A. Senglet, 7318; female and 3 males on slide, Mazandaran Province, near Amol, forest, sifting, 18.VII.1973, leg. A. Senglet, 7329b; 4 females, 3 males and juvenile on slide, Mazandaran Province, Aliabad, 30.VII.1974, leg. A. Senglet, 7475; female on slide, Gilan Province, road to Dyavaherdeh, 1100–1300 m a.s.l., 7.VIII. 1974, leg. A. Senglet, 7484.

Etymology. The name of the new species is referring to its exceptionally short macrochaetae Ml.

Diagnosis. Habitus typical of the genus *Deutonura*. Dorsal tubercles present and well developed. 2+2 large pigmented eyes. Buccal cone relatively long and wide, labrum without ogival sclerifications. Head without chaetae E, O and L3. Tubercles Cl and Af separate. No granular area between chaetae A and B on head. Tubercles De on Th. II and III with 3 and 4 chaetae, respectively. Tubercles Di on Abd. V not bilobed. Cryptopygy not developed. Male ventral organ present.

Description. General. Body length (without antennae): 0.7 (juvenile) to 1.7 mm (holotype: 0.85 mm). Colour of the body white. 2+2 large black eyes, in a typical arrangement for the genus (Figs 42, 43).

Chaetal morphology. Dorsal ordinary chaetae of five types: long macrochaetae (Ml), short macrochaetae (Mc), very short macrochaetae (Mcc), mesochaetae and microchaetae. Long macrochaetae thickened, slightly arc-like or straight, narrowly sheathed, serrated, apically rounded and extended at apex (Figs 42, 43, 50, 52). Macrochaetae Mc and Mcc morphologically similar to long macrochaetae, but much shorter (Figs 42, 43, 50). Mesochaetae similar to ventral chaetae, thin, smooth and pointed.

Table 11. Chaetotaxy of *Deutonura breviseta* sp. nov.: Chaetotaxy of antennae.

Segment, Group	Number of chaetae	Segment, Group	Number of chaetae adult
I	7	IV	or, 8 S, i, 12 mou, 6 brs, 2 iv
II	12		
III	5 sensilla AO III		
ve	5	ap	8 bs, 5 miA
vc	4	ca	2 bs, 3 miA
vi	4	cm	3 bs, 1 miA
d	5	cp	8 miA, 1 brs

Table 12. Chaetotaxy of *Deutonura breviseta* sp. nov.: Postcephalic chaetotaxy.

	Terga				Legs				
	Di	De	Dl	L	Scx2	Cx	Tr	Fe	T
Th. I	1	2	1	–	0	3	6	13	19
Th. II	3	2+s	3+s+ms	3	2	7	6	12	19
Th. III	3	3+s	3+s	3	2	8	6	11	18
							Sterna		
Abd. I	2	3+s	2	3			VT: 4		
Abd. II	2	3+s	2	3			Ve: 5; chaeta Ve1 present		
Abd. III	2	3+s	2	3			Vel: 5; Fu: 5 me, 0 mi		
Abd. IV	2	2+s	3	6			Vel: 4; Vec: 2; Vei: 2; Vl: 4		
Abd. V	(3+3)		5+s				Ag: 3; Vl: 1, L‘: 1		
Abd. VI		7					Ve: 14; An: 2 mi		

Microchaetae similar to mesochaetae, but clearly shorter (Figs 42, 43). S-chaetae of terga thin, smooth and short, notably shorter than nearby macrochaetae (Figs 42, 50, 51).

Antennae. Typical of the genus. Dorsal chaetotaxy of Ant. III–IV as in Fig. 46 and Table 11. S-chaetae of Ant. IV of medium length and relatively thin, sensillum sgd short and straight (Fig. 46). Apical vesicle distinct, trilobate (Figs 44, 45). Ventral chaetotaxy of Ant. III as in Fig. 47 and Table 11, ventral chaetotaxy of Ant. IV as Table 11.

Mouthparts. Buccal cone relatively short and wide, labral sclerifications nonogival (Fig. 42). Labrum chaetotaxy: 2/2, 4. Labium with four basal, three distal and four lateral chaetae, papillae x absent. Maxilla styliform mandible thin and tridentate.

Dorsal chaetotaxy and tubercles. Head without granular area between chaetae A and B. Elementary tubercles DE and EE on head absent (Fig. 42). Head without chaetae E, O and L3, chaeta D free (Figs 42, 43). Chaetae Ocm and Ocp of nearly equal length. Chaetae De2 on head usually as Mcc, rarely as mi (Fig. 42). Chaeta Dl6 on head as Mcc or mi. Th. I with tubercles Di and De not fused. Chaetae Di3 on Th. II–III free. On Th. III, chaetae De2 slightly shorter than De3 (Fig. 42). On Abd. I–III, chaetae De2 distinctly shorter than De3 (Fig. 50). Cryptopygy absent, Abd. VI well visible from above.

Ventral chaetotaxy. On head, groups Vea, Vem and Vep with 3, 4 and 4 chaetae, respectively. Group Vi on head with 6 chaetae. On Abd. IV, furca rudimentary without microchaetae. Male with thick and forked chaetae (male ventral organ) around genital aperture (Abd. V). On Abd. V, chaetae Vl and L’ present (Fig. 48).

Legs. Chaetotaxy of legs as in Table 12. Claw without internal tooth (Fig. 49). On tibiotarsi, chaeta M present and chaetae B4 and B5 relatively long and pointed.

Remarks. *Deutonura breviseta* sp. nov. seems to be closest to *D. persica* Smolis, Shayanmehr & Yoosefi-Lafooraki, 2018 recently described from the northern part of Iran (Mazandaran Province, Smolis et al. 2018). However, these species differ in numerous characters, including the number of lateral labial chaetae (in *breviseta*, four, in *persica*, three), the presence of chaetae C on the head (in *breviseta*, present, in *persica*, absent), the number of chaetae (L+So) on the head (in *breviseta*, 9, in *persica* 8), the presence of chaetae Dl3 on the head (in *breviseta*, present, in *persica*, absent), the presence of microchaetae on furca rudimentary (in *breviseta*, absent, in *persica*, present) and the presence of cryptopygy (in *breviseta*, present, in *persica*, absent). Additionally, male ventral organ in *D. breviseta* sp. nov. is built of thickened and forked chaetae on Abd. V only (in *persica*, also on Abd. III, IV and VI).

***Deutonura sengleti* sp. nov.**

http://zoobank.org/15B48E2F-B8EF-4C46-8A2F-CC09CEDDD62A
Figs 53–61, Tables 13–15

Type material. ***Holotype***: female on slide, Iran, Gilan Province, Shahrbijar, tree hole, humus, sifting, 6.IX.1973, leg. A. Senglet, sample 7366. ***Paratypes*:** 2 males on slide, same data as holotype.

Other material. Iran, 2 males on slide, Gilan Province, Limir, large trees in marsh, sifting, 28.VI.1973, leg. A. Senglet, 7306; female, 2 males and juvenile on slide, Gilan Province, road to Jirandeh, 1000 m a.s.l., forest, 9.VIII.1974, leg. A. Senglet, 7486; female, male and juvenile on slide, Gilan Province, near Asalem (37°38'N, 48°48'E), 1800 m a.s.l., tree holes, sifting, 10.VI.1975, leg. A. Senglet, 7516; 2 males and juvenile on slide, Gilan Province, near Asalem (37°40'N, 48°52'E), 1200 m a.s.l., tree holes, sifting, 10.VI.1975, leg. A. Senglet, 7517; female on slide Gilan Province, Asalem (37°45'N, 48°57'E), leaves and tree holes, sifting, 11.VI.1975, leg. A. Senglet, 7519; male on slide, Mazandaran Province, near Amol, forest, sifting, 18.VII.1973, leg. A. Senglet, 7329b; male on slide, Mazandaran Province, road to Tchorteh, 800 m a.s.l., tree and leaves, sifting, 5.VIII.1974, leg. A. Senglet, 7482.

Etymology. The new species is dedicated to Antoine Senglet, collector of the Iranian material studied and prominent Swiss Arachnologist.

Diagnosis. Habitus typical of the genus *Deutonura*. Dorsal tubercles present and well developed. 2+2 large pigmented eyes. Buccal cone relatively long and narrow, labrum without ogival sclerifications. Head without chaetae O, So2 and L3. Tubercles Cl and Af separate. No granular area between chaetae A and B on head. Tubercles De on Th. II and III with 3 and 4 chaetae, respectively. Tubercles Di on Abd. V not bilobed. Cryptopygy not developed. Male ventral organ present.

Description. General. Body length (without antennae): 0.85 (juvenile) to 1.55 mm (holotype: 1.45 mm). Colour of the body bluish-grey. 2+2 large black eyes, in a typical arrangement for the genus (Fig. 53).

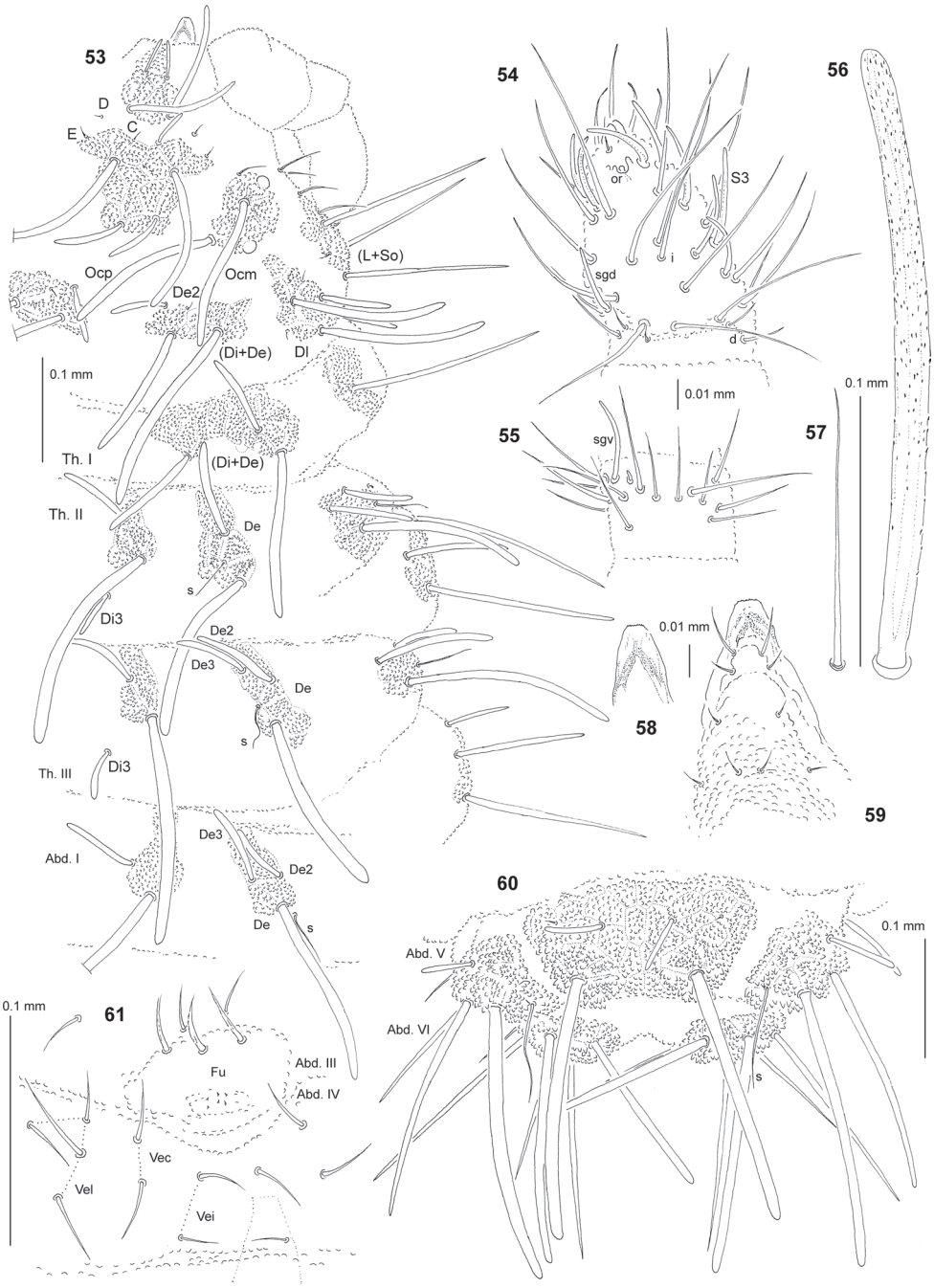

Figures 53–61. *Deutonura sengleti* sp. nov. **53** chaetotaxy of head, Th. and Abd. I (holotype), dorsolateral view **54** dorsal chaetotaxy of Ant. III–IV **55** ventral chaetotaxy of Ant. III **56** chaeta Di1 of Abd. V **57** sensillum of Abd. V **58** apical part of labrum **59** chaetotaxy and ventral sclerifications of labrum **60** dorsal chaetotaxy of Abd. V–VI (holotype) **61** ventral chaetotaxy of Abd. III–IV (adult male).

Table 13. Chaetotaxy of *Deutonura sengleti* sp. nov.: Cephalic chaetotaxy–dorsal side.

Tubercle	Number of chaetae	Types of chaetae	Names of chaetae
Cl	4	Ml	F
		Mc	G
Af	10	Ml	B
		Mc	A
		Mcc or mi	C
		mi	D, E
Oc	3	Ml	Ocm, Ocp
		mi	Oca
(Di+De)	4	Ml	Di1, De1
		Mc	Di2
		mi or Mcc	De2
Dl	6	Ml	Dl5, Dl1
		Mc	Dl3, Dl4
		mi or Mcc	Dl2
		mi	Dl6
(L+So)	8	Ml	L1, L4, So1
		me	So3–6
		mi or Mcc	L2

Chaetal morphology. Dorsal ordinary chaetae of five types: long macrochaetae (Ml), short macrochaetae (Mc), very short macrochaetae (Mcc), mesochaetae and microchaetae. Long macrochaetae thickened, slightly arc-like or straight, narrowly sheathed, serrated, cylindrical, apically rounded (Figs 53, 56, 60). Macrochaetae Mc and Mcc morphologically similar to long macrochaetae, but much shorter (Figs 53, 60). Mesochaetae similar to ventral chaetae, thin, smooth and pointed. Microchaetae similar to mesochaetae, but clearly shorter (Figs 53, 60). S-chaetae of terga thin, smooth and short, notably shorter than nearby macrochaetae (Figs 53, 57, 60).

Antennae. Typical of the genus. Dorsal chaetotaxy of Ant. III–IV as in Fig. 54 and Table 14. S–chaetae of Ant. IV long and relatively thin, S3 notably longer than others, sensillum sgd of medium size and straight (Fig. 54). Apical vesicle distinct, trilobate. Ventral chaetotaxy of Ant. III as in Fig. 55 and Table 14.

Mouthparts. Buccal cone relatively long and narrow, labral sclerifications non-ogival (Figs 58, 59). Labrum chaetotaxy: 4/2, 4 (Fig. 59). Labium with four basal, three distal and four lateral chaetae, papillae x absent. Maxilla styliform mandible thin and tridentate.

Dorsal chaetotaxy and tubercles. Head without granular area between chaetae A and B. Elementary tubercles DE and EE on head absent (Fig. 53). Head without chaetae O, L3 and So2, chaeta D free. Chaetae C as Mcc or mi (Fig. 53). Chaetae Ocm and Ocp of nearly equal length. Chaetae De2 on head as mi or rarely Mcc (Fig. 53). Th. I with tubercles Di and De fused (Fig. 53). Chaetae Di3 on Th. II–III free. On Th. III, chaetae De2 slightly longer than De3 (Fig. 53). On Abd. I–III, chaetae De2 shorter than De3. Cryptopygy absent, Abd. VI well visible from above.

Ventral chaetotaxy. On head, groups Vea, Vem and Vep with 3, 4 and 4 chaetae, respectively. Group Vi on head with 6 chaetae. On Abd. IV, furca rudimentary with 6 minute microchaetae without visible chaetopores (Fig. 61). Male with thick and forked

Table 14. Chaetotaxy of *Deutonura sengleti* sp. nov.: Chaetotaxy of antennae.

Segment, Group	Number of chaetae	Segment, Group	Number of chaetae adult
I	7	IV	or, 8 S, i, 12 mou, 6 brs, 2 iv
II	12		
III	5 sensilla AO III		
ve	5	ap	8 bs, 5 miA
vc	4	ca	2 bs, 3 miA
vi	4	cm	3 bs, 1 miA
d	5	cp	8 miA, 1 brs

Table 15. Chaetotaxy of *Deutonura sengleti* sp. nov.: Postcephalic chaetotaxy.

	Terga				Legs				
	Di	De	Dl	L	Scx2	Cx	Tr	Fe	T
Th. I	3		1	–	0	3	6	13	19
Th. II	3	2+s	3+s+ms	3	2	7	6	12	19
Th. III	3	3+s	3+s	3	2	8	6	11	18
							Sterna		
Abd. I	2	3+s	2	3			VT: 4		
Abd. II	2	3+s	2	3			Ve: 5; chaeta Ve1 present		
Abd. III	2	3+s	2	3			Vel: 4–5; Fu: 5 me, 6 mi		
Abd. IV	2	2+s	3	6			Vel: 4; Vec: 2; Vei: 2; Vl: 4		
Abd. V	(3+3)		5+s				Ag: 3; Vl: 1, L‘: 1		
Abd. VI		7					Ve: 14; An: 2 mi		

chaetae (male ventral organ) on furca rudimentary (Abd. IV, Fig. 61) and around genital aperture (Abd. V). On Abd. V, chaetae Vl and L’ present.

Legs. Chaetotaxy of legs as in Table 15. Claw without internal tooth. On tibiotarsi, chaeta M present and chaetae B4 and B5 of medium size and pointed.

Remarks. The new species runs in the most recent key to *Deutonura* species (Deharveng et al. 2015) to *D. caerulescens* Deharveng, 1982 from France (Deharveng 1982). However, these species differ in the number of chaetae (L+So) on the head (in *sengleti*, 8, in *caerulescens*, 9–10), the presence of microchaetae on furca rudimentary (in *sengleti*, present, in *caerulescens*, absent), the number of chaetae L on Abd. III and IV (in *sengleti*, 3 and 6 chaetae, in *caerulescens*, 4 and 8 chaetae), the number of chaetae on tubercle (De+Dl+L) of Abd. V (in *sengleti*, 5+s, in *caerulescens*, 7+s) and ratio of chaetae Di1:Di2:Di3 on Abd. V (in *sengleti*, 1:4:16, in *caerulescens*, 1:2:4 or 1:3:7).

Deutonura iranica **sp. nov.**

http://zoobank.org/A3E5E3DA-122E-4C11-888D-CF1265288184
Figs 62–71, Table 16–18

Type material. ***Holotype***: juvenile (second instar) on slide, Iran, West Azerbaijan Province, Choj (38°37'N, 45°02'E), 1.VI.1975, leg. A. Senglet, sample 7503.

Etymology. The species name refers to the country of its collecting.

Diagnosis. Habitus typical of the genus *Deutonura*. Dorsal tubercles present and well developed. 2+2 large pigmented eyes. Buccal cone relatively long and narrow,

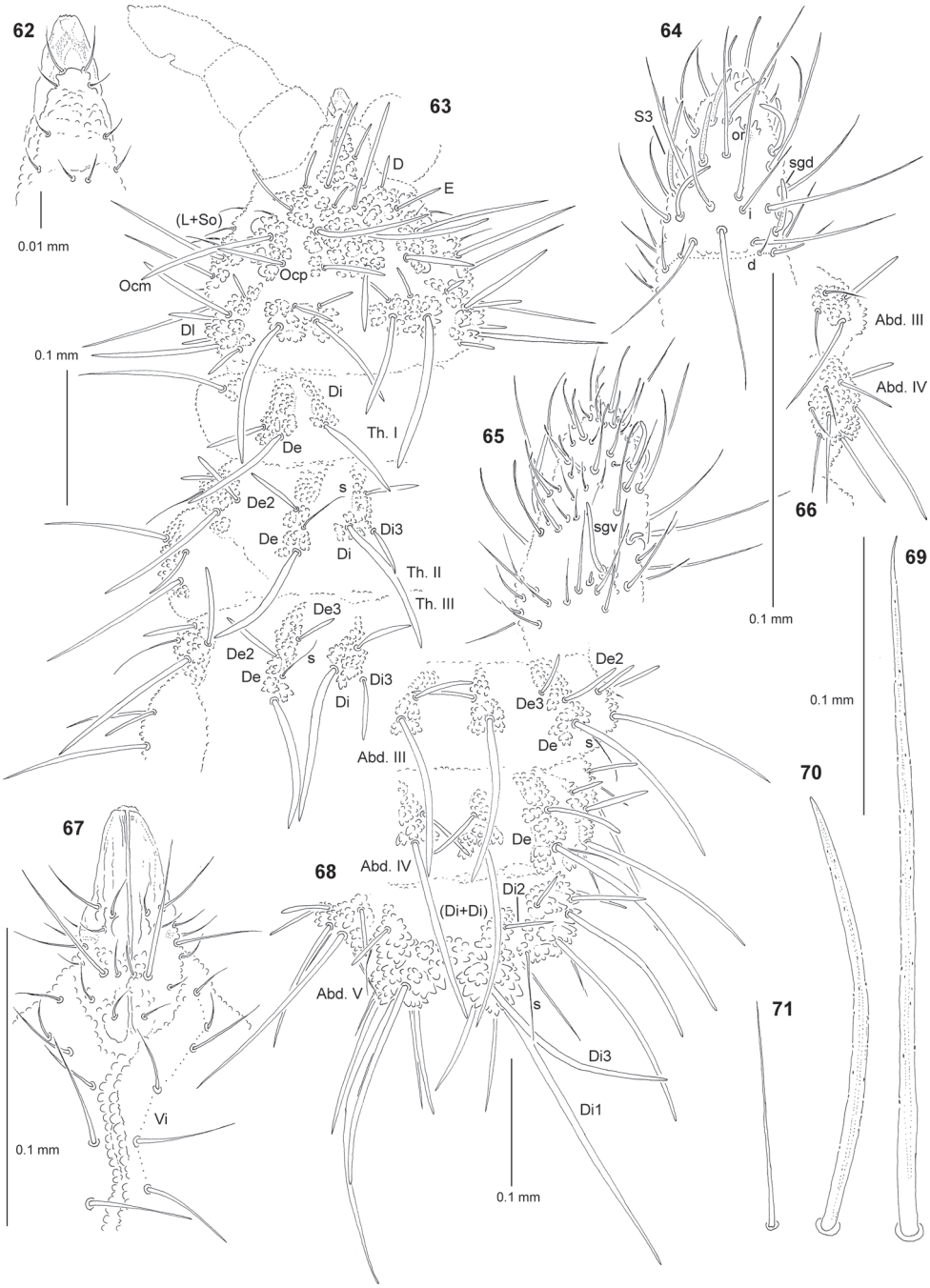

Figures 62–71. *Deutonura iranica* sp. nov.: **62** chaetotaxy and ventral sclerifications of labrum **63** chaetotaxy of head and Th. (holotype), dorsolateral view **64** dorsal chaetotaxy of Ant. III–IV **65** ventral chaetotaxy of Ant. III–IV **66** chaetotaxy of tubercles L of Abd. III–IV, ventral view **67** chaetotaxy of labium and group Vi **68** dorsal chaetotaxy of Abd. III–VI (holotype) **69** chaeta Di1 of Abd. V **70** chaeta Di2 of Abd. V **71** sensillum of Abd. V.

Table 16. Chaetotaxy of *Deutonura iranica* sp. nov.: Cephalic chaetotaxy–dorsal side.

Tubercle	Number of chaetae	Types of chaetae	Names of chaetae
Cl	4	M	F
		Mc	G
Af	10	Ml	B
		Mc	A, E
		Mcc	C, D
Oc	3	Ml	Ocm
		Mc	Ocp
		mi	Oca
(Di+De)	4	Ml	Di1, De1
		Mcc	Di2, De2
Dl	6	Ml	Dl5, Dl1
		Mc	Dl3, Dl4
		Mcc	Dl2, Dl6
(L+So)	7	Ml	L1, L4, So1
		me	So3–6

Table 17. Chaetotaxy of *Deutonura iranica* sp. nov.: Chaetotaxy of antennae.

Segment, Group	Number of chaetae	Segment, Group	Number of chaetae II instar
I	7	IV	or, 8 S, i, 10 mou, 4 brs, 2 iv
II	12		
III	5 sensilla AO III		
ve	5	ap	8 bs, 5 miA
vc	4	ca	2 bs, 3 miA
vi	4	cm	3 bs, 1 miA
d	5	cp	8 miA, 1 brs

labrum without ogival sclerifications. Head without chaetae O, So2, L2 and L3. Tubercles Cl and Af separate. No granular area between chaetae A and B on head. Tubercles De on Th. II and III with 3 and 4 chaetae, respectively. Tubercles Di on Abd. V bilobed. Cryptopygy strongly developed.

Description. General. Body length (without antennae): holotype: 1.05 mm. Colour of the body white. 2+2 large black eyes, in a typical arrangement for the genus (Fig. 63).

Chaetal morphology. Dorsal ordinary chaetae of five types: long macrochaetae (Ml), short macrochaetae (Mc), very short macrochaetae (Mcc), mesochaetae and microchaetae. Long macrochaetae relatively thin, arc-like or straight, narrowly sheathed, feebly serrated, apically sharply pointed (Figs 63, 68–70). Macrochaetae Mc and Mcc morphologically similar to long macrochaetae, but much shorter (Figs 63, 68). Mesochaetae similar to ventral chaetae, thin, smooth and pointed. Microchaetae similar to mesochaetae, but clearly shorter. S-chaetae of terga thin, smooth and short, shorter than nearby macrochaetae (Figs 63, 68, 71).

Antennae. Typical of the genus. Dorsal chaetotaxy of Ant. III–IV as in Fig. 64 and Table 17. S-chaetae of Ant. IV long and relatively thin, S3 notably longer than others, sensillum sgd of medium size and straight (Fig. 64). Apical vesicle distinct, trilobate. Ventral chaetotaxy of Ant. III–IV as in Fig. 65 and Table 17.

Mouthparts. Buccal cone relatively long and narrow, labral sclerifications non-ogival (Figs 62, 67). Labrum chaetotaxy: 4/2, 4 (Fig. 62). Labium with four basal,

Table 18. Chaetotaxy of *Deutonura iranica* sp. nov.: Postcephalic chaetotaxy.

	Terga				Legs				
	Di	**De**	**Dl**	**L**	**Scx2**	**Cx**	**Tr**	**Fe**	**T**
Th. I	1	2	1	-	0	3	6	13	19
Th. II	3	2+s	3+s+ms	3	2	7	6	12	19
Th. III	3	3+s	3+s	3	2	8	6	11	18
							Sterna		
Abd. I	2	3+s	2	3			VT: 4		
Abd. II	2	3+s	2	3			Ve: 5; chaeta Ve1 present		
Abd. III	2	3+s	2	4			Vel: 5; Fu: 4 me, 0 mi		
Abd. IV	2	2+s	3	8			Vel: 4; Vec: 2; Vei: 2; Vl: 4		
Abd. V	(3+3)		7+s				Ag: 3; Vl: 1, L‘: 1		
Abd. VI		7					Ve: 14; An: 2 mi		

three distal and four lateral chaetae, papillae x absent (Fig. 67). Maxilla styliform mandible thin and tridentate.

Dorsal chaetotaxy and tubercles. Head without granular area between chaetae A and B. Elementary tubercles DE and EE on head present (Fig. 63). Head without chaetae O, L2, L3 and So2. Chaetae C as Mcc. Chaetae Ocp notably shorter than Ocm. Chaetae De2 on head as Mcc (Fig. 63). Th. I with tubercles Di and De not fused. Chaetae Di3 on Th. II–III connected with tubercle Di. On Th. III, chaetae De2 slightly longer than De3 (Fig. 63). On Abd. I–III, chaetae De2 longer than De3 (Fig. 68). Cryptopygy present and strongly developed, Abd. VI invisible from above (Fig. 68).

Ventral chaetotaxy. On head, groups Vea, Vem and Vep with 4, 3 and 4 chaetae, respectively. Group Vi on head with 6 chaetae (Fig. 67). Tubercles L on Abd. III and IV with 4 and 6 chaetae, respectively (Fig. 66). On Abd. IV, furca rudimentary without microchaetae. On Abd. V, chaetae Vl and L’ present.

Legs. Chaetotaxy of legs as in Table 18. Claw without internal tooth. On tibiotarsi, chaeta M present and chaetae B4 and B5 of medium size and pointed.

Remarks. Since juveniles (beginning from the first instar) of the subfamily Neanurinae are characterised by the complete chaetotaxy of the head, thorax and abdomen, we decided to describe the new species despite having only one specimen of the second instar. *D. iranica* sp. nov. runs in the most recent key to *Deutonura* species (Deharveng et al. 2015) to *D. gibbosa* Porco, Bedos & Deharveng, 2010, a form common and widespread in southern France (the Alps and Jura), Switzerland, Italy and Slovenia (Porco et al. 2010). Both species are readily distinguished from most members of the genus by the presence of very prominent and conspicuously bilobed tubercle (Di+Di) on the penultimate abdominal segment. This unique character is additionally associated with the specific chaetotaxic arrangement of chaetae Di, with their shift backwards. *D. iranica* sp. nov. can be easily separated from *D. gibbosa* by the presence of white body colour (in *gibbosa* deep to light blue), the presence of 7 chaetae on cephalic tubercle (L+So) (in *gibbosa*, 8–9 chaetae), the presence of cephalic chaetae Ocp equal chaetae A (in *gibbosa*, chaetae Ocp distinctly longer than A) and the presence of 4 lateral labial chaetae (in *gibbosa*, 3 chaetae).

***Paravietnura rostrata* sp. nov.**
http://zoobank.org/E4B57858-235D-4FCC-99D6-A7AFBE6848A7
Figs 72–82, Tables 19–21

Type material. ***Holotype*:** juvenile (second instar) on slide, Iran, Gilan Province, Shahrbijar, tree hole, humus, sifting, 6.IX.1973, leg. A. Senglet, sample 7366.

Etymology. The name of the new species referring to its exceptionally-long buccal cone.

Diagnosis. Habitus typical of the genus *Paravietnura* with stumpy and short body. Macrochaetae long thick and widely sheathed. 2+2 large pigmented eyes. Buccal cone extremely long and narrow, labrum with ogival sclerifications. Tubercle (Af + 2Oc) with chaetae B and Ocm, chaetae A and Ocp absent. Tubercle Cl without chaetae G. Tubercle (Dl+L+So) with 9 chaetae. Furca rudimentary with minute and difficult microchaetae, without chaetopores.

Description. General. Body length (without antennae): holotype: 0.45 mm. Colour of the body bluish. 2+2 large black eyes, in a typical arrangement for the genus (Fig. 75).

Chaetal morphology. Dorsal ordinary chaetae of five types: long macrochaetae (Ml), short macrochaetae (Mc), very short macrochaetae (Mcc), mesochaetae and microchaetae. Long macrochaetae thickened, arc-like, widely sheathed, strongly serrated, apically rounded (Figs 75, 79, 81). Macrochaetae Mc and Mcc morphologically similar to long macrochaetae, but much shorter (Figs 75, 79). Mesochaetae similar to ventral chaetae, thin, smooth and pointed. Microchaetae similar to mesochaetae, but clearly shorter (Figs 75, 79). S–chaetae of terga thin, smooth and short, shorter than nearby macrochaetae (Figs 75, 79, 82).

Antennae. Typical of the genus. Dorsal and ventral chaetotaxy of Ant. III–IV as in Figs 72–74 and Table 20. S-chaetae of Ant. IV relatively short and thin (Fig. 72), sensillum sgd of medium size and straight (Fig. 73), sensillum sgv relatively long and slightly s-shaped (Fig. 74). Apical vesicle distinct, bilobate (Fig. 72).

Mouthparts. Buccal cone extremely elongated with labral sclerifications ogival (Figs 76, 77). Labrum chaetotaxy: 0/2, 4, without prelabral chaetae (Fig. 76). Labium with three basal, three distal and two lateral chaetae, papillae x absent (Fig. 77). Maxilla styliform mandible thin and tridentate.

Dorsal chaetotaxy and tubercles. Chaetotaxy of head as in Fig. 75 and Table 19. Chaetotaxy of Th. and Abd. As in Figs 75, 79 and Table 21. On Th. I, tubercle De with one chaeta (Fig. 75). On Th. II and III, chaetae Di 3 absent. Th. II and III with two chaetae De (Fig. 75). On Abd. IV, chaetae Di1 distinctly longer than Abd. V (Fig. 79). On Abd. V, chaetae Di2 and Di3 absent. Tubercle Di of Abd. IV partially fused (Fig. 79). Cryptopygy present and strongly developed, Abd. VI invisible from above (Fig. 79).

Ventral chaetotaxy. On head, groups Vea, Vem and Vep with 3, 2 and 4 chaetae, respectively. Group Vi on head with 5 chaetae (Fig. 77). On Abd. IV, furca rudimentary with 4 minute microchaetae and 4 mesochaetae (Fig. 78). On Abd. V, chaetae Vl present and L' absent.

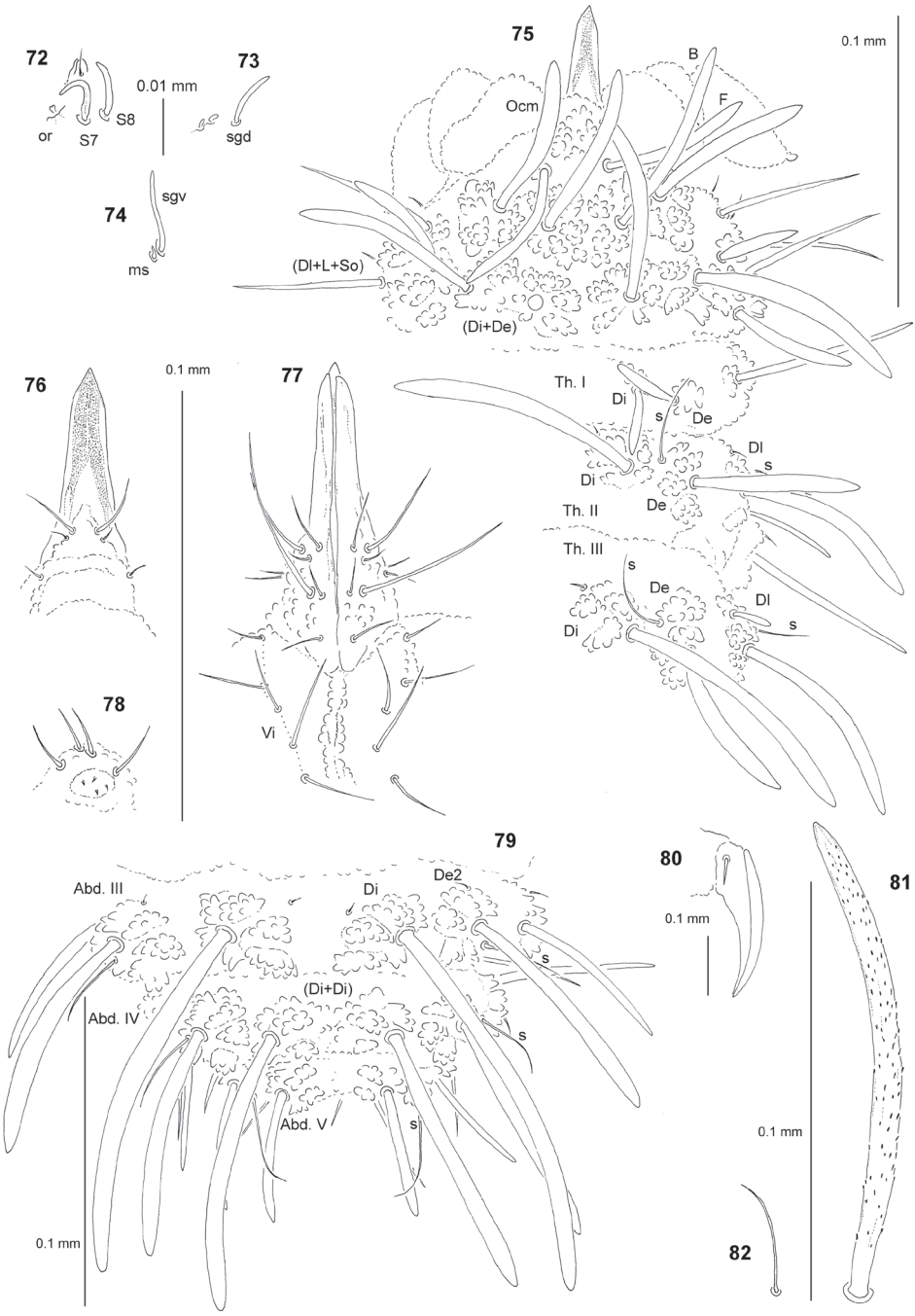

Figures 72–82. *Paravietnura rostrata* sp. nov.: **72** apical part of Ant. IV, dorsal view **73** sensillum sgd and microsensilla of AOIII, dorsolateral view **74** sensillum sgv and microsensillum of Ant. III **75** chaetotaxy of head and Th. (holotype), dorsolateral view **76** chaetotaxy and ventral sclerifications of labrum **77** chaetotaxy of labium and group Vi **78** furca rudimentary **79** dorsal chaetotaxy of Abd. III–VI (holotype) **80** claw of leg III, lateral view **81** chaeta Di1 of Abd. III **82** sensillum of Abd. IV.

Table 19. Chaetotaxy of *Paravietnura rostrata* sp. nov.: Cephalic chaetotaxy–dorsal side.

Tubercle	Number of chaetae	Types of chaetae	Names of chaetae
Cl	2	Ml	F
(Af+2Oc)	4	Ml	B, Ocp
(Di+De)	2	Ml	Di1, De1
(Dl+L+So)	9		impossible to recognise

Table 20. Chaetotaxy of *Paravietnura rostrata* sp. nov.: Chaetotaxy of antennae.

Segment, Group	Number of chaetae	Segment, Group	Number of chaetae II instar
I	7	IV	or, 8 S, i, 10 mou, 4 brs, 2 iv
II	11		
III	5 sensilla AO III		
ve	5	ap	8 bs, 5 miA
vc	4	ca	2 bs, 3 miA
vi	4	cm	3 bs, 1 miA
d	4	cp	8 miA, 1 brs

Table 21. Chaetotaxy of *Paravietnura rostrata* sp. nov.: Postcephalic chaetotaxy.

	Terga				Legs				
	Di	De	Dl	L	Scx2	Cx	Tr	Fe	T
Th. I	1	1	1	–	0	3	6	13	19
Th. II	2	1+s	2+s+ms	3	2	7	6	12	19
Th. III	2	1+s	2+s	3	2	8	6	11	18
							Sterna		
Abd. I	2	2+s	2	2			VT: 4		
Abd. II	2	2+s	2	2			Ve: 3; chaeta Ve1 present		
Abd. III	2	2+s	2	2			Vel: 3; Fu: 4 me, 4 mi		
Abd. IV	(1+1)	1+s	3	3			Vel: 2; Vec: 2; Vei: 2; Vl: 4		
Abd. V		4+s					Ag: 2; Vl: 1		
Abd. VI		7					Ve: 11; An: 1mi		

Legs. Chaetotaxy of legs as in Table 21. Claw without internal tooth (Fig. 80). On tibiotarsi, chaeta M present and chaetae B4 and B5 of medium size and pointed.

Remarks. No doubt, the new species is the third member of the remarkable Neanurinae genus *Paravietnura* Smolis & Kuznetsova, 2018 described recently from the Caucasus (Smolis and Kuznetsova 2018). *Paravietnura rostrata* sp. nov. seems to be the closest to *P. notabilis* Smolis & Kuznetsova, 2018; however, it can be easily separated from the mentioned species because of the reduction of its cephalic chaetotaxy (in *rostrata*, chaetae G and Ocp absent, in *notabilis*, present), extremely elongated labrum, which is well visible from above (in *notabilis*, feebly elongated and practically invisible from above), absence of prelabral chaetae (in *notabilis*, 2 chaetae present), the presence of 1+1 chaetae De on Th. I (in *notabilis*, 2+2 chaetae present), the absence of chaetae Di3 on Th. (in *notabilis*, present), reduction of the number of chaetae De on Th. II and III (in *rostrata*, 1+s chaetae, in *notabilis*, 2+s and 3+s chaetae, respectively), the absence of chaetae De2 and De3 on Abd. I–III (in *notabilis*, present), the fusion of tubercles Di on Abd. IV (in *notabilis*, not fused) and the presence of 1 chaeta Di on Abd. V (in *notabilis*, 3 chaetae Di present).

New Records

Cryptonura maxima Smolis, Falahati & Skarżyński, 2012

Material. Iran, Mazandaran Province, Baladeh, 2200 m a.s.l., 12.VII.1974, leg. A. Senglet, sample 7459; numerous specimens on slide, Iran Mazandaran Province, Aliabad, 30.VII.1974, leg. A. Senglet, 7475.

Note. Up to date, the species was known from the Elburz Mts. in Golestan Province (Smolis et al. 2012).

Cryptonura persica Smolis, Falahati & Skarżyński, 2012

Material. Iran, Mazandaran Province, near Gorgan, forest, mosses, sifting, 20.VII.1973, leg. A. Senglet, sample 7332; Mazandaran Province, near Shahpasand, leaves, sifting, 29.VII.1974, leg. A. Senglet, 7473; West Azerbaijan Province, Choj (38°37'N, 45°02'E), 1.VI.1975, leg. A. Senglet, 7503; Golestan Province, near Tangrah (37°23'N, 55°50'E), 16.VII.1975, leg. A. Senglet, 7552; North Khorasan Province, near Tangrah (37°20'N, 56°01'E), 16.VII.1975, leg. A Senglet, 7553; Golestan Province, near Loveh (37°20'N, 55°44'E / 700 m a.s.l.), 21.VIII.1975, leg. A. Senglet, 7572; Golestan Province, near Loveh (37°18'N, 55°43'E / 1200 m a.s.l.), 21.VIII.1975, leg. A Senglet, 7573; Semnan Province, near Loveh (37°19'N, 55°46'E / 1300 m a.s.l.), 22.VIII.1975, leg. A. Senglet, 7574.

Note. Similarly to the previous species, *C. persica* was known exclusively from the Elburz Mts. in Golestan Province (Smolis et al. 2012). The outlined records, from provinces West Azerbaijan, Mazandaran, Semnan and North Khorasan, shows that this form seems to be quite common and widespread in north-western Iran.

Deutonura persica Smolis, Shayanmehr & Yoosefi-Lafooraki, 2018

Material. Iran, Gilan Province, near Asalem (37°42'N, 48°53'E), 450 m a.s.l., tree holes, sifting, 10.VI.1975, leg. A. Senglet, sample 7518; Iran, Mazandaran Province, Ivel (36°14'N, 53°37'E / 1500 m a.s.l.), under stones, 11.VII.1975, leg. A Senglet, 7547A.

Note. Until now, the species was known from its type locality only: Hezarjarib Forest in region Neka in Mazandaran Province (Smolis et al. 2018).

Endonura longirostris Smolis, Shayanmehr, Kuznetsova & Yoosefi-Lafooraki, 2017

Material. Iran, Mazandaran Province, Nashtarud, forest, reserve, sifting, 10.VII.1973, leg. A. Senglet, sample 7318; Iran, Mazandaran Province, near Delaam, forest,

4.VIII.1974, leg. A. Senglet, 7478; Golestan Province, near Loveh (37°20'N, 55°44'E / 700 m a.s.l.), 21.VIII.1975, leg. A. Senglet, 7572.

Note. Up to now, this very characteristic member of the genus *Endonura* was known from two localities in Mazandaran Province (Smolis et al. 2017).

Endonura paracentaurea Smolis, Shayanmehr, Kuznetsova & Yoosefi-Lafooraki, 2017

Material. Iran, Gilan Province, Limir, ;large trees in marsh, sifting, 28.VI.1973, leg. A. Senglet, sample 7306; Gilan Province, Shahrbijar, tree hole, humus, sifting, 6.IX.1973, leg. A. Senglet, 7366; Mazandaran Province, road to Tchorteh, 800 m a.s.l., tree and leaves, sifting, 5.VIII.1974, leg. A. Senglet, 7482.

Note. Until now, *Endonura paracentaurea* was recorded exclusively from Mazandaran Province (Smolis et al. 2017).

Neanura deharvengi Smolis, Shayanmehr & Yoosefi-Lafooraki, 2018

Material. Iran, Gilan Province, Limir, big trees in marsh, sifting, 28.VI.1973, leg. A. Senglet, sample 7306; Mazandaran Province, Nashtarud, forest, reserve, sifting, 10.VII.1973, leg. A. Senglet, 7318; Mazandaran Province, Kiasar, very dry forest, sifting, 22.VII.1973, leg. A. Senglet, 7334.

Note. To date, this unique member of the genus *Neanura* MacGillivray, 1893 characterised by strong reduction of cephalic chaetotaxy, was recorded from two localities in Mazandaran Province only (Smolis et al. 2018).

Neanura muscorum (Templeton, 1835)

Material. Iran, Gilan Province, Zandżan (36°43'N, 48°21'E), 15.IX.1973, leg. A. Senglet, sample 7372.

Note. Up to now, this cosmopolitan and the most widespread member of the subfamily Neanurinae was recorded from three Iranian provinces: Zanjan, Gilan and Mazandaran (Cox 1982, Yahyapour 2012).

Protanura papillata Cassagnau & Delamare Deboutteville, 1955

Material. Iran, Kermanshah Province, Geravand, 5.VIII.1973, leg. A. Senglet, sample 7344.

Note. This species is known from Lebanon, Israel and Iran (Smolis et al. 2016b). The present record is the third from Kermanshah Province.

Discussion

Until recently, the whole knowledge on richness and diversity of Iranian Neanurinae was based solely on a Cox's (1982) paper, in which four European and rather common taxa, i.e. *Neanura muscorum* and *Bilobella aurantiaca* (Caroli, 1912) were mentioned. However, the last decade has resulted in a real explosion of research on Iranian Collembola. Taking into account all recent data, one can conclude that Neanurinae fauna of Iran contains 21 species of the following genera: *Bilobella* Caroli, 1912 – 1; *Cryptonura* Cassagnau, 1979 – 2; *Deutonura* Cassagnau, 1979 – 5; *Endonura* Cassagnau, 1979 – 8; *Neanura* MacGilliwray, 1893 – 2; *Paravietnura* Smolis & Kuznetsova, 2018 – 1; *Persanura* Mayvan, Smolis & Skarżyński, 2015 – 1; *Protanura* Börner, 1906 and *Thaumanura* Börner, 1932 – 1 (Cox 1982; Smolis et al. 2012; Mayvan et al. 2015b; Smolis et al. 2016a, b, 2017; Smolis and Kuznetsova 2018; Smolis et al. 2018). Despite the fact that the image of diversity and richness of Iranian Neanurinae is still incomplete, some general comments can be made.

Firstly, the Iranian fauna is characterised by a remarkable percentage of endemites, since seventeen species are known exclusively from this country. This number is probably underestimated as earlier records of some taxa, i.e. *Bilobella aurantiaca*, *Thaumanura echinata* (Kos, 1940) and *Deutonura decolorata* (Gama & Gisin, 1964 in: Gisin 1964) are rather unlikely and should be revised. Such a high number of endemites is certainly noteworthy; nevertheless, it is a known and rather general phenomenon for this group of springtails. Research conducted, both in tropical and temperate forests, indicated that Neanurinae have a strong tendency to speciation and their fauna on a larger geographical scale is often characterised by a high degree of endemism (e.g. Deharveng 1979; Cassagnau and Palacios-Vargas 1983; Deharveng and Weiner 1984; Cassagnau and Deharveng 1984; Cassagnau 1988, 1996; Greenslade 1994; Palacios-Vargas and Simón Benito 2007; Janion et al. 2011; Queiroz and Deharveng 2015; Smolis 2017).

Secondly, in terms of species richness, this fauna should be treated even today as very rich. Especially, the Hyrcanian forest, where sixteen species of the subfamily were noted, seems to be not only a national but also a regional hot spot. The observed situation, however, may not be especially surprising as this huge and diversified area covers almost one million hectares and ranges from west to east through five Iranian Provinces: Ardabil, Gilan, Mazandaran, Golestan and North Khorasan. In addition, this forest is a worldwide and commonly-known refuge for many iconic and spectacular mammals, i.e. the Persian leopard *Panthera pardus ciscaucasica*, trees, i.e. the Persian ironwood *Parrotia persica*, the Caspian locust tree *Gleditsia capsica* and insects, i.e. the longhorn beetle *Parandra caspia*, the red flat beetle *Cucujus muelleri* (e.g. Sagheb-Talebi et al. 2014; Mayvan et al. 2015a; Müller et al. 2015; Bussler 2017).

Finally, current and especially future knowledge (many regions of Iran still remain unexplored, see Shayanmehr et al. 2013, Fig. 2) of the Iranian Neanurinae fauna could shed light on key issues such as its origin and relationship with fauna of neighbouring

regions. For example, the similarity of Iranian fauna to that of the Caucasus (presence of genera *Paravietnura* and *Persanura*) and the east Mediterranean region (presence of *Protanura papillata* and genus *Cryptonura*) should already be underlined.

Acknowledgements

The work was financially supported by the Institute of Environmental Biology, Faculty of Biological Science, University of Wrocław, Poland (project no. 1076/Ś/IBŚ/2020). We are grateful to Prof. Louis Deharveng and Prof. Javier Arbea who reviewed the manuscript. We are also much indebted to the Editor Prof. Wanda Maria Weiner for helpful remarks.

References

Axelson WM (1905) Einige neue Collembolen aus Finland. Zoologisher Anzeiger 28: 788–794.

Bellinger PF, Christiansen KA, Janssens F (2020) Checklist of the Collembola of the world. http://www.collembola.org [Accessed 13 July 2020]

Börner C (1906) Das System der Collembolen nebst Beschreibung neuer Collembolen des Hamburger Naturhistorischen Museums. Mitteilungen aus den Naturhistorischen Museum in Hamburg, XXIII. Jahrgang, 2. Beiheft zum Jahrbuch der Hamburgischen Wissenschaftlichen Austalten, XXIII, 1905, Hamburg 1906, 147–188.

Börner C (1932) Apterygota. In: Brohmer P (Ed.) Fauna von Deutschland, 4th ed. Auflage 4, Leipzig, 136–143.

Bussler H (2017) *Cucujus muelleri* sp. nov. aus den kaspischen Gebirgswäldern des Iran (Coleoptera: Cucujidae). Nachrichtenblatt der Bayerischen Entomologen 66(3/4): 54–58.

Caroli E (1912) Contribuzioni alla conosceza dei Collemboli italiani. I. La tribu degli Achorutini. Archivio Zoologico Italiano 6: 349–374.

Cassagnau P (1979) Les Collemboles Neanuridae des Pays Dinaro-Balkaniques: leur interêt phylogénétique et biogéographique. Biologia Gallo – Hellenica 8: 185–203.

Cassagnau P (1988) Les Collemboles Neanurinae des Masif du sud de l'Inde et de Ceylan. Travaux du Laboratoire d'écobiologie des Arthropodes Edaphiques, Toulouse 5(4): 21–51.

Cassagnau P (1996) Collemboles Neanurini primitifs d'Afrique et de Madagascar. Annales de la Société entomologique de France 32(2): 121–161.

Cassagnau P, Deharveng L (1984) Collemboles des Philippines. 1. Les lobelliens multicolores de montagnes de Luzon. Travaux du Laboratoire d'écobiologie des Arthropodes Edaphiques, Toulouse 5(1): 1–11.

Cassagnau P, Delamare Deboutteville C (1955) Mission Henri Coiffait (1951). 3. Collemboles. Archives de Zoologie Expérimentale et Génerale 91: 365–395.

Cassagnau P, Palacios-Vargas JG (1983) Contribution a l'étude des Collemboles Neanurinae d'Amerique Latine. Travaux de Laboratoire d'Écobiologie des Arthropodes Édaphiques, Toulouse 4(1): 1–16.

Cassagnau P, Péja N (1979) Diagnoses préliminaries de quelques Neanuridae de Grèce et d'Albanie. Biologia Gallo – Hellenica 8: 205–222.

Cox P (1982) The Collembola fauna of north and north western Iran. Entomologist's Monthly Magazine 118: 39–43.

Deharveng L (1979) Contribution à la connaissance des Collemboles Neanurinae de France et de la Peninsule Iberique. Travaux du Laboratoire d'Écobiologie des Arthropodes Edaphiques, Toulouse 1: 1–61.

Deharveng L (1982) Contribution à l'étude des *Deutonura* du groupe *phlegraea*. Travaux de Laboratoire d'Écobiologie des A rthropodes Édaphiques, Toulouse 3(2): 1–20.

Deharveng L (1983) Morphologie évolutive des Collemboles Neanurinae en particulier de la lignée néanurienne. Travaux de Laboratoire d'Écobiologie des Arthropodes Édaphiques, Toulouse 4: 1–63.

Deharveng L (1989) The genus *Paranura* Axelson, 1902 in Thailand (Collembola Neanurinae). Tropical Zoology 2: 103–121. https://doi.org/10.1080/03946975.1989.10539432

Deharveng L, Bedos A (1992) *Blasconurella*, a new genus of Neanurinae from Thailand, with five new species. Tropical Zoology 5: 299–311. https://doi.org/10.1080/03946975.1992.10539201

Deharveng L, Weiner WM (1984) Collemboles de Corée du Nord III–Morulinae et Neanurinae. Travaux de Laboratoire d'Écobiologie des Arthropodes Édaphiques, Toulouse 4: 1–61.

Deharveng L, Suhardjono Y (2000) *Sulobella yoshii*, a New Genus New Species of Lobellini (Collembola: Neanurinae) from South Sulawesi, with Comments on the Tribe Lobellini. Contributions from the Biological Laboratory Kyoto University 29(2): 83–87.

Deharveng L, Mouloud SA, Bedos A (2015) A new species of *Deutonura* (Collembola: Neanuridae: Neanurinae) from Algeria, with revised diagnosis of the genus and key to the western Palearctic species. Zootaxa 4000(4): 464–472. https://doi.org/10.11646/zootaxa.4000.4.5

Gisin H (1964) Collemboles d'Europe. VI. Revue suisse de Zoologie 71(20): 383–391. https://doi.org/10.5962/bhl.part.75615

Greenslade P (1994) Collembola. In: Houston WWK (Ed.) Zoological catalogue of Australia. Volume 22. Protura, Collembola, Diplura. CSIRO, Melbourne, 19–138.

Janion C, Bedos A, Deharveng L (2011) The genus *Ectonura* Cassagnau, 1980 in South Africa (Collembola: Neanuridae: Neanurinae), with a key to South African Neanurinae. ZooKeys 136: 31–45. https://doi.org/10.3897/zookeys.136.1744

Ji-Gang J, Cheng-Wang H, Yun-Xia L (2018) A new species of *Lobellina* and first record of *Vietnura* from China (Collembola: Neanuridae: Neanurinae). ZooKeys 807: 13–28. https://doi.org/10.3897/zookeys.807.24941

Kos F (1940) Terricole Collembolen aus Slovenien. Glasnik, Bulletin de la Société Scientifique de Skoplje 22: 136–168.

Luo Y, Palacios-Vargas JG (2016) On the genus *Paralobella* (Collembola: Neanurinae: Lobellini) with description of a new Chinese species. Zootaxa 4066(3): 343–350. https://doi.org/10.11646/zootaxa.4066.3.10

MacGillivray AD (1893) North American Thysanura – IV. Canadian Entomologist 25: 313–318. https://doi.org/10.4039/Ent25313-12

Mayvan MM, Shayanmehr M, Scheu S (2015a) Depth distribution and inter-annual fluctuations in density and diversity of Collembola in an Iranian Hyrcanian Forest. Soil Organisms 87(3): 239–247.

Mayvan MM, Smolis A, Skarżyński D (2015b) *Persanura hyrcanica*, a new genus and species of Neanurinae (Collembola: Neanuridae) from Iran, with a key to genera of the tribe Neanurini. Zootaxa 3918: 552–558. https://doi.org/10.11646/zootaxa.3918.4.4

Müller J, Thorn S, Baier R, Sagheb-Talebi K, Barimani HV, Seibold S, Ulyshen MD, Gossner MM (2016) Protecting the forests while allowing removal of damaged trees may imperil saproxylic insects biodiversity in the Hyrcanian Beech Forests of Iran. Conservation Letters 9(2): 106–113. https://doi.org/10.1111/conl.12187

Palacios-Vargas JG, Deharveng L (2014) First record of the genus *Australonura* Cassagnau 1980 (Collembola: Neanuridae) in the New World, with description of new species from Paraguay. Zootaxa 3779(1): 33–47. https://doi.org/10.11646/zootaxa.3779.1.6

Palacios-Vargas JG, Simón Benito JC (2007) A new genus and three new species of Neanuridae (Collembola) from North America. Journal of Cave and Karst Studies 69(3): 318–325. https://doi.org/10.3958/0147-1724-32.3.169

Porco D, Bedos A, Deharveng L (2010) Description and DNA barcoding assessment of the new species *Deutonura gibbosa* (Collembola: Neanuridae: Neanurinae), a common springtail of Alps and Jura. Zootaxa 2639: 59–68. https://doi.org/10.11646/zootaxa.2639.1.6

Queiroz GC, Deharveng L (2015) New genus, new species and new record of Neanurinae (Collembola, Neanuridae) for the Neotropics. Zootaxa 4020(1): 134–152. https://doi.org/10.11646/zootaxa.4020.1.5

Sagheb-Talebi K, Sajedi T, Pourhashemi M (2014) Forests of Iran – a treasure from the past, a hope for the future. Plant and Vegetation vol. 10, 152 pp. https://doi.org/10.1007/978-94-007-7371-4

Shayanmehr M, Yahyapour E, Kahrarian M, Yoosefi-Lafooraki E (2013) An Introduction to Iranian Collembola (Hexapoda): an update to the species list. ZooKeys 335, 69–83. https://doi.org/10.3897/zookeys.335.5491

Smolis A (2008) Redescription of four Polish *Endonura* Cassagnau, 1979 (Collembola, Neanuridae, Neanurinae), with a nomenclature of the ventral chaetae of antennae. Zootaxa 1858: 9–36. https://doi.org/10.11646/zootaxa.1858.1.2

Smolis A (2017) Contribution to the knowledge of Neanurinae of Vietnam with description of three new species (Collembola, Neanuridae). ZooKeys 688: 15–23. https://doi.org/10.3897/zookeys.688.12307

Smolis A, Deharveng L (2006) *Vitronura mascula*, a new species of Neanurinae (Collembola: Neanuridae) from northern Vietnam, with a key to the species of the genus. Revue suisse de Zoologie 113: 263–268. https://doi.org/10.5962/bhl.part.80349

Smolis A, Deharveng L (2015) Diversity of *Paranura* Axelson, 1902 (Collembola: Neanuridae: Neanurinae) in Pacific Region of Russia and United States. Zootaxa 4033(2): 203–236. https://doi.org/10.11646/zootaxa.4033.2.2

Smolis A, Deharveng L, Kaprus' IJ (2011) Studies on the non-European *Endonura* Cassagnau, 1979 (Collembola, Neanuridae, Neanurinae). Zootaxa 3004: 45–56. https://doi.org/10.11646/zootaxa.3004.1.4

Smolis A, Falahati A, Skarżyński D (2012) The genus *Cryptonura* Cassagnau, 1979 (Collembola: Neanuridae: Neanurinae) in Iran. Zootaxa 3530: 51–58. https://doi.org/10.11646/zootaxa.3530.1.5

Smolis A, Greenslade P (2020) New Lobellini (Collembola: Neanuridae) from Queensland contribute to understanding distribution and ecology of Australian fauna. Austral Entomology 59: 253–264. https://doi.org/10.1111/aen.12460

Smolis A, Kuznetsova N (2018) *Paravietnura* gen. n., an intriguing genus of Neanurini from the Caucasus (Collembola, Neanuridae, Neanurinae). Zookeys 739: 41–54. https://doi.org/10.3897/zookeys.739.22041

Smolis A, Shayanmehr M, Yoosefi-Lafooraki E (2018) New members of the genera *Neanura* MacGilliwray, 1893 and *Deutonura* Cassagnau, 1979 (Collembola: Neanuridae) from the Middle East. European Journal of Taxonomy 406: 1–16. https://doi.org/10.5852/ejt.2018.406

Smolis A, Kahrarian M, Piwnik A, Skarżyński D (2016a) *Endonura* Cassagnau in Iran, with a key of the genus (Collembola, Neanuridae, Neanurinae). Zookeys 553: 53–71. https://doi.org/10.3897/zookeys.553.6009

Smolis A, Shayanmehr M, Kuznetsova N, Yoosefi-Lafooraki E (2017) Three new remarkable species of the genus *Endonura* Cassagnau, 1979 from the Middle East and Central Asia (Collembola, Neanuridae, Neanurinae, Neanurini). Zookeys 673: 135–151. https://doi.org/10.3897/zookeys.673.12084

Smolis A, Skarżyński D, Kahrarian M, Kaprus' IJ (2016b) Redescription of *Protanura papillata* Cassagnau & Delamare Deboutteville, 1955 (Collembola, Neanuridae, Neanurinae), with new records from Middle East, and with supplemented diagnosis and key to the genus. Zootaxa 4092(2): 293–300. https://doi.org/10.11646/zootaxa.4092.2.11

Smolis A, Skarżyński D, Pomorski RJ, Kaprus' IJ (2007) Redescription of *Endonura taurica* (Stach, 1951) and *E. quadriseta* Cassagnau & Péja, 1979, and description of two new species of the genus *Endonura* Cassagnau, 1979 (Collembola: Neanuridae: Neanurinae) from the Crimea (Ukraine). Zootaxa 1442: 19–35. https://doi.org/10.11646/zootaxa.1442.1.2

Templeton R (1835) Thysanura Hiberbnicae, or descriptions of such species of spring-tailed insects (Podura and Lepisma, Lin.) as have been observed in Ireland. Transactions of the Entomological Society of London 1(2): 89–98. https://doi.org/10.1111/j.1365-2311.1838.tb00147.x

Yahyapour E (2012) Faunistic Study on Collembola (Insecta: Apterygota) in Sari Regions. MSc thesis, Sari, Vol. 1. Sari Agricaltural Science and Natural Resources University, Iran, 96 pp. [in Persian with English abstract]

Yossi R (1976) On some Neanurid Collembola of Southeast Asia. Nature and life in Southeast Asia 7: 257–299.

Zhi-Chun M, Jian-Xiu C (2008) A new species of *Lobellina* (Collembola: Neanuridae) from China. Zootaxa 4033(2): 203–236.

ZooKeys 992: 139–155 (2020)
doi: 10.3897/zookeys.992.57028
https://zookeys.pensoft.net

RESEARCH ARTICLE

A peer-reviewed open-access journal
ZooKeys
Launched to accelerate biodiversity research

Observations of the foraging behavior and activity patterns of the Korean wood mouse, *Apodemus peninsulae*, in China, using infra-red cameras

Dianwei Li[1,2], Jingwei Hao[1], Xu Yao[1], Yang Liu[1], Ting Peng[1], Zhimin Jin[1], Fanxing Meng[1]

1 *College of Life Sciences and Technology, Mudanjiang Normal University, No. 191 Wenhua Road, Mudanjiang, Heilongjiang 157011, China* **2** *Heilongjiang Academy of Forestry, No. 134 Haping Road, Harbin, Heilongjiang 150081, China*

Corresponding author: Dianwei Li (lidianwei@mdjnu.edu.cn)

Academic editor: R. López-Antoñanzas | Received 29 July 2020 | Accepted 19 October 2020 | Published 12 November 2020

http://zoobank.org/73251911-BEEB-4CA9-A1F1-49121EEB856D

Citation: Li D, Hao J, Yao X, Liu Y, Peng T, Jin Z, Meng F (2020) Observations of the foraging behavior and activity patterns of the Korean wood mouse, *Apodemus peninsulae*, in China, using infra-red cameras. ZooKeys 992: 139–155. https://doi.org/10.3897/zookeys.992.57028

Abstract

Apodemus peninsulae, a dominant rodent species in temperature forests of northeastern China, is a model animal to explore the ecological functions of reciprocal coevolution of animals and plants. From August to October 2016, 24 infra-red cameras were installed to study the feeding behavior and activity patterns of *A. peninsulae* in its natural environment. By analyzing 5618 video records, we found that feeding behavior, followed by motor and sentinel behaviors, was their main activity. In the behavior spectra, motor behavior (creep, walk, and skip), feeding behavior (forage, feeding, transport, hoarding, and clean), and sentinel behavior (alert, flee, banishment, and coexistence) accounted for 57.96%, 40.36%, and 1.68% of their behavior, respectively. The peak of feeding behavior occurred between 18:00 and 23:00, and feeding behavior frequency, duration, and activity rhythms differ among August to October. Furthermore, activity was the greatest after sunset and before sunrise, indicating a nocturnal lifestyle; however, from August to October, the start time of the activity was earlier, and the end time was later than usual. On average, mice spent 21.6 ± 11.6 times/night feeding, with a duration of 63.58 ± 98.36 s; while they spent less time in foraging, 39.05 ± 51.63 s. We found a significant difference in feeding and foraging frequency, with mice spending on average 10.84 ± 9.85 times/night and 9.23 ± 11.17 times/night, respectively. Our results show that feeding and foraging behavior is also influenced by light intensity, suggesting a preference for crepuscular periods of the day. Infra-red cameras are very useful in detecting activity patterns of animals that are not easily observable; these cameras are able to capture a large amount of valuable information for research into ecological functions.

Keywords
Activity rhythm, feeding behavior, Glires, infra-red camera

Introduction

Through adaptive evolution, animals respond to environmental factors, as well as their physiology, in order to adapt to their environment (Lehner 1996; Halles and Stenseth 2000; Pearson and Theimer 2004; Seri et al. 2018; Tang et al. 2020). They do this in a range of ways, including adjusting their behavior in response to environmental changes, such a daily circadian rhythm, temperature, competition, predation avoidance, and resource availability, as well as their own physiology (Flannigan and Stookey 2002; Li et al. 2019; Tang et al. 2020). As a result, they form specific behavior patterns and activity rhythms. Therefore, it is important to understand how animals adapt and adjust their behavior to their environment and to assess the mechanisms that drive these patterns.

Foraging activity of animals involves a wide spectrum of behaviors used in the quest to find food. Foraging and feeding behaviors are often linked together, and animals will use a combination of strategies. Foraging and feeding behaviors include finding, obtaining, processing, ingesting, and hoarding, following specific pattern specific to the animal. Depending on the need, feeding can occur at the site where food is found or can be moved and consumed somewhere else. The decision to do so is dependent on external pressures such as predation, the time available for foraging, and environmental factors such as temperature (Halles and Stenseth 2000; Pearson and Theimer 2004; Seri et al. 2018). In learning the factors that affect the feeding and foraging behavior spectra of animals, we hope to gain further insight into adaptive capability, activity intensity, which will give us a clearer understanding on adaptive strategies of animals as well as niche dimensions in specific communities (Lehner 1996; Halles and Stenseth 2000; Pearson and Theimer 2004; Seri et al. 2018; Tang et al. 2020).

Infra-red (IR) cameras have been found to be highly beneficial to ecological studies of cryptic animals, those that are active at night when it is difficult to see them, or those that occur in hard to reach locations. Moreover, IR cameras have many benefits, such as being non-invasive, capacity for long-term monitoring with 24 hour or longer monitoring (Karanth 1995; Rowcliffe et al. 2008; O'Connell et al. 2020), low cost, low environmental interference, resistance to environmental changes, and ability to record greatly hidden species and complex terrain (Karanth 1995; Rowcliffe et al. 2008; Mondol et al. 2009; O'Connell et al. 2010; Zhang et al. 2013; Claridge et al. 2019). In addition, IR cameras can capture a large amount of information in the natural state (O'Connell et al. 2010), including population structure, species diversity, and some information on spatial distribution (Mondol et al. 2009; Zhang et al. 2013; Claridge et al. 2019). As a result, IR cameras have been widely used in studies involving field monitoring, quantity estimation, habitat characteristics, individual recognition, behavior patterns, and activity rhythm (Mondol et al. 2009; Zhang et al. 2013; Claridge et al. 2019). For example, in studies involving mammals in the superorder Glires, IR

cameras have been widely used to assess species diversity and estimate population density (Zhang et al. 2013). However, in smaller-bodied species of Glires, such information is lacking. Much of the research has been conducted on larger species of Glires: Sino-Mongolia beaver *Caster fiber birulai*, Asiatic brush-tailed porcupine *Atherurus macrourus* and red-bellied squirrel *Callosciurus erythralus* (Liu et al. 2015; Wen et al. 2016; Wang et al. 2019; Tang et al. 2020). Thus, more research is needed using IR cameras to study the behavior of smaller-bodies species of Glires.

The Korean wood mouse, *Apodemus peninsulae*, is a dominant species of the Glires community in temperate forests in northeastern China, inhabiting a variety of habitats such as forests, shrubs, glades, grasslands, and farmlands at the forest margins. This species feeds on and stores a variety of seeds and fruits from plants such as *Quercus mongolican*, *Pinus koraiensis*, and *Corylus mandshurica* (Lu and Zhang 2005; Park et al. 2014; Liu et al. 2015; Li et al. 2018). As a keystone species in the forest ecosystem, *A. peninsulae* is not only a primary consumer and seed disperser, but also an important food resource for carnivores. Research on *A. peninsulae* has mainly focused on population dynamics, food storage, nest activity, body temperature, and distribution (Lu and Zhang 2005; Park et al. 2014; Liu et al. 2015; Li et al. 2018; Masaki et al. 2005). However, there were no reports on feeding behavior and activity patterns in *A. peninsulae* under natural conditions. However, Lu and Zhang (2005) did report on the activity rhythm and seed hoarding of this species under laboratory and artificial fence conditions. Due to the limitation of space and human interference, these studies could not fully reflect the natural activity rules of Gires. Our study used IR cameras to monitor the feeding behavior of *A. peninsulae* in its natural environment. Our results will provide a new perspective on the various application of IR cameras as a non-invasive tool for monitoring and studying the ecology of animal behavior in natural settings.

Site and methods

Study area and research site selection

The study was conducted from June 2015 to October 2016. The research site was in a forested area of Hengdaohezi town, Hailin City (44°44'N–44°55'N, 129°6'E–129°15'E, elevation 460–600 m), at the northern end of the Changbai Mountains in northeastern China, the east vein of the main ridge of Zhangguangcai Mountain. The mountain runs northwest-southeast. The climate is temperate continental monsoon, with four distinct seasons and a hot rainy season. The maximum temperature is 37 °C, the minimum temperature is –44.1 °C, and the annual average temperature is 2.3–3.7 °C. About 100–160 days in the year are frost free. The first frost is in late September, and the last frost is in late April to early May. Precipitation is concentrated in June to September and varies between 400 mm and 800 mm. The forests in this area are dominated by secondary vegetation. There is a high abundance and diversity of Glires, largely dominated by combinations of various species such as *A. peninsulae*, *A. agrarius*, and *Clethrionomys rufocanus*.

In the theropencedrymion, three alternative plots with less human interference were selected for research. For each plot, we first used the rat traps method to investigate the presence of small Glires in the area. The plot with the largest capture rate of *A. peninsulae* was selected as the research site. The chosen site was 100 m × 150 m and at an altitude of 533–552 m.

Infra-red camera settings

In the study plot, four sample strips with an interval of 20 m were set, and six IR cameras (Ltl Acorn, LTL-6310MC) were installed in each sample strip. The IR camera interval was 20 m, with 24 cameras in total. The IR cameras were set to the photo + video mode. Each camera was set to take three shots after triggering and then to automatically record for 15 s after every 30 s interval. Cameras automatically recorded the date, time, environmental temperature, and other information. Cameras were fixed on tree trunks, or other fixed objects, about 30 cm above the ground, and baits (marked seeds of *Quercus mongolican*, *Pinus koraiensis*, and *Corylus mandshurica*) were placed on the ground approximately 30–80 cm in front of the camera. Ten days later, cameras were retrieved to collect and analyze the photos and videos.

Recording and characterization of behaviors

Once the target animal was identified, the following observations were recorded, characterized, and later analyzed in order to construct the feeding and foraging behavior spectrum. The characterization included noting the type, frequency, and duration of behaviors exhibited during feeding and foraging. Due to the short duration of the video recording interval, 30 s, the video recording time, location of activity, and state of the target animal before and after the activity was used to assess whether the activity was continuous. The activity was considered to be continuous if the location and behavior did not change for the duration of the recording.

Measuring of environmental variables: environment temperature, light intensity, sunrise, and sunset time

The environmental temperature was measured with the IR cameras, while light intensity was measured during early, middle, and late stage of the survey period, respectively. The measurements were taken once an hour only between 17:00 and 20:00 in the evening and 3:00 and 5:00 in the morning. For the sunrise and sunset time, we referred to local climate data and calculated the median.

Statistical analysis

The data was tested for normality and equality of variance using the Kolmogorov-Smirnov and Levene's test of homogeneity. Data was treated with respective tests depending on whether they met or did not met the assumptions of normality. The

Kruskal-Wallis H test (nonparametric test) was used to compare the significant differences in behavior frequency, behavior duration, temperature, and light intensity among the three months. The t-test (Parametric test) or Mann-Whitney U test (nonparametric test) was used to test the differences between the different months. The association between feeding frequency, light intensity, and temperature was tested using the Pearson Correlation analysis. All data were expressed as mean ± sd and statistical significance was accepted when $\alpha < 0.05$. All statistical analyses were conducted in SPSS 22.0 software.

Results

Species diversity and composition of Glires in the study area

Among the 6383 effective recorded activities in the video, 5618 were of *A. peninsulae*, accounting for 85.73% of all the Glire species in the area. Other recorded Glires include *Tamias sibiricus* with 523 records, squirrel with 226 records, and *Clethrionomys rufocanus* with 16, accounting for 7.98%, 3.45%, and 2.84%, respectively. Therefore, *A. peninsulae* was the absolute dominant species in the selected research plot.

Classification and definition of foraging behaviors of *A. peninsulae*

Apodemus peninsulae behavior was analyzed from the video records. The main behavior patterns are as follows:

Motor behavior

A series of animal behaviors with obvious spatial displacements in different positions through various types of movement.

- **Creep (slow movement).** The abdomen of the body is on the ground, the forelimbs are stretched forward and flat on the ground, and then the two hindlimbs move forward simultaneously in a creeping movement. This kind of movement is the slowest, is used as the completion of short-distance movement and often occurs during foraging and feeding.
- **Walk (medium-speed movement).** The abdomen is off the ground; the limbs move alternately as the body stretches. The speed and distance in this kind of the movement are between creep and skip. It is used as complete short and medium-distance displacement and often occurs during foraging.
- **Skip (fast movement).** The hind limbs quickly kick off the ground, the body jumps forward and upward, and the displacement occurs in the form of a parabolic trajectory; the flying height is 10–30 cm, including a single skip and multiple consecutive skips, without other accompanying behaviors. This kind of movement often occurs during transport.

Feeding behavior

A series of behaviors exhibited by animals during feeding.

- **Forage:** when animals are searching for food by walking and creeping using their senses of smell and vision. They usually search over a large area before finding a concentrated food source and continue to search in a smaller area after finding the food source. Animals often exhibit the following behaviors: sniffing, looking around, forearm digging, and other search actions with single short skips (Fig. 1a).
- **Feeding:** when animals are handling and eating food. When feeding, they usually do not move around, but they do occasionally creep, squat, or lie on the ground with hind limb support. The abdomen is on the ground, the back is raised, the forelimbs are on the ground or slightly raised and the two front paws grasp the food to assist in processing the seed coat and biting and chewing the food (Fig. 1b).
- **Transport:** when animals are moving their food from where it was found, but not eating or processing it immediately. Transport occurs after foraging, and animals usually leave quickly by running or skipping. The direction of transport is scattered.
- **Hoarding:** when animals, after transporting the food in a short distance, do not eat or process the food but stores it in a place. This can be a concentrated area (concentrated hoarding) or scattered spots (scattered hoarding) within the foraging area. Usually, the food is buried in the soil and the litter using the mouth to carry the food and forelimbs to dig.
- **Clean:** when animals self-groom by scratching to clean or groom the fur of the cheeks, neck, and chest with mouth, forelimbs, and hindlimbs. It usually occurs after or during feeding.

Sentinel behavior

A series of behaviors of animals exhibited in response to risks and disturbances in the environment, and vigilance in response to what is in the environment to avoid being depredated.

- **Alert:** animals immediately interrupt foraging, feeding and other activities; animals stay still by squatting while lifting the forelimbs, standing up slightly, bowing back, sniffing, listening, and observing the surrounding environment (Fig. 1c).
- **Flee:** animals immediately interrupt their ongoing activity and leave quickly by running fast with skip or continuous large distance skips after perceiving the danger or disturbance.
- **Banishment:** animals immediately interrupt ongoing activities when another rodent appears within the same area where it is foraging or feeding. Animals will quickly move to the other rodent by skipping to chase it away.
- **Coexistence:** when two rodents forage within the same area without any competition or showing any aggression towards each other. Both animals conduct their own forage or feeding behavior with at least 30 cm between one another (Fig. 1d).

Figure 1. Some behaviors of *A. peninsulae.* **a** forage **b** feeding **c** alert **d** coexistence.

Feeding behavior strategy

Activity time of *A. peninsulae*

The start and end time of activity was consistent with sunrise and sunset; the percentage of activity time of *A. peninsulae* after sunset and sunrise was 100%, and 99.96%, respectively. Only two observations of activities that extended past sunrise by 30 minutes were found (Table 1). There was a seasonal, as well as night and day, effect on activity patterns, and much of the activity in summer was shorter than in autumn. From August to October, as the temperatures become cooler from August to October, the activity time starts to become longer. In August, *A. peninsulae* activity was at 37.1% of the whole day but increased to 52.3% and 52.2% in September and October, respectively.

Feeding behavior frequency and duration

Forage, feeding, and transport in feeding behavior were the main activities of *A. peninsulae* and were accompanied with motor and sentinel behavior. Of the total number of records (4403) of various types of behaviors, 57.96% (2552) were motor, 40.36%

Table 1. The activity time of *A. peninsulae* and partial climatic characteristics.

Month	Earliest time	Latest time	Sunset time	Sunrise time	Temperature (°C)	Illumination (Lx)
8	19:08:48	04:02:09	18:40 (18:31–18:47)	4:18 (4:12–4:24)	19.1 ± 2.2	371.4 ± 938.9
9	17:21:37	05:54:53	17:19 (17:10–17:29)	5:12 (5:06–5:18)	10.0 ± 1.6	64.6 ± 138.5
10	17:00:46	05:31:10	16:46 (16:37–16:55)	5:34 (5:28–5:40)	4.3 ± 1.4	16.3 ± 38.4

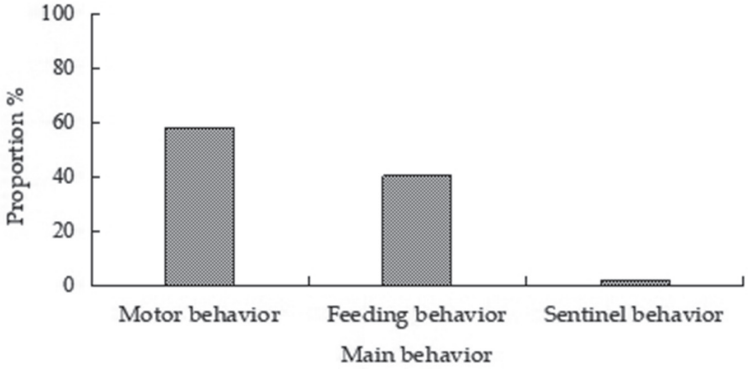

Figure 2. Proportion of three types behaviors of *A. peninsulae.*

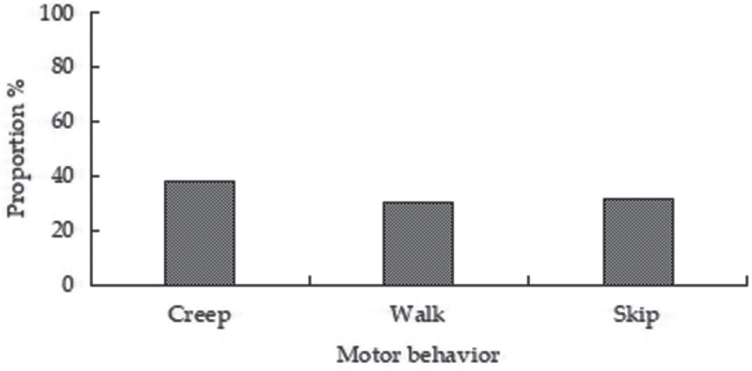

Figure 3. Proportion of motor behaviors of *A. peninsulae*.

(1777) were feeding, and 1.68% (74) were sentinel behaviors (Fig. 2). Of motor behaviors, creep, walk, and skip accounted for 38.24%, 30.41%, and 31.35% of behavior, respectively (Fig. 3). Of feeding behaviors, foraging, feeding, transport, and cleaning accounted for 48.79%, 35.85%, 14.01%, and 1.35%, respectively (Fig. 4). Hoarding behavior after transport could not be recorded due to the limitation of camera monitoring range. In sentinel behavior, alert, flee, banishment, and coexistence accounted for 35.14%, 40.54%, 4.05%, and 20.27%, respectively (Fig. 5).

Table 2. Frequency and duration of feeding behavior of *A. peninsulae* in different months.

Month	Frequency(time/night)				Duration (s)	
	Activity	Forage	Feeding	Transport	Forage	Feeding
8	7.2 ± 2.8	4.58 ± 2.87	4.17 ± 4.83	2.48 ± 1.86	42.78 ± 44.95	91.10 ± 118.02
9	29.7 ± 7.8	21.60 ± 10.02	12.30 ± 10.55	4.89 ± 5.90	47.05 ± 66.80	68.51 ± 102.98
10	15.7 ± 7.5	10.10 ± 8.36	11.35 ± 14.09	6.06 ± 4.83	29.16 ± 30.36	53.83 ± 88.72
Total	21.6 ± 11.6	10.84 ± 9.85	9.23 ± 11.17	4.37 ± 4.57	39.05 ± 51.63	63.58 ± 98.36

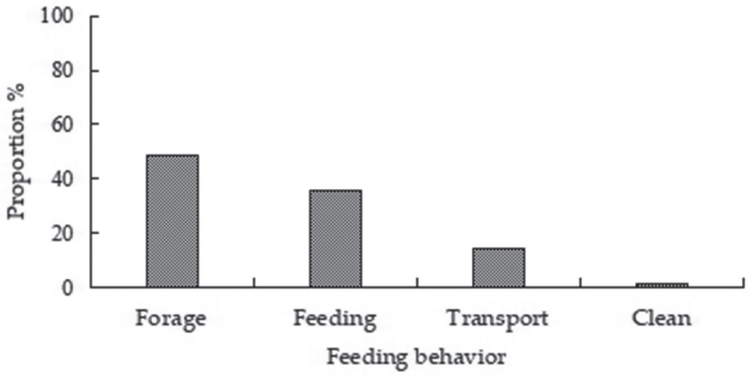

Figure 4. Proportion of feeding behaviors of *A. peninsulae.*

Figure 5. Proportion of sentinel behaviors of *A. peninsulae*.

Feeding behavior frequency varied significantly in different months (H = 82.848, df = 2, P < 0.001). Total frequency was 21.6 ± 11.6 times/night (4.2–41.6 times / night, N = 26), of which 7.2 ± 2.8 times/night (4.2–10.5 times/night, N = 5) in August, 29.7 ± 7.8 times/night (17.9–41.6 times/night, N = 14) in September, which was the most frequent month, and 15.7 ± 7.5 times (4.5–25.4 times/night, N = 7) in October. The frequency of activities in August was significantly less than that in September (t = –9.220, P < 0.001) and October (t = –2.382, P < 0.05), and the frequency of activities in September was higher than October (t = 3.931, P < 0.01) (Table 2).

Forage and feeding frequency were the highest in September, followed by October, and lowest in August (forage: $H = 36.163$, df = 2, $P < 0.001$; feeding: $H = 10.262$, df = 2, $P < 0.01$). The transport frequency in October was the highest, followed by September, and lowest in August (H = 6.018, df = 2, $P < 0.05$). There was no difference in the duration of forage in each month ($H = 1.318$, df = 2, $P > 0.05$), but the feeding duration was significant difference (H = 7.008, df = 2, $P < 0.05$) and the feeding duration in August was significantly longer than September and October (September: $Z = -2.348$, $P < 0.05$; October: $Z = -2.602$, $P < 0.01$).

The frequency and duration of three feeding behaviors were all different. The average frequency of forage, feeding and transport was 10.84 ± 9.85 times/night, 9.23 ± 11.17 times/night, and 4.37 ± 4.57 times/night, respectively. The frequency of forage was significantly higher than feeding and transport ($H = 23.092$, df = 2, $P < 0.001$). Only in September did the frequency of three behaviors show significant differences from August to October ($H = 25.614$, df = 2, $P < 0.001$) (Table 2). The average duration of forage and feeding was 39.05 ± 51.63 s and 63.58 ± 98.36 s, respectively. Feeding duration was significantly longer than forage ($Z = -6.704$, $P < 0.001$) and it showed different differences in August, September, and October ($Z = -3.930$, $P < 0.001$; $Z = -2.295$, $P < 0.05$; $Z = -5.478$, $P < 0.001$).

Feeding activity rhythm

Our observations show that the peak of feeding behavior occurs between 18:00 and 23:00 and varies from month to month. In August, only a single feeding peak was observed which started after 19:00, peaking between 22:00 and 23:00, and reducing after 3:00. In September and October, the activity started after 17:00, peaking between 18:00 and 20:00, which was earlier than that in August. In addition, the frequency of feeding was significantly higher than that in August, after 20:00, with a smooth curve and began to decrease after 4:00 (Fig. 6).

A. peninsulae showed a highest activity frequency on the first day it encountered a food source, with an average of 32.7 ± 7.1 times/night, then followed by daily feeding frequency between 10 and 22 times. This trend varied from month to month, with the feeding peak in August and decreasing thereafter. The feeding frequency showed the highest peaks on days 1, 4, 7, and 9 in September, and on days 1, 8, and 10 in October (Fig. 7).

Environmental factors and feeding behavior

From August to October, the temperature and light intensity decreased month by month. The temperature ($H = 223.041$, df = 2, $P < 0.001$) and light intensity ($H = 14.812$, df = 2, $P < 0.001$) from August to October showed significant differences. There was a strong positive association between temperature and feeding behavior during the month of September ($R = 0.361$, $P < 0.001$), but not during August and October (August: $R = 0.118$, $P > 0.05$; October: $R = -0.036$, $P > 0.05$; Fig. 8). Overall,

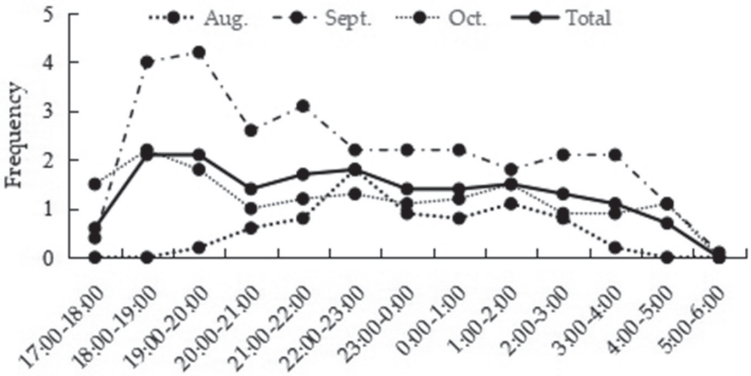

Figure 6. The night activity rhythm of *A. peninsulae* in different months.

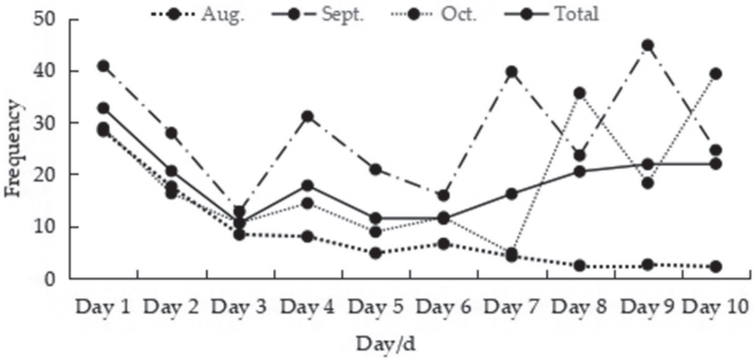

Figure 7. The activity rhythm of *A. peninsulae* during the study.

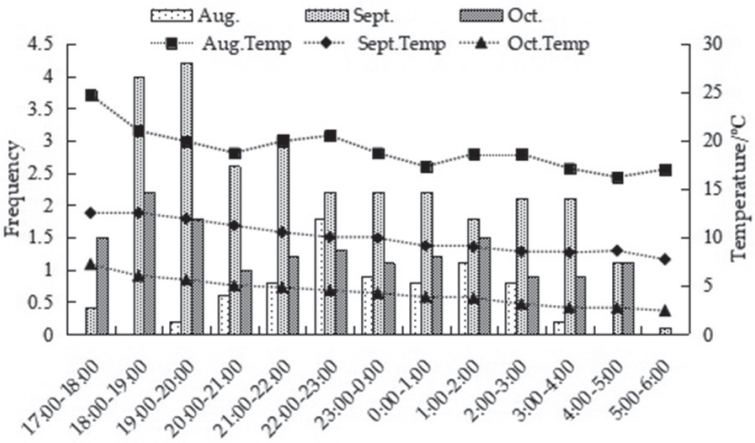

Figure 8. Interactions between temperature and feeding behavior of *A. peninsulae*.

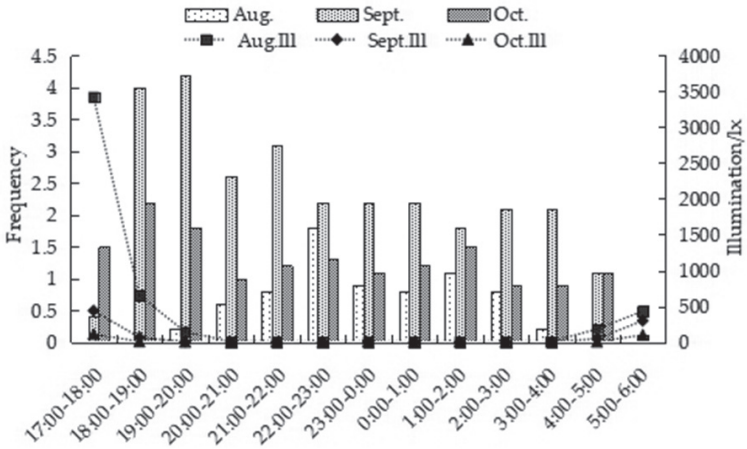

Figure 9. Interactions between illumination and feeding behavior of *A. peninsulae*.

feeding behavior was strongly associated with light intensity across the months, mainly September ($R = 0.472$, $P < 0.001$), and August ($R = 0.294$, $P < 0.05$), but this was not the case for October ($R = 0.167$, $P > 0.05$) (Fig. 9).

Discussion

Feeding behavior spectra of *A. peninsulae*

Apodemus peninsulae spends the majority of its active time feeding and exhibits some motor behaviors and sentinel behaviors during feeding. Our results show that foraging was the most frequent behavior and feeding was the longest behavior. *A. peninsulae* usually fed *in situ* when first encountering seeds, then transported seeds for later feeding or storage. The animals compensated for energy loss by reducing the frequency of foraging activity and spending more time to increase other activities such as sentinel behaviors so that they were more vigilant. Due to the limitation of the monitoring range of the camera, we were unable to follow post-transport feeding and hoarding activities, leading to an inaccurate calculation. We had similar results to Li et al. (2018) who showed that *A. peninsulae* was a scatter-hoarding animal which spent little time in feeding on seeds *in situ* (15.1%), but rather more time on post-transport feeding (20.4%) and hoarding (41.2%). Due to the existence of pressures, such as a complex and changeable environment, predation by natural enemies, and inter- and intraspecies competition, the combined feeding mode with *in situ* feeding, transport feeding, and scattered hoarding could help them to obtain greater benefits on the basis of reducing predation risk and decreasing competitive pressure (Clarke and Kramer 1994; Leaver and Daly 2001; Vander 2003, 2010; Vander and Beck 2012; Wang et al. 2013; Lichti et al. 2015).

Feeding and transport in *A. peninsulae* play two completely opposite roles in vegetation regeneration. On the one hand, feeding on a large number of seeds is harmful to forest regeneration (Lichti et al. 2015), while on the other, the transported and stored seeds exceed the demand, and any remaining seeds can potentially sprout and promote plant regeneration. In scatter-hoarding animals, it is common that caches are forgotten and plants can generate from those. Thus, the scatter-hoarding strategy effectively promotes plant regeneration and is a significant contributor to stabilizing plant population structure and maintaining the species diversity (Vander 2001; Preston and Jacobs 2009; Lichti et al. 2015). In response to the seasonal changes and the impacts on food resources, coupled with the north temperate climate, *A. peninsulae* showed different requirements to meet different life activities at different times. For example, in summer when resources were abundant and temperature and light intensity were suitable, *A. peninsulae* spent more time in feeding *in situ* and less time on other motor activities such as foraging and hoarding. However, when temperatures began to cool in the fall and resources were getting depleted, *A. peninsulae* began spending more time on foraging and transport activities, suggesting that they were storing food in order to successfully overwinter. This is an adaptation strategy in response to the seasonal changes of food and environment and is important for survival and reproduction of the species now and in the future (Vander 2001; Murray et al. 2006; Chang et al. 2010; Lichti et al. 2015).

Activity rhythm of *A. peninsulae* and affecting factors

Activity rhythm is a comprehensive adaptation to obtain the greatest survival benefits under various conditions and is affected by a variety of internal and external factors. Among them, solar radiation, light intensity, and environmental temperature are the main factors that affect animal activity rhythm (Roll et al. 2006). The change of the length of day and night is an effective constraining factor of the distribution of an animal's activity time; thus, it is particularly important to allocate its activity time appropriately to the available time (Dunbar 1992). Studies have confirmed that light was an important factor for the activities of Glires, and strictly nocturnal animals were inactive during the daylight period. Our study showed that the frequency of feeding behavior of *A. peninsulae* was strongly correlated with light intensity, showing an increased frequency of activity with a reduction in light intensity. This indicates that the nocturnal activity of these rodents is influenced by the intensity of light, since they are adapted to functioning at low light, twilight, and dusk. Most *Apodemus* spp. are either nocturnal, crepuscular, or both (Wolton 1983). Thus, it is unsurprising that these behaviors are consistent with what we observed in our study. In addition, the activity time of *A. peninsulae* showed seasonal differences, with shorter activity time in summer and longer time in autumn. The difference between the two seasons was up to 4 h, supporting the idea that temperature also influences activity patterns (Park et al. 2014).

Temperature is known to have considerable effect on changes in the daily activity rhythm in animals (Watanuki and Nakayama 1993; Corp et al. 1997; Hu et al. 2002).

Environment temperature has an important effect on the night activity of Glires (Corp et al. 1997), with rodent species adjusting their foraging times and activities in response to changes in temperature (Hu et al. 2002). Usually, *A. peninsulae* is more active at relatively warm temperatures (the average daily temperature is 0 °C) (Park et al. 2014), but it can adapt well to changes in environmental temperatures without having severe impact on its activities. As *A. peninsulae* does not hibernate in the cold months, it likely survives by greatly reducing foraging and feeding activities (Chang et al. 2010; Park et al. 2014).

Benefits and applications of IR cameras in the ecological studies

Studies under laboratory conditions have shown that *A. peninsulae* can be active both day and night in the spring (May), and the activity duration at night is more than that in day (Ji et al. 2005) , suggesting that seasonal difference may have an effect on animal activity rhythm. However, our data captured by IR cameras or radio monitoring with little human interference, shows more realistic behavioral patterns than laboratory studies. IR cameras reveal the strictly nocturnal and crepuscular lifestyle of *A. peninsulae*, and while it is relatively difficult to observe the behavior of nocturnal animals in the natural environment, IR cameras can provide an effective method to capture realistic information.

IR cameras have been used to assess species diversity survey and population density estimation in large mammals (Rowcliffe et al. 2008; Mondol et al. 2009; Zhang et al. 2013). However, IR cameras are less used in studies on small rodents (Zhang et al. 2013). Nocturnal small mammals are difficult to identify to individuals through photos or videos taken at night due to the lack of "natural marks". Identifying gender and age is just as difficult (Zhang et al. 2013). IR cameras have their own shortcomings. The effectiveness of these cameras depend on the probability, for example, that the study animal will appear at the site, the activities will be within the field of vision of the camera, and that the photos and videos will be in focus and clear; the cameras will also capture a high number of repeat records of the same individuals (Mondol et al. 2009; O'Connell et al. 2010; Zhang et al. 2013). Here, we found that the behaviors recorded by IR camera were fewer in number than in laboratory studies, but we captured more information on abundance compared to traditional surveys in natural environment (O'Connell et al. 2010; Liu et al. 2015; Li et al. 2018; Claridge et al. 2019; Nichols et al. 2019).

Conclusion

Infra-red cameras were used to record in natural conditions the feeding behavior of a small species of Glires, *A. peninsulae*, with both nocturnal and crepuscular behavior. In the behavior spectra, feeding behavior followed by motor and sentinel behaviors were the main activities of this species. It spent the majority of its active time feeding

and foraging. The behavior was influenced by light intensity, suggesting a preference for crepuscular periods of the day. This species' activities had significant seasonal differences and is seen as an adaptation strategy in response to seasonal changes in food and the environment. Our results show that IR cameras are highly useful in ecological studies of species of Glires that are not easily observable. IR cameras are able to capture much valuable information on ecological functions.

Acknowledgments

We are grateful to the people who helped install infra-red cameras and collect behaviorial data in Hengdaohezi. We thank the anonymous reviewers for their constructive comments on the manuscript. This research was funded by the Science Research Project of the Education Department of Heilongjiang Province (1353ZD005), the Innovation Research Project of Mudanjiang Normal University (GP2019004), and the Doctoral Research Fund of Mudanjiang Normal University (MNUB201907).

References

Chang G, Xiao Z, Zhang Z (2010) Effects of burrow condition and seed handling time on hoarding strategies of Edward's long-tailed rat (*Leopoldamys edwardsi*). Behavioural Processes 85: 163–166. https://doi.org/10.1016/j.beproc.2010.07.004

Claridge AW, Paull DJ, Welbourne DJ (2019) Elucidating patterns in the occurrence of threatened ground-dwelling marsupials using camera-traps. Animals 9: 913. https://doi.org/10.3390/ani9110913

Clarke MF, Kramer DL (1994) Scatter-hoarding by a larder-hoarding rodent: intraspecific variation in the hoarding behaviour of the eastern chipmunk, *Tamias striatus*. Animals 48: 299–308. https://doi.org/10.1006/anbe.1994.1243

Corp N, Gorman ML, Speakman JR (1997) Ranging behaviour and time budgets of male wood mice *Apodemus sylvaticusin* different habitats and seasons. Oecologia 109: 242–250. https://doi.org/10.1007/s004420050079

Dunbar RIM (1992) Time: a hidden constraint on the behavioural ecology of baboons. Behavioral Ecology and Sociobiology 31: 35–49. https://doi.org/10.1007/BF00167814

Flannigan G, Stookey JM (2002) Day-time time budgets of pregnant mares housed in tie stalls: a comparison of draft versus light mares. Applied Animal Behaviour Science 78: 125–143. https://doi.org/10.1016/S0168-1591(02)00085-0

Halles S, Stenseth NC (2000) Activity patterns in small mammals, an ecological approach. Springer, Berlin – New York, 322 pp. https://doi.org/10.1007/978-3-642-18264-8

Hu ZJ, Guo C, Wang Y, Zhang MH, Chen ZQ (2002) Daily activity rhythms of Yangtze vole. Chinese Journal of Zoology 37: 18–22.

Ji CY, Li Q, Yang CW (2005) Study on circadian activity rhythms of *Apodemus speciosus* Temminck. Journal of Mudanjiang Normal University (Natural Sciences Edition) 04: 1–3.

Karanth KU (1995) Estimating tiger *Panthera tigirs* populations from camera-trap data using capture-recapture models. Biological Conservation 71: 333–338. https://doi.org/10.1016/0006-3207(94)00057-W

Leaver LA, Daly M (2001) Food caching and differential cache pilferage: a field study of coexistence of sympatric kangaroo rats and pocket mice. Oecologia (Berlin) 128: 577–584. https://doi.org/10.1007/s004420100686

Lehner PN (1996) Handbook of Ethological Methods. Cambridge University Press, Cambridge, 694 pp.

Lichti NI, Steele MA, Swihart RK (2015) Seed fate and decision-making processes in scatter-hoarding rodents. Biological Reviews 92: 474–504. https://doi.org/10.1111/brv.12240

Li DW, Jin ZM, Yang CY, Yang CW, Zhang MH (2018) Scatter-hoarding the seeds of sympatric forest trees by *Apodemus peninsulae* in a temperate forest in northeast China. Polish Journal of Ecology 66: 382–394. https://doi.org/10.3161/15052249PJE2018.66.4.006

Li YH, Huang ZH, Zhou QH, Ma GZ, Huang CM (2019) Daily activity pattern in Assamese macaques inhabiting limestone forest, southwest Guangxi, China. Global Ecology and Conservation 20: e00709. https://doi.org/10.1016/j.gecco.2019.e00709

Liu D, Huang X, Chu H, Liu Y, Zhang F, Chen G, Qi Y (2015) Activity rhythms of Sino-Mongolia beaver (*Caster fiber birulai*) measured with infrared camera traps in Xinjiang, China. Arid Zone Research 32: 205–211.

Lu J, Zhang Z (2005) Food hoarding behaviour of large field mouse *Apodemus peninsulae*. Acta Theriologica 50: 51–58. https://doi.org/10.1007/BF03192618

Masaki M, Koshimoto C, Tsuchiya K, Nishiwaki A, Morita T (2005) Body temperature profiles of the Korean field mouse *Apodemus peninsulae* during winter aggregation. Mamm Study 30: 33–40. https://doi.org/10.3106/1348-6160(2005)30[33:BTPOTK]2.0.CO;2

Mondol S, Karanth KU, Kumar NS, Gopalaswamy AM, Andheria A, Ramakrishnan U (2009) Evaluation of noninvasive genetic sampling methods for estimating tiger population size. Biological Conservation 142: 2350–2360. https://doi.org/10.1016/j.biocon.2009.05.014

Murray AL, Barber AM, Jenkins SH, Longland WS (2006) Competitive environment affects food-hoarding behavior of Merriam's kangaroo rats (*Dipodomys merriami*). Journal of Mammalogy 87: 571–578. https://doi.org/10.1644/05-MAMM-A-172R1.1

Nichols M, Ross J, Glen AS, Paterson AM (2019) An evaluation of systematic versus strategically-placed camera traps for monitoring feral cats in New Zealand. Animals 9: 687. https://doi.org/10.3390/ani9090687

O'Connell AF, Nichols JD, Karanth KU (2010) Camera Traps in Animal Ecology: Methods and Analyses. Springer, Tokyo, 280 pp. https://doi.org/10.1007/978-4-431-99495-4

Park SJ, Rhim SJ, Lee EJ, Lee WS, Maguire CC (2014) Home range, activity patterns, arboreality, and day refuges of the Korean wood mouse *Apodemus peninsulae* (Thomas, 1907) in a temperate forest in Korea. Mammal Study 39: 209–217. https://doi.org/10.3106/041.039.0404

Pearson KM, Theimer TC (2004) Seed-caching responses to substrate and rock cover by two *Peromyscus* species: implications for pinyon pine establishment. Oecologia 141: 76–83. https://doi.org/10.1007/s00442-004-1638-8

Preston SD, Jacobs LF (2009) Mechanisms of cache decision making in fox squirrels (*Sciurus niger*). Journal of Mammalogy 90: 787–795. https://doi.org/10.1644/08-MAMM-A-254.1

Roll U, Dayan T, Kronfeld SN (2006) On the role of phylogeny in determining activity patterns of rodents. Ecology and Evolution 20: 479–490. https://doi.org/10.1007/s10682-006-0015-y

Rowcliffe J, Field J, Turvey S, Carbone C (2008) Estimating animal density using camera traps without the need for individual recognition. Journal of Applied Ecology 45: 1228–1236. https://doi.org/10.1111/j.1365-2664.2008.01473.x

Seri H, Chammem M, Ferreira LM, Kechnebou M, Khorchani T, Silva SR (2018) Effects of seasonal variation, group size and sex on the activity budget and diet composition of the addax antelope. African Journal of Range & Forage Science 35: 89–100. https://doi.org/10.2989/10220119.2018.1477831

Tang CB, Wang GH, Shi ZP, Li SQ, Huang ZH, Wang ZX, Zhou QH (2020) Activity rhythm and time budget of the red-bellied squirrels (*Callosciurus erythralus*) based on infrared camera data. Journal of Guangxi Normal University 38: 133–139.

Vander Wall SB (2001) The evolutionary ecology of nut dispersal. Botanical Review 67: 74–117. https://doi.org/10.1007/BF02857850

Vander Wall SB (2003) Effects of seed size of wind-dispersed pines (*Pinus*) on secondary seed dispersal and the caching behavior of rodents. Oikos 100: 25–34. https://doi.org/10.1034/j.1600-0706.2003.11973.x

Vander Wall SB (2010) How plants manipulate the scatter-hoarding behavior of seed-dispersing animals. Philosophical Transactions of the Royal Society B-biological Sciences 365: 989–997. https://doi.org/10.1098/rstb.2009.0205

Vander Wall SB, Beck MJ (2012) A comparison of frugivory and scatter-hoarding seed-dispersal syndromes. Biological Reviews 78: 10–31. https://doi.org/10.1007/s12229-011-9093-9

Wang B, Ye CX, Cannon CH, Chen J (2013) Dissecting the decision making process of scatter-hoarding rodents. Oikos 122: 1027–1034. https://doi.org/10.1111/j.1600-0706.2012.20823.x

Wang G, Shi Z, Li, S, Lu C, Zhou Q (2019) Preliminary observation on the activity rhythm and time budget of the Asiatic brush-tailed porcupine (*Atherurus macrourus*) based on camera-trapping data. Acta Theriologica Sinica 39: 62–68.

Watanuki Y, Nakayama Y (1993) Age difference in activity pattern of Japanese monkeys: effects of temperature, snow, and diet. Primates 34: 419–430. https://doi.org/10.1007/BF02382651

Wen LJ, Guo YM, Huang J, Song Y (2016) The activity rhythm of the Asiatic brush-tailed porcupine *Atherurus macrourus* and its correlation with the phases of the moon. Chinese Journal of Zoology 51: 347–352.

Wolton RJ (1983) The activity of free-ranging wood mice *Apodemus sylvaticus*. Journal of Animal Ecology 52: 781–794. https://doi.org/10.2307/4453

Zhang SS, Bao YX, Wang YN, Fang PF, Ye B (2013) Estimating rodent density using infrared-triggered camera technology. Acta Ecologica Sinica 33: 3241–3247. https://doi.org/10.5846/stxb201202290272

ZooKeys 992: 157–181 (2020)
doi: 10.3897/zookeys.992.53975
https://zookeys.pensoft.net

RESEARCH ARTICLE

A peer-reviewed open-access journal
ZooKeys
Launched to accelerate biodiversity research

Monopis jussii, a new species (Lepidoptera, Tineidae) inhabiting nests of the Boreal owl (*Aegolius funereus*)

Marko Mutanen[1], Peter Huemer[2], Jonna Autto[3], Ole Karsholt[4], Lauri Kaila[5]

1 *Ecology and Genetics Research Unit, P.O.Box 3000, FI-90014 University of Oulu, Finland* **2** *Tiroler Landesmuseen-Betriebsgesellschaft m.b.H., Innsbruck, Austria* **3** *Apajatie 11, FI-96800 Rovaniemi, Finland* **4** *Zoological Museum, Natural History Museum of Denmark, Universitetsparken 15, DK-2100 Copenhagen, Denmark* **5** *Finnish Museum of Natural History, Zoology Unit, P.O.Box 17, FI-00014 University of Helsinki, Finland*

Corresponding author: Marko Mutanen (marko.mutanen@oulu.fi)

Academic editor: E.J. van Nieukerken | Received 6 May 2020 | Accepted 26 August 2020 | Published 12 November 2020

http://zoobank.org/AB14E1B0-0314-4D0E-A42C-0276F0AE6C52

Citation: Mutanen M, Huemer P, Autto J, Karsholt O, Kaila L (2020) *Monopis jussii*, a new species (Lepidoptera, Tineidae) inhabiting nests of the Boreal owl (*Aegolius funereus*). ZooKeys 992: 157–181. https://doi.org/10.3897/zookeys.992.53975

Abstract

Monopis jussii Kaila, Mutanen, Huemer, Karsholt & Autto, **sp. nov.** (Lepidoptera, Tineidae) is described as a new species. It is closely related to the widespread and common *M. laevigella* ([Denis & Schiffermüller], 1775), but differs in its distinct COI DNA barcode sequences, four examined nuclear loci as well as details in forewing coloration and pattern. Most reared specimens of *M. jussii* have emerged from the nest remnants of the Boreal owl (*Aegolius funereus* (Linnaeus, 1758)), but also nests of the Ural owl (*Strix uralensis* Pallas, 1771) and the Great tit (*Parus major* Linnaeus, 1758) have been observed as suitable habitats. Based on the present knowledge, the new species has a boreo-montane distribution as it is recorded only from northern Europe and the Alps. Several extensive rearing experiments from *Strix* spp. nest remnants from southern Finland did not produce any *M. jussii*, but thousands of *M. laevigella*, suggesting that the species is lacking in the area or, more unlikely, that the nest of these owl species do not serve as good habitat for the new species. This unexpected species discovery highlights, once again, the usefulness of DNA barcoding in revealing the cryptic layers of biodiversity. To serve stability we select a neotype for *Tinea laevigella* [Denis & Schiffermüller], 1775, and discuss the complicated synonymy and nomenclature of this species.

Keywords
boreo-montane, cryptic diversity, DNA barcoding, nuclear marker

Introduction

The lepidopteran fauna of Central and North Europe has been investigated for a longer time and more intensively than that of any other region in the world. Consequently, discoveries of species new to the region are nowadays uncommon and usually involve expansive or invasive species. Large-scale efforts to build taxonomically comprehensive regional DNA barcode reference libraries have, however, resulted in a boost in discoveries of overlooked species during the last 15 years, as demonstrated by the increase of new species descriptions e.g. in the family Gelechiidae by Huemer et al. (2020). Characteristic to the new discoveries is that they often concern unexpected cases of cryptic diversity among well-known and often widespread species. Examples of such recent findings, originally detected as deep intraspecific splits in DNA barcode sequences, include *Leptidea reali* Reissinger, 1990 (Dinca et al. 2011), *Olethreutes subtilana* (Falkovitsh, 1959) (Segerer et al. 2010), *Phalonidia udana* (Guenée, 1845) (Mutanen et al. 2012a), *Epinotia cinereana* (Haworth, 1811) (Mutanen et al. 2012b), *Nemophora scopolii* Kozlov, Mutanen, Lee & Huemer, 2016 (Kozlov et al. 2017), several *Elachista* spp. (Mutanen et al. 2013) and *Hoplodrina alsinides* (Costantini, 1922) (Huemer et al. 2020).

There are many more additional cases of potential cryptic diversity in European Lepidoptera, as dozens of species show high levels of genetic polymorphism in their mitochondrial DNA (Mutanen et al. 2016, Huemer et al. 2020). While polymorphism in the mitochondrial DNA may result from multiple other phenomena, including mitochondrial introgression and retained ancestral polymorphism, many of those cases are likely to result from cryptic diversity.

An intraspecific split of the mitochondrial DNA being reflected in the nuclear genome in sexually reproducing species and in sympatry would strongly suggest the presence of cryptic diversity, because, unlike mitochondrial DNA, nuclear DNA is subject to genetic recombination. From this starting point, we sequenced four nuclear markers of *Monopis laevigella* ([Denis & Schiffermüller], 1775), a widespread and common species of tineid moths, showing a deep sympatric genetic split in its DNA barcode region in Europe (Gaedike 2019). Despite the limited number of analyzed specimens, the results provided unequivocal genetic support for the presence of two biologically distinct species. Subsequent morphological examination revealed consistent differences in the adult wing patterns, providing additional support for the overlooked cryptic diversity. Additionally, based on the presently available data, the two species show overlapping, but different ranges and based on the present knowledge, also a different ecology. Based on these grounds, we here describe one of the taxa as new to science.

Material and methods

The material examined was acquired from the following collections:

ITJ Research collection of Juhani Itämies
MUT Research collection of Marko & Tomi Mutanen
MZH Finnish Museum of Natural History, Helsinki, Finland
TLMF Tiroler Landesmuseum Ferdinandeum, Innsbruck, Austria
ZMUO Zoological Museum, University of Oulu, Finland
ZSM Zoologische Staatssammlung München, Germany

Terminology of genitalia follows Robinson and Nielsen (1993) and Gaedike (2019).

Preparation of genitalia generally follows the method outlined by Robinson (1976). Male genitalia were mounted in dorso-ventral position as it was considered to best show shapes of diagnostic structures, even if the shape of the gnathos is not optimally expressed. Male genitalia were stained using Eosin, female genitalia as well as abdominal pelts of both sexes using Chlorazol black. Structures were embedded in Euparal. Images were edited using Corel PHOTO-PAINT (2019).

Species of Tineidae have been systematically sequenced for the standard barcode region of the mitochondrial COI (cytochrome c oxidase subunit 1) in the connection of ongoing regional or national DNA barcoding projects in the Alps (Lepidoptera of the Alps campaign) and Finland (FinBOL). DNA barcode sequencing was conducted at the Canadian Centre for DNA Barcoding (CCDB, Biodiversity Institute of Ontario, University of Guelph) using standard Sanger protocols as explained in deWaard et al. (2008). We successfully sequenced 87 specimens of *Monopis* representing twelve species, the newly described species included. Five European species of *Monopis* (*M. luteocostalis* Gaedike, 2006, *M. henderickxi* Gaedike & Karsholt, 2001, *M. christophi* Petersen, 1957, *M. pallidella* Zagulajev, 1955 and *M. barbarosi* (Koçak, 1981)) were not included in this sampling. Each of them is morphologically clearly distinct from *M. jussii* sp. nov. (Gaedike 2019). Full collection and taxonomic data as well as voucher photographs, DNA sequences and GenBank accession numbers of all these specimens are available in the Barcode of Life Data Systems (BOLD; Ratnasingham and Hebert 2007) in the public dataset DS-MONOJUS at https://dx.doi.org/10.5883/DS-MONOJUS. Collection data of the specimens are also given in Table 1. Some of the COI sequences used in this study were previously published in Mutanen et al. (2016), the others are novel.

Four nuclear genes, *carbamoylphosphate synthase domain protein* (CAD), *elongation factor 1 alpha* (EF-1a), *cytosolic malate dehydrogenase* (MDH) and *wingless*, were sequenced at the University of Oulu, Finland. These genes were chosen primarily based on the high amplification success rate in other Tineidae, but also based on our previous experience on their general good functionality to provide useful taxonomic information between closely related species. In these analyses, three specimens of *M. laevigella* and two specimens of *M. jussii*, all collected from Finland, were included. Legs

Table 1. Summary of the collection data of barcoded specimens of *Monopis* used in this study. For more details, see the public BOLD dataset at https://dx.doi.org/10.5883/DS-MONOJUS.

Species	Sample ID	Sequence length	Collector(s)	Collection date	Country	Province	Site	Latitude	Longitude
Monopis burmanni	TLMF Lep 18816	658	Huemer P.	13-Jun-2006	Austria	Tyrol	Nordtirol, Kranebitter Innaue	47.265	11.323
Monopis burmanni	TLMF Lep 18234	658	Huemer P.	05-Jun-2015	Austria	Tyrol	Nordtirol, Ellbachtal, unterer Kaiserboden	47.539	11.926
Monopis crocicapitella	TLMF Lep 06512	658	O. Rist	23-Sep-2005	Austria	Vienna	Wien Stadlau	48.217	16.467
Monopis crocicapitella	TLMF Lep 03882	658	Huemer P.	21-May-2004	Spain	Comunidad Valenciana	Valencia, El Saler, Albufera	39.3255	-0.312972
Monopis fenestratella	MM18616	658	Marko Mutanen	1997	Finland	N	Mäntsälä	60.688	25.168
Monopis fenestratella	MM18615	658	Marko Mutanen	1997	Finland	N	Mäntsälä	60.688	25.168
Monopis fenestratella	MM08511	658	Marko Mutanen	larva 1997-1998	Finland	Ta	Pälkäne		
Monopis fenestratella	MM08510	552	Marko Mutanen	larva 1997-1998	Finland	Ta	Pälkäne		
Monopis imella	TLMF Lep 19836	658	Buchner P.	29-Aug-2014	Austria		Niederoesterreich, Sollenau	47.905	16.266
Monopis imella	TLMF Lep 25734	639	Huemer P.	07-Sep-2016	Austria		Burgenland, Jois SW, Hackelsberg	47.9539	16.7747
Monopis imella	TLMF Lep 25735	638	Huemer P.	07-Sep-2016	Austria		Burgenland, Jois SW, Hackelsberg	47.9539	16.7747
Monopis imella	TLMF Lep 23122	658	Huemer P.	26-May-2017	Austria		Burgenland, Hackelsberg	47.9528	16.7733
Monopis imella	TLMF Lep 19838	658	Buchner P.	17-Aug-2014	Austria		Niederoesterreich, Sollenau	47.905	16.266
Monopis imella	MM18899	658	Kari Vaalamo, Bo Wikström	13-Jul-2002-19-Jul-2002	Finland	Al	Kökar	59.9031	20.74
Monopis imella	MM18898	658	Pekka Sundell, M. Varesvuo, L. Jalonen, Kalle Lundsten	25-Aug-2004-10-Sep-2004	Finland	Al	Kökar	59.92	20.898
Monopis imella	MM26020	658	Huotari, Laasonen	08-Jul-2014	Hungary	Tokaj	Tarcal	48.0512	21.1811
Monopis imella	MM26021	658	Huotari, Laasonen	08-Jul-2014	Hungary		Tokaj, Tarcal	48.0512	21.1811
Monopis jussii	MM17525	658	Marko Mutanen	2001	Finland	Oba	Ylikiiminki	64.984	26.153
Monopis jussii	MM18626	658	Panu Välimäki & Marko Mutanen	2006	Finland	Oba	Oulu	64.9768	25.3056
Monopis jussii	MM15526	658	Marko Mutanen	larva 2001	Finland	Oba	Ylikiiminki		
Monopis jussii	TLMF Lep 09795	658	Huemer P.	23-Jun-2006	Italy	South Tyrol	Suedtirol, Tiers E, Plafetscher Wald	46.472	11.596

Species	Sample ID	Sequence length	Collector(s)	Collection date	Country	Province	Site	Latitude	Longitude
Monopis laevigella	TLMF Lep 09306	658	Huemer P.	19-Jun-2012	Austria	Tyrol	Nordtirol, Oberpettnau, Platten	47.301	11.126
Monopis laevigella	TLMF Lep 10365	658	Huemer P.	16-Jun-2013	Austria	Tyrol	Nordtirol, Tiefenbachklamm/ Brandenberg	47.484	11.864
Monopis laevigella	TLMF Lep 10441	658	Huemer P.	16-May-2013	Austria	Tyrol	Nordtirol, Tiefenbachklamm/ Brandenberg	47.484	11.864
Monopis laevigella	TLMF Lep 07389	658	Huemer P.	25-May-2008	Austria	Tyrol	Nordtirol, Telfs/ Moritzen SW, Innau	47.299	11.05
Monopis laevigella	TLMF Lep 10354	658	Huemer P.	16-Jun-2013	Austria	Tyrol	Nordtirol, Tiefenbachklamm/ Brandenberg	47.484	11.864
Monopis laevigella	TLMF Lep 07970	658	Huemer P.	25-May-2012	Austria	Vorarlberg	Umg. Zwischenwasser, Ueble Schlucht, Eingang	47.267	9.667
Monopis laevigella	MM19355	658	O. Martin	larva 14-Oct-2004	Denmark	Sjaelland	Nez, Bognaes, Egehoved		
Monopis laevigella	MM17303	658	Tomi Mutanen	09-Jun-2010	Finland	Ab	Salo	60.335	23.088
Monopis laevigella	MM17522	658	Henrik Bruun	01-Apr-2007	Finland	Ab	Nauvo	60.225	21.945
Monopis laevigella	MM21029	658	Ali Karhu	27-Jun-2008-29-Jun-2008	Finland	Ka	Liperi	62.552	29.167
Monopis laevigella	MM21028	658	Ali Karhu	1-Jun-2010-25-Jul-2010	Finland	Ka	Liperi	62.551	29.226
Monopis laevigella	MM21026	658	Ali Karhu	03-Jul-2007	Finland	Ka	Liperi	62.563	29.013
Monopis laevigella	MM21025	658	Ali Karhu	2005	Finland	Ka	Liperi	62.511	29.475
Monopis laevigella	MM17524	606	Marko Mutanen	30-Jun-1997	Finland	Oba	Hailuoto	64.968	24.671
Monopis laevigella	MM15527	658	Marko Mutanen	30-Jun-2001	Finland	Oba	Oulu	64.977	25.306
Monopis laevigella	MM10119	658	Marko Mutanen, Nestori Mutanen, Anttoni Mutanen	12-Jul-2008	Finland	Oba	Kiiminki	65.071	25.725
Monopis laevigella	MM18625	658	Panu Välimäki	21-Jun-2000	Finland	St	Luvia	61.29	21.587
Monopis laevigella	MM17526	658	Juhani Itaemies	14-Feb-2005	Finland	St	Eurajoki	61.193	21.417
Monopis laevigella	TLMF Lep 27537	658	Huemer P.	29-Jun-2019	Italy	Piedmont	Fenestrelle, ca. 0,7 km NE Pequerel	45.0517	7.07111

Species	Sample ID	Sequence length	Collector(s)	Collection date	Country	Province	Site	Latitude	Longitude
Monopis laevigella	TLMF Lep 12113	658	Huemer P.	17-Jul-2013	Italy	South Tyrol	Suedtirol, N Zwischenwasser/ St. Lorenzen	46.739	11.873
Monopis laevigella	TLMF Lep 11818	658	Huemer P.	25-Jul-2013	Italy	South Tyrol	Suedtirol, Franzenshoehe / Stilfserjoch	46.534	10.486
Monopis laevigella	TLMF Lep 02066	658	Huemer P.	01-Jul-2010	Italy	South Tyrol	Suedtirol, Ritten/ Obergruenwald	46.597	11.439
Monopis laevigella	TLMF Lep 05368	658	Huemer P., Tarmann G. M.	01-Aug-2011	Macedonia		Mavrovo NP, Radika valley, around bridge, 10 km NNW Sveta Voda	41.789	20.547
Monopis monachella	TLMF Lep 08436	658	Huemer P.	25-Jul-2012	Austria	Vorarlberg	Lustenau, Schweizer Ried, AZE Haeusle S	47.446	9.69
Monopis monachella	TLMF Lep 19839	658	Buchner P.	07-Jun-2014	Austria		Niederoesterreich, Sollenau	47.905	16.266
Monopis monachella	MM13366	658	Marko Mutanen, Panu Välimäki	2008	Finland	Ab	Dragsfjärd	60.011	22.498
Monopis monachella	MM11934	658	Marko Mutanen, Panu Välimäki	2007	Finland	N	Hanko	59.836	23.236
Monopis monachella	MM17249	658	Lauri Kaila	21-Aug-2005	Finland	N	Tammisaari	59.829	23.612
Monopis monachella	MM12377	658	Marko Mutanen, Panu Välimäki	2007	Finland	Sa	Imatra	61.108	28.799
Monopis neglecta	TLMF Lep 07250	658	Sumpich J.	10-Jun-2010	Austria	Lower Austria	Hardegg Umgebung/ Thaya Haenge	48.854	15.858
Monopis neglecta	TLMF Lep 17583	658	Deutsch H.	30-Aug-2002	Austria	Tyrol	Osttirol, Lengberg	46.801	12.891
Monopis neglecta	TLMF Lep 06608	658	Rist O.	11-Jun-2010	Austria	Vienna	Wien Mauer	48.15	16.25
Monopis nigricantella	TLMF Lep 03881	658	Huemer P.	07-Sep-2005	Spain	Comunidad Valenciana	Valencia, El Saler, Albufera	39.3255	-0.312972
Monopis nigricantella	TLMF Lep 03879	658	Huemer P.	18-May-2004	Spain	Comunidad Valenciana	Valencia, El Saler, Albufera	39.3255	-0.312972
Monopis nigricantella	TLMF Lep 03878	658	Huemer P.	22-May-2004	Spain	Comunidad Valenciana	Valencia, Santa Pola, Playa del Pinet	38.1583	-0.625278

Species	Sample ID	Sequence length	Collector(s)	Collection date	Country	Province	Site	Latitude	Longitude
Monopis nigricantella	TLMF Lep 03880	658	Huemer P.	08-Sep-2005	Spain	Comunidad Valenciana	Valencia, El Saler, Albufera	39.3255	-0.312972
Monopis obviella	TLMF Lep 15096	636	Huemer P.	19-Jun-2014	Austria	Tyrol	Nordtirol, Baumkirchen W	47.296	11.552
Monopis obviella	TLMF Lep 09367	658	Huemer P.	02-Jun-2012	Austria	Tyrol	Nordtirol, Flaurling NW, Innau	47.302	11.121
Monopis obviella	TLMF Lep 08054	658	Huemer P.	15-Jun-2012	Austria	Vorarlberg	Bludesch, Bludescher Magerrasen E, Umg. Jordan	47.203	9.747
Monopis obviella	TLMF Lep 09962	658		19-Jun-13	Austria	Vorarlberg	Umg.Langenegg, Langenegg-Leiten, Fohren	47.467	9.883
Monopis obviella	TLMF Lep 25739	658	Huemer P.	07-Sep-2016	Austria		Burgenland, Jois SW, Hackelsberg	47.9539	16.7747
Monopis obviella	TLMF Lep 19832	658	Buchner P.	29-Aug-2014	Austria		Niederoesterreich, Sollenau	47.905	16.266
Monopis obviella	MM18928	658	Kari Vaalamo, Bo Wikström	19-Jul-2008-23-Jul-2008	Finland	Al	Lemland	59.9564	20.0116
Monopis obviella	MM06790	658	Marko Mutanen	13-Jul-2007	Finland	Al	Lemland	60.026	19.961
Monopis obviella	MM21130	658	Marko Mutanen, Tomi Mutanen, Anttoni Mutanen, Nestori Mutanen	16-Jul-2011	Finland	N	Hanko	59.834	23.013
Monopis obviella	TLMF Lep 27604	658	Huemer P.	28-Jun-2019	Italy	Piedmont	Fenestrelle, ca. 1 km WNW Pequerel	45.0497	7.05139
Monopis obviella	TLMF Lep 27794	630	Huemer P.	23-Jul-2019	Italy	Piedmont	Fenestrelle, ca. 0,7 km NE Pequerel	45.0517	7.07111
Monopis obviella	TLMF Lep 10292	658	Huemer P.	25-Jun-2013	Italy	South Tyrol	Suedtirol, Margreid/ Fennerschlucht	46.288	11.201
Monopis obviella	TLMF Lep 02169	658	Huemer P.	04-Jun-2010	Italy	South Tyrol	Suedtirol, Montiggl/ Kleiner Priol	46.428	11.3
Monopis obviella	TLMF Lep 12282	658	Huemer P.	05-Jul-2013	Italy	South Tyrol	Suedtirol, Schleiser Leiten	46.698	10.517
Monopis spilotella	MM04157	658	Marko Mutanen		Finland	Le	Enontekiö	68.997	20.744

Species	Sample ID	Sequence length	Collector(s)	Collection date	Country	Province	Site	Latitude	Longitude
Monopis spilotella	MM24137	658	Marko Mutanen, Anttoni Mutanen, Nestori Mutanen	05-Jul-2014	Finland	Lkoc	Muonio	67.9178	23.7466
Monopis spilotella	MM03158	658	Marko Mutanen	2006	Finland	Oba	Kiiminki	65.071	25.725
Monopis spilotella	MM02304	658	Marko Mutanen, Panu Välimäki	2006	Finland	Sa	Imatra	61.108	28.799
Monopis weaverella	TLMF Lep 15166	658	Huemer P.	09-Jun-2014	Austria	Tyrol	Nordtirol, Ellbachtal, unterer Kaiserboden	47.539	11.926
Monopis weaverella	TLMF Lep 15178	658	Huemer P.	09-Jun-2014	Austria	Tyrol	Nordtirol, Ellbachtal, unterer Kaiserboden	47.539	11.926
Monopis weaverella	TLMF Lep 18561	658	Huemer P.	20-Jul-2005	Austria	Tyrol	Nordtirol, Umg. Innsbruck, Samertal, Jaegerkar	47.34	11.382
Monopis weaverella	TLMF Lep 07388	658	Huemer P.	25-May-2008	Austria	Tyrol	Nordtirol, Telfs/ Moritzen SW, Innau	47.299	11-May
Monopis weaverella	TLMF Lep 09220	658	Huemer P.	06-Jun-2010	Austria	Tyrol	Nordtirol, Walchsee/ Schwemm N	47.661	12.298
Monopis weaverella	MM21138	658	Marko Mutanen ,Tomi Mutanen	18-Jun-2011	Finland	Ab	Nauvo	60.192	21.923
Monopis weaverella	MM13581	658	Marko Mutanen, Panu Välimäki	2008	Finland	Ab	Dragsfjärd	60.011	22.498
Monopis weaverella	MM21027	658	Ali Karhu	21-Jun-2004-23-Jun-2004	Finland	Ka	Liperi	62.552	29.167
Monopis weaverella	MM04159	658	Marko Mutanen		Finland	Le	Enontekiö	68.997	20.744
Monopis weaverella	MM04158	658	Marko Mutanen		Finland	Le	Enontekiö	68.997	20.744
Monopis weaverella	MM02600	639	Marko Mutanen, Panu Välimäki	2006	Finland	Sa	Imatra	61.108	28.799
Monopis weaverella	TLMF Lep 22008	658	Schaefer W.	07-Aug-2015	Germany		Kefenrod	50.35	9.21667

of dry and pinned adult specimens were used for extraction of genomic DNA with DNeasy Blood & Tissue Kit (Qiagen). We largely followed the sequencing protocol by Wahlberg and Wheat (2008), but PCR clean-up was carried out with ExoSAP-IT (Affymetrix, Santa Clara, CA, USA) and Sephadex columns (Sigma-Aldrich, St. Louis, MO, USA). Additionally, sequencing was performed using an ABI 3730 DNA Analyzer (Applied Biosystems, Foster City, CA, USA). Sequences were checked and edited using BioEdit software (Hall 1999). The sequences were uploaded to a VoSeq database (Peña and Malm 2012). The same dataset was used to generate fasta files for Neighbor-Joining analyses.

Minimum genetic p-distance barcode divergence between *M. laevigella* and *M. jussii* was calculated using analytical tools in BOLD Systems v. 4.0 (http://www.boldsystems.org). Neighbor-joining trees for the barcode region for all included *Monopis* species and specimens as well as four nuclear genes for five analyzed specimens of *M. laevigella* and *M. jussii* were constructed under p-distance model using Mega 7.0 (Kumar et al. 2016). The trees were stylized using CorelDraw v. 20.0.0.633.

Results

DNA sequencing resulted in a barcode of 552 bp or longer for 81 specimens. All except seven specimens yielded a full-length (654 bp) barcode. BOLD's barcode gap analysis showed that all included species have highly species-specific DNA barcodes with the mean of minimum divergences (p-distance model) to the nearest species being 10.01% (range 4.43–17.58%) (Figure 1). The minimum divergence between *M. laevigella* and *M. jussii* is 4.43%.

For each nuclear gene, data of only a single specimen of two analyzed *M. jussii* specimens were retrieved. Informative (i.e. data from both species available) sequence lengths by genes were as follows: CAD: 336 bp, EF-1a: 410 bp, MDH: 334 bp, wingless: 307 bp. Genetic p-distances between the two species were: CAD: 2.1%, EF-1a: 2.2%, MDH: 1.5%, and wingless: 4.1%. As a rule, the specimen of *M. jussii* formed a sister to the two or three specimens of *M. laevigella* (Figure 2).

Monopis jussii **Kaila, Mutanen, Huemer, Karsholt & Autto, sp. nov.**
http://zoobank.org/288523EF-4785-4711-B5DF-483D42057841
Figures 3–9

Type material. ***Holotype*** ♂ (Figure 3): FINLAND, PPe Yli-Kiiminki, larva 2001, ex nest of *Aegolius funereus*, M. Mutanen leg. R. Gaedike prep. 8607. (ZMUO).

Paratypes. FINLAND • 7 ♂ 16 ♀, PPs Kiiminki, 65.1163°N, 25.8291°E, Larva 1995, ex nest of *Aegolius funereus*, L. Kaila prep. 6317, 6325, 6326, M. Mutanen leg. (ZMUO); Finland: 10 ♂, 16 ♀, PPe Yli-Kiiminki, larva 2001, ex nest of *Aegolius funereus*, L. Kaila prep. 6314, 6315, 6316, 6322, 6323, 6324, R. Gaedike prep. 8606,

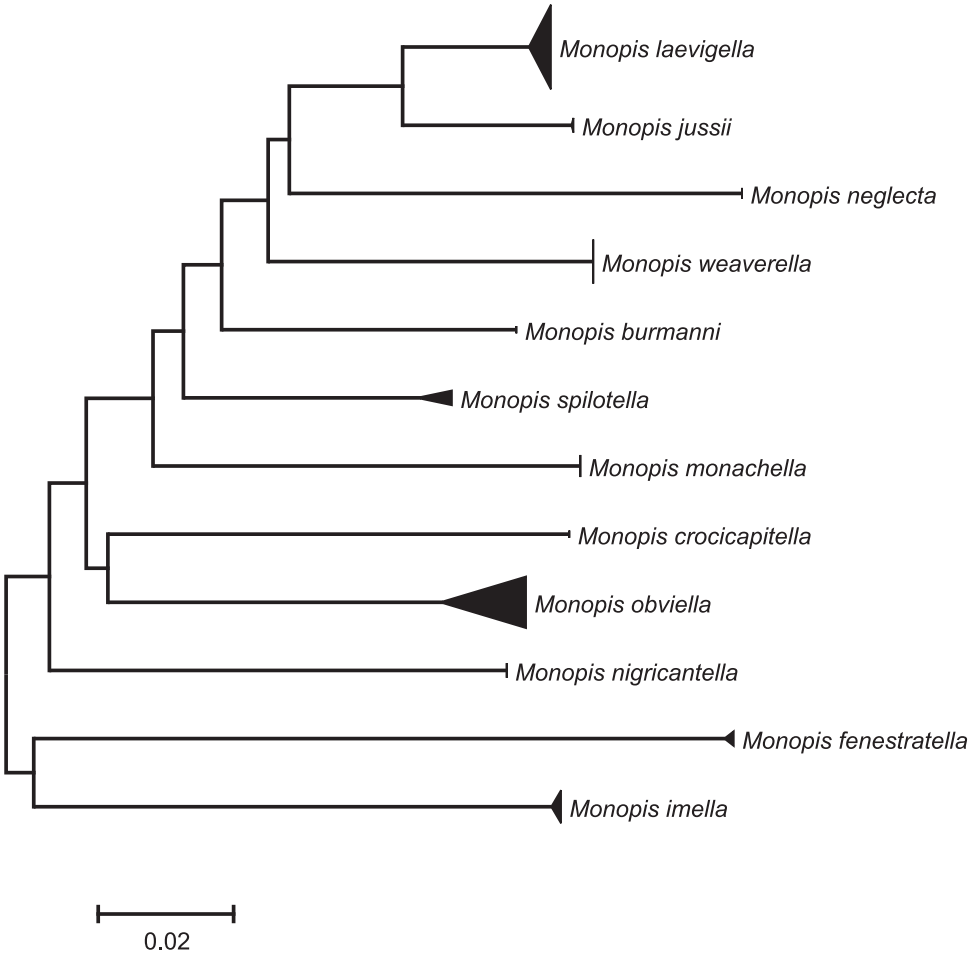

Figure 1. A compressed Neighbor-Joining tree DNA barcode region of European *Monopis* with most European species represented. The depth of the triangle is proportional to the intraspecific genetic variability within species and the height to sampling intensity.

8607, 8698, DNA samples MM15526, MM17525, M. Mutanen leg. (ZMUO); • 2 ♀, Oba Utajärvi, Pälli, 64.8363°N, 26.21°E, larva 1980 ex nest of *Aegolius funereus*, J. Itämies leg. (ITJ); • 3 ♂ 3 ♀, Kn Puolanka, Piltunkijärvi, 64.7618°N, 27.3151°E, larva 18.6.1976 ex nest of *Aegolius funereus* (1974), M. Rikkonen leg. (ZMUO); • 2 ♂, Kn Vaala, Otermajärvi, 64.6724°N, 27.1047°E, larva 12 Jun 1976 ex nest of *Aegolius funereus* (1974), M. Rikkonen leg. (ZMUO); • 1 ♀, Kn Kajaani, 64.2263°N, 27.7932°E, VYÖ 1210 *ad luc* 15. –21 Jun 2006, DNA sample MM 17523, R. Leinonen leg. (ZMUO). ITALY • 1 ♀, Südtirol, Tiers E, Plafetscher Wald, 1600–1650 m, 46.472°N, 11.596°E, 23 Jun 2006, leg. Huemer, DNA sample TLMF Lep 09795 (TLMF).

Other material. FINLAND • 7 ♂ 4 ♀, Ta Valkeakoski, Sääksmäki, 61.2326°N, 24.1137°E, ex larva (host unknown); 1992, S. Karhula leg. (MZH); • 2 ♀, Kn Kajaani,

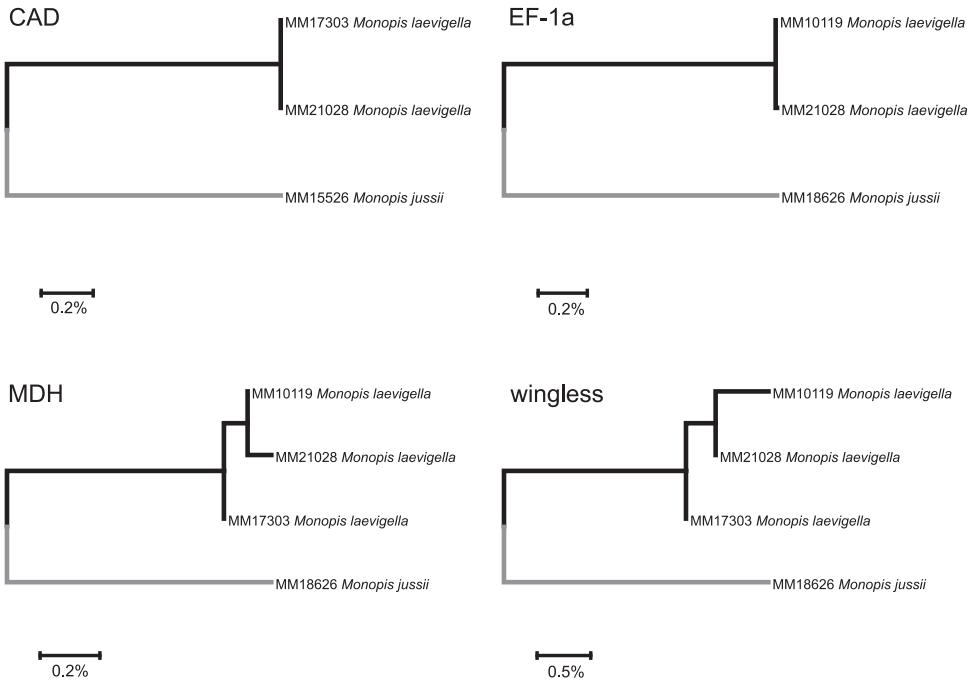

Figure 2. Comparison of genetic variability in four nuclear genes, CAD, EF-1a, MDH and wingless, between *Monopis laevigella* and *M. jussii* sp. nov.

Karankalahti, 64.2222°N, 27.721°E, ex larva 2016 from nest of *Strix uralensis*, Itämies & Kyrki leg. (ZMUO); 1 ♀, PPe: Oulu, Oinaansuo, 65.0249°N, 25.6209°E, larva 28 Apr 1992 in nest of *Parus major*, J. Itämies leg. (ZMUO); • 1 ♀, EP Jurva, 62.7002°N, 22.0153°E, ex larva 2006, H. Vuorinen leg. (ZMUO); 2 ♀, Ks Kuusamo, 66.2565°N, 29.2807°E, ex larva 1975, J. Viramo leg. (ZMUO); • 1 ♂ 1 ♀, Ks Salla, Värriö, R1 & R3, 30 Jun 1989 & 21 Jul 1987, Erkki Pulliainen leg. (ZMUO); • 1 ♀, Li Inari, Kivijoki, 68.6125°N, 28.3509°E, 15 Jul 1993, E. & L. Laasonen leg. (ZMUO); • 1 ♂, Ks Kuusamo, Autiotalo, 66.3591°N, 29.6029°E, 28 Jun 1995, E. & L. Laasonen leg. (ZMUO); • 1 ♂, PPn Rovaniemi, 66.5509°N, 25.7619°E, 17 Jun 1992, T. Mutanen leg. (ZMUO); • 1 ♀, EnL Enontekiö, Saana, 69.0456°N, 20.8554°E, 11 Jul 2016, Marko, Nestori & Anttoni Mutanen leg. (ZMUO); • 1 ♀, Pedersöre, 8 Jul 1939, Sjöholm leg. (ZMUO); • 1 ♀, Om Jakobstad, 63.7098°N, 22.6489°E, 21 Jun 1936, E. Sjöholm leg. (ZMUO); 2 ♂, KP Haapajärvi, Harjunniemi, 63.7434°N, 25.3292°E, ad luc. 3 Jul 1975 & 6 Jul 1975, A. Kosonen leg. (ZMUO); NORWAY • Finnmark Alta, Mattisfossen-Sakkopadne, 5 Jul 1973, J. Kyrki leg. (ZMUO); SWEDEN • Härjedalen, Vemdalen, 3 Jul 1947, Henrik Bruun leg. (ZMUO).

Diagnosis. *Monopis jussii* sp. nov. is externally close to *M. laevigella*, but the forewing appears darker, as it is less mottled with pale scales, especially along the margins (Figures 4, 5). Fringes are yellow and with a clear fringe line in *M. laevigella* but grey and without the fringe line in *M. jussii*. Besides the genetic markers, the forewing col-

Figure 3. The holotype male of *Monopis jussii* sp. nov. PPe Yli-Kiiminki, larva 2001, ex nest of *Aegolius funereus*, M. Mutanen leg., R. Gaedike prep. 8607. (Coll. ZMUO).

our is indeed the best clue to separate these species. There is nevertheless some variation, especially in *M. laevigella*. Both male and female genitalia vary considerably, as do those of *M. laevigella*. The variation in all characters of genitalia overlaps between these species, and, apparently, they cannot be identified by genital characters. For variation of *M. laevigella* see also Gaedike (2019). Moreover, *M. weaverella* (Scott, 1858) and *M. neglecta* Šumpich & Liška, 2011 may occasionally fall within the morphological variation of these two species, especially in females. The males of *M. weaverella* and *M. neglecta* can however be distinguished from *M. laevigella* and *M. jussii* by the shape of gnathos, best decipherable in lateral view (see Gaedike 2019): gnathos arms are straight, triangular in *M. weaverella* and *M. neglecta*, angled particularly in anterior margin in *M. laevigella* and *M. jussii*.

Description. Forewing length 5.8–8.5 mm (n = 8 ♂ and 8 ♀) (note that the specimens are reared which may have affected their size). Maxillary palpus, labial palpus and head ochreous yellow; outer side of labial palpus with dark grey scales, second segment distally bristled. Scape of antenna ochre with pecten formed of bristle-shaped scales, pedicel and flagellum dark brown. Thorax dark grey, dorsomedially variably intermixed or entirely with pale ochre scales; tegula dark grey, apically often paler grey or ochre. Fore and mid leg inwardly ochre, outwardly leaden grey, apex of tibia and tarsal segments

Figure 4. Comparison of habitus between *Monopis laevigella* and *M. jussii* sp. nov. **A–C** *M. laevigella* female **D–F** *M. laevigella* male **G–I** *M. jussii* paratype, females **J–L** *M. jussii* paratype, males.

ochre. Hind leg inwardly pale, outwardly ochre, intermixed with grey scales; spurs and apex of tibia and tarsal articles ochre. Forewing dark grey, variably mottled with pale grey scales; costa narrowly and variably sometimes ochre; basal scales of termen with alternating pale ochre and grey scales, distal scales of termen unicolorous grey, contrast between distally paler basal scales and darker distal scales giving an impression of faint fringe line; silvery grey spot somewhat basal of middle of wing length at fold. Hind wing bluish grey with somewhat darker grey veins; fringe basally narrowly ochre, otherwise grey. Underside of wings grey with ochre margin; underside of hindwing dark grey along costal margin. Abdomen leaden grey, basal segments ventrally more or less ochre.

Male genitalia (Figure 6). Uncus elongate, triangular, laterally with long, hair-like scales, distally pointed, bifid. Gnathos arms angled in the middle, tapered toward hook-shaped apex. Basal and distal margins of tegumen reinforced, U-shaped, anter-

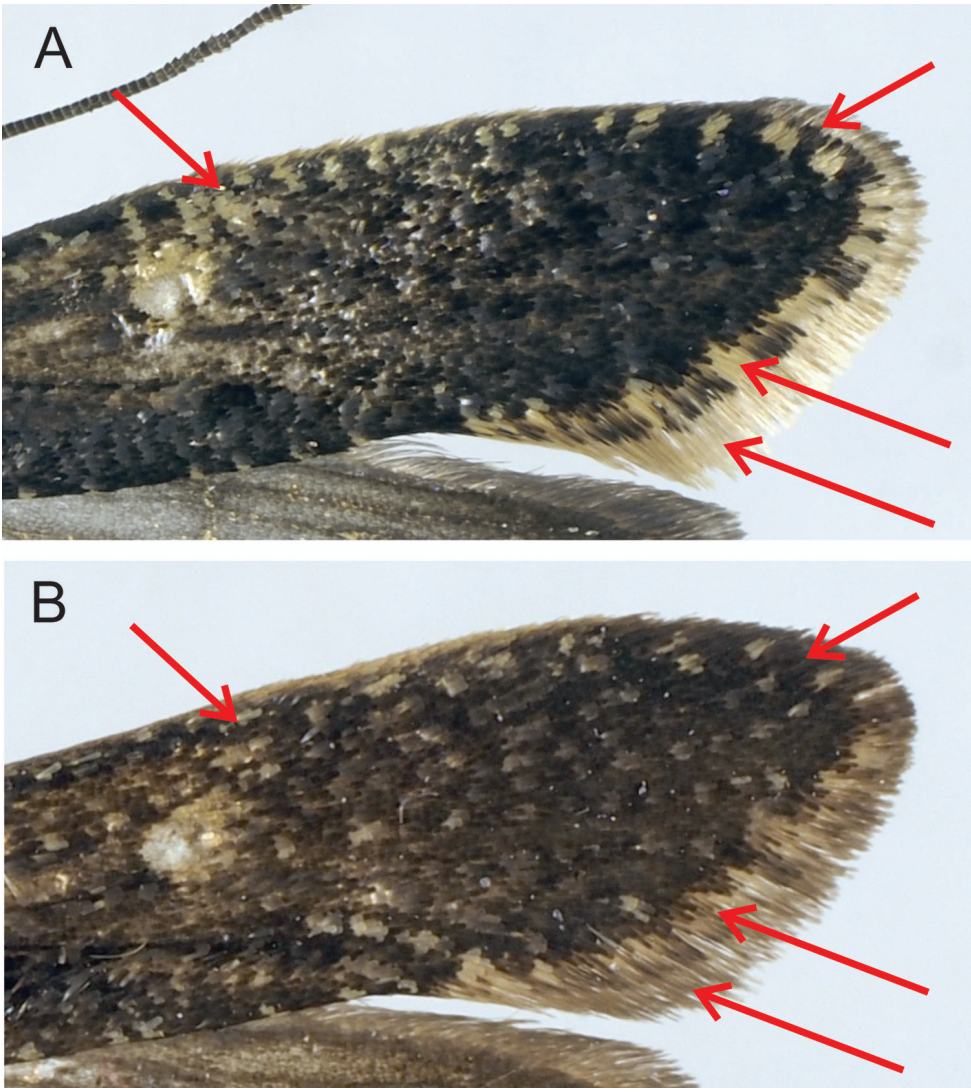

Figure 5. Comparison of forewing patterns of *Monopis laevigella* (**A**) and *M. jussii* sp. nov. (**B**). The arrows indicate differences in fringe colour (yellow/grey), fringe line (present/absent; chequered/non-chequered) and forewing costa (many white scales between the costa and the dorsal spot/few white scales between the costa and the dorsal spot).

ior margin more deeply. Shape of valva highly variable, gradually varying from ovoid and basally broadest to somewhat elongate and medially widest; distally round. Every aspect of saccus variable; straight or somewhat undulate, apically little or very much widened; length also very variable. Phallus straight and nearly parallel-sided, slightly widened at basal 1/3; length compared to that of saccus impossible to establish due to variation in length of saccus. Phallus distally inserted in cylindrical, internally spinose anellus. Vesica distally densely spinose, devoid of cornuti.

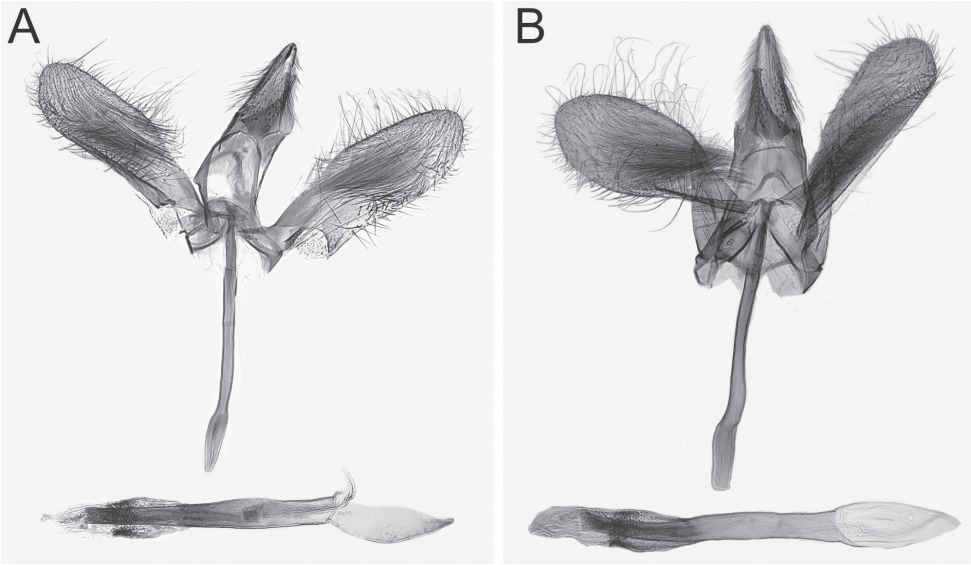

Figure 6. Overview of male genitalia of *Monopis jussii* sp. nov. **A** paratype, Finland, Kiiminki, M. Mutanen leg., L. Kaila prep. 6317 **B** Finland, Yli-Kiiminki, M. Mutanen leg., L. Kaila prep. 6315.

Female genitalia (Figures 7–9). Papilla analis membranous, elongate, distally round, with a few setae. Apophysis posterioris as long as segments 7+8, posteriorly starting as continuation of papilla analis, slender, anteriorly slightly widened, apex cut. Apophysis anterioris 1/3 length of and slightly stouter than apophysis posterioris, twice as long as 8th segment, distally not widened. Ovipositor telescopic, with two retractile nodes; with a few stout setae. Ventral pseudapodemes (*sensu* Davis and Robinson 1999) not decipherable. Tergum 8 posteriorly somewhat sclerotized. Ostium a widely U-shaped opening, laterally bordered as posteriorly curved rim, laterad shallowly emarginated in posterior direction, emargination with a few long setae; devoid of microtrichia but minutely granulose. Length of antrum variable, narrowed toward colliculum; colliculum tubular, length variable, 2–4 times as long as wide, usually narrowed in the middle. Ductus bursae between colliculum and corpus bursae membranous, as long as apophysis anterioris. Corpus bursae oval, 3 times as long as wide; in approximately the middle to posterior 1/3 ca. 12 elongate, sharply spicular or dentate signa forming transverse band.

Genetic characterisation. Clearly distinguishable by its DNA barcode from all other species of *Monopis* barcoded globally so far (Figure 1). Genetically the closest species with a minimum divergence of 4.43% is *M. laevigella*. Intraspecific divergence among four barcoded specimens from Finland and Italy is 0.15%. Additionally, the species show 1.5–4.1% interspecific divergence in the nuclear genes of *CAD*, *EF-1a*, *MDH* and *wingless* (Figure 2).

Etymology. The species is dedicated to Dr Juhani (Jussi) Itämies, a Finnish expert of Lepidoptera who, as far as we know, is the first to have reared this species. He has

Figure 7. Overview of female genitalia of *Monopis jussii* sp. nov., paratype, Finland, Yli-Kiiminki, M. Mutanen leg., L. Kaila prep. 6324.

also spent most of his life on faunistic research of Finnish Lepidoptera and has done incredible work in elucidating the life history of numerous microlepidopteran species.

Distribution. From our available observations *M. jussii* seems to have a boreomontane distribution pattern. It is widely distributed in Finland and also recorded from Norway (Finnmark) and Sweden (Härjedalen). Records from the Alps seem rare with a proved, barcode-based locality in the Italian Dolomites and two further unpublished records (ZSM, A. Segerer) in the Bavarian Alps.

Biology. So far reared on five different occasions from the nest bottoms of the Boreal owl (*Aegolius funereus*). Two specimens in the collection of ZMUO have been reared from the nest of the Ural owl (*Strix uralensis*) and one specimen from the nest

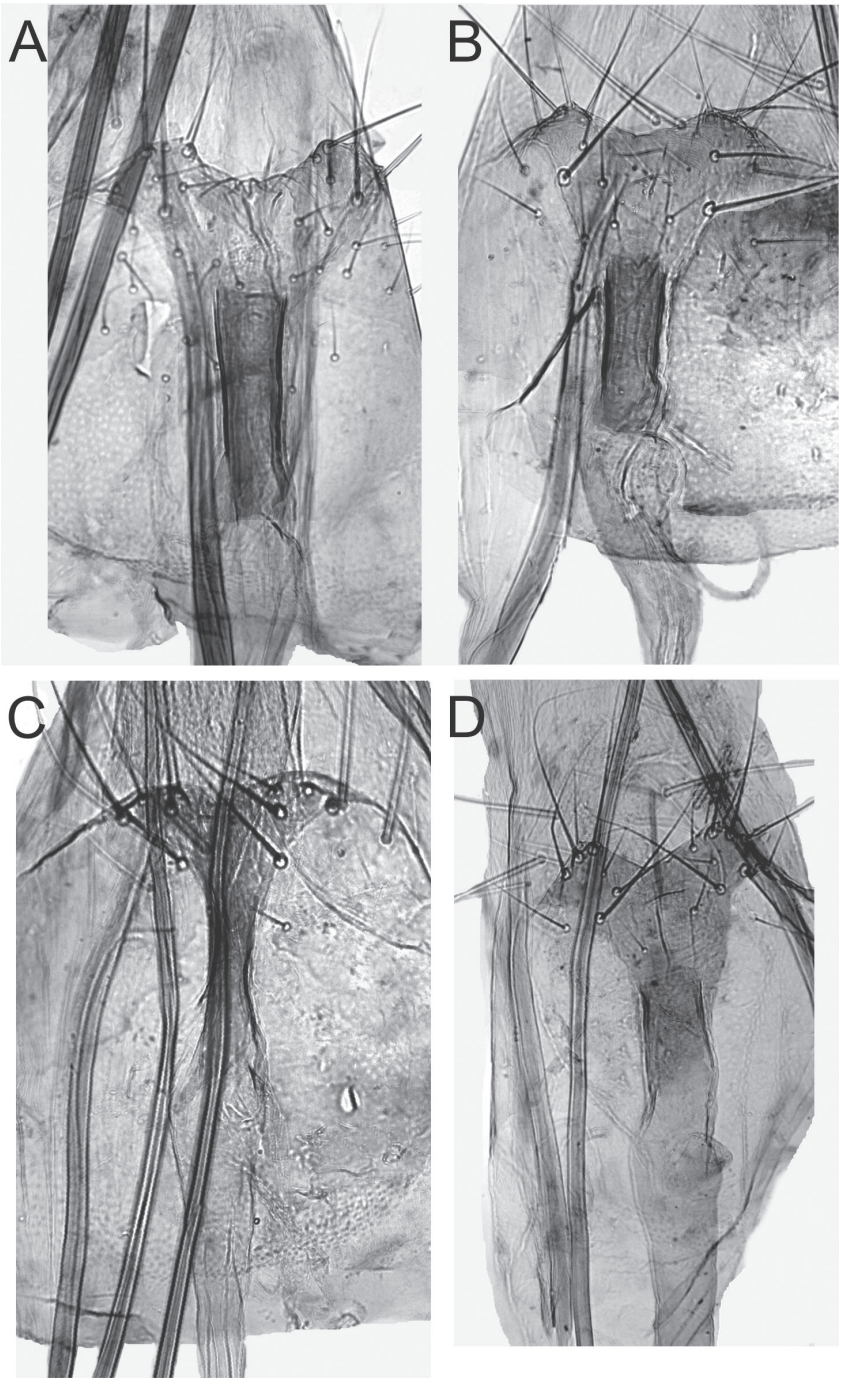

Figure 8. Details of ostium bursae and colliculum of female genitalia of *Monopis jussii* sp. nov. **A** paratype, Finland, Yli-Kiiminki, M. Mutanen leg., L. Kaila prep. 6324 **B** paratype, Finland, Kiiminki, M. Mutanen leg., L. Kaila prep. 6325 **C** paratype, Finland, Yli-Kiiminki, M. Mutanen leg., L. Kaila prep. 6322 **D** paratype, Finland, Kiiminki, M. Mutanen leg., L. Kaila prep. 6326.

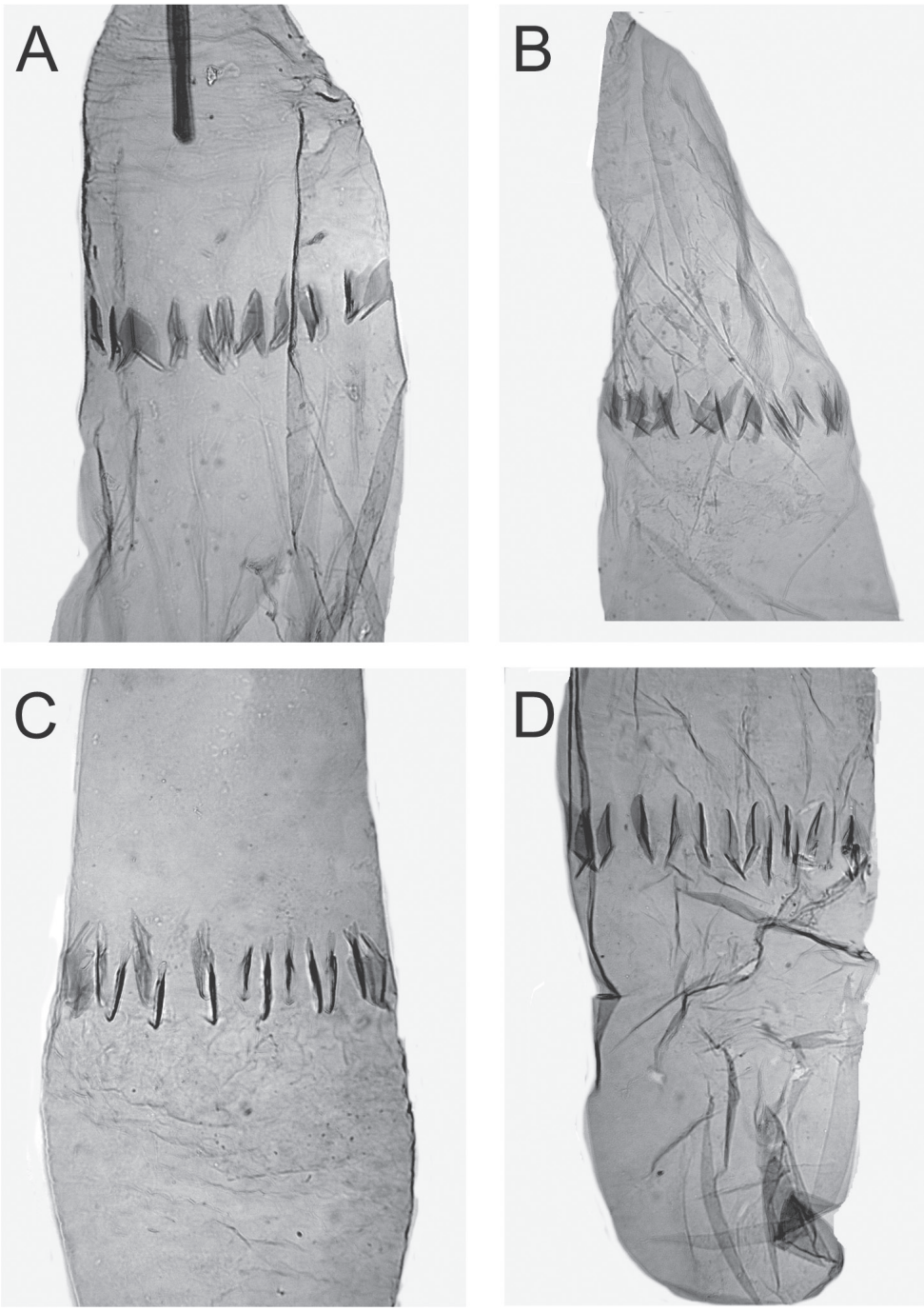

Figure 9. Signa of corpus bursae of female genitalia of *Monopis jussii* sp. nov. **A** paratype, Finland, Yli-Kiiminki, M. Mutanen leg., L. Kaila prep. 6324 **B** paratype, Finland, Kiiminki, M. Mutanen leg., L. Kaila prep. 6325 **C** paratype, Finland, Yli-Kiiminki, M. Mutanen leg., L. Kaila prep. 6322 **D** paratype, Finland, Kiiminki, M. Mutanen leg., L. Kaila prep. 6326.

of the Great tit (*Parus major*). Additionally, three reared specimens of two different rearing events do not state anything about the origin. One specimen has been found in a vacated house. Thirteen specimens in coll. ZMUO and a specimen from the Italian Alps in coll. TLMF have been collected in the wild between 17 June to 21 July, which matches well with the flight time of other *Monopis* species of these regions.

Taxonomic remarks on *Monopis laevigella*

Monopis jussii sp. nov. is most closely related to *M. laevigella* and can easily be confused with that species (see above). We therefore re-evaluate available names in the *M. laevigella* species group.

Monopis laevigella ([Denis & Schiffermüller], 1775).
Tinea laevigella [Denis & Schiffermüller], 1775: 139.

Misidentifications

Tinea rusticella Hübner, 1796: 61, pl. 3, fig. 17; a junior synonym of *Haplotinea insectella* (Fabricius, 1794) (Zeller, 1852: 153–154).
Recurvaria rustica Haworth, 1828: 548; unjustified emendation of *Tinea rusticella* Hübner, 1796.
Tinea saturella Haworth, 1828: 562, unavailable.
Tinea vestianella sensu Stephens, 1835: 344; a misidentification of *Phalaena* (*Tinea*) *vestianella* Linnaeus, 1758.
Blabophanes rusticella ab. *semispilotella* Strand, 1900: 225; unavailable name, deemed infrasubspecific according to ICZN Art. 45.6.2 from use of the term "ab."; a misidentification of *M. weaverella* (Scott, 1858) (Gaedike 2019).

Neotype selection

Tinea laevigella was described from an unspecified number of specimens collected in the area of Vienna, Austria ([Denis & Schiffermüller], 1775). The collection was later deposited in the "Hof-Naturalien-Kabinett" and destroyed by fire during the Vienna Rebellion on 31st of October 1848 (Speta 2003). Since this species can be confused with *M. jussii* sp. nov. and several other congeneric taxa we designate as neotype a male specimen from Austria to preserve stability (Figure 10). It is labelled "AUSTRIA occ. Nordtirol / Brandenberg / Tiefenbachklamm / 11°51'52"E, 47°29'4"N / 645 m, 16.6.2013 / leg. Huemer" "DNA Barcode / TLMF Lep 10354" (TLMF).

Tinea rusticella was figured twice by Hübner in the eighth volume of his *Sammlung europäischer Schmetterlinge*, first it was validly described on page 61, pl. 3, fig. 17 (1796) and later a different species was figured on pl. 49, fig. 339 (1813). Hübner (1825) considered them conspecific, and he referred to both figures when he erected the monotypic genus *Monopis*.

Figure 10. Neotype male of *Monopis laevigella* from Austria, here designated. AUSTRIA occ. Nordtirol / Brandenberg / Tiefenbachklamm / 11°51'52"E, 47°29'4"N / 645 m, 16.6.2013 / leg. Huemer" "DNA Barcode / TLMF Lep 10354". (Coll. TLMF).

Zeller (1852) was probably the first to question whether Hübner's two figures of *Tinea rusticella* represented the same species. He referred to Hübner's fig. 339 (1813) when dealing with the species, which became known as *Monopis rusticella* [= *Monopis laevigella* ([Denis & Schiffermüller], 1775)], and rejected that Hübner's fig. 17 (1796) could be of a specimen of that species, suggesting that it could be *Tinea misella* Zeller, 1839 [= *Haplotinea insectella* (Fabricius, 1794)]. *Tinea rusticella* Hübner, 1813 is both a misidentification and a homonym of *Tinea rusticella* Hübner, 1796 and thus permanently invalid.

Haworth (1828: 548) named the species twice. First with reference to Hübner's pl. 3, fig. 17 as *Recurvaria rustica*, which is an unjustified emendation and thus an objective synonym of *Tinea rusticella* (Hübner, 1796) [= *Haplotinea insectella* (Fabricius)], and later in the same work Haworth (op. cit.: 339), again with reference to Hübner's pl. 3, fig. 17, proposed the name *Tinea saturella* in synonymy with *Tinea rusticella*. Because *Tinea saturella* was described in synonymy with *Tinea rusticella* it was always considered a synonym of that species (viz. *Monopis rusticella*), but because Haworth referred only to Hübner's fig. 17 (and not to fig. 339) it is an objective junior synonym of *Tinea rusticella* Hübner, 1796, and thereby a subjective junior synonym of *Haplotinea insectella* (Fabricius). However, as the name *Tinea saturella* has never been made available under the provision of Art. 11.6. of the Code (ICZN 1999) and adopted as the name of a taxon before 1961, we consider it as unavailable.

Although *Monopis* Hübner 1825 was described as a monotypic genus, it is based on a partly misidentified species. We consider Zeller (1852) as First Reviser of *Tinea rusticella* Hübner, restricting the name to the species now (and also by Zeller 1852) known as *Monopis laevigella* ([Denis & Schiffermüller], 1775).

Discussion

Compared with many other groups of Lepidoptera, the species diversity of Tineidae is generally poorly investigated. Hundreds of species deposited in museum collections remain undescribed (Robinson 2009). It is likely that many more species remain entirely undiscovered globally. The European fauna is comparatively well understood, and the fauna of the entire continent has recently been taxonomically reviewed in two monographs (Gaedike 2015, 2019). New species discoveries are uncommon, particularly for central and northern parts of Europe. An example of a recent species discovery is that of *Monopis neglecta* Šumpich & Liška, 2011, a species that morphologically is nearly indistinguishable from *M. weaverella* (Scott, 1858) (see Gaedike 2019). While no genetic data were provided for *M. neglecta* in the original description, the DNA barcode sequences provided in the present study confirm its status as a separate species from *M. weaverella*. It is encouraging that although the species of Tineidae are often difficult to tell apart from each other morphologically, no cases of barcode sharing in the European fauna are known. Evidently, therefore, DNA barcoding provides an efficient way to investigate their diversity in less thoroughly explored areas as well.

Based on the available distributional data, *Monopis jussii* has a much more limited range than *M. laevigella*. It is possible, if not likely, that it is a member of boreo-montane faunal elements, being distributed in the boreal region on the one hand and in the Alps below the timberline on the other hand. It is likely absent from the lowlands of Central Europe. It would not be surprising if the species turns out to be present in other European mountain systems and the eastern Palearctic. Based on the large number of examined museum specimens from the ZMUO and MZH collections, the species is widely present in northern Finland south to ca. 64° N but becomes much scarcer towards the more southern localities. The southernmost verified records from Finland are from the province of Tavastia australis (ca. 61° N).

Based on our own and other experiences (Robinson 2009, Gaedike 2019), *Monopis laevigella* is not strict regarding the source of its food, but it seems to prefer cavity-breeding birds, possibly because their nests are usually dry. Several extensive rearing experiments of nest bottoms of various birds, mostly the Tawny Owl (*Strix aluco* Linnaeus, 1758) and the Ural Owl (*S. uralensis* Pallas, 1771), from southern Finland have yielded large numbers of *M. laevigella*, which is usually present in every nest in large numbers. In an experiment by MM in 2017 with 13 nest bottoms of *Strix* spp., probably thousands of *M. laevigella* emerged. Among several dozen pinned specimens sampled from each nest, none represents *M. jussii*. Other species that are regularly or often

present in the nests of *Strix* spp. in Finland are *Niditinea striolella* (Matsumura, 1931) (usually emerges in great numbers too), *Tinea svenssoni* Opheim, 1965 (present in almost all nests), *Tinea steueri* Petersen, 1966 (not present in every nest) and *Monopis fenestratella* (Heyden, 1863) (present in most nests but is cryptic in behaviour). While it is possible that *M. jussii* has stricter habitat requirements and that it has a strong preference for the Boreal Owl, we find this possibility unlikely. The Boreal owl, the Ural owl, as well as the Great tit are all cavity breeders, rendering the nest conditions between these species very similar. In rearing conditions, tineids are not selective for the origin of food and readily feed on mammal hairs too. It is more likely that *Monopis jussii* has been reared mostly from the nests of the Boreal owl just because it is a more common owl species within the moth's main distribution in Finland than either of the two *Strix* species present in Finland. Further rearing experiments, optimally systematically from different species of birds, would bring additional valuable information on the habitat requirements of *M. jussii* and several other species of Tineidae.

Monopis laevigella has a Holarctic distribution (Landry and Pohl 2018, Gaedike 2019). Many specimens of this species have been barcoded from the Nearctic region, both from Canada and the U.S.A. They fall in two clusters, both of which are highly distinct from the clade consisting of *M. jussii* and the Palearctic *M. laevigella* (data only partially public in BOLD). In the Neighbor-Joining trees neither of these clusters is placed as sister to the Palearctic *M. laevigella* + *M. jussii* clade, suggesting that they represent distinct taxa and even that their closest relative is not *M. laevigella*. However, due to the limited phylogenetic information content of the DNA barcode region, verification of both scenarios requires more rigorous and thorough taxonomic and phylogenetic scrutiny.

Acknowledgements

We are grateful to Leif Aarvik, Reinhard Gaedike, Peter Buchner, Bob Heckford, and Juhani Itämies for providing information and help with many kinds of matters during the preparation of this study. DNA barcoding was conducted at the Centre for Biodiversity Genomics, to whose staff we are grateful for their continuous support. Thomas Pape, Natural History Museum of Denmark, kindly advised on questions about nomenclature. Sequencing was financially supported by the Academy of Finland, Kone foundation and Finnish Cultural foundation through grants to the Finnish Barcode of Life project and furthermore supported by the Promotion of Educational Policies, University and Research Department of the Autonomous Province of Bolzano - South Tyrol with funds to the projects "Genetische Artabgrenzung ausgewählter arktoalpiner und boreomontaner Tiere Südtirols" and "Erstellung einer DNA-Barcode-Bibliothek der Schmetterlinge des zentralen Alpenraumes (Süd-, Nord- und Osttirol)". Andrew Liston kindly checked the English language. Finally, we are indebted to Bengt Å. Bengtsson, an anonymous reviewer, and Erik J. van Nieukerken for many useful comments on the earlier version of this paper.

References

Davis DR, Robinson GS (1999) The Tineoidea and Gracillarioidea. In: Kristensen NP (Ed.) Lepidoptera, moths and butterflies. Vol 1: Evolution, systematics and biogeography. Handbook of Zoology 4(35), Walter de Gruyter, Berlin, New York, 91–119.

Denis M, Schiffermüller I (1775) Ankündung eines systematischen Werkes von den Schmetterlingen der Wienergegend herausgegeben von einigen Lehrern am k. k. Theresianum. Augustin Bernardi, Wien, 322 pp. [pls. frontispece, 1–1b]

Dinca V, Lukhtanov VA, Talavera G, Vila R (2011) Unexpected layers of cryptic diversity in wood white *Leptidea* butterflies. Nature Communications 2: 324. https://doi.org/10.1038/ncomms1329

Gaedike R (2015) Tineidae I (Dryadaulinae, Hapsiferinae, Euplocaminae, Scardiinae, Nematopogoninae and Meessinae). In: Nuss M, Karsholt O, Huemer P (Eds) Microlepidoptera of Europe 7. Brill, Leiden/Boston, 308 pp. https://doi.org/10.1163/9789004289161

Gaedike R (2019) Tineidae II (Myrmecozelinae, Perissomasticinae, Tineinae, Hieroxestinae, Teichobiinae and Stathmopolitinae). In: Karsholt O, Mutanen M, Nuss M (Eds) Microlepidoptera of Europe 9. Brill, Leiden/Boston, 248 pp. https://doi.org/10.1163/9789004387515

Haworth AH (1828) Lepidoptera Britannica, sistens digestionem novam insectorum Lepidopterorum quae in magna Britannica reperiuntur, larvarum pabulo, temporeque pascendi; expansion alarum, mensibusque volandi, synonymis atque locis observationibusque variis vol 4. J. Murray, London, 513–609. https://doi.org/10.1080/14786442808674667

Hübner J (1796–1836) Sammlung europäischer Schmetterlinge 8. Augsburg. (Tineae-Schaben): 1–78 [1796], 71 pls 1–71 (1796-[1836]).

Hübner J (1816–1825) Verzeichniss bekannter Schmettlinge. Augsburg, 431 pp. https://doi.org/10.5962/bhl.title.48607

Huemer P, Haxaire J, Lee KM, Mutanen M, Pekarsky O, Ronkay L (2020) Revision of the genus *Hoplodrina* Boursin, 1937 (Lepidoptera, Noctuidae, Xyleninae). I. *Hoplodrina octogenaria* (Goeze, 1781) and its sister species *H. alsinides* (Costantini, 1922) sp. rev. in Europe. ZooKeys 927: 75–97. https://doi.org/10.3897/zookeys.927.51142

Huemer P, Karsholt O (2010) Gelechiidae II. (Gelechiinae: Gnorimoschemini). Microlepidoptera of Europe vol 6. Apollo Books. Stenstrup, Denmark, 586 pp. https://doi.org/10.1163/9789004260986_002

Huemer P, Karsholt O, Aarvik L, Berggren K, Bidzilya A, Junnilainen J, Landry J-F, Mutanen M, Nupponen K, Segerer A, Šumpich J, Wieser C, Wiesmair B, Hebert PDN (2020) DNA barcode library for European Gelechiidae (Lepidoptera) suggests greatly underestimated species diversity. ZooKeys 921: 141–157. https://doi.org/10.3897/zookeys.921.49199

ICZN (1999) International Code of Zoological Nomenclature, Fourth Edition. International Trust for Zoological Nomenclature, The Natural History Museum London, London, 306 pp.

Kozlov MV, Mutanen M, Lee KM, Huemer P (2017) Cryptic diversity in the long-horn moth *Nemophora degeerella* (Lepidoptera: Adelidae) revealed by morphology, DNA barcodes and genome-wide ddRAD-seq data. Systematic Entomology 42: 329–346. https://doi.org/10.1111/syen.12216

Kumar S, Stecher G, Tamura K (2016) MEGA7: Molecular evolutionary genetics analysis version 7.0. Molecular Biology and Evolution 33: 1870–1874. https://doi.org/10.1093/molbev/msw054

Landry JF, Pohl GR (2018) 16. Family Tineidae Latreille, 1810. In: Pohl GR et al. Annotated Checklist of the Moths and Butterflies (Lepidoptera) of Canada and Alaska. Pensoft series Faunistica 118: 46–50.

Mutanen M, Aarvik L, Huemer P, Kaila L, Karsholt O, Tuck K (2012a) DNA barcodes reveal that the widespread European tortricid moth *Phalonidia manniana* (Lepidoptera: Tortricidae) is a mixture of two species. Zootaxa 3262: 1–21. https://doi.org/10.11646/zootaxa.3262.1.1

Mutanen M, Aarvik L, Landry JF, Segerer A, Karsholt O (2012b) *Epinotia cinereana* (Haworth, 1811) bona sp., a Holarctic tortricid distinct from *E. nisella* (Clerck, 1759) (Lepidoptera: Tortricidae: Eucosmini) as evidenced by DNA barcodes, morphology and life history. Zootaxa 3318: 1–25. https://doi.org/10.11646/zootaxa.3318.1.1

Mutanen M, Kaila L, Tabell J (2013) Wide-ranging barcoding aids discovery of one-third increase of species richness in presumably well-investigated moths. Scientific Reports 3: 2901. https://doi.org/10.1038/srep02901

Mutanen M, Kivelä SM, Vos RA, Doorenweerd C, Ratnasingham S, Hausmann A, Huemer P, Dincă V, van Nieukerken EJ, Lopez-Vaamonde C, Vila R, Aarvik L, Decaëns T, Efetov KA, Hebert PDN, Johnsen A, Karsholt O, Pentinsaari M, Rougerie R, Segerer A, Tarmann G, Zahiri R, Godfray HCJ (2016) Species-Level Para- and Polyphyly in DNA Barcode Gene Trees: Strong Operational Bias in European Lepidoptera. Systematic Biology 65: 1024–1040. https://doi.org/10.1093/sysbio/syw044

Peña C, Malm T (2012) VoSeq: a voucher and DNA sequence web application. PLoS One.7(6), e39071. https://doi.org/10.1371/journal.pone.0039071

Robinson GS (1976) The preparation of slides of Lepidoptera genitalia with special reference to the Microlepidoptera. Entomologist's Gazette 27: 127–132.

Robinson GS (2009) Biology, distribution and diversity of tineid moths. Natural History Museum, Kuala Lumpur, 143 pp.

Robinson G, Nielsen ES (1993) Tineid genera of Australia (Lepidoptera). *Monographs on Australian Lepidoptera* 2. CSIRO Publishing, Melbourne, 344 pp. https://doi.org/10.1071/9780643105102

Scott J (1858) A supposed new species of *Tinea* allied to *rusticella*. The Zoologist 16: 5964–5965.

Segerer AH, Haslberger A, Grünewald T (2010) Occurrence of *Olethreutes subtilana* (Falkovitsh, 1959) in Central Europe uncovered by DNA barcoding (Tortricidae: Olethreutinae). Nota Lepidopterologica 33: 209–218.

Speta F (2003) Ignaz Schiffermüller (1727–1806) – eine Biographie. Denisia 8: 11–14.

Stephens JF (1834) Illustrations of British Entomology or, a Synopsis of Indigenous Insects: containing their generic and specific distinctions with an account of their metamorphoses, times of appearance, localities, food, and economy, as far as practicable. London. Insecta Haustellata 4: 1–436, pls 23–41.

Strand E (1900) Einige arktische Aberrationen von Lepidopteren. Entomologische Nachrichten 26: 225–226.

Šumpich J, Liška J (2011) In: Šumpich, J.: Motýli Národnich parku Podyjí a Thayatal. Die Schmetterlinge der Nationalparke Podyjí und Thayatal. Správa Národního parku Podyfí, Znojmo, 1–488.

Wahlberg N, Wheat CW (2008) Genomic outposts serve the phylogenomic pioneers: designing novel nuclear markers for genomic DNA extractions of Lepidoptera. Systematic Biology 57: 231–242. https://doi.org/10.1080/10635150802033006

Zeller PC (1852) Die Schaben mit langen Kiefertastern. Linnaea Entomologica 6: 81–197.